

**Assessing uncertainties of in situ
FAPAR measurements across
different forest ecosystems**

**Implications for the validation of
satellite derived FAPAR products**

Birgitta Maria Putzenlechner

Dissertation zur Erlangung des Doktorgrades
an der Fakultät für Geowissenschaften
der Ludwig-Maximilians-Universität München

Vorgelegt von

Birgitta Maria Putzenlechner

Aus München

München, 2019

Erstgutachter: Prof. Dr. Ralf Ludwig

Zweitgutachter: Prof. Dr. Arturo Sanchez-Azofeifa

Tag der Fertigstellung: 18.12.2019

Tag der mündlichen Prüfung: 02.03.2020

Every tree reaching for light will cast shadows. There are, however, sunspots in every forest.

Acknowledgements

After winded paths through the forests, this thesis finally comes to an end. The journey related to this thesis has been a challenge in many ways and the accomplishments of this work would not have been possible without the support of several people whom I hereby want to express my sincere gratitude to. First, I want to thank my supervisor, Prof. Dr. Ralf Ludwig, for giving me the opportunity to start this PhD project and the constant guidance and encouragement to accomplish it. I am also grateful for supporting me to travel as going abroad as well as participating in numerous conferences and workshops was key to elaborate my research design. Finally, I am grateful for having had the opportunity to teach, which I perceived as both a professional and personal enrichment in my academic career. I also want to thank my second supervisor, Prof. Dr. Arturo Sánchez-Azofeifa for the profound scientific guidance throughout this whole journey. Thanks to his outstanding expertise in the field of forest ecology, monitoring and remote sensing, the in-depth discussions were important to reach scientific milestones. I am also thankful to him for hosting me at the University of Alberta in the framework of the Jointly Delivered Doctoral Degree Program with LMU. In this regard, I want to thank the whole CEOS-Tropi-Dry lab team, especially Sofia Calvo, Saulo Castro, Felipe Alencastro and Iain Sharp for sharing their experience and knowledge on the Albertan and Costa Rican sites with me.

As being recipient of a research stipend, I am very thankful to the financial support and professional skills courses offered by the MICMoR Research School, funded by the Helmholtz Association. I also want to thank my mentor Dr. Ralf Kiese for his advice on setting up the monitoring network in Graswang and the time he invested for our regular thesis committee meetings. Special thanks also go to Dr. Elija Bleher for taking good care of organizational and funding issues related to the MICMoR curriculum. After all, the numerous workshops, fellows' retreats and presentations at research forums expanded my scientific horizon.

At LMU Munich, I want to thank Dr. Philip Marzahn for investing his time to refine methodologies and publication strategies. Special thanks also go to Benjamin Müller, who was always willing to share his R skills and discuss statistical methods. I particularly enjoyed sharing my office with Dr. Lingxiao Wang and Verena Huber-García – thank you for the good spirit. In this regard, a very special thanks goes to Vera Erfurth for guiding me through university's bureaucracy or keeping my chocolate level constant.

Apart from these people, I am extremely thankful for the support of my parents who kept believing in me during the most difficult times. I also want to thank my friends Franziska Teusel and Dr. Franziska Koch for inspiring me to become a scientist and the constant encouragements to reach this goal. I finally thank Philipp Koal for the dedicated support he offered me throughout the last years as a scientist, teammate and partner to make the best out of little boxes and me in the middle of the forest.

Summary

Carbon balances are important for understanding global climate change. Assessing such balances on a local scale depends on accurate measurements of material flows to calculate the productivity of the ecosystem. The productivity of the Earth's biosphere, in turn, depends on the ability of plants to absorb sunlight and assimilate biomass. Over the past decades, numerous Earth observation missions from satellites have created new opportunities to derive so-called “essential climate variables” (ECVs), including important variables of the terrestrial biosphere, that can be used to assess the productivity of our Earth's system. One of these ECVs is the “fraction of absorbed photosynthetically active radiation” (FAPAR) which is needed to calculate the global carbon balance. FAPAR relates the available photosynthetically active radiation (PAR) in the wavelength range between 400 and 700 nm to the absorption of plants and thus quantifies the status and temporal development of vegetation. In order to ensure accurate datasets of global FAPAR, the UN/WMO institution “Global Climate Observing System” (GCOS) declared an accuracy target of 10% (or 0.05) as acceptable for FAPAR products. Since current satellite derived FAPAR products still fail to meet this accuracy target, especially in forest ecosystems, in situ FAPAR measurements are needed to validate FAPAR products and improve them in the future. However, it is known that in situ FAPAR measurements can be affected by significant systematic as well as statistical errors (i.e., “bias”) depending on the choice of measurement method and prevailing environmental conditions. So far, uncertainties of in situ FAPAR have been reproduced theoretically in simulations with radiation transfer models (RTMs), but the findings have been validated neither in field experiments nor in different forest ecosystems. However, an uncertainty assessment of FAPAR in field experiments is essential to develop practicable measurement protocols.

This work investigates the accuracy of in situ FAPAR measurements and sources of uncertainties based on multi-year, 10-minute PAR measurements with wireless sensor networks (WSNs) at three sites on three continents to represent different forest ecosystems: a mixed spruce forest at the site “Graswang” in Southern Germany, a boreal deciduous forest at the site “Peace River” in Northern Alberta, Canada and a tropical dry forest (TDF) at the site “Santa Rosa”, Costa Rica. The main statements of the research results achieved in this thesis are briefly summarized below:

Uncertainties of instantaneous FAPAR in forest ecosystems can be assessed with Wireless Sensor Networks and additional meteorological and phenological observations. In this thesis, two methods for a FAPAR bias assessment have been developed. First, for assessing the bias of the so-called two-flux FAPAR estimate, the difference between FAPAR acquired under diffuse light conditions and two-flux FAPAR acquired during clear-sky conditions can be investigated. Therefore, measurements of incoming and transmitted PAR are required to calculate the two-flux FAPAR estimate as well as observations of the ratio of diffuse-to-total incident radiation. Second, to assess the bias of not only the two- but also

the three-flux FAPAR estimate, four-flux FAPAR observations must be carried out, i.e. measurements of top-of-canopy (TOC) PAR albedo and PAR albedo of the forest background. Then, to quantify the bias of the two and three-flux estimate, the difference with the four-flux estimate can be calculated.

Main sources of uncertainty of in situ FAPAR measurements are high solar zenith angle, occurrence of colored leaves and increased wind speed. At all sites, FAPAR observations exhibited considerable seasonal variability due to the phenological development of the forests (Graswang: 0.89 to 0.99 \pm 0.02; Peace River: 0.55 to 0.87 \pm 0.03; Santa Rosa: 0.45 to 0.97 \pm 0.06). Under certain environmental conditions, FAPAR was affected by systemic errors, i.e. bias that go beyond phenologically explainable fluctuations. The in situ observations confirmed a significant overestimation of FAPAR by up to 0.06 at solar zenith angles above 60° and by up to 0.05 under the occurrence of colored leaves of deciduous trees. The results confirm theoretical findings from radiation transfer simulations, which could now for the first time be quantified under field conditions. As a new finding, the influence of wind speed could be shown, which was particularly evident at the boreal location with a significant bias of FAPAR values at wind speeds above 5 ms⁻¹.

The uncertainties of the two-flux FAPAR estimate are acceptable under typical summer conditions. Three-flux or four-flux FAPAR measurements do not necessarily increase the accuracy of the estimate. The highest average relative bias of different FAPAR estimates were 2.1% in Graswang, 8.4% in Peace River and -4.5% in Santa Rosa. Thus, the GCOS accuracy threshold of 10% set by the GCOS was generally not exceeded. The two-flux FAPAR estimate was only found to be biased during high wind speeds, as changes in the TOC PAR albedo are not considered in two-flux FAPAR measurements. Under typical summer conditions, i.e. low wind speed, small solar zenith angle and green leaves, two-flux FAPAR measurements can be recommended for the validation of satellite-based FAPAR products. Based on the results obtained, it must be emphasized that the three-flux FAPAR estimate, which has often been preferred in previous studies, is not necessarily more accurate, which was particularly evident in the tropical location.

The discrepancies between ground measurements and the current Sentinel-2 FAPAR product still largely exceed the GCOS target accuracy at the respective study sites, even when considering uncertainties of FAPAR ground measurements. It was found that the Sentinel-2 (S2) FAPAR product systematically underestimated the ground observations at all three study sites (i.e. negative values for the mean relative bias in percent). The highest agreement was observed at the boreal site Peace River with a mean relative deviation of -13% ($R^2=0.67$). At Graswang and Santa Rosa, the mean relative deviations were -20% ($R^2=0.68$) and -25% ($R^2=0.26$), respectively. It was argued that these high discrepancies resulted from both the generic nature of the algorithm and the higher ecosystem complexity of the sites Graswang and Santa Rosa. It was also found that the temporal aggregation method of FAPAR ground data should be well considered for comparison with the S2 FAPAR product, which refers to daily

averages, as overestimation of FAPAR during high solar zenith angles could distort validation results. However, considering uncertainties of ground measurements, the S2 FAPAR product met the GCOS accuracy requirements only at the boreal study site. Overall, it has been shown that the S2 FAPAR product is already well suited to assess the temporal variability of FAPAR, but due to the low accuracy of the absolute values, the possibilities to feed global production efficiency models and evaluate global carbon balances are currently limited.

The accuracy of satellite derived FAPAR depends on the complexity of the observed forest ecosystem. The highest agreement between satellite derived FAPAR product and ground measurements, both in terms of absolute values and spatial variability, was achieved at the boreal site, where the complexity of the ecosystem is lowest considering forest structure variables and species richness.

These results have been elaborated and presented in three publications that are at the center of this cumulative thesis. In sum, this work closes a knowledge gap by displaying the interplay of different environmental conditions on the accuracy of situ FAPAR measurements. Since the uncertainties of FAPAR are now quantifiable under field conditions, they should also be considered in future validation studies. In this context, the practical recommendations for the implementation of ground observations given in this thesis can be used to prepare sampling protocols, which are urgently needed to validate and improve global satellite derived FAPAR observations in the future.

Zusammenfassung

Projektionen zukünftiger Kohlenstoffbilanzen sind wichtig für das Verständnis des globalen Klimawandels und sind auf genaue Messungen von Stoffflüssen zur Berechnung der Produktivität des Erdökosystems angewiesen. Die Produktivität der Biosphäre unserer Erde wiederum ist abhängig von der Eigenschaft von Pflanzen, Sonnenlicht zu absorbieren und Biomasse zu assimilieren. Über die letzten Jahrzehnte haben zahlreiche Erdbeobachtungsmissionen von Satelliten neue Möglichkeiten geschaffen, sogenannte „essentielle Klimavariablen“ (ECVs), darunter auch wichtige Variablen der terrestrischen Biosphäre, aus Satellitendaten abzuleiten, mit deren Hilfe man die Produktivität unseres Erdsystems computergestützt berechnen kann. Eine dieser „essenziellen Klimavariablen“ ist der Anteil der absorbierten photosynthetisch aktiven Strahlung (FAPAR) die man zur Berechnung der globalen Kohlenstoffbilanz benötigt. FAPAR bezieht die verfügbare photosynthetisch aktive Strahlung (PAR) im Wellenlängenbereich zwischen 400 und 700 nm auf die Absorption von Pflanzen und quantifiziert somit Status und die zeitliche Entwicklung von Vegetation. Um möglichst präzise Informationen aus dem globalen FAPAR zu gewährleisten, erklärte die UN/WMO-Institution zur globalen Klimabeobachtung, das „Global Climate Observing System“ (GCOS), ein Genauigkeitsziel von 10% (bzw. 0.05) FAPAR-Produkte als akzeptabel. Da aktuell satellitengestützte FAPAR-Produkte dieses Genauigkeitsziel besonders in Waldökosystemen immer noch verfehlen, werden dringen in situ FAPAR-Messungen benötigt, um die FAPAR-Produkte validieren und in Zukunft verbessern zu können. Man weiß jedoch, dass je nach Auswahl des Messsystems und vorherrschenden Umweltbedingungen in situ FAPAR-Messungen mit erheblichen sowohl systematischen als auch statistischen Fehlern beeinflusst sein können. Bisher wurden diese Fehler in Simulationen mit Strahlungstransfermodellen zwar theoretisch nachvollzogen, aber die dadurch abgeleiteten Befunde sind bisher weder in Feldversuchen noch in unterschiedlichen Waldökosystemen validiert worden. Eine Unsicherheitsabschätzung von FAPAR im Feldversuch ist allerdings essenziell, um praxistaugliche Messprotokolle entwickeln zu können.

Die vorliegende Arbeit untersucht die Genauigkeit von in situ FAPAR-Messungen und Ursachen von Unsicherheit basierend auf mehrjährigen, 10-minütigen PAR-Messungen mit drahtlosen Sensornetzwerken (WSNs) an drei verschiedenen Waldstandorten auf drei Kontinenten: der Standort „Graswang“ in Süddeutschland mit einem Fichten-Mischwald, der Standort „Peace River“ in Nord-Alberta, Kanada mit einem borealen Laubwald und der Standort „Santa Rosa“, Costa Rica mit einem tropischen Trockenwald. Die Hauptaussagen der in dieser Arbeit erzielten Forschungsergebnisse werden im Folgenden kurz zusammengefasst:

Unsicherheiten von FAPAR in Waldökosystemen können mit drahtlosen Sensornetzwerken und zusätzlichen meteorologischen und phänologischen Beobachtungen quantifiziert werden. In dieser Arbeit wurden zwei Methoden für die Bewertung von Unsicherheiten entwickelt. Erstens, um den

systematischen Fehler der sogenannten „two-flux“ FAPAR-Messung zu beurteilen, kann die Differenz zwischen FAPAR, das unter diffusen Lichtverhältnissen aufgenommen wurde, und FAPAR, das unter klaren Himmelsbedingungen aufgenommen wurde, untersucht werden. Für diese Methode sind Messungen des einfallenden und transmittierten PAR sowie Beobachtungen des Verhältnisses von diffuser zur gesamten einfallenden Strahlung erforderlich. Zweitens, um den systematischen Fehler nicht nur der „two-flux“ FAPAR-Messung, sondern auch der „three-flux“ FAPAR-Messung zu beurteilen, müssen „four-flux“ FAPAR-Messungen durchgeführt werden, d.h. zusätzlich Messungen der PAR Albedo des Blätterdachs sowie des Waldbodens. Zur Quantifizierung des Fehlers der „two-flux“ und „three-flux“ FAPAR-Messung kann die Differenz zur „four-flux“ FAPAR-Messung herangezogen werden.

Die Hauptquellen für die Unsicherheit von in situ FAPAR-Messungen sind ein hoher Sonnenzenitwinkel, Blattfärbung und erhöhte Windgeschwindigkeit. An allen drei Untersuchungsstandorten zeigten die FAPAR-Beobachtungen natürliche saisonale Schwankungen aufgrund der phänologischen Entwicklung der Wälder (Graswang: 0,89 bis 0,99 \pm 0,02; Peace River: 0,55 bis 0,87 \pm 0,03; Santa Rosa: 0,45 bis 0,97 \pm 0,06). Unter bestimmten Umweltbedingungen war FAPAR von systematischen Fehlern, d.h. Verzerrungen betroffen, die über phänologisch erklärbare Schwankungen hinausgehen. So bestätigten die in situ Beobachtungen eine signifikante Überschätzung von FAPAR um bis zu 0,06 bei Sonnenzenitwinkeln von über 60° und um bis zu 0,05 bei Vorkommen gefärbter Blätter der Laubbäume. Die Ergebnisse bestätigen theoretische Erkenntnisse aus Strahlungstransfersimulationen, die nun erstmalig unter Feldbedingungen quantifiziert werden konnten. Als eine neue Erkenntnis konnte der Einfluss der Windgeschwindigkeit gezeigt werden, der sich besonders am borealen Standort mit einer signifikanten Verzerrung der FAPAR-Werte bei Windgeschwindigkeiten über 5 ms⁻¹ äußerte.

Die Unsicherheiten der „two-flux“ FAPAR-Messung sind unter typischen Sommerbedingungen akzeptabel. „Three-flux“ oder „four-flux“ FAPAR-Messungen erhöhen nicht unbedingt die Genauigkeit der Abschätzung. Die höchsten durchschnittlichen relativen systematischen Fehler verschiedener Methoden zur FAPAR-Messung betragen 2,1% in Graswang, 8,4% in Peace River und -4,5% in Santa Rosa. Damit wurde der durch GCOS festgelegte Genauigkeitsschwellenwert von 10% im Allgemeinen nicht überschritten. Die „two-flux“ FAPAR-Messung wurde nur als fehleranfällig bei hohe Windgeschwindigkeiten befunden, da Änderungen der PAR-Albedo des Blätterdachs bei der „two-flux“ FAPAR-Messung nicht berücksichtigt werden. Unter typischen Sommerbedingungen, also geringe Windgeschwindigkeit, kleiner Sonnenzenitwinkel und grüne Blätter, kann die „two-flux“ FAPAR-Messung für die Validierung von satellitengestützten FAPAR-Produkten empfohlen werden. Auf Basis der gewonnenen Ergebnisse muss betont werden, dass die „three-flux“ FAPAR-Messung, die in

bisherigen Studien häufig bevorzugt wurde, nicht unbedingt weniger fehlerbehaftet sind, was sich insbesondere am tropischen Standort zeigte.

Die Abweichungen zwischen Bodenmessungen und dem aktuellen Sentinel-2 FAPAR-Produkt überschreiten auch unter Berücksichtigung von Unsicherheiten in der Messmethodik immer noch weitgehend die GCOS-Zielgenauigkeit an den jeweiligen Untersuchungsstandorten. So zeigte sich, dass das S2 FAPAR-Produkt die Bodenbeobachtungen an allen drei Studienstandorten systematisch unterschätzte (d.h. negative Werte für die mittlere relative Abweichung in Prozent). Die höchste Übereinstimmung wurde am borealen Standort Peace River mit einer mittleren relativen Abweichung von -13% ($R^2=0,67$) beobachtet. An den Standorten Graswang und Santa Rosa betrug die mittleren relativen Abweichungen jeweils -20% ($R^2=0,68$) bzw. -25% ($R^2=0,26$). Es wurde argumentiert, dass diese hohen Abweichungen auf eine Kombination sowohl des generisch ausgerichteten Algorithmus als auch der höheren Komplexität beider Ökosysteme zurückgeführt werden können. Es zeigte sich außerdem, dass die zeitlichen Aggregation der FAPAR-Bodendaten zum Vergleich mit S2 FAPAR-Produkt, das sich auf Tagesmittelwerte bezieht, gut überlegt sein sollte, da die Überschätzung von FAPAR während eines hohen Sonnenzenitwinkels in den Bodendaten die Validierungsergebnisse verzerren kann. Unter Berücksichtigung der Unsicherheiten der Bodendaten erfüllte das S2 FAPAR Produkt jedoch nur am boreale Untersuchungsstandort die Genauigkeitsanforderungen des GCOS. Insgesamt hat sich gezeigt, dass das S2 FAPAR-Produkt bereits gut zur Beurteilung der zeitlichen Variabilität von FAPAR geeignet ist, aber aufgrund der geringen Genauigkeit der absoluten Werte sind die Möglichkeiten, globale Produktionseffizienzmodelle zu speisen und globale Kohlenstoffbilanzen zu bewerten, derzeit begrenzt.

Die Genauigkeit von satellitengestützten FAPAR-Produkten ist abhängig von der Komplexität des beobachteten Waldökosystems. Die höchste Übereinstimmung zwischen satellitengestütztem FAPAR und Bodenmessungen, sowohl hinsichtlich der Darstellung von absolutem Werten als auch der räumlichen Variabilität, wurde am borealen Standort erzielt, für den die Komplexität des Ökosystems unter Berücksichtigung von Waldstrukturvariablen und Artenreichtum am geringsten ausfällt.

Die dargestellten Ergebnisse wurden in drei Publikationen dieser kumulativen Arbeit erarbeitet. Insgesamt schließt diese Arbeit eine Wissenslücke in der Darstellung des Zusammenspiels verschiedener Umgebungsbedingungen auf die Genauigkeit von situ FAPAR-Messungen. Da die Unsicherheiten von FAPAR nun unter Feldbedingungen quantifizierbar sind, sollten sie in zukünftigen Validierungsstudien auch berücksichtigt werden. In diesem Zusammenhang können die in dieser Arbeit genannten praktische Empfehlungen für die Durchführung von Bodenbeobachtungen zur Erstellung von Messprotokollen herangezogen werden, die dringend erforderlich sind, um globale satellitengestützte FAPAR-Beobachten validieren und zukünftig verbessern zu können.

Contents

| | |
|--|------|
| Acknowledgements | IV |
| Summary..... | V |
| Zusammenfassung..... | VIII |
| List of Figures | XII |
| List of Tables | XII |
| Abbreviations | XIII |
| 1 Introduction..... | 14 |
| 1.1 FAPAR and radiative transfer in forests | 16 |
| 1.2 Monitoring FAPAR in forests..... | 17 |
| 1.3 State-of-the-art: uncertainty of FAPAR observations..... | 19 |
| 1.3.1 Uncertainties of direct FAPAR measurements | 19 |
| 1.3.2 Validation of satellite derived FAPAR products with ground data ... | 21 |
| 2 Research design | 24 |
| 2.1 Aims and goals..... | 24 |
| 2.1.1 Assessing variability and uncertainty of in situ FAPAR with WSNs . | 24 |
| 2.1.2 Validating satellite derived FAPAR products considering uncertainty and ecosystem complexity | 25 |
| 2.2 Acquisition of ground data | 26 |
| 2.2.1 Natural environments of the study sites | 26 |
| 2.2.2 Experimental set-ups of WSNs | 30 |
| 3 Scientific Publications | 34 |
| 3.1 Paper I: Assessing the variability and uncertainty of two-flux FAPAR measurements in a conifer-dominated forest. In: Agricultural and Forest Meteorology | 34 |
| 3.2 Paper II: Accuracy assessment on the number of flux terms needed to estimate in situ fAPAR. In: International Journal of Applied Earth Observation and Geoinformation..... | 51 |
| 3.3 Paper III: Validation of Sentinel-2 FAPAR products using ground observations across three forest ecosystems. In: Remote Sensing of Environment..... | 67 |
| 4 Synthesis..... | 89 |
| 4.1 Conclusions | 89 |
| 4.2 Future Outlook | 93 |
| References | 94 |

List of Figures

| | |
|---|----|
| Figure 1: The energy budget of PAR fluxes in the soil-forest-atmosphere system | 17 |
| Figure 2. Locations of the three study sites. | 26 |
| Figure 3. The mixed-coniferous forest at the site Graswang | 27 |
| Figure 4. The boreal-deciduous forest at Peace River | 28 |
| Figure 5. The tropical dry forest at Santa Rosa | 28 |
| Figure 6. Hexagonal sampling scheme of WSN nodes. | 31 |
| Figure 7. Experimental set-ups of the three study sites for permanent FAPAR and meteorological observations. | 18 |

List of Tables

| | |
|--|----|
| Table 1. Species composition and forest structure variables of the study sites. | 29 |
| Table 2: Sampling protocols for measuring TOC PAR albedo and forest background albedo..... | 32 |
| Table 3: Practical recommendations for the development of sampling protocols for in situ FAPAR measurements with WSNs..... | 91 |

Abbreviations

ANN - artificial neuronal network
AVHRR - Advanced Very-High-Resolution Radiometer
DBH - diameter at breast height
DHP - digital hemispherical photography
ECV - essential climate variable
ESA - European Space Agency
FAPAR - fraction of absorbed photosynthetic active radiation
FCOVER - fractional cover
GCOS - Global Climate Observing System
GPP - global primary production
HCI - Holdridge complexity index
LAI - leaf area index
LiDAR - light detection and ranging
LUE - light use efficiency
LUT - lookup table
LM - linear model
MODIS - Medium Range Imaging Spectrometer
NDVI - normalized difference vegetation index
NIR - near infrared
NLM - non-linear model
NPP - net primary production
PAR - photosynthetic active radiation
PEM - production efficiency model
RTM - radiative transfer model
R² - coefficient of determination
S2 - Sentinel-2
SZA - solar zenith angle
TDF - tropical dry forest
TERENO - Terrestrial Environmental Observatories
TOC - top-of-canopy
UAV - unmanned aerial vehicle
VI - vegetation index
WSN - wireless sensor network

1 Introduction

The plants' ability to assimilate biomass from sunlight sets the boundary condition for the productivity of ecosystems. As the humanity's production of food, fiber, wood, grain fed to livestock and fuel depends on photosynthesis, it is crucial for society to understand, quantify and model global carbon balances (Ryu et al., 2019). With photosynthesis being the essential driver of the global carbon cycle and thus strongly coupled with the climate system (Heimann and Reichstein, 2008, Sellers et al., 2018), reliably assessed fluxes between the terrestrial biosphere and the atmosphere are necessary to develop strategies aiming at constraining carbon emissions and mitigate future climate change. Over the past decades, interdisciplinary efforts between plant physiology and earth system sciences in combination with new sensor technologies have improved the multiscale understanding of the productivity of ecosystems (e.g., Beer et al., 2010, Farquhar et al., 1980, Sellers et al., 1997). Further, the increasing availability of biophysical variables from numerous Earth Observation satellite missions has opened new opportunities to monitor and quantify the state and dynamics of vegetation (e.g., Disney et al., 2016, Myneni et al., 2002, Prince and Goward, 1995).

For understanding global carbon balances and assess ecosystem production, Running (2012) proposed net primary production (NPP) as a measurable planetary boundary and noted that for more than 30 years, global NPP exhibited an interannual variability of less than 2%. Further, it was noted that humans currently appropriated 38% of the global NPP, but 53% of global NPP were not harvestable (i.e., plant growth on root systems, preserved land or remote areas). Hence, it was concluded that less than 10% of total global NPP theoretically remained for additional future use by humans (Running, 2012). Thus, for a responsible and thus sustainable use of resources by humanity, precise estimates of NPP are crucial. NPP results from the difference between global primary production (GPP) and autotrophic respiration and can be assessed with production efficiency models (PEMs) (McCallum et al., 2009). PEMs are driven by satellite remote sensing observations, specifically long-term records on so-called essential climate variables (ECVs) (GCOS, 2011). According to GCOS (2011), an ECV is a physical, chemical or biological variable or a group of linked variables that critically contributes to the characterization of the Earth's climate. One of the terrestrial ECVs is FAPAR, the fraction of absorbed photosynthetic active radiation. By definition, FAPAR (often also written "fAPAR" or "fPAR") relates photosynthetic active radiation (PAR) to the absorption of plants within the wavelength region of 400 to 700 nm (Möttus et al., 2011). Thus, it is a dimensionless quantity, varying between zero (e.g. over deserts) and one, although this maximum value is never measured in practice because some of the incoming light is always reflected (GCOS, 2011). FAPAR is considered the primary source of information about vegetation status because it is directly related to plant development (Prince and Goward, 1995). For its key role in many ecosystem processes, FAPAR is a key variable in production efficiency modeling

as PEMs typically rely on the light use efficiency (LUE) model, which indicates that dry matter production is linearly related to PAR absorbed by the plant (Anderson et al., 2000, Monteith et al., 1977). Besides information on PAR and LUE, which is in turn dependent on surface and air temperature, vapor pressure deficit and soil moisture, accurate estimates on FAPAR are required (McCallum et al., 2009).

With the increasing availability of satellite remote sensing data, numerous algorithms have been developed to retrieve FAPAR from space (e.g., Baret et al., 2007, Carrer et al., 2013, Gitelson, 2019, Li et al., 2015, Liu et al., 2019, Liu et al., 2018, Myneni et al., 1997, Tao et al., 2016) to generate global FAPAR datasets (e.g., Baret et al., 2011, Disney et al., 2016, Li et al., 2017a, Myneni et al., 2002, Weiss and Baret, 2016). Besides using FAPAR datasets as inputs for PEMs, satellite derived FAPAR products have also been used for the monitoring of photosynthetic activity (Gobron et al., 2006), vegetation cover (Liu and Treitz, 2018, Mougin et al., 2014), biomass production (Meroni et al., 2014), the evolution of drought events (Cammalleri et al., 2019, Cammalleri and Vogt, 2018, Gobron et al., 2005, Peng et al., 2019), tree phenology (Gond et al., 1999, Verstraete et al., 2008) and variations of foliage chlorophyll (Zhang et al., 2013). Recently, numerous studies have evaluated available FAPAR products, reporting considerable discrepancies in terms of absolute values and temporal stability (D'Odorico et al., 2014, McCallum et al., 2010, Pickett-Heaps et al., 2014, Tao et al., 2015). However, accurate estimates of FAPAR are urgently needed, as discrepancies of FAPAR inputs have been identified as a major contributor to seasonal discrepancies in NPP (McCallum et al., 2009). Therefore, the GCOS has declared a target accuracy of 10% (or 0.05 in absolute values) as acceptable for FAPAR products in their overall guideline for the quality of ECVs (GCOS, 2011). To improve current retrieval methods for satellite derived FAPAR products, they highlighted that “further efforts need to be made to develop and promote standard protocols to measure FAPAR in the field” (GCOS, 2011). In addition to that, to improve global FAPAR estimates, studies have highlighted the need for uncertainty information considered in both remote sensing and in situ FAPAR products (D'Odorico et al., 2014, Gobron, 2015). Now, almost one decade after the release of the GCOS framework, FAPAR in situ data is still scarce and well-defined protocols are lacking (Ganguly et al., 2014, Gobron, 2015, Wang et al., 2016). In fact, recent studies admit that the significance of their validation has been compromised by the availability and quality of ground data (Li et al., 2015, Liu et al., 2019, Liu et al., 2018). It is therefore of great importance, to investigate new and efficient ways to acquire FAPAR ground data and quantify and assess uncertainties involved.

This cumulative thesis has been carried out to determine and quantify the contribution of related uncertainty sources included in FAPAR ground observations in forest ecosystems. It is organized as follows: In section 1.1, a brief summary of the radiative transfer processes relevant for the acquisition of FAPAR in forests is given. An overview on possible methods to acquire FAPAR in forests

is presented in section 1.2. Based on these fundamental concepts, section 1.3 discusses the sources of uncertainty of FAPAR that have been identified in ground observations so far and how uncertainty has been addressed in validation activities. Section 2 then presents the research design, including the specific aims and goals (2.1) as well as information on the experimental sites and set-ups for the acquisition of FAPAR ground data (2.2). The three peer-reviewed publications building up this cumulative thesis are presented in section 3. Finally, a conclusion of the main findings and an outlook on potential future work is given in section 4.

1.1 FAPAR and radiative transfer in forests

Plants use available PAR for photosynthesis from direct sunlight, scattered light, diffuse radiation and PAR reflected from the ground. Thus, FAPAR is determined by the radiation balance of PAR fluxes which includes the following quantities (**Fig. 1**): instantaneously incoming solar radiation in the PAR domain (PAR_{IN}), PAR reflectance at the TOC-level (R_{TOC}), PAR transmission down to surface-level (PAR_{TRANS}), PAR reflected by the soil (R_{SOIL}) as well as the contribution of horizontal fluxes entering and exiting a canopy target (PAR_H) (Chen, 1996, Widlowski, 2010). In relation to total incoming radiation, incoming PAR accounts to roughly 45%, but this ratio is dependent on altitude, water vapor content and solar zenith angle (SZA) (Larcher, 2003). Incoming PAR interacts with vegetation components, resulting in absorption, transmittance and multiple scattering processes. The radiative transfer equation for FAPAR is formulated as follows:

$$FAPAR = 1 - R_{TOC} - \frac{PAR_{TRANS}}{PAR_{IN}} (1 - R_{SOIL}) + PAR_H \quad (1)$$

where $FAPAR$ is the Fraction of Absorbed Photosynthetic Active Radiation, R_{TOC} the PAR reflectance at the TOC-level, PAR_{TRANS} the PAR transmission down to surface-level, R_{SOIL} the PAR reflected by the soil and PAR_H the contribution of horizontal fluxes (Widlowski, 2010).

Typically, leaves reflect about 6-10% of the incoming radiation while the soil reflects only about 2% thereof (Larcher, 2003). Most of the absorption take place in the uppermost part of the sun crown, depending on solar elevation and sky condition. Generally, diffuse radiation can reach deeper into the canopies (Leuchner et al., 2012, Ollinger, 2011). FAPAR ranges from 0.90 to 0.97 in dense broadleaf deciduous and coniferous evergreen forests during summer, and varies between 0.30 and 0.50 during the dormant period (Larcher, 2003). In general, the total area of foliage mainly determines how much incoming solar radiation is intercepted by the canopy, with the intensity exponentially decreasing with increasing leaf cover (Ollinger, 2011). Due to the complexity of scattering processes in forests, the relationship between forest structure and the variability of light transmittance is not linear so that simple forest structure variables such as stem density, basal area, tree height or diameter at breast height (DBH) are not always useful predictors of light availability in forest stands (Montgomery and Chazdon, 2001, Ollinger, 2011). Instead, depending on the arrangement of leaves within the stand (i.e.,

clumping) and the inclination of leaves towards incident radiation (i.e., leaf angle distribution), the attenuation and scattering of incoming radiation vary considerably (Hovi et al., 2017, Ollinger, 2011). Due to differences in direct and diffuse radiation field, canopy architecture, species composition and density as well as phenological development, FAPAR is a highly variable quantity across different forest ecosystems and within single forest stands both spatially and temporally (Baldocchi et al., 1986, Capers and Chazdon, 2004, Ross and Sulev, 2000).

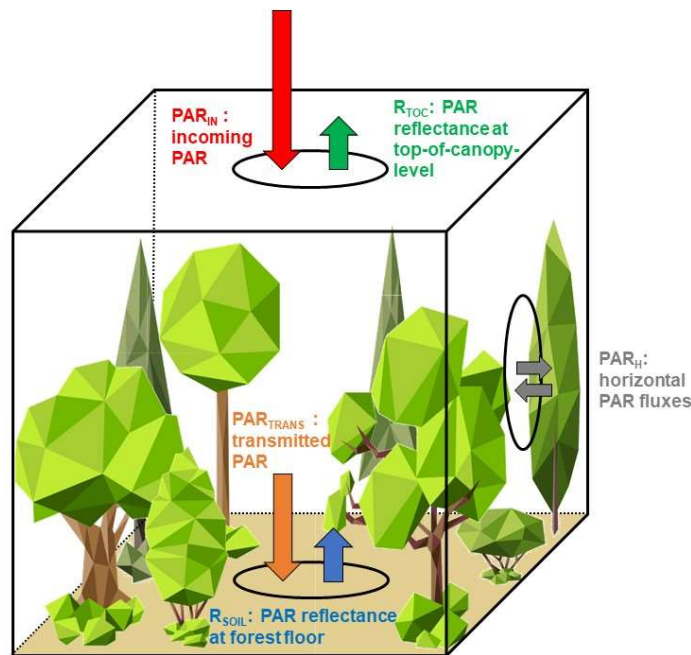


Figure 1: The energy budget of PAR fluxes in the soil-forest-atmosphere system. The sizes of the arrows for R_{TOC} , R_{SOIL} , PAR_{TRANS} and PAR_H correspond approximately to their respective proportion to PAR_{IN} .

1.2 Monitoring FAPAR in forests

FAPAR of forest ecosystems is derived from satellite remote sensing or acquired with ground measurements. Numerous approaches exist to estimate FAPAR from various satellite sensors, such as AVHRR (Sellers et al., 1994, Zhu et al., 2013), MODIS (Myneni et al., 2002, Myneni et al., 1997), MISR (Knyazikhin et al., 1998, Yu et al., 2000), SPOT/VEGETATION (Baret et al., 2011, Li et al., 2015), CYCLOPES (Baret et al., 2007) as well as Sentinel-2 (S2) (Weiss and Baret, 2016). Retrieval approaches can be classified into three groups (Ganguly et al., 2014): 1) linear models (LMs) or non-linear models (NLMs), 2) radiative transfer models (RTMs), 3) artificial neuronal networks (ANNs) and combinations thereof. With a long tradition in remote sensing, LM methods have been used to relate reflectance values or a vegetation index (VI) to FAPAR (Majasalmi and Rautiainen, 2016). As the relationship between the normalized difference vegetation index (NDVI) and FAPAR has often been reported to be close to linear (Myneni and Williams, 1994), NDVI has been widely used to derive FAPAR with LMs (e.g., Fensholt et al., 2004, Gitelson, 2019, Rahman and Lamb, 2016, Zhu et al., 2013). However, it is well-known that NDVI tends to saturate under conditions of moderate-to-high aboveground biomass due to

saturation of reflectance in the VIS and due to general limitations of the normalized difference approach (e.g., Sakowska et al., 2016). In general, the disadvantage of LMs or NLMs is that they are site-, time- and species-specific and thus poorly suited for large-scale operational use (Houborg et al., 2007, Wang and Tenhunen, 2004). In contrast, RTMs use physical equations to describe the light energy balance in the vegetation canopy to predict canopy reflectance and biophysical parameters, such as leaf area index (LAI) and FAPAR. For example, the MODIS FAPAR standard products (MCD15A2) are retrieved from reflectance data in red and near infrared (NIR) channels by using a lookup table (LUT) technique that is based on a radiative transfer equation (Myneni et al., 1997). More recently, RTMs based on the law of energy conservation (Fan et al., 2014) and spectral-invariant theory (Stenberg et al., 2013) have been proposed. The ANN methods are networks of relatively simple radiative transfer processes that require multiband reflectance and several auxiliary datasets to derive FAPAR from non-linear and non-parametric equation systems (Baret et al., 2007, Yuan et al., 2015). For example, the algorithm of the operational S2 FAPAR product was developed with an ANN trained over the PROSPECT+SAIL RTM on S2 TOC reflectance (Li et al., 2015, Weiss and Baret, 2016). As such, the algorithm is an evolution of FAPAR retrievals with ANNs applied for VEGETATION, MERIS, SPOT, and LANDSAT satellites (Li et al., 2015, Weiss and Baret, 2016).

Satellite derived FAPAR products require validation with ground data. Methods for monitoring FAPAR at the ground can be distinguished into direct and indirect methods. As direct FAPAR measurements are cost and labor intensive, FAPAR is often determined indirectly (Ganguly et al., 2014). Therefore, measurements of gap fraction retrieved from digital hemispherical photography (DHP) (Claverie et al., 2013, Djamai et al., 2019, Liu et al., 2018, Nestola et al., 2017), measurements of LAI (Fensholt et al., 2004, Pinty et al., 2011) or observations of fractional cover (FCOVER) are used (Liu and Treitz, 2018, Pickett-Heaps et al., 2014). In theory, direct FAPAR measurements would require measuring all PAR fluxes of the radiative transfer equation (Eq. 1). As measuring all five quantities is unfeasible with currently available measurement techniques, FAPAR is estimated by ignoring certain flux terms or making assumptions upon. Depending on the number of flux terms considered, direct FAPAR measurements are distinguished into two-, three- and four-flux estimates (Eq. 2-4) (Widlowski, 2010). The four-flux FAPAR estimate $FAPAR_4$ ignores horizontal PAR fluxes so that the remaining equation can be formulated as:

$$FAPAR_4 = 1 - R_{TOC} - \frac{PAR_{trans}}{PAR_{in}} (1 - R_{soil}) \quad (2)$$

The three-flux FAPAR estimates $FAPAR_{3(1)}$ and $FAPAR_{3(2)}$ make assumptions on PAR reflected from the background by either (1) assuming PAR reflected from the background to equal to TOC reflected PAR or by (2) ignoring PAR reflected from the background which results in the following to equations:

$$FAPAR_{3(1)} = (1 - R_{TOC}) \left(1 - \frac{PAR_{trans}}{PAR_{in}}\right) \quad (3.1)$$

$$FAPAR_{3(2)} = 1 - R_{TOC} - \frac{PAR_{trans}}{PAR_{in}} \quad (3.2)$$

Finally, the two-flux FAPAR $FAPAR_2$ estimate only considers incoming PAR and transmitted PAR through the canopy, which reduces the equation to:

$$FAPAR_2 = 1 - \frac{PAR_{trans}}{PAR_{in}} \quad (4)$$

Direct PAR measurements can be carried out with commercially available PAR sensors arranged in wireless sensor networks (WSNs) to ensure synchronized sampling. An overview on different available PAR sensors has been provided by (Akitsu et al., 2017).

1.3 State-of-the-art: uncertainty of FAPAR observations

In their framework for the quality assurance of ECVs, the GCOS demands that “further efforts need to be made to develop and promote standard protocols to measure FAPAR in the field” (GCOS, 2011). As a prerequisite for developing these “standard protocols”, sources of uncertainties need to be identified and quantified. In this regard, the following two sections report on the state-of-the art on the knowledge of uncertainties of direct in situ FAPAR observations and their previous consideration in satellite remote sensing validation activities.

1.3.1 Uncertainties of direct FAPAR measurements

The currently high discrepancies among different satellite derived FAPAR products highlight the value of independent ground data, which is, however, known to be affected by considerable uncertainties and bias¹. Bias of ground data may arise from the sampling scheme (referred to as sampling bias) and the estimating scheme (referred to as estimating bias), corresponding to the terms “statistical” and “systematic errors”, respectively. From an RTM simulation study of a tall open-canopy forest, Widlowski (2010) presented the first comprehensive investigation of the bias of in situ FAPAR observations. Several factors were investigated regarding their role for sampling bias: the size of the experimental domain of interest, the number of samples required for a given accuracy level as well as the geometry of the sampling scheme. As for domain size, Widlowski (2010) stated that the area for carrying out measurements should be greater than 30 x 30 m² as the contribution of horizontal fluxes became significant with reduced domain size. Regarding the number of samples needed for a given accuracy level, Widlowski (2010) recommended to perform measurements with at least 10 flux samples. Otherwise, the quality of FAPAR values may depend largely on the chance of locations of the sensors on the forest floor. Despite this recommendation, recent studies still rely on measurements with single or un-synchronized hand-held devices (e.g., using the SUNSCAN device by Liu et al. (2018)). As the variability of FAPAR is higher under clear sky conditions than under overcast sky conditions (Leuchner

¹ In this thesis, the term “bias” is defined as the difference between actual FAPAR and “true FAPAR”.

et al., 2011), a higher number of samples is required to reduce sampling bias. Regarding the geometry of the sampling scheme, Widlowski (2010) found that grid-based sampling schemes are largely equivalent to random sampling schemes and transect-based sampling schemes should be carried out at angles of 90° to the azimuth of the direct solar radiation source. This means that transect-based sampling schemes must be adapted to the solar position and are thus restricted to short-term experiments only (e.g., Liu et al., 2018).

There is only limited knowledge on the spatial dimension of sampling bias, but even less is known on its temporal dimension. As FAPAR changes already during a single day, the GCOS (2011) stated that “a detailed sampling strategy is required, covering [...] temporal intervals much smaller than the typical [...] revisit time of space-based sensors”. Validation studies often perform measurements during single dates only (e.g., Liu et al., 2018, Steinberg et al., 2006, Tao et al., 2015). However, to study the seasonal dynamics of FAPAR, permanent monitoring of FAPAR is necessary. Additionally, the existing literature lacks an investigation of the influence of different aggregation schemes and temporal sampling intervals. The influence of temporal aggregation scheme should be considered, particularly because most satellite derived FAPAR products are developed under the assumption that instantaneous FAPAR acquired at 10:00 or 14:00 local solar time is a good approximation of daily integrated FAPAR (Baret et al., 2011, Camacho et al., 2013, Martínez et al., 2013).

Regarding uncertainties of in situ FAPAR data arising from the estimating scheme, experiments with RTMs have demonstrated that the accuracy of FAPAR is affected by the applied estimation approach as well as certain environmental conditions (Kobayashi et al., 2014, Widlowski, 2010). So far, these theoretical findings lack validation in the field. Regarding the choice of estimating scheme, the two-flux FAPAR estimate was found to perform best in open forest canopies under typical summer conditions (Widlowski, 2010). This finding is in contrast with the current scientific practice of preferring the three-flux FAPAR estimate (e.g., D’Odorico et al., 2014, Nestola et al., 2017, Rankine et al., 2014, Senna et al., 2005, Tao et al., 2015). Given also the diversity of experimental set-ups used for direct FAPAR measurements, there seems to be no consensus on a preferred measurement approach, i.e. considering two-, three or four flux terms for the estimation of FAPAR. In addition, uncertainties of acquired ground data are not addressed in the existing studies (e.g., D’Odorico et al., 2014, Nestola et al., 2017, Rankine et al., 2014, Senna et al., 2005, Tao et al., 2015), which hampers the transparent validation of satellite derived FAPAR products.

Regarding the influence of environmental conditions, it has been shown that major sources of uncertainties are changes in illumination conditions, seasonal changes related to tree phenology (i.e. colored autumn leaves, LAI) and changes in forest background albedo, e.g. during the presence of snow. As for illumination conditions, it has been confirmed in field experiments (Leuchner et al., 2011) that FAPAR estimates are affected by a considerable bias under clear-sky conditions and high SZAs (i.e.,

above 60°). Recently, FAPAR observations carried out at boreal sites have confirmed that the overestimation bias of FAPAR under high SZA and clear-sky conditions is crucial especially at conifer-dominated forest stands (Majasalmi et al., 2017). Majasalmi et al. (2017) also demonstrated that the seasonal difference of FAPAR between instantaneous and daily averages of FAPAR at a boreal site crosses the threshold accuracy set by the GCOS (2011). Regarding the influence of colored leaves and forest background albedo, Widłowski (2010) simulated large influences on the accuracy of FAPAR which have not been investigated in field-conditions so far.

Overall, even though total PAR irradiance is typically monitored as part of the standard observation protocol at ecological and radiation research sites (e.g. FLUXNET, LTER, and SURFRAD), few of these sites generate all the necessary other measurements required to close the radiation budget and derive a reliable estimate of the canopy FAPAR at the scale of the observing space-borne sensor (GCOS, 2011). In addition to that, despite latest findings and progress in theoretical understanding of FAPAR and its uncertainties, there is still a lack of validation in the field to understand which sources of uncertainty need to be mainly considered in the development of the urgently needed sampling protocols. In the last decade, Wireless Sensors Networks (WSN) have opened new possibilities in environmental monitoring by ensuring cost and labor efficient options for multi-sensor and multi-temporal sampling also in forest ecosystems (Pastorello et al., 2011) that could reduce sampling and investigate estimating bias in field conditions. Although WSNs have already demonstrated their potential for FAPAR observations (Castro and Sanchez-Azofeifa, 2018, Nestola et al., 2017, Rankine et al., 2014), WSN with multiple PAR sensors have not yet been used to evaluate the uncertainties of ground data.

1.3.2 Validation of satellite derived FAPAR products with ground data

Numerous studies conducted with the goal of intercomparing and validating existing satellite derived FAPAR products confirm considerable discrepancies among FAPAR products (D'Odorico et al., 2014, Martínez et al., 2013, McCallum et al., 2010, Pickett-Heaps et al., 2014, Pinty et al., 2011, Tao et al., 2015). Product uncertainties of biophysical remote sensing products may generally arise from different sensors and their calibration, atmospheric correction, SZA correction, underlying land cover map or assumptions thereof and the general large variety of underlying retrieval algorithms (Ganguly et al., 2014). Generally, FAPAR products perform better in shrubland and crop sites, but are less accurate over forests for several reasons. As forests present a larger value range for FAPAR values, they also allow for more possible deviations among products (Tao et al., 2015). Another issue is that most algorithms are developed and validated over cropland, whereas FAPAR ground data in forests is still scarce (Gobron, 2015). And after all, forests with their complex architecture allow for more interactions with photons, which requires more sophisticated RTMs that are more difficult to parameterize. In

tropical forests, several canopy layers and the difficulty to obtain ground measurements further hampers the accurate retrieval of FAPAR, which is reflected in two recent studies highlighting that product discrepancies were particularly high in tropical forest regions (Xiao et al., 2018, Xu et al., 2018). Further, in their recent investigations on the spatio-temporal consistency and uncertainty of AVHRR and MODIS FAPAR products, Xu et al. (2018) note that more accurate ground measurements and better representation of different vegetation types indifferent LAI/FPAR ranges are required to refine the uncertainty evaluation of the AVHRR LAI/FPAR product. This conclusion is not new, as already the GCOS (2011) noted that “networks of in situ experimental sites should be expanded to become representative of a wider range of biomes”.

Thus, given the current situation, it is evident that satellite derived FAPAR products need to be validated intensively with ground data to improve retrieval algorithms and FAPAR estimates for forested areas. However, the literature review of existing FAPAR validation studies reveals the following major issues and deficits:

- 1) different underlying FAPAR definitions,
- 2) differences in spatial and temporal scale between ground data and satellite sensor,
- 3) limited temporal and spatial sampling of ground data as well as
- 4) unknown uncertainties of ground data and/or no discussion thereof.

Regarding deficit no. 1), it has to be noted that satellite derived FAPAR products which are based on RTM simulations often relate to absorption by green vegetation elements, referred to as “green FAPAR” (GCOS, 2011). In field conditions, PAR radiation is also attenuated by trunks and branches so that measurements obtained by PAR sensors consider the absorption of all vegetation components and thus relate to the concept of “total FAPAR” (GCOS, 2011). Another difference related to the definition of FAPAR that is often found in satellite derived FAPAR products relates to the direction of the illumination source. While “Black-sky FAPAR” considers only direct light as present under clear sky, “white-sky FAPAR” results from anisotropic radiation only under diffuse, overcast illumination conditions (GCOS, 2011). Typically, satellite derived FAPAR products only consider “black-sky FAPAR”, whereas direct PAR measurements also contain “white-sky FAPAR” (Liu et al., 2019).

Regarding deficit no. 2), i.e. the aggregation of ground data to sensor resolution, validation activities face the situation that FAPAR products have commonly been available at kilometric (e.g. GEOV1 FAPAR product from SPOT/VEGETATION) and hectometric (e.g. PROBA-V FAPAR product) spatial resolutions, thereby not matching the spatial resolution desired for agricultural and forestry applications (Clevers and Gitelson, 2013). Thus, efforts have been made to downscale products by using auxiliary optical remote sensing observations (e.g., Li et al., 2017a, Wang et al., 2016). With ESA’s S2

mission, a FAPAR product with decametric spatial resolution is available, thereby enabling the monitoring of vegetation productivity and dynamics on the scale of single forest stands (Drusch et al., 2012, Frampton et al., 2013). So far, the capabilities of S2 to capture spatial variability have not been validated in field conditions.

As for deficit no. 3), i.e. the issue of limited temporal and spatial sampling of ground data, recent studies aiming at the validation of remote sensing FAPAR products still rely on radiation measurements performed with only few radiation sensors, often acquired for several dates only. For example, the assessments of different satellite derived FAPAR products by D'Odorico et al. (2014) and Tao et al. (2015) relied on PAR flux measurements acquired at one single location per site, thereby limiting their outcome for a comprehensive validation. Recently, Liu et al. 2018 validated a new FAPAR retrieval method for various sensor systems using indirect FAPAR observations based on DHP in combination with direct FAPAR observations acquired with a handheld device (SUNSCAN) for two days. Gobron (2015) summarized that for the rare case that direct PAR measurements are available to generate a FAPAR ground reference, only few sites are equipped to perform a multi-temporal validation of satellite derived FAPAR products.

Regarding deficit no. 4), the abovementioned recent studies (i.e., D'Odorico et al., 2014, Liu et al., 2018, Tao et al., 2015) have neither assessed nor discussed uncertainties of ground data. Recently, Nestola et al. (2017) presented the results of a validation study of two satellite derived FAPAR products at a mountainous deciduous forest site and found high agreement of different ground measurement methods, e.g. between direct FAPAR observations based on PAR sensors and DHP measurements. However, it remains unclear whether the FAPAR ground data was affected by commonly known sources of uncertainties, such as the presence of colored leaves during the senescence period. Further, Liu et al. 2019 proposed a new FAPAR retrieval algorithm for “white-sky” FAPAR and validated only against indirect FAPAR observations, i.e. FAPAR retrieved from DHPs.

Given these deficits, it becomes evident that there is not only an urgent need for ground measurements and associated uncertainty information for different forest ecosystems, but also an urgent need for considering uncertainties of ground data in satellite validation activities.

2 Research design

Overall, this thesis assesses uncertainties of FAPAR based on direct PAR measurements in field conditions. The following sections present the aims and goals as well as the experimental approach for the acquisition of ground data with WSNs in three different forest ecosystems.

2.1 Aims and goals

It is of high importance to understand and consider uncertainties of FAPAR ground data in validation activities and global production efficiency modeling. This cumulative thesis consists of three scientific publications dealing with the assessment of FAPAR uncertainties and their influence on using FAPAR ground data for other purposes, such as the validation of satellite derived FAPAR products. In all three papers, it is generally hypothesized that uncertainties of FAPAR ground measurements can be assessed and quantified based on long-term observations with WSNs. The following subsections present the relevant underlying research questions investigated in the publications.

2.1.1 Assessing variability and uncertainty of in situ FAPAR with WSNs

FAPAR in forest ecosystems is known to be highly variable, as the light environment of a forest is characterized by a unique set-up of multiple transmittance, absorptance and reflectance processes resulting from both structural components such as crown architecture, stem density and leaf angles as well as biophysical properties of leaves (i.e., leaf pigments) (Möttus et al., 2011, Ollinger, 2011). Depending on the phenological status of the canopy, FAPAR presents substantial dynamics throughout the growing season. It is important to understand which portion of the variability observed can be attributed to sources of uncertainty which requires specific methods for the bias assessment. Thus, the first research question is:

Q1: How can the bias of instantaneous FAPAR observations be assessed in field conditions?

According to theoretical findings based on RTM simulations, crucial environmental variables are the illumination conditions under varying SZA and the ratio of diffuse-to-total incident radiation, leaf color and the occurrence of snow (Widlowski, 2010). However, other sources of uncertainty may play a role as well which have not been investigated in RTM simulations. In this regard, wind speed is considered as a potential source of uncertainty, as higher wind speeds may affect leaf angles and thus scattering and reflectance properties of the canopy (Ollinger, 2011, Roden, 2003). Thus, the second question to be investigated is:

Q2: Which environmental conditions are key sources of uncertainty in FAPAR ground observations?

It is important to investigate this question at different study sites with different species composition and forest structure as well as climatic constraints to derive more general conclusions and recommendations.

For developing sampling protocols, it is further important to understand the choice of estimating and sampling scheme and the feedbacks with certain environmental conditions identified as key sources of uncertainties and relate identified bias to the accuracy threshold set by the GCOS (2011). This leads to the following questions:

Q3: What is the bias of FAPAR ground observations associated to the estimating scheme?

Q4: What is the bias of FAPAR ground observations associated to sampling size?

2.1.2 Validating satellite derived FAPAR products considering uncertainty and ecosystem complexity

Recent satellite missions provide globally available information on the status and dynamics of vegetation. Several FAPAR products are available, such as the S2 FAPAR product (Weiss and Baret, 2016). As satellite derived FAPAR products rely on globally applicable, generalized retrieval methods and often do not have prior information on the land cover type, it is not surprising that deviations between ground data and satellite derived FAPAR product have been found to be relatively high, especially in forest ecosystems (D'Odorico et al., 2014, Tao et al., 2015, Xiao et al., 2019). Previous studies aiming at the validation of satellite derived FAPAR products have been compromised by not considering uncertainties of ground data. Instead, only few sensors are used (e.g., Tao et al., 2015) or in situ FAPAR estimates are based on indirect retrieval methods (Li et al., 2015, Liu et al., 2019). This is in contrast to several authors demanding to include uncertainties of ground data into the validation process (Ganguly et al., 2014, Gobron, 2015). Based on this deficit, the following research question can be formulated:

Q5: What is the bias between ground data and recent satellite derived FAPAR products under uncertainty constraints?

For the investigation of *Q5*, the recent S2 FAPAR lends itself to be validated with the FAPAR ground measurements, as its decametric spatial resolution enables the monitoring of single forest stands. In addition to that, validation activities have been restricted to agricultural areas so far (Djamai et al., 2019), which is a common limitation of FAPAR validation studies (e.g., Claverie et al., 2013, Gitelson, 2019). Another issue is that most validation studies have been carried out in temperate forests (McCallum et al., 2010, Nestola et al., 2017, Pinty et al., 2011) or semi-arid environments (Fensholt et al., 2004, Huemmrich et al., 2005, Martínez et al., 2013, Pickett-Heaps et al., 2014), also missing a comparison of different ecosystems.

In this regard, it must be stressed again that FAPAR is determined by ecosystem function and structure and will thus vary substantially across different ecosystems. This brings up the hypothesis that deviations between ground data and satellite derived product are higher with increasing ecosystem complexity, which in turn raises the following research question:

Q6: How does ecosystem complexity influence deviations between ground and satellite derived FAPAR estimates?

Ecosystem complexity can be characterized by both structural (e.g. stem density, basal area, tree height) and ecological characteristics (e.g., number of different species, number of horizontal layers) of a forest stand.

2.2 Acquisition of ground data

The results presented in this thesis were obtained based on direct PAR measurements collected at three different study sites. The following sections present the natural environment of these sites and the experimental set-ups. The initial implementation of WSNs, maintenance of sensors and data collection were carried out independently at the German site. For a comparison of ecosystems, existing data was made available thanks to the close cooperation with the University of Alberta.

2.2.1 Natural environments of the study sites

Investigations on the uncertainty of FAPAR in forests was carried out at three different forest sites (**Fig. 2**). Although one single forest stand comprises distinct structural characteristics, the selection of study sites oriented itself on the aim of representing temperate, boreal and tropical forest biomes, showing typical species composition for the respective ecosystem.

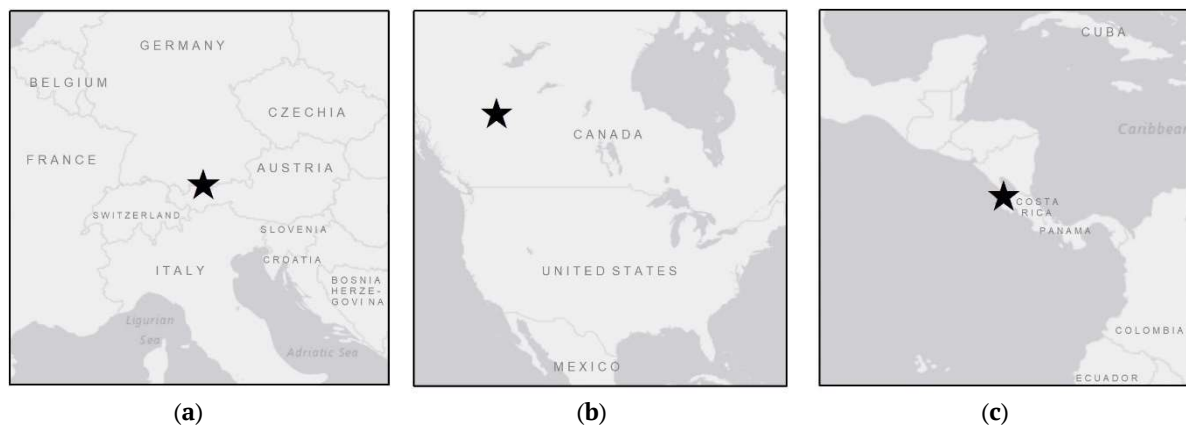


Figure 2. Locations of the three study sites; (a) “Graswang”, Germany, Central Europe, (b) “Peace River”, Alberta, Canada, North America and (c) “Santa Rosa”, Costa Rica, Central America.

The Central European site “Graswang” is located in Southern Germany, approx. 80 km south of Munich (**Fig. 2a**). The site is part of the pre-Alpine TERENO research project for long-term environmental research (Zacharias et al., 2011) and was equipped with a WSN for continuous FAPAR observations in 2015. The forest stand is situated in a sub-alpine valley at 900 m a.s.l., surrounded by slopes of the Ammer Mountains, reaching up to 2340 m. The climate is warm-temperate and fully humid (according to Köppen’s classification), with mean annual air temperature of 6.8 °C (monthly mean temperatures range from -2.5 °C in January to 15.6 °C in July) and mean annual precipitation

around 1,300 mm according to 5-year records of the meteorological station operated by KIT/IMK-IFU, Garmisch-Partenkirchen, Germany. Snowfall occurs typically between November and March, but snow-free episodes in winter are not unusual as well. The vegetation period spans from late April to the end of September. The site is located on flat terrain and comprises a mid-aged spruce-dominated mixed-coniferous forest (**Fig. 3a-b**). Species composition was inventoried in November 2015 (**Table 1**) and revealed that 82% of the basal area is occupied by Norway spruce (*Picea abies*), which is also the dominating species in South German commercial timberlands (Buras and Menzel, 2019). Deciduous species are European beech (*Fagus sylvatica*, 14%) and Sycamore maple (*Acer pseudoplatanus*, 4%). The forest floor is composed of several species of low-growing herbs (**Fig. 3c, Table 1**).

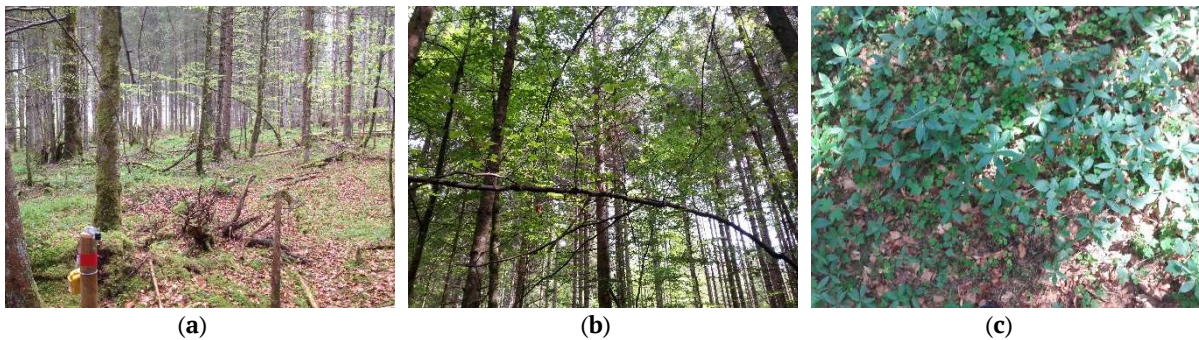


Figure 3. The mixed-coniferous forest at the site Graswang; (a) forest with WSN nodes in the foreground, (b) crown region around early vegetation period, (c) herbal vegetation at the forest floor in mid-summer.

The Peace River Environmental Monitoring Super Site is located in Northern Alberta, Canada (“Peace River”) in the forest biome of the so-called aspen parkland (**Fig. 4**). Here, the dominating tree is trembling aspen (*Populus tremuloides*), interspersed by other deciduous species. The site is part of the joint industry-research forestry region for Ecosystem Management Emulating Natural Disturbance (EMEND) for large-scale boreal forest preservation and harvest experimentation (Spence and Volney, 1999). The climate is humid continental with cool summers and cold winters, with a mean annual temperature of 1.2 °C and annual precipitation sum of 400 mm. Typically, first snowfall occurs around mid of October, building up a snow cover which lasts until the end of April. Consequently, the vegetation period is relatively short, usually starting not before mid of May and ending until the mid of September. The old-growth forest stand is characterized by two distinct vertical layers of vegetation (**Fig. 4a-b**) with an observed decreasing woody density with height (Rankine et al., 2014, Taheriazad et al., 2016). The first layer reaches up to 15-20 m in height and is composed predominantly of trembling aspen (**Table 1**). The understory canopy is composed of large shrubs such as green alder, reaching up to 4 m (**Fig. 4c, Table 1**).

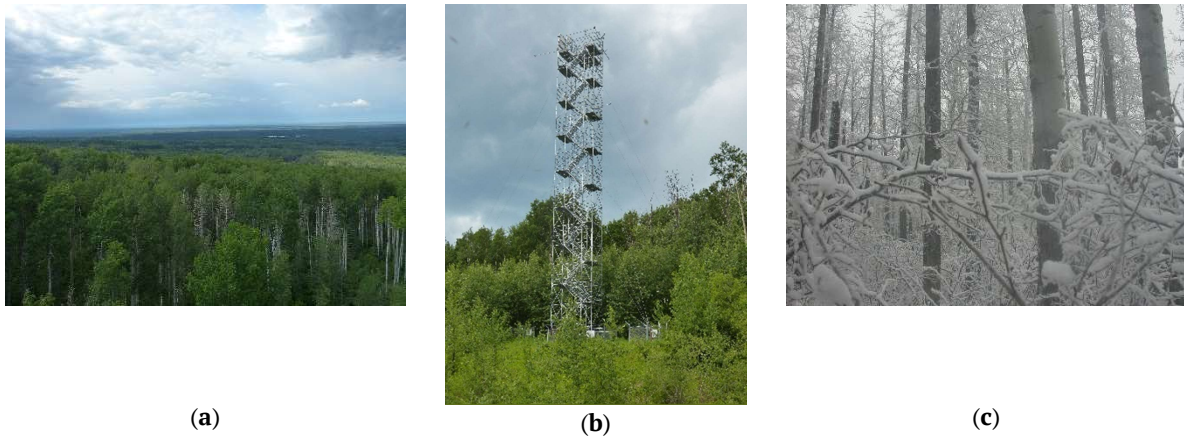


Figure 4. The boreal-deciduous forest at Peace River; (a) Panorama on the forest from the flux tower (photo by Philip Marzahn); (b) 30 m tall flux tower for meteorological observations (photo by Philip Marzahn); (c) understory vegetation in winter (photos (a) and (b) by Philip Marzahn).

The Santa Rosa National Park Environmental Monitoring Super Site (“Santa Rosa”) is located in the Province of Guanacaste, Costa Rica (**Fig. 1c**). The climate is tropical-monsoonal with a six-month dry season (December to May) and a highly variable precipitation ranging from 900 to 2,600 mm with the mean around 1,600 mm (Kalacska et al., 2004). Before the site received its actual status as a conservation area, deforestation has happened across the entire region due to clearing lands for pasture, agriculture, timber extraction and tourism (Sanchez-Azofeifa, 1996). As a result, various stages of 0-400-year-old secondary forest successions can be found (Li et al., 2017b). The sub-sites “Perros”, “Principe” and “Kakubari” are located in forests of an intermediate successional stage, which consists of two vertical canopy layers (**Fig. 5a-b**). The upper canopy layer is composed of fast growing deciduous species and few evergreen species (<10%) (Fig. 5b) whereas the understory consists of lianas and shade tolerant species (**Fig. 5b, Table 1**) (Arroyo-Mora et al., 2005). During the dry season, almost all vegetation species, except for a few evergreen species, lose their leaves and fall into a dormant stage (**Fig 5c**).

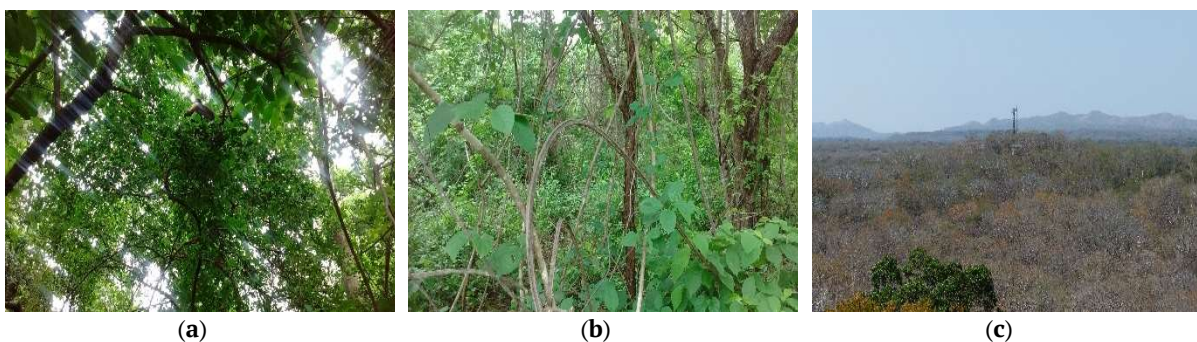


Figure 5. The tropical dry forest at Santa Rosa; (a) crown area (photo by Philip Marzahn), (b) understory vegetation with lianas (photo by Philip Marzahn), (c) forest during dry season with evergreen tree in the foreground and flux tower in the background (photo by Ralf Ludwig).

Table 1 shows that the sites differ substantially in both structural and biodiversity-related variables. To summarize the site characteristics for quantitative analysis, the Holdridge complexity

index (HCI) serves as a measure of ecosystem complexity (Holdridge and Tosi, 1967). It is calculated as follows:

$$HCI = \frac{HDBS}{10^3} (2)$$

where H is the mean tree height, D the number of stems per 0.1 ha, B the basal area in m² per ha and S the total number of tree species. A modified formula for secondary forests was used (Lugo et al., 1978), considering only trees with $DBH > 5$ cm.

Table 1. Species composition and forest structure variables of the study sites.

| Site names | Graswang, Germany | Peace River, Canada | Santa Rosa, Costa Rica |
|---|---|--|---|
| Geographical locations and altitudes | 47.5708° N, 11.0326° E; 864 m | 56.7441° N, 118.3439° W; 870 m | “Principe”: 10.8543° N, 85.6080° W; “Perros”: 10.8437° N, 85.6275° W; “Kakubari”: 10.8431° N, 5.616875° W; 300 m |
| Forest biomes | Temperate mixed-coniferous forest | Boreal-deciduous forest | Tropical dry forest |
| Trees: names of dominant species | <i>Picea abies</i> (Norway spruce), <i>Fagus sylvatica</i> (European beech), <i>Acer pseudoplatanus</i> (sycamore maple); | <i>Populus tremuloides</i> (trembling aspen), <i>Populus balsamifera</i> (balsam poplar); | <i>Luehea speciosa</i> , <i>Lonchocarpus minimiflorus</i> , <i>Guazuma ulmifolia</i> (bastard cedar), <i>Byrsonima crassifolia</i> ; |
| Understory vegetation: names of dominant species | <i>Oxalis acetosella</i> (wood sorrel), <i>Mercurialis perennis</i> (dog's mercury) | <i>Alnus crispa</i> (green alder), <i>Rosa acicularis</i> (prickly rose) | <i>Amphilophium paniculatum</i> , <i>Davila kunthii</i> , <i>Annona reticulata</i> , <i>Ocotea veraguensis</i> , <i>Hirtella racemosa</i> |
| Species density | 3 | 2 | 29 |
| S [no. of tree species (0.1 ha)⁻¹] | | | |

| | | | |
|--|------------|------------|------------|
| DBH: MEAN ± | 13.4 ± 9.5 | 30.6 ± 8.2 | 12.5 ± 7.8 |
| SD [cm] | | | |
| Stem Density D | 231 | 41 | 120 |
| [no. of stems | | | |
| (0.1 ha)⁻¹] | | | |
| Basal Area B | 4.8 | 2.4 | 1.9 |
| [m² (0.1 ha)⁻¹] | | | |
| Tree Height H: | 14.4 ± 2.3 | 26.5 ± 4.5 | 9.6 ± 3.2 |
| MEAN ± SD [m] | | | |
| HCI | 48 | 1 | 64 |

2.2.2 Experimental set-ups of WSNs

At all three sites, the experimental set-up for the FAPAR measurements consisted of WSNs of self-powered nodes (model ENV-Link-Mini-LXRS, LORD MicroStrain, Cary, NC, USA). The nodes were deployed in a hexagonal topology (**Fig. 6a**), as this sampling scheme was found to ensure signal quality and connectivity by maximizing the sensing area covered by a given number of nodes (Mortazavi et al., 2014, Younis and Akkaya, 2008). To account for the different footprint of PAR measurements, which is dependent on the height of the canopy, nodes were deployed in 20 m spacing at the sites Santa Rosa and Peace River and 10 m spacing at Graswang. The nodes were equipped with quantum PAR sensors (model SQ-110, Apogee, Logan, UT, USA; field of view 180°; uncertainty estimates: cosine response ±5% at 75° SZA, temperature response 0.06±0.06% per °C, calibration uncertainty ±5% and non-stability <2% y⁻¹). The PAR sensors were mounted at 1.3 m height on wooden poles and aimed upward to either measure incoming PAR (PAR_{in}) outside the forests or transmitted PAR (PAR_{trans}) inside the forests (**Fig. 6b**).

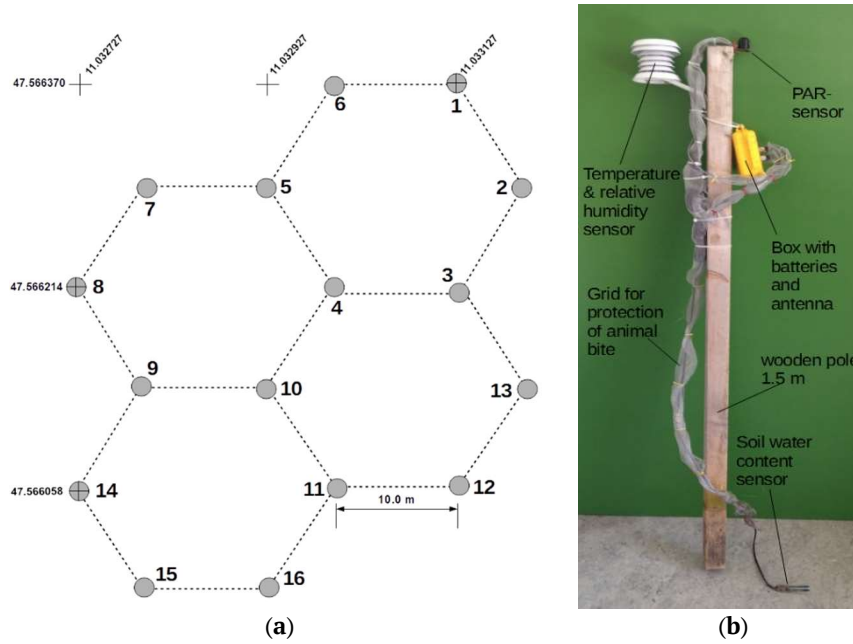


Figure 6. Hexagonal sampling scheme of WSN nodes; (a) Example of hexagonal sampling scheme with 10 m spacing between the nodes at Graswang; (b) WSN node with PAR sensor and other environmental sensors (not used in this thesis).

Figure 7 illustrates the experimental settings of the sites. At Graswang, the reference sensor for PAR_{in} was placed on open grassland (Fig. 7a), while it was measured right above the WSN on towers at Peace River and Santa Rosa (Fig. 7b-c). Overall, PAR_{trans} was acquired with 16 sensors at Graswang, 22 sensors at Peace River and 35 sensors at Santa Rosa (19 at “Kakubari”, 10 at “Principe” and 6 at “Perros”), respectively. While measurements of PAR_{in} and PAR_{trans} are essential to calculate the two-flux FAPAR estimate, observations of TOC PAR albedo (R_{TOC}) are required to calculate three- and four-flux FAPAR estimates. For obtaining four-flux FAPAR estimates, measurements of PAR reflected from the forest soil are needed to calculate forest background albedo (R_{soil}) are needed. Table 2 provides an overview on how R_{TOC} and R_{soil} were acquired at the three sites.

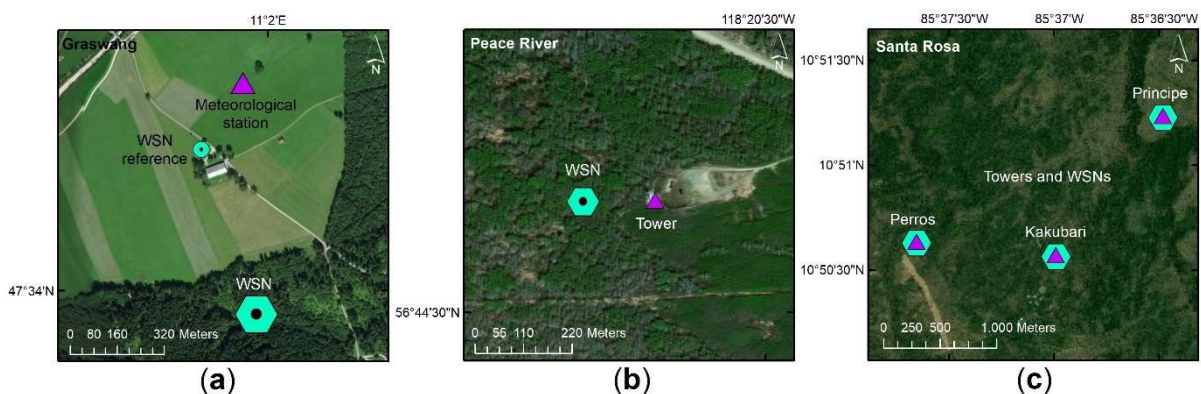


Figure 7. Experimental set-ups of the three study sites for permanent FAPAR and meteorological observations. Hexagonal symbols refer to WSNs, triangles refer to towers with meteorological stations; (a) Graswang with reference node and meteorological station on open grassland, (b) Peace River with reference sensor and meteorological station on a tower and (c) Santa Rosa with the three sub-sites “Perros”, “Principe” and “Kakubari”, each of them equipped with reference sensor and meteorological station mounted on towers.

Table 2: Sampling protocols for measuring TOC PAR albedo and forest background albedo.

| Site names | Graswang | Peace River | Santa Rosa |
|------------|---|---|--|
| R_{TOC} | <ul style="list-style-type: none"> approximated with UAV flights twice per year to cover the partly and fully foliated vegetation periods two opposite quantum PAR sensors connected to an environmental monitoring node hexacopter model DJI F550 Flame Wheel, DJI Innovations, Shenzhen, China aggregation of the 10 min flight time based on 1 Hz PAR measurements | <ul style="list-style-type: none"> measured every 10 min 30 m high flux tower two opposite quantum PAR sensors connected to an environmental monitoring node synchronized with all WSN observations | <ul style="list-style-type: none"> measured every 10 min 30 m high flux towers two opposite quantum PAR sensors connected to an environmental monitoring node synchronized with all WSN observations |
| R_{soil} | <ul style="list-style-type: none"> measured every 10 min upward and downward directed sensors for PAR_{trans} and PAR_{soil} mounted at 3 m height, covered in plastic boxes | <ul style="list-style-type: none"> measured every 10 min downward directed PAR_{soil} sensors mounted at nodes for PAR_{trans} | <ul style="list-style-type: none"> measured every 10 min downward directed PAR_{soil} sensors mounted at nodes for PAR_{trans} |

The configuration for all nodes of the WSN and data download were carried out with a portable receiver (frequencies ranging from 2.405 GHz to 2.480 GHz) equipped with USB interface (model WSDA-Base-104 USB Base Station, MicroStrain, Cary, NC, USA) to connect to a portable computer equipped with the software “Node Commander” (version 2.17.0, LORD MicroStrain, Cary, NC, USA). At Peace River and Santa Rosa, data aggregation was operationally carried out with a base station equipped with an outdoor transceiver (model WSDA-1000 Wireless Sensor Data Aggregator, MicroStrain, Cary, NC, USA) positioned on the towers. Sensors were configured to measure instantaneous PAR every 10 min synchronously (~1 ns). Data was uploaded to “Enviro-Net” (<http://www.enviro-net.org/>), a web platform for sensor data management, near real-time visualization and analysis (Pastorello et al., 2011).

3 Scientific Publications

This cumulative thesis comprises three peer-reviewed scientific publications in international journals. Two of these three publications have been published, one is currently under review. The following sub-sections list the publications with information on the respective journal, its 5-year impact factor and the status of publishing. Additionally, the contribution of each author is explained and short information on the content and its relation to the research questions presented in section 2.1 is given. Thus, the papers are not listed in chronological order, but rather follow the order of underlying research questions. Paper no. I presents an assessment of the variability and uncertainty of two-flux FAPAR observations in a conifer-dominated forest in the Bavarian Alps, Germany. The paper focuses on one site and on FAPAR estimating approach (i.e., two-flux approach) only, as sources of variability and uncertainty with respect to phenological and meteorological conditions are presented in detail. Paper no. II investigates these identified sources of uncertainty in a more generalized way for three different ecosystems: the Graswang site, a boreal-deciduous forest in Northern Alberta, Canada, and a tropical dry forest in Guanacaste, Costa Rica. In addition, the paper reflects upon the uncertainties of three- and four-flux estimates. Paper no. III then assesses and discusses the current accuracy of a satellite derived FAPAR product (S2) considering the identified sources of uncertainties at the abovementioned three ecosystems.

3.1 Paper I: Assessing the variability and uncertainty of two-flux FAPAR measurements in a conifer-dominated forest. In: Agricultural and Forest Meteorology

Citation: BIRGITTA PUTZENLECHNER, PHILIP MARZAHN, RALF KIESE, RALF LUDWIG AND ARTURO SÁNCHEZ-AZOFEIFA (2019): *Assessing the variability and uncertainty of two-flux FAPAR measurements in a conifer-dominated forest*. Agricultural and Forest Meteorology, 264, 149-163.

Journal: Agricultural and Forest Meteorology (Elsevier)

5-year Impact Factor: 5.317

Status: published

Research outline: This article focuses on the assessment of spatial variability and uncertainty of two-flux FAPAR measurements at the TERENO site Graswang. This site was chosen as it is easily accessible for regular maintenance activities so that data gaps could not hamper high resolution time series which was required for the detailed analysis of the influence of environmental conditions on the uncertainty of FAPAR. In addition to that, the TERENO meteorological station offered not only general meteorological observations of high quality (i.e., no data gaps due to easy maintenance access), but also observations of diffuse radiation which was indispensable for the methodological approach,

requiring the ratio of diffuse-to-total incident radiation. The two-flux estimate was chosen as previous investigations with RTM simulations (Widlowski, 2010) have identified its uncertainties to be acceptable under typical summer conditions. In addition to that, no measurements from a tower are required, so that it is a cost and labor efficient estimating approach that is thus relatively easy to implement in future studies aiming at the validation of satellite derived FAPAR products. The investigations of FAPAR uncertainties were carried out with respect to different environmental conditions. Specifically, influences of illumination conditions with SZA and the ratio of diffuse-to-total incident radiation, wind speed, leaf color and snow coverage on the variability and uncertainty of two-flux FAPAR estimates were assessed. The methodological approach follows the assumption that FAPAR acquired under diffuse light conditions is close to “true FAPAR” as it is not influenced by the SZA. To reveal the uncertainty of the two-flux FAPAR measurements, the difference between FAPAR acquired under diffuse light conditions and two-flux FAPAR acquired during a certain environmental condition (e.g., high SZA) was calculated. A positive (negative) value obtained from this difference was interpreted as an indication for an underestimation (overestimation) of “true” FAPAR by the two-flux FAPAR estimate. The article investigates the following research questions:

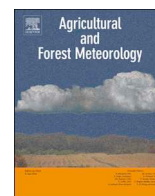
Q1: How can the bias of instantaneous FAPAR observations be assessed in field-conditions?

Q2: Which environmental conditions are key sources of uncertainty in FAPAR ground observations?

Q3: What is the bias of FAPAR ground observations associated to sample sizes?

Scientific value: The paper adds to the investigation of common sources of uncertainty that are known from RTM simulations but have not been validated in field-conditions before. In addition to that, the influence of wind speed was investigated for the first time. By demonstrating the potential of permanent WSN monitoring activities to ensure multi-year FAPAR observations with associated uncertainty information, the paper paves the way for expanding the investigations of FAPAR uncertainties using WSNs to other FAPAR estimate schemes and ecosystems.

Authors' contributions: The study conception was developed by BP and AS-A. Methodology was developed by BP and PM. Acquisition, analysis and interpretation of data was carried out by BP. Data curation was done by BP and AS-A. Funding was acquired by RL, RK and AS-A. Project administration was carried out by RK, RL, PM and BP. Supervision was given by RL, RK and AS-A. The original draft was written by BP, while all other authors commented and revised critically and thus contributed to the final draft.



Assessing the variability and uncertainty of two-flux FAPAR measurements in a conifer-dominated forest

Birgitta Putzenlechner^{a,*}, Philip Marzahn^a, Ralf Kiese^b, Ralf Ludwig^a, Arturo Sanchez-Azofeifa^c

^a Department of Geography, Ludwig-Maximilians Universität, Luisenstr. 37, 80333, Munich, Germany

^b Institute of Meteorology and Climate Research Atmospheric Environmental Research (IMK-IFU), Karlsruhe Institute of Technology, Kreuzeckbahnstr. 19, 82467, Garmisch-Partenkirchen, Germany

^c Earth and Atmospheric Sciences Department, University of Alberta, 1-26 Earth Sciences Building, Edmonton, T6G2E3, Alberta, Canada

ARTICLE INFO

Keywords:

FAPAR
Fraction of absorbed photosynthetically active radiation
Forest
Spatio-temporal variability
In-situ data
Uncertainty

ABSTRACT

The estimation of the Fraction of Absorbed Active Radiation (FAPAR) and its uncertainties is key for understanding global carbon balances. This work investigates the variability and associated uncertainties of in-situ two-flux FAPAR observations attributed to changes in phenological and meteorological conditions. Specifically, we assessed influences of illumination conditions with solar zenith angle and the ratio of diffuse-to-total incident radiation, wind speed, leaf color and snow coverage on the variability of two-flux FAPAR. We assumed FAPAR acquired under diffuse light conditions to be closest to “true” FAPAR as it is not influenced by the solar zenith angle. To reveal the uncertainty of the two-flux FAPAR measurements, we investigated the difference ($\Delta_{\text{two-flux}}$) between FAPAR acquired under diffuse light conditions and two-flux FAPAR acquired during a certain environmental condition (e.g. large solar zenith angle). A positive (negative) value obtained from this difference was interpreted as an indication for an underestimation (overestimation) of “true” FAPAR by the two-flux FAPAR estimate, as found in previously investigations with canopy radiative transfer models (RTM).

Therefore, permanent PAR measurements were carried out 2015–2017 in a sub-alpine, spruce-dominated forest in Southern Germany using a Wireless Sensor Network (WSN). FAPAR observations exhibited considerable seasonal variability (0.89 to 0.99 ± 0.03) despite the dominance of evergreen spruces. The in-situ observations confirm significant overestimation of FAPAR by up to 0.06 under solar zenith angles above 60° and by up to 0.05 during the presence of colored autumn leaves, similarly to the results obtained from previous studies with canopy RTMs. Additionally, our results indicate an effect of wind speed which we consider crucial at sites where high wind speeds occur more frequently. Overall, this study shows the potential of permanent WSN monitoring activities to ensure multi-year FAPAR observations with associated uncertainty information that are demanded to validate satellite-derived FAPAR products in forest ecosystems.

1. Introduction

The state and dynamics of plants interacting with sunlight play an essential role in the global carbon balance. The Fraction of Absorbed Photosynthetically Active Radiation (FAPAR) relates PAR (400–700 nm) to the absorption of plants and represents a key variable for many ecosystem processes (Möztus et al., 2011). Due to its importance for ecosystem research (Gower et al., 1999; Prince and Goward, 1995), FAPAR is considered as an essential climate variable (ECV) by the Global Climate Observing System (GCOS, 2011). With the increasing availability of satellite imagery, algorithms have been developed to derive FAPAR from vegetation reflectance properties based on canopy radiative transfer models (RTM), artificial neuronal

networks, lookup tables or their combination (e.g. Baret et al., 2007; Carrer et al., 2013; Li et al., 2015; Myneni et al., 1997; Tao et al., 2016). Several studies have evaluated available FAPAR products, showing considerable discrepancies that exceed the accuracy target of 0.05 (or 10%) for FAPAR products set by GCOS (2011) particularly in forest ecosystems (Disney et al., 2016; D’Odorico et al., 2014; McCallum et al., 2010; Pickett-Heaps et al., 2014; Tao et al., 2015). To improve global FAPAR estimates, studies have highlighted the need for uncertainty information considered in both remote sensing and in-situ FAPAR products (e.g. D’Odorico et al., 2014). However, ground data is scarce, and in addition to that, well-defined measurement protocols are still lacking (Ganguly et al., 2014; Wang et al., 2016).

In principal, FAPAR is determined by the radiation balance equation

* Corresponding author.

E-mail address: b.putzenlechner@igf.geo.uni-muenchen.de (B. Putzenlechner).

which relates the following quantities: instantaneously incoming solar radiation in the PAR domain, PAR reflectance at the top-of-canopy-level, PAR transmission down to surface-level, PAR albedo of the surface as well as the contribution of horizontal fluxes entering and exiting the canopy target (Chen, 1996; Widlowski, 2010). In field conditions, direct measurements of all these quantities would require sophisticated, cost and labor-expensive experimental set-ups. Thus, certain terms of the equation are usually ignored or approximated, resulting in so-called FAPAR estimates that are differentiated by the number of flux contributions considered. The so-called two-flux FAPAR estimate, for example, ignores all terms except incoming and transmitted PAR (Appendix A, Eq. (A.1)).

Several studies have given direct FAPAR estimates based on different approaches, with a large variety of experimental set-ups and sensor systems being used (Awal et al., 2006; Huemmrich et al., 2005; Nestola et al., 2017; Senna et al., 2005; Serrano et al., 2000; Steinberg et al., 2006; Ter-Mikaelian et al., 1999). Instead of estimating the radiative transfer equation by direct PAR measurements, FAPAR is also often determined indirectly using gap fraction retrieved from hemispherical photography (Li et al., 2015), measurements of LAI (Fensholt et al., 2004; Pinty et al., 2011) or observations of fractional cover (Pickett-Heaps et al., 2014). More recently, modeling approaches have been preferred (Hovi et al., 2017; Majasalmi et al., 2017; Stenberg et al., 2016). Even though it is well-known that spatial variability of light is particularly high in forest ecosystems (Baldocchi et al., 1986; Leuchner et al., 2011; Ollinger, 2011; Ross et al., 1998), most studies aiming at the validation of remote sensing FAPAR products rely on radiation measurements performed with only few sensors, and do not provide information on the uncertainty of the ground estimates (e.g. D'Odorico et al., 2014; Tao et al., 2015).

Considering the need for FAPAR in-situ observations from a larger number of flux sensors, the two-flux FAPAR estimate has the advantage of being relatively cost and labor efficient as i.e. the installation of a tower for measuring top-of-canopy reflectance is not required. However, regarding uncertainties of in-situ FAPAR data obtained from direct radiation measurements, experiments with RTMs have demonstrated that accuracy is considerably affected depending on actual environmental conditions and estimation method being used (Kobayashi et al., 2014; Widlowski, 2010). Widlowski (2010) showed in an RTM experiment in open-canopy forest that the accuracy of FAPAR estimates, also the two-flux estimate, is mainly affected by changes in solar zenith angle (SZA), seasonal changes related to tree phenology (i.e. colored autumn leaves, LAI) and changes in forest background albedo during the presence of snow. For FAPAR acquired under diffuse (anisotropic) light conditions, also known as “white-sky FAPAR”, for example, the influence of SZA has been found to be negligible, in contrast to FAPAR obtained under clear sky conditions (“black-sky FAPAR”), as FAPAR estimates that ignore lateral light fluxes (i.e. two- and three flux approaches) miss out a significant portion of the light field under large SZAs (Widlowski, 2010). As another example, Widlowski (2010) showed that bright autumn leaves lead to an “overestimation bias” of the two-flux FAPAR estimate as the top-of-canopy reflectance is increased so that the difference between “true” FAPAR (considering all flux components) and the two-flux FAPAR estimate yielded in a negative value. Recently, Majasalmi et al. (2017) demonstrated that the seasonal difference of FAPAR (simulated based on photon recollision probability) between instantaneous and daily averages of FAPAR at a boreal site crosses the threshold accuracy set by GCOS (2011). Despite these latest findings and progress in theoretical understanding of FAPAR and its uncertainties, there is still a lack of validation in the field to understand which sources of uncertainty need to be mainly considered in the development of urgently needed sampling protocols.

In this study, it is hypothesized that varying meteorological and phenological conditions and their influence on the two-flux FAPAR estimate can be assessed and quantified based on field observations. Therefore, our specific objectives were to (a) characterize overall

spatial and temporal variability of two-flux FAPAR observations in a conifer-dominated forest, (b) assess the influence of illumination conditions with (1) ratio of diffuse-to-total incident radiation d/Q and (2) SZA, (3) wind speed (WS), (4) leaf color (LC) as well as (5) snow coverage (SC) and to (c) assess their relevance as sources of uncertainty. With the exception of wind speed, all variables are known to be sources of variability for two-flux FAPAR observations (Widlowski, 2010). With transmittance and scattering within canopies being strongly influenced by leaf angle orientation (Ollinger, 2011), we additionally investigated whether there is an influence of wind speed on FAPAR.

To ensure multiple, continuous and synchronized PAR measurements, we used a Wireless Sensor Network (WSN) as monitoring technology (Pastorello et al., 2011). In a sub-alpine conifer-dominated forest site in Southern Germany, we carried out measurements of incoming and transmitted PAR to calculate the two-flux FAPAR estimate. Meteorological and phenological information were gathered by an automated camera and a meteorological station. The observation system for instantaneous FAPAR ensured accurate and long-term PAR measurements to reveal the uncertainty underlying two-flux FAPAR monitoring in conifer-dominated forests.

2. Materials and methods

2.1. Study site

Measurements of FAPAR were carried out in a spruce-dominated forest stand located approximately 90 km southwest of Munich, Germany (47.5708°N 11.0326°E, 864 m a.s.l.) (Fig. 1). The site is part of the pre-Alpine TERENO project (Terrestrial Environmental Observatories) aimed to conduct long-term environmental research on the impacts of climate change on terrestrial ecosystems in the Ammer river catchment in Upper Bavaria, Germany (Zacharias et al., 2011). The site is situated on a flat alluvial plain in a sub-alpine valley surrounded by the slopes of the Ammer Mountains reaching up to 1800 m altitude. The climate is characterized by warm and humid summers and cool snowy winters (annual precipitation: approx. 1300 mm; mean air temperature: 6.8 °C, ranging from −2.5 °C in January to 15.6 °C in July).

2.2. Forest structure and composition

In December 2015, a forest inventory was carried out to determine species and diameter at breast height (DBH) of all trees (DBH > 3 cm) within the WSN including a buffer of 10 m around the outer sensor locations. The average tree height of the mid-aged forest was estimated to 15 m, the species composition survey resulted in 82% Norway spruce (*Picea abies*), 14% European beech (*Fagus sylvatica*) and 4% Sycamore maple (*Acer pseudoplatanus*). Basal area and stem density of the sampled plot accounted for 47.9 m² ha^{−1} and 2309 stems ha^{−1}, respectively. Table 1 shows overall basal area and percentages of basal area of different tree species in the 10 m-surrounding of 16 sensor locations in the forest. Basal area of all trees in buffer zones varies from 37.9 to 68.3 m² ha^{−1}, basal area of deciduous trees ranges from 3 to 34%.

2.3. Experimental set-up for FAPAR observations

The set-up for the two-flux FAPAR measurements consisted of a WSN of self-powered nodes (model ENV-Link-Mini-LXRS, LORD MicroStrain, Cary, NC, USA). Each node was equipped with a commercially available quantum PAR sensor (model SQ-110, Apogee, Logan, UT, USA; field of view 180°) aimed upward to measure incoming PAR (PAR_{in}) outside the forest and transmitted PAR (PAR_{trans}) inside the forest. Sensors were mounted on wooden poles using angle connectors to ensure correct leveling and at 1.3 m height above the ground to avoid influences from understory vegetation. Product specific uncertainty estimates for the PAR sensors are given by the manufacturer as follows: cosine response ± 5% at 75° SZA, temperature response

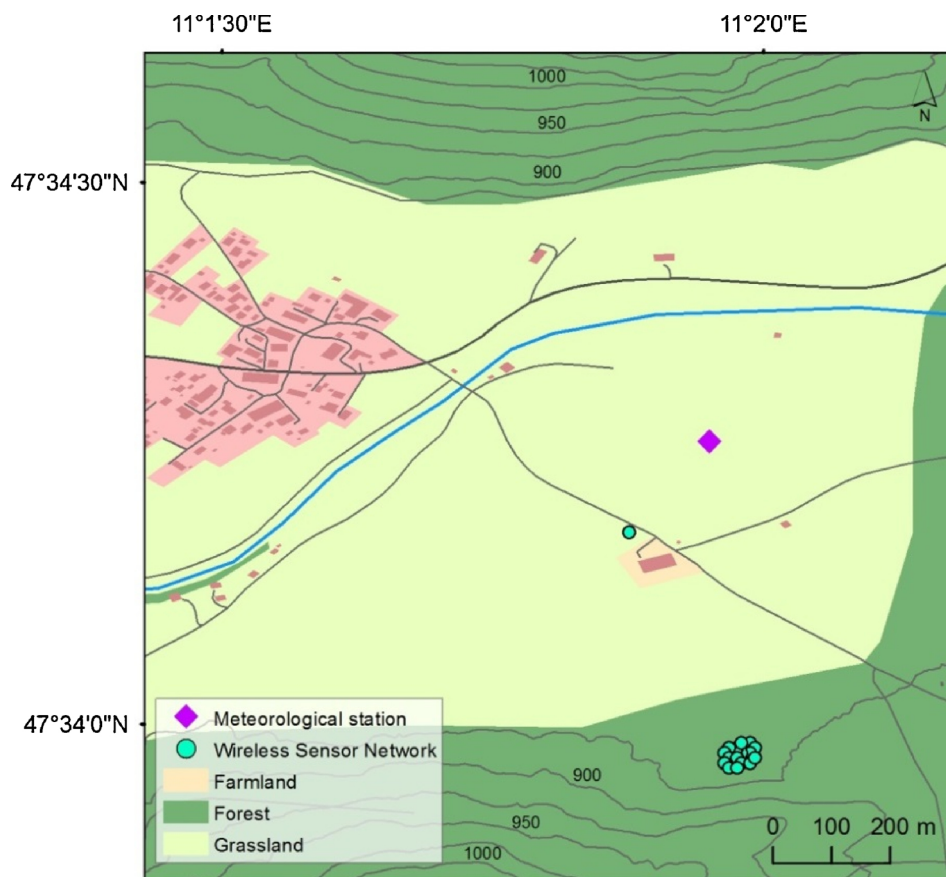


Fig. 1. Location of the experimental site. Terrain information was taken from the DEM provided by the Free State of Bavaria, Germany; Land cover information was taken from Open Street Map.

Table 1

Basal area and percentage of basal areas of different tree species in the 10 m-surrounding of each sensor location in the forest.

| Position ID in WSN | Basal area [m ² ha ⁻¹] | Basal area of spruces [%] | Basal area of beeches [%] | Basal area of maples [%] |
|--------------------|---|---------------------------|---------------------------|--------------------------|
| 1 | 47.1 | 94.3 | 5.7 | 0.0 |
| 2 | 68.3 | 94.3 | 5.7 | 0.0 |
| 3 | 53.6 | 96.7 | 3.3 | 0.0 |
| 4 | 40.3 | 95.5 | 4.5 | 0.0 |
| 5 | 52.8 | 79.2 | 20.8 | 0.0 |
| 6 | 41.7 | 65.9 | 7.3 | 26.8 |
| 7 | 51.7 | 82.1 | 17.4 | 0.5 |
| 8 | 42.0 | 93.1 | 6.2 | 0.6 |
| 9 | 46.6 | 91.9 | 8.1 | 0.0 |
| 10 | 61.5 | 82.0 | 17.1 | 0.9 |
| 11 | 67.2 | 81.4 | 15.6 | 3.0 |
| 12 | 37.9 | 77.7 | 19.5 | 2.7 |
| 13 | 39.0 | 95.1 | 4.9 | 0.0 |
| 14 | 48.3 | 92.2 | 7.8 | 0.0 |
| 15 | 50.4 | 79.4 | 19.0 | 1.6 |
| 16 | 47.3 | 81.7 | 13.5 | 4.8 |

0.06 ± 0.06% per °C, calibration uncertainty ± 5% and non-stability < 2% y⁻¹. Regarding the purpose of using PAR measurements of the SQ-110 PAR product for FAPAR estimates, Akitsu et al. (2017) found a difference of -7.7 × 10⁻⁴ from a reference standard FAPAR. Thus, this accuracy satisfies the threshold of 10% set by GCOS (2011) when used for not-partially cloudy sky under summer conditions.

PAR_{in} was measured approx. 300 m outside the forest in open grassland and PAR_{trans} with 16 PAR sensors with 10 m-spacing inside the forest (Fig. 2). The location and size of the area for the observations of PAR_{trans} was selected by the following considerations: To limit

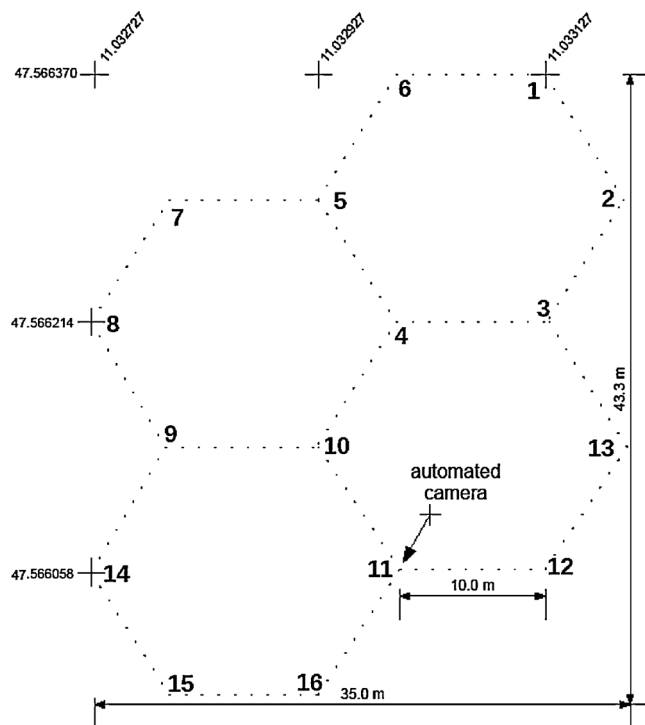


Fig. 2. Experimental set-up for PAR observations in the forest. Each of the 16 nodes was equipped with a PAR sensor pointed upward at 1.3 m height to perform synchronized measurements of transmitted PAR every 10 min. The viewing direction of the automated camera is indicated with an arrow.

influences of lateral light fluxes, we a) installed the nodes at least 80 m away from the forest edge to avoid edge effects and b) chose a domain of interest not smaller than $30 \times 30 \text{ m}^2$, following the recommendation by Widłowski (2010) who found emerging non-zero net horizontal fluxes resulting in unacceptably high bias of the two-flux FAPAR estimate for smaller areas. We chose a hexagonal sampling scheme with the nodes at the vertices since this sampling scheme maximizes the sensing area covered by the given number of nodes and at the same time ensures signal quality and connectivity (Mortazavi et al., 2014; Younis and Akkaya, 2008). Apart from that, the hexagonal sampling belongs to grid-based sampling approaches that have been found to be unaffected by the direction of the direct light source (solar azimuth angle) when compared to transect sampling approaches (Leblanc et al., 2002; Widłowski, 2010).

The configuration of the WSN and data download was carried out with a commercially available portable receiver (frequencies ranging from 2.405 GHz to 2.480 GHz) equipped with USB interface (model WSDA-Base-104 USB Base Station, MicroStrain, Cary, NC, USA) to connect to a portable computer equipped with the software “Node Commander” (version 2.17.0, LORD MicroStrain, Cary, NC, USA). The nodes of the WSN were configured to measure the instantaneous PAR every 10 min synchronously ($\sim 1 \text{ ns}$).

2.4. Meteorological data

We used data on meteorological conditions obtained from the TERENO meteorological environmental research station located approx. 450 m outside the forest on open grassland. Shortwave incoming radiation, wind speed and air temperature were measured at 2 m height (model WXT520, Vaisala, Vantaa, Finland). Observations on diffuse radiation conditions were obtained from a sunshine pyranometer (model SPN1, Delta-T, Cambridge, UK) and used to calculate the ratio of diffuse-to-total incident radiation (d/Q). From the original data logged at 20 Hz integration interval every 1 min, timesteps were selected every 10 min corresponding to the acquisition time of the synchronized nodes of the WSN. Volumetric water content in the forest was measured with seven sensors in 5 cm depth (model EC-5, Decagon, Pullman, WA, USA) (i.e. nodes 2, 5, 6, 9, 12, 14, 16 in Fig. 2). An overview of meteorological conditions in the observation period is shown in Fig. B1, Appendix B.

2.5. Observations of forest phenology

For daily observations of forest phenology, an automated self-powered camera (model Snapshot Mini 5.0, Dörr, Neu-Ulm, GER; 5 MP resolution, 640×480 pixels) was installed at 1.3 m height looking horizontally towards one of the nodes of the WSN and its canopy region above (Fig. 2). The camera was programmed to take one photo every six hours (i.e. approx. at 0 a.m., 6 a.m., 12 a.m. and 6 p.m.). From each day, the photo taken closest to noontime was selected. The photos were used for visual monitoring to determine the progress of leaf color change and leaf fall as well as to identify periods of snow coverage. Therefore, subset images were extracted as region of interest with only branches and leaves of the trees (Fig. C1, Appendix C). Time series of redness and greenness were calculated using the approach used by Sonnentag et al. (2012) who recommended to calculate the 90-percentile of all green (red) daytime values within a three-day window to the center (“three-day-90-percentile”) to reduce influences of varying illumination conditions.

2.6. Processing of two-flux FAPAR

All data was processed and analyzed using the statistical software R (<https://cran.r-project.org/>). The location of the site with its surrounding slopes required a shadow exclusion routine in the pre-processing of acquired PAR data. Therefore, we determined timesteps of

shadowed sensors based on the solar zenith and azimuth angles and a digital elevation model (DEM) with 5 m spatial resolution (DEM 5, Free State of Bavaria, <https://www.ldbv.bayern.de>) by using the R-package “insol” (<http://www.meteoexploration.com/R/insol/index.html>). Any PAR data affected by topographic shadows were excluded from the time series. With the sensors for PAR_{in} and $\text{PAR}_{\text{trans}}$ being separated by 300 m, shadowing caused by moving clouds needed to be considered. As a first step, we excluded all timesteps with $\text{PAR}_{\text{trans}} \geq \text{PAR}_{\text{in}}$. Based on the measurements of the meteorological station (Fig. 1), we additionally excluded all data acquired during mixed illumination conditions ($0.2 \leq d/Q < 0.9$) in the uncertainty assessment (Section 2.9).

Two-flux FAPAR was calculated based on measurements of PAR_{in} and $\text{PAR}_{\text{trans}}$ for every 10 min daylight timestep (t) a) individually at each (i) of the 16 (n) sensor locations in the forest (“individual FAPAR”, $\text{FAPAR}_{i,t}$) and b) as spatial average (“domain FAPAR”, $\text{FAPAR}_{d,t}$) using the following approach:

$$\text{FAPAR}_{i,t} = 1 - \frac{\text{PAR}_{\text{trans},t}}{\text{PAR}_{\text{in},t}} \quad (1a)$$

$$\text{FAPAR}_{d,t} = \frac{1}{n} \sum_{i=1}^n \text{FAPAR}_{i,t} \quad (1b)$$

2.7. Characterization of spatio-temporal variability

Understanding the spatio-temporal variability of FAPAR is needed to discuss sources of uncertainty. For assessing the representation of spatial variability of FAPAR across the forest stand with our experimental set-up, we performed statistical testing between distributions of domain FAPAR and individual FAPAR. As FAPAR follows a not-normal distribution, we used the nonparametric Mann–Whitney (MW test) and Kolmogorov–Smirnov test (KS test) to check up on equality of the central tendency and equality of distributions as null hypothesis (0.05-significance level), respectively.

To investigate the numbers of samples required to capture a certain amount of spatial variability of FAPAR, we calculated the coefficient of variation (CV, in %) of domain FAPAR as a function of the number of samples (i.e. sensors). For varying numbers of sensors (2–16), all possible sensor-ID combinations out of the 16 locations were determined as the binomial coefficient. For the combinations, we calculated the maximum CV of all timesteps. We distinguished between different environmental conditions with combinations of WS , SZA and d/Q . As the results refer to the statistical error of FAPAR (which can be decreased with a higher number of samples), previously described as “sampling bias” of FAPAR (Widłowski, 2010), we evaluated obtained values of maximum CV with the accuracy target of 10% set by GCOS (2011).

Time series of domain FAPAR were processed for the years 2015 and 2016. To distinguish the contribution of different species composition to domain FAPAR, we aggregated individual FAPAR under diffuse light conditions ($d/Q \geq 0.9$) according to the proportions of basal areas of different tree species (Table 1). Thus, $\text{FAPAR}_{\text{spruces}}$ and $\text{FAPAR}_{\text{beeches}}$ refer to weekly aggregated domain FAPAR of sensors with more than 90% and less than 80% basal area of spruces in their 10 m-surrounding, respectively. The intersections of the curves of $\text{FAPAR}_{\text{spruces}}$ and $\text{FAPAR}_{\text{beeches}}$ were used to identify key phenological changes as transmitted fractions of PAR under Norway spruce are known to be higher than for European beech (Leuchner et al., 2011).

2.8. Assessing sources of variability

We fitted a Generalized Linear Model (GLM) with d/Q , SZA , WS , LC and SC as explanatory variables to assess their contribution to the variability of domain FAPAR. Stepwise logistic regression was applied to a) account for the strict value range of FAPAR ($0 \leq \text{FAPAR} \leq 1$) (Wang, 2006) and b) identify the best fitting model based on the

Table 2

Selection criteria and classification schemes were used to filter domain FAPAR for the uncertainty assessment of different variables. Time periods of FAPAR_{white} ($d/Q \geq 0.9$, $WS < 2 \text{ m s}^{-1}$) were adapted to the periods of time of classified and selected domain FAPAR.

| Variable(s) | Classification scheme | Selection scheme domain FAPAR | Selection scheme FAPAR _{white} |
|--|---|--|---|
| Illumination conditions (SZA and d/Q) | varying SZA and d/Q | $WS < 2 \text{ m s}^{-1}$ Jun–Aug 2015 and 2016 | Jun–Aug 2015 and 2016 |
| Wind speed (WS) | varying WS | $d/Q \geq 0.9$ Jun–Aug 2015 and 2016 | Jun–Aug 2015 and 2016 |
| Leaf color (LC) | FAPAR _{green} , FAPAR _{yellow} , FAPAR _{red} | $d/Q \geq 0.9$ $WS < 2 \text{ m s}^{-1}$ Sep–Nov 2016 before first snowfall | Sep 2016 |
| Snow coverage (SC) | FAPAR _{no} , FAPAR _{partly} , FAPAR _{snow} | $d/Q \geq 0.9$ $WS < 2 \text{ m s}^{-1}$ Mar–Apr 2017 before bud burst | Mar–Apr 2017 before bud burst |

minimum Akaike information criterion (AIC). We obtained p-values for the estimated coefficients of the logistic regression using the Wald test (Venables and Ripley, 2002). LC and SC were defined as factor (categorical) variables with different periods of leaf color and snow coverage based on visual interpretations of the automated camera. The different categories of LC were defined for color periods of beech leaves, i.e. predominantly green (FAPAR_{green}), yellow (FAPAR_{yellow}) and red (FAPAR_{red}) and defoliated (FAPAR_{noleaves}) as baseline. For SC, we distinguished periods with completely (FAPAR_{snow}) and partly snow coverage (FAPAR_{partly}) as well as the absence of snow (FAPAR_{no}). We calculated the Nagelkerke pseudo R² as overall measure for the goodness of fit of the GLM (Nagelkerke, 1991).

2.9. Uncertainty assessment

To examine the relevance of each explanatory variable as a source

of uncertainty for the two-flux FAPAR estimate, we compared different distributions of domain FAPAR using MW and KS test (0.05-significance level). To avoid interactions with other variables, we applied selection schemes to the classified explanatory variables as shown in Table 2. For example, to assess the influence of snow-covered forest floor on two-flux FAPAR, we selected data acquired in early spring before leaf unfolding, as in autumn the early snow events would overlap with leaf color change. A comprehensive overview showing classification and selection schemes for the uncertainty assessment is shown in Table 2.

We then calculated the difference between average reference domain FAPAR and domain FAPAR within the same period of time (Table 2), in the following referred to as $\Delta_{\text{two-flux}}$. As reference domain FAPAR, we used domain FAPAR under diffuse light conditions and calm air ($d/Q \geq 0.9$ and $WS < 2 \text{ m s}^{-1}$) (FAPAR_{white}) as it can be assumed to be unaffected by influences of SZA, WS, LC and SC, corresponding to a refined definition of the commonly-known term “white-sky FAPAR” (Baret et al., 2007). With the concept of $\Delta_{\text{two-flux}}$, we refer to the study of Widlowski (2010), who considered the difference between simulated reference FAPAR (considering all flux terms of the radiative transfer equation) and simulated FAPAR estimates (e.g. two-flux estimate) as the “estimating bias” of instantaneous FAPAR observations. In our study, “true” FAPAR remains unknown as only two-flux FAPAR is measured so that using the same term “bias” as Widlowski (2010) would be misleading. However, as the value of FAPAR_{white} can be assumed to be closest to “true” FAPAR (no influences of SZA and WS), we considered the sign of $\Delta_{\text{two-flux}}$ as an indication for an overestimation (negative value) or underestimation (positive value) of the two-flux FAPAR as described by Widlowski (2010) for different environmental conditions.

3. Results

3.1. Variability of incoming and transmitted PAR and exclusion of topographic shadows

Observations of PAR_{in} and PAR_{trans} determined approx. 14,000 FAPAR observations per vegetation period. While PAR_{in} is largely determined by available radiation according to the course of the sun,

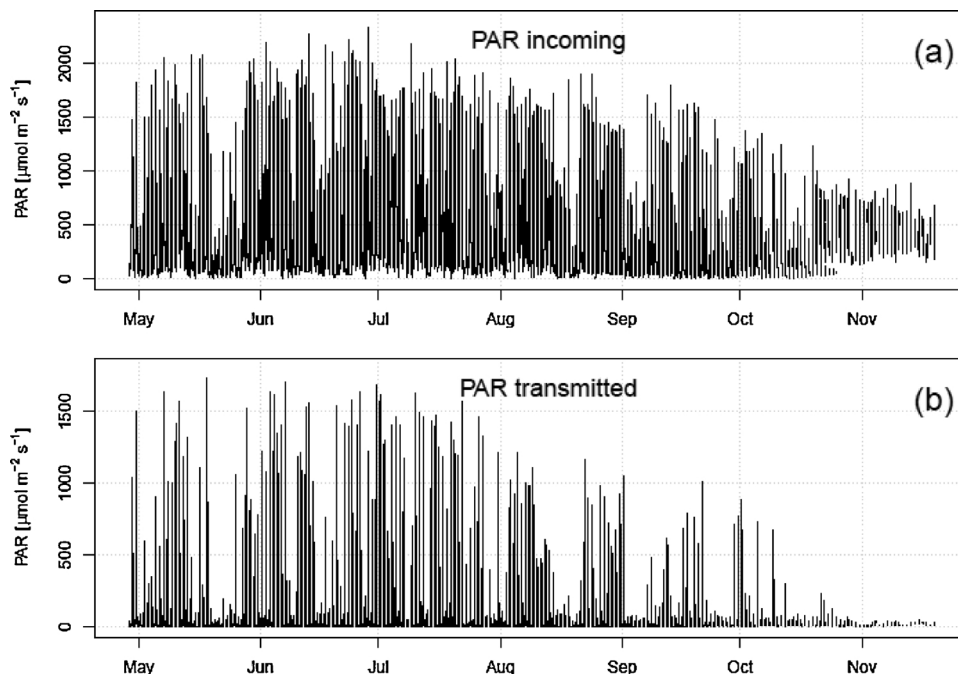


Fig. 3. PAR measured every 10 min in 2015: (a) incoming PAR measured outside the forest and (b) average transmitted PAR obtained from 16 sensors inside the forest.

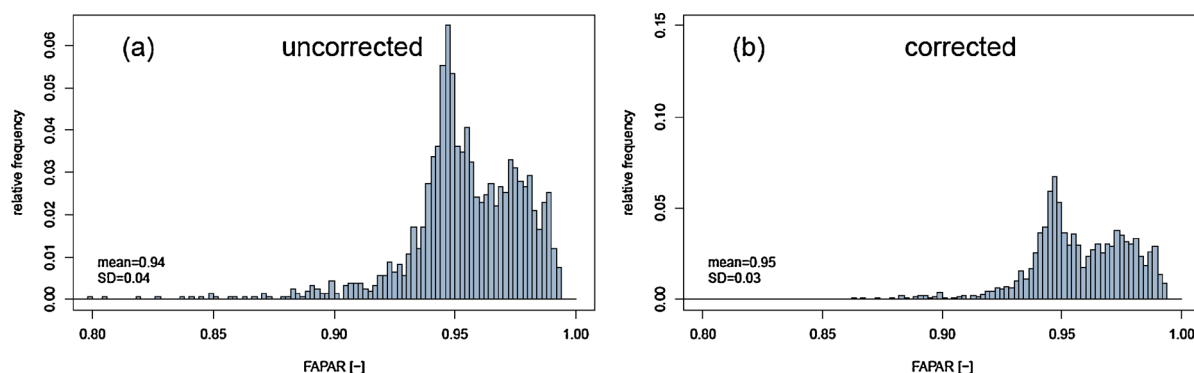


Fig. 4. Histogram of domain FAPAR based on the 10 min mean of 16 sensors in 2015 and 2016 (a) before and (b) after the exclusion of topographic shadows.

PAR_{trans} shows a modified seasonal course according to the phenological development and status of the canopy (Fig. 3). Around the solar noon in midsummer, PAR_{in} ranged from $400 \mu\text{mol m}^{-2} \text{s}^{-1}$ during overcast conditions up to $2300 \mu\text{mol m}^{-2} \text{s}^{-1}$ during clear sky. With leaves of beech and maple trees still growing in May, solar elevation around noon was already high so that the maximum PAR_{trans} of $1700 \mu\text{mol m}^{-2} \text{s}^{-1}$ was reached one month earlier than maximum PAR_{in} . Over the whole investigation period, PAR_{trans} (mean = $26 \mu\text{mol m}^{-2} \text{s}^{-1}$, SD = $29 \mu\text{mol m}^{-2} \text{s}^{-1}$) accounted to 4% of PAR_{in} (mean = $598 \mu\text{mol m}^{-2} \text{s}^{-1}$, SD = $497 \mu\text{mol m}^{-2} \text{s}^{-1}$), exhibiting higher seasonal variability.

Overall, between 9 and 15% of daylight timesteps were affected by topographic shadowing, depending on sensor location. Before the exclusion of shadows, the FAPAR distribution showed higher frequencies of values below 0.85 (Fig. 4a), which occurred under the constellation that the sensor for PAR_{in} was shadowed while the sensors for PAR_{trans} remained in direct sunlight. After the exclusion, FAPAR followed a bimodal, not normal distribution (KS test: $D = 0.80$, $p < 0.001$) with the mean at 0.95 and SD of 0.03 (Fig. 4b). Removing shadow-affected data resulted in the abrupt fade outs of PAR before reaching zero values in late October or in early morning/late evening (Fig. 3).

3.2. Spatio-temporal variability of FAPAR

Given the dominance of spruce trees, the seasonal difference of domain FAPAR between the summery maximum (0.99) and spring and autumn values (0.89) accounted to 0.1 (Fig. 5). These weak seasonal dynamics were mainly influenced by the phenological development of the beech trees. The weekly aggregated domain FAPAR differentiated for varying percentages of spruce trees reveals differences due to species composition (Fig. 6). Compared to $FAPAR_{spruces}$, $FAPAR_{beeches}$ was slightly higher (+0.01) during foliated months compared to defoliated months. Throughout the whole vegetation period, domain FAPAR exhibited periods with higher and lower variability (Fig. 5). A common feature for both years can be seen in late autumn: here, domain FAPAR showed exceptionally low SD in combination with pronounced fluctuations of the mean despite leaves of beech trees had completely fallen.

Inter-annual differences are observable with the intersection points in spring and autumn as well as in the maximum summery FAPAR value reached (Fig. 6). In 2016, both spring and autumn intersections between $FAPAR_{beeches}$ and $FAPAR_{spruces}$ were observed three weeks later than in 2015. Further, the summer of 2015 showed episodes with lower values than recorded in 2016, particularly for $FAPAR_{beeches}$. In autumn 2016, higher values for both $FAPAR_{spruces}$ (0.96) and $FAPAR_{beeches}$ (0.94) are observed than in 2015 (0.93 and 0.91).

Regarding inter-sensor differences due to spatial variability across the site, Fig. 7 shows differences of individual FAPAR recordings. Based on the MW test, three sensor pairs out of the 120 pairs of value distributions possible from 16 PAR sensors could not be assumed to be

different regarding their central tendency (i.e. sensor combinations (2,6): $p = 0.58$, (3,13): $p = 0.22$, (6,12): $p = 0.23$). Further, each of the individual FAPAR distributions differed significantly from domain FAPAR ($p < 0.001$).

3.3. Sources of variability in domain FAPAR and uncertainty assessment

Overall, 12,679 complete sets of explanatory variables were available to fit the GLM. Illumination conditions, characterized by d/Q and SZA , changed permanently throughout the day and season. SZA around the solar noon ranged from 24° in midsummer up to values above 60° after mid of October. Most of the time (60% of timesteps), FAPAR was acquired under diffuse light conditions ($d/Q > 0.9$), with only 10% of timesteps classified as clear sky conditions ($d/Q < 0.2$). In summer 2015 and 2016 (Jun–Aug), average WS accounted to 1.5 m s^{-1} (SD: 1.1 m s^{-1}), with roughly 97% of FAPAR data being measured with WS below 4 m s^{-1} . Dates of color changes of beech leaves were identified for autumn 2016: leaf fall started at the end of October and peaked around the beginning of November; later, a snow event interrupted the fall of the remaining brown leaves.

The stepwise logistic regression identified the GLM with all environmental variables (d/Q , SZA , WS , LC , SN) as the best model fit (i.e. with the minimum AIC; Nagelkerke pseudo $R^2 = 0.99$) to explain domain FAPAR. Highly significant contributions were found for d/Q (regr. coef. = -1.28 , $p < 0.001$), SZA (0.01 , $p < 0.001$) and LC (0.58 , $p < 0.001$), while WS (0.00 , $p = 0.07$) and SC (-0.08 , $p = 0.08$) showed only marginal explanatory power. In the following, the results of the uncertainty assessment for each explanatory variable are given.

Fig. 8a–c show how d/Q altered the value distributions of domain FAPAR for small ($SZA < 40^\circ$), medium ($40^\circ \leq SZA < 60^\circ$) and larger SZAs ($SZA \geq 60^\circ$). In general, FAPAR acquired in diffuse light conditions was slightly lower than FAPAR acquired in direct light conditions. The variability of domain FAPAR was higher under clear sky conditions than under diffuse light conditions for medium and low SZAs (Fig. 8a–b). FAPAR acquired under largest SZAs, however, showed low variability even for clear sky conditions (Fig. 8c). With decreasing d/Q , the value distributions of FAPAR changed from a unimodal to a bimodal, left-skewed shape. In contrast to medium and small SZA (Fig. 8a–b), a less skewed distribution was found for large SZA and low d/Q (Fig. 8c), with a local maximum at 0.97 and the mode of the distribution shifted to 0.99.

Fig. 8d summarizes Fig. 8a–c by showing domain FAPAR found at different ranges of SZA under nearly clear sky conditions ($d/Q < 0.2$) as well as $FAPAR_{white}$. The differences in central tendency for domain FAPAR distributions between lowest and largest SZA class were significant (MW test: $W = 4,857,931$, $p < 0.001$). Overall, $\Delta_{two-flux}$ ranged from -0.02 for smallest SZA to -0.06 at largest SZA .

The influence of wind speed on FAPAR distributions is shown in Fig. 9. For WS below 5 m s^{-1} , domain FAPAR stays almost constant. However, for high WS ($\geq 5 \text{ m s}^{-1}$), domain FAPAR changes by 0.01,

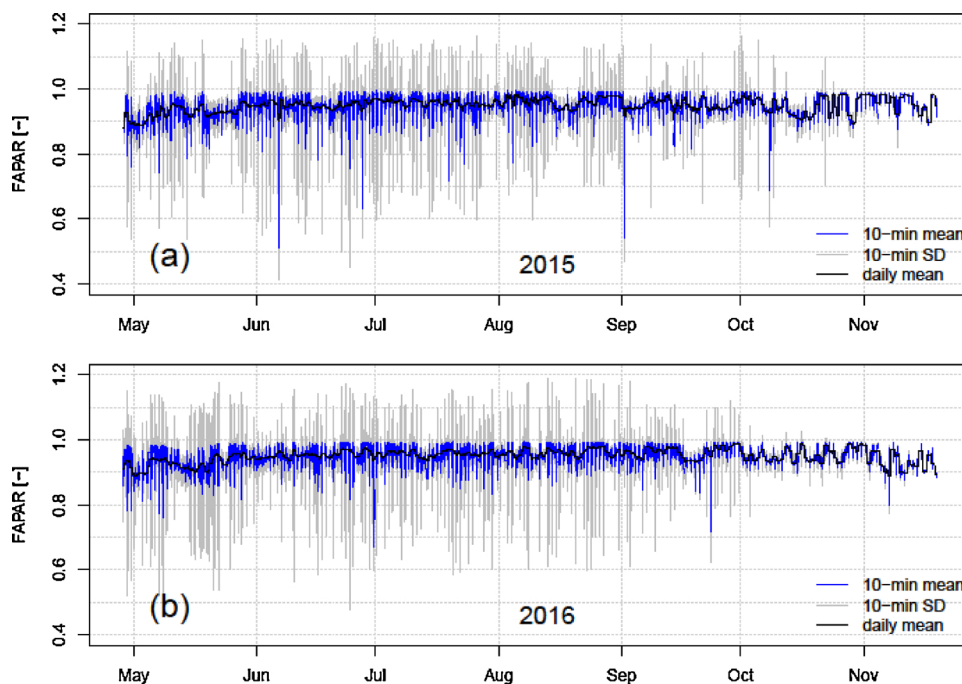


Fig. 5. Domain FAPAR with SD for each 10 min timestep and daily aggregated domain FAPAR for the vegetation periods of (a) 2015 and (b) 2016.

though not significantly (MW test: $p > 0.05$ for all combinations of classified FAPAR shown in Fig. 9a). Nevertheless, under higher WS, the value distribution shifts from unimodal to bimodal with a second maximum around 0.89 (Fig. 9b). Again, this change in the shape of distribution was not found to be significant.

Spatial variability (CV) of domain FAPAR decreased exponentially with a higher number of sensors depending on d/Q , SZA and WS (Fig. 10). Overall (“all” in Fig. 10), the deployment of 16 sensors

reduced the spatial variability by 64% compared to the case of two sensors, with CV always below 10%. The decrease of CV with increasing sample size differed depending on illumination conditions. While FAPAR in diffuse light conditions presented almost constant variability across different numbers of sensors (value range of CV: 3–5%), a minimum of five sensors was needed to achieve a CV below 10% under clear sky conditions. High WS further augmented the number of samples needed to achieve a certain level of CV under both clear and

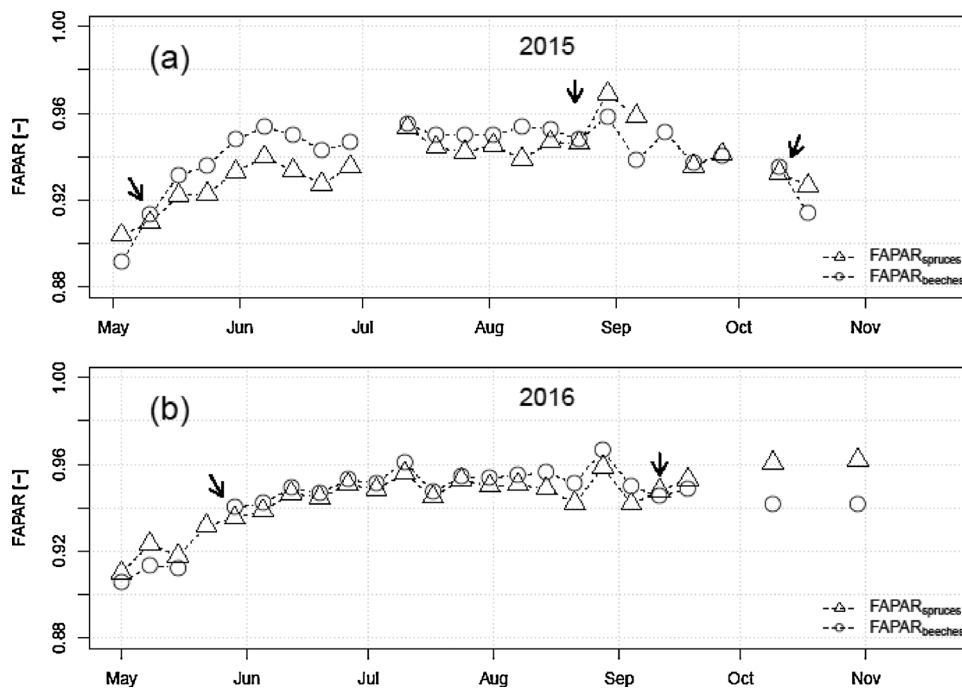


Fig. 6. Weekly aggregated domain FAPAR in diffuse light conditions for different percentages of the basal area of spruces (FAPARspruces with basal area $\geq 90\%$ and FAPARbeeches with basal area $< 80\%$) located 10 m around the sensors, arrows indicating intersection points.

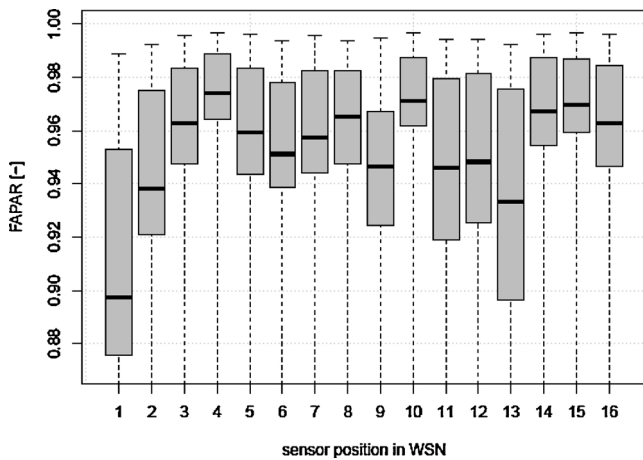


Fig. 7. FAPAR measured in 2015 at different sensor locations.

overcast sky conditions. Lowest variability (CV ~1%) was present under clear sky conditions and large SZA.

As for the influence of leaf color, the visual observations were supported by the three-day-90th-percentile of redness and greenness values calculated from the subset photos of the automated camera (Fig. 11a). The progress of leaf color change became apparent in the last third of October, when redness increased considerably towards its maximum at the end of October and dropped according to the observed peak of leaf fall. Fig. 11b shows that the peak coloring of beech leaves coincided with highest FAPAR values (0.98) within the investigation period: around the peak of leaf fall, FAPAR exhibited a sharp decline, as PAR_{trans} increased with the loss of foliage. In contrast to FAPAR_{green}, fluctuations of FAPAR_{yellow} exhibited higher amplitudes while the mean

of both periods remained equal (mean: 0.94, SD: 0.01). FAPAR distributions during different color periods (Fig. 12a) show that the distribution changed from unimodal (FAPAR_{green}) to bimodal (FAPAR_{yellow}). Differences between FAPAR_{red} and FAPAR_{green} were significant for both central tendency (MW test: $W = 2522, p < 0.001$) and value distributions (KS test: $D = 0.52, p < 0.001$). $\Delta_{two-flux}$ attributed to LC in autumn 2016 accounted for -0.01 on average, reaching up to -0.05 around the peak of leaf colors.

The influence of SC on FAPAR distributions is shown in Fig. 12b. FAPAR_{no}, FAPAR_{partly} and FAPAR_{snow} presented significantly different distributions (KS test: $p < 0.05$). With the occurrence of snow, the mode of FAPAR distributions increases, accompanied by a flattening out of the distribution. Compared to FAPAR_{snow}, FAPAR_{partly} exhibited fewer fluctuations at the far ends of the distribution, also indicating an increase of the mode, although not as pronounced. Overall, $\Delta_{two-flux}$ for FAPAR_{snow} accounted to 0.01.

4. Discussion

4.1. Role of pre-processing

We showed results of an uncertainty assessment for two-flux FAPAR observations in a conifer-dominated forest. The fact that the variability of domain FAPAR was reduced by 25% after the exclusion of topographic shadowing demonstrates that topographic shadows represented a major influence on the variability of domain FAPAR. The exclusion of topographic shadows eliminated extremely low values of domain FAPAR induced under the constellation that the sensor for PAR_{in} was shaded while sensors for PAR_{trans} would remain in direct sunlight. Thus, the exclusion of topographic shadows had the disadvantage that parts of the data could not be used for the uncertainty assessment, which affected timesteps under large SZA and clear sky conditions. On the

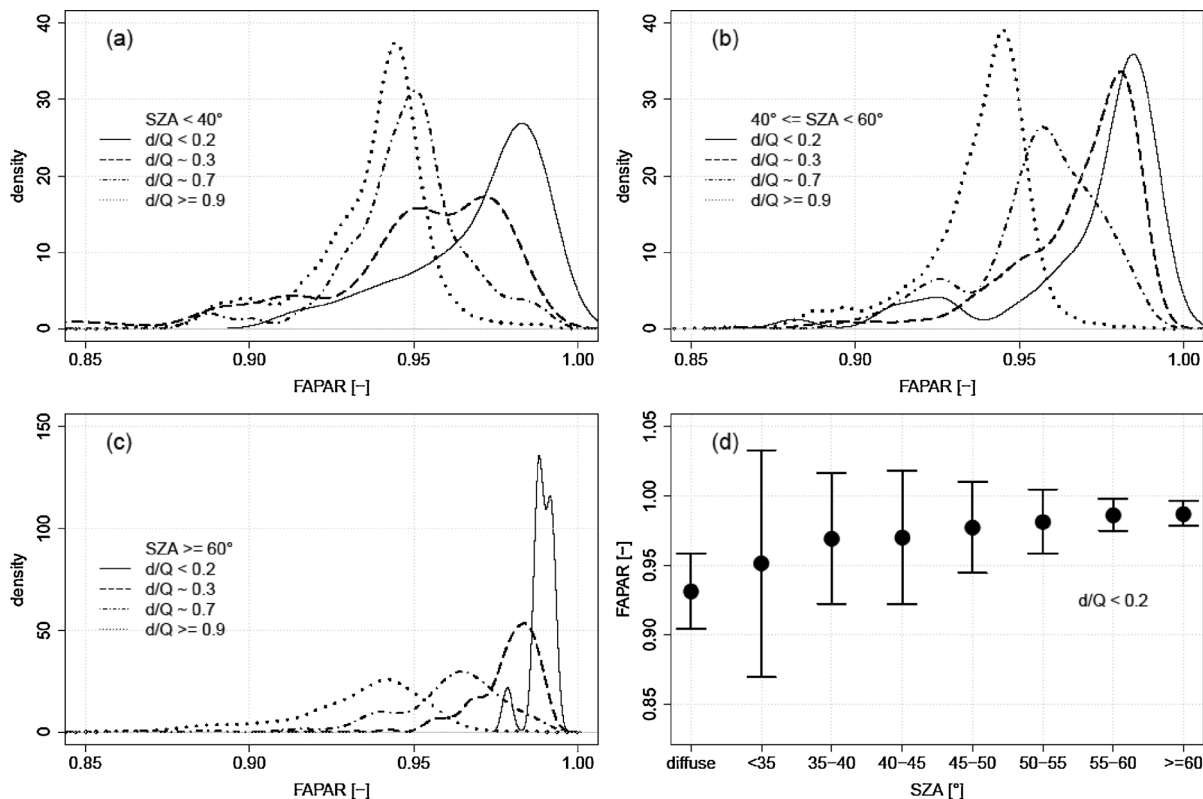


Fig. 8. Influence of d/Q on summerly domain FAPAR (Jun–Aug 2015 and 2016): (a) small SZA, (b) medium SZA, (c) large SZA; (d) domain FAPAR (\pm SD) for different SZA and diffuse illumination conditions (FAPAR_{white}).

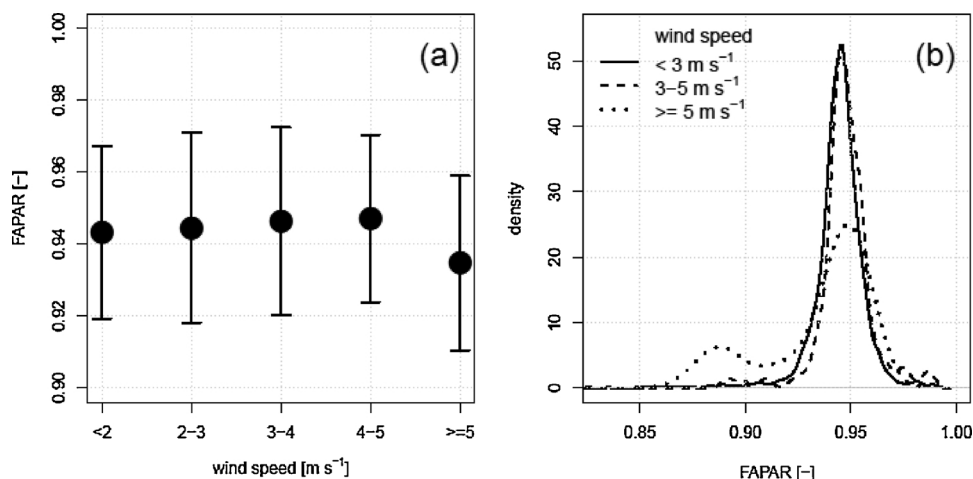


Fig. 9. FAPAR measured under diffuse light conditions June to August 2015 and 2016 classified for different wind speed conditions: (a) domain FAPAR with SD and (b) density distributions of FAPAR.

other hand, the influence of SZA on domain FAPAR and its consequences for uncertainty of the two-flux FAPAR estimate could only be assessed with topographic shadowing being excluded.

4.2. Sources of spatio-temporal variability

Our results further showed that the weak seasonal dynamics of domain FAPAR (± 0.1) resulted from the dominance of evergreen spruces while the main contribution to the seasonality of FAPAR was attributed to beech, showing also inter-annual differences. The lower absolute values of domain FAPAR in the summer of 2015 are supported by low summerly precipitation records (413 mm vs. 570 mm in 2016) as well as higher air temperatures (17.1 °C in 2015 vs. 15.5 °C in 2016), and thus decreased soil water content as observed at least in the upper layer of the forest soil (Appendix B, Fig. B1). Here, we see potential to further study the effect of water scarcity on FAPAR at local scale, as it has been done on regional and continental scale (Gobron et al., 2005;

Meroni et al., 2014).

The results of the GLM showed significant contributions of illumination conditions with SZA and d/Q and LC, and marginal influences of WS and SC. The highly significant contribution of d/Q is in accordance with previous studies that highlighted illumination conditions as a major source of variability in FAPAR observations (Hutchison et al., 1980; Leuchner et al., 2011; Möttus, 2004; Ross et al., 1998). Measurements of two-flux FAPAR showed the quasi-symmetric unimodal value distribution typical for diffuse light conditions (e.g. Baldocchi et al., 1986; Hutchison et al., 1980; Leuchner et al., 2011; Sinclair and Knoerr, 1982). Thus, the low variability of domain FAPAR observed under diffuse light conditions explains the episodes of low SD observed in summerly domain FAPAR (Fig. 5). Further, the observed slightly lower FAPAR values obtained under diffuse light are in accordance with other studies that explained this phenomenon with the conical shape of coniferous trees, presenting larger gaps that facilitate the penetration of diffuse radiation into the canopy with the consequence of increasing

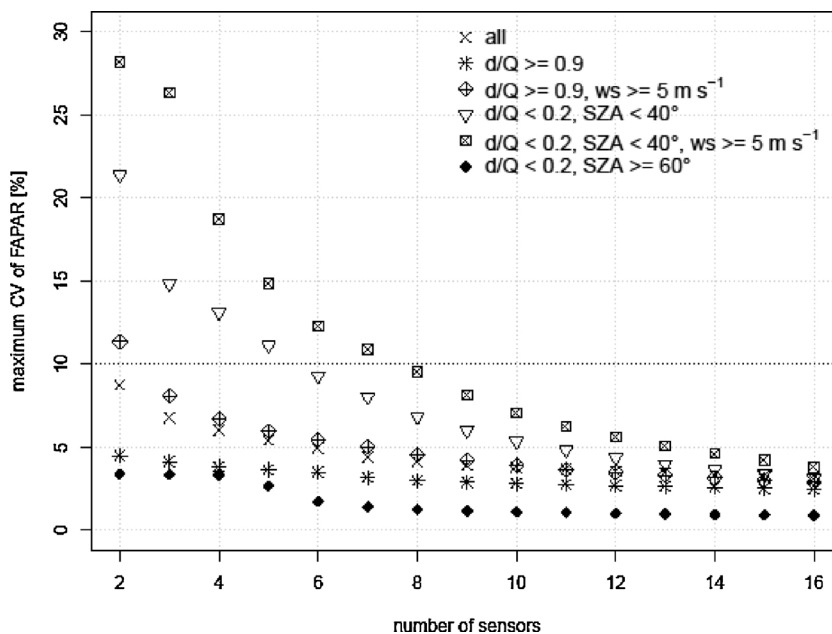


Fig. 10. The maximum coefficient of variation (CV) of domain FAPAR as a function of the number of samples for varying environmental conditions. The dotted line refers to the accuracy target of 10% set by GCOS (2011) for FAPAR products.

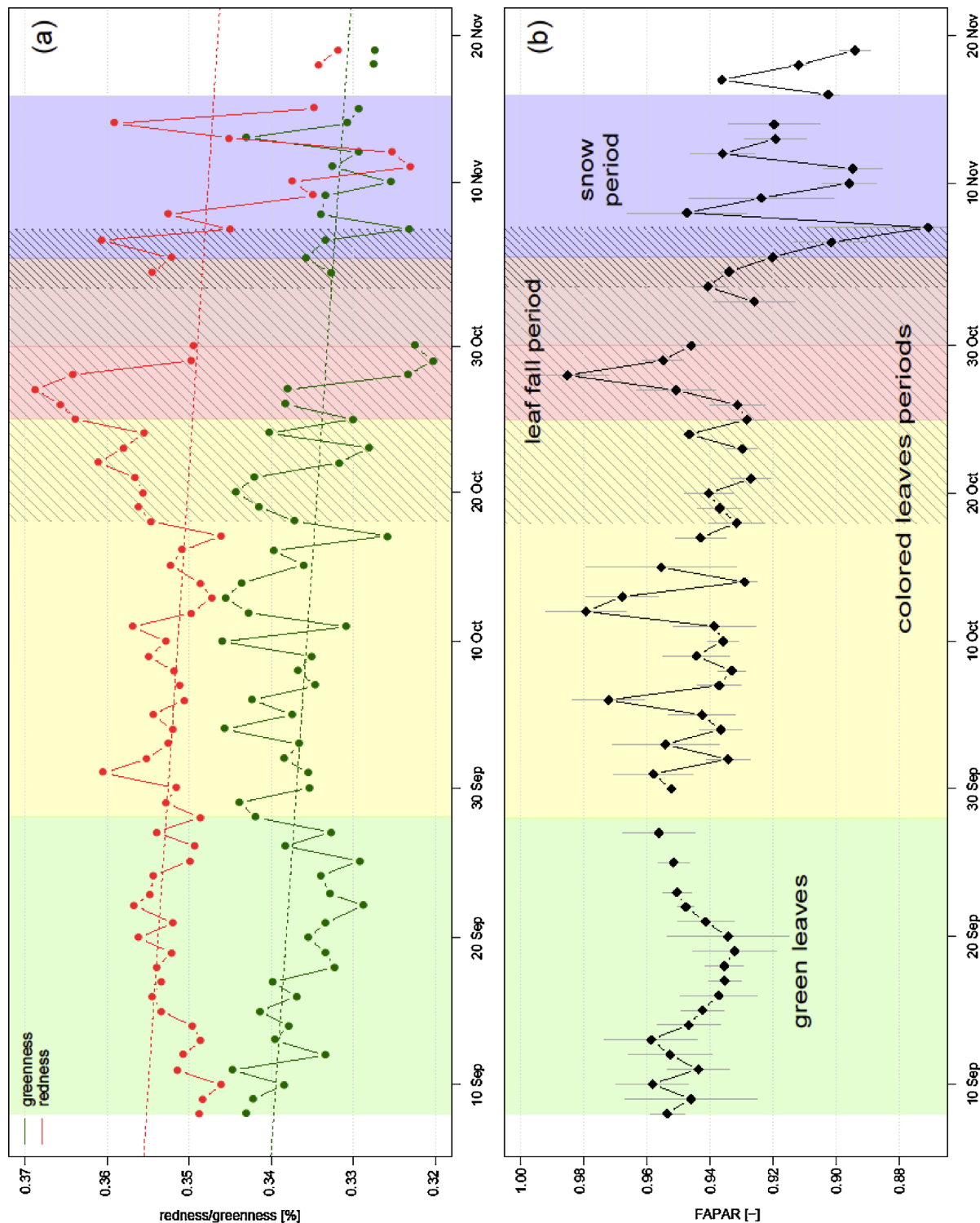


Fig. 11. Autumn 2016 during different periods of leaf color and leaf fall (hatched areas) of beech leaves: (a) redness and greenness as the three-day 90-percentile of the canopy region of the photos of an automated camera and (b) daily domain FAPAR and SD acquired under diffuse light conditions. (For interpretation of the references to colour in this figure legend, the reader is referred to the web version of this article).

transmission rates (Leuchner et al., 2011; Morgan et al., 1985).

The low absolute values and slow decrease of CV obtained under diffuse light conditions (Fig. 10) indicate that already two sensors capture the spatial variability across the given site. However, as satellite derived FAPAR products are limited to cloudless images, validation sampling campaigns aim at sampling under clear sky conditions,

for which CV as a measure of variability was found to be four times higher than for two sensors. The higher variability found under clear sky conditions results from the observed left-skewed-bimodal distribution observed under low to medium SZAs (Fig. 8a–b). Left-skewness has been explained by Leuchner et al. (2011) with the occurrence of sunspots on the forest floor, leading to lower FAPAR values.

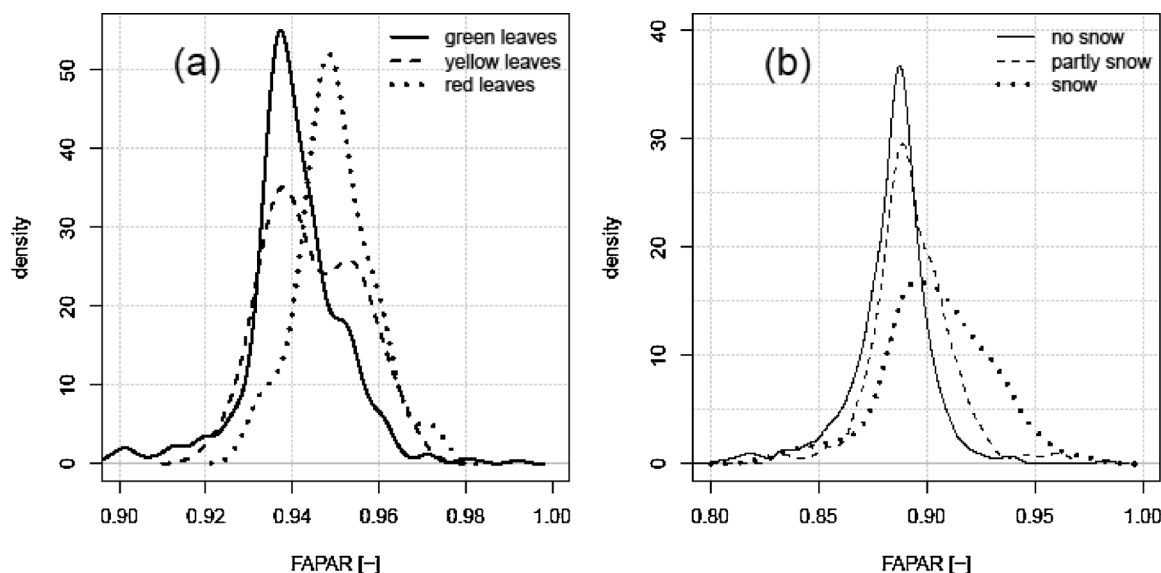


Fig. 12. Distributions of domain FAPAR under diffuse light conditions for different periods of (a) leaf colors of beech leaves and (b) snow coverage.

4.3. Influence of environmental conditions on the uncertainty of two-flux FAPAR

Our results demonstrate that at larger SZA (above 60°), the two-flux FAPAR estimate misses out on large parts of the variability of the light field, with overall low spatial variability (Fig. 10) and only several local maxima (Fig. 8c) instead of the original skewness compared to domain FAPAR acquired under small SZA (Fig. 8a). The observed local maxima could indicate the contribution of lateral light fluxes, as has also been suggested by Leuchner et al. (2011). Consequently, the increase of domain FAPAR after the senescence period observed as a common feature in both years (Fig. 5) can be explained with the overestimation observed during larger SZA and clear sky conditions. Here, our results are similar to the findings of Widłowski (2010) who simulated an overestimation by up to 0.05 for larger SZAs ($\geq 60^\circ$) in open spruce forest. Typically, the overestimation has been found to be more pronounced in coniferous forest because the conical tree shapes cause more interception at large SZA, resulting in increased reflectance and reduced transmittance (Widłowski, 2010).

The observed overestimation by up to 0.06 at our site crosses the accuracy threshold set by GCOS (2011). However, as the $\Delta_{\text{two-flux}}$ for SZA equals more than half of the seasonal variability (± 0.1), it will have greater (ecological) significance than at a different site with higher seasonal dynamics. As the forest site is still interspersed with deciduous trees, we expect higher overestimation for pure spruce forest, commonly found across Central and North European managed forests, as it has been indicated by Majasalmi et al. (2017). Further, with the elimination of timesteps due to topographic shadowing with largest SZA (above 70°), the influence of SZA could still be underestimated. Finally, the significant influence of SZA could lead to the recommendation to use FAPAR ground data acquired in diffuse light conditions shortly before or after a satellite overpass, which requires permanent monitoring activities as possible with the WNS technology.

For wind speeds above 5 m s^{-1} , we found increased spatial variability, an indication for an underestimation of FAPAR and overall no significant explanatory power in the GLM. The assessment of wind speed is hindered by the fact that over the two-year observation period, high wind speeds were not observed frequently. The underestimation of domain FAPAR by 0.01 attributed to the observed second maximum in the value distribution (Fig. 9) could result from changed leaf angle orientation from horizontal to (semi-)upright and thus more light

entering deeper into the canopy. Canopy RTMs already include the representation of leaf angle distribution, simulating lower reflectance under vertical leaf orientation (Asner, 1998; Verhoef, 1984). However, further investigations with measurements of top-of-canopy reflectance are required for a comprehensive evaluation of underlying processes.

For leaf color, results showed a significant contribution of beech trees on the variability of domain FAPAR despite the dominance of evergreen spruce. Pronounced fluctuations of $\text{FAPAR}_{\text{yellow}}$ (Fig. 11) could result from the contributions of bright and relatively large yellow leaves of maple trees, followed by leaf fall as maple trees showed earlier senescence than beech trees. The overestimation of fAPAR by 0.05 during peak color period (Fig. 12a) supports findings of Widłowski (2010), who simulated an overestimation by up to 0.1 for beech due to increased reflectance of bright autumn leaves. Thus, we expect the influence of leaf color to be more pronounced at forest stands dominated by beech. Further, since for $\text{FAPAR}_{\text{red}}$, a considerable amount of foliage had already fallen, the overestimation could have been higher, provided that a higher proportion of colored leaves had remained in the canopy. Thus, the duration of the peak leaf color period as well as the amount of colored foliage in the canopy and in turn the influence of leaf color on the two-flux FAPAR may vary year-by-year.

Snow coverage was not identified as a significant explanatory variable for domain FAPAR. This could arise from the fact that snow coverage occurred only on several days in the observation period. Nevertheless, our results showed tendencies for an overestimation ($\Delta_{\text{two-flux}} = -0.01$) which is in contrast to Widłowski (2010) who found a drastic underestimation between 0.25 and 0.3 for the two-flux estimate which was explained with a higher proportion of PAR_{in} and $\text{PAR}_{\text{trans}}$ reflected upwards due to the high albedo of snow-covered forest floor. However, our observed right-skewed value distributions for $\text{FAPAR}_{\text{partly}}$ and $\text{FAPAR}_{\text{snow}}$ (Fig. 12b) could indicate an effect of snow accumulation in the crowns, especially on the dense branches of spruce trees, which could also explain the high difference between $\text{FAPAR}_{\text{spruces}}$ and $\text{FAPAR}_{\text{beeches}}$ observed in autumn 2016 (Fig. 6). Manninen and Stenberg (2009) showed that total forest albedo under the occurrence of snow was largely determined not only by the albedo of the forest floor itself, but also by the presence of snow-covered/frost-covered canopy. Given our results, we support their conclusion that changes in top-of-canopy snow accumulation needs to be considered in canopy RTMs.

4.4. Sampling numbers under uncertainty constraints

Our investigations on the spatial variability across the site revealed significant differences between sensor locations despite the dominance of spruce at this site. This is in accordance with numerous studies that pointed out the high spatial variability in forest ecosystems because of complex interactions of scattering and absorbance arising from canopy structure and density (Leuchner et al., 2011; Ollinger, 2011). Although the recommendation of deploying multiple devices in the field is not a new (e.g. Reifsnyder et al., 1971), our results emphasize once again the need for sampling with more than one device for validating satellite-derived FAPAR products, as it has recently been done by Nestola et al. (2017). Given the high variability found under clear sky conditions and higher wind speeds and given the fact that optical remote sensing FAPAR products are dependent on clear sky conditions, we generally support the recommendation by Widłowski (2010) that ten PAR sensors should be the utmost minimum number of samples for reasonably accurate FAPAR observations. In this regard, we see potential for applying the WSN technology to match the resolution of new decametric satellite derived FAPAR products (e.g. Sentinel-2). Our results showed that 16 sensors considerably reduced the variability to an acceptable level at the given site (i.e. by almost two third compared to two devices) (Fig. 10). We believe that the WSN monitoring approach could therefore reappraise the current conception of direct FAPAR observations being neither verifiable due to underlying uncertainties (e.g. Rahman et al., 2015) nor feasible in terms of labor intensity.

5. Conclusions

We presented the results of an uncertainty assessment of 10 min two-flux FAPAR observations at a sub-alpine conifer-dominated forest stand in Southern Germany. The variability of FAPAR was found to be mainly attributed to illumination conditions and leaf color, while influences of wind speed and snow coverage were found to present only marginal influences over the two-year observation period. To reveal the uncertainty of the two-flux FAPAR estimate, we accounted for the sign and absolute value of the difference ($\Delta_{\text{two-flux}}$) between domain FAPAR acquired under diffuse light conditions and calm air (FAPAR_{white}) and domain FAPAR during different meteorological or phenological conditions (e.g. large SZA). A negative (positive) value of $\Delta_{\text{two-flux}}$ was interpreted as an indication for an overestimation (underestimation) of “true” FAPAR by the two-flux FAPAR estimate, as found in previously investigations with canopy RTMs. The following findings could be used in the development of sampling protocols for the validation of satellite-derived FAPAR products:

Appendix A

Eq. (A.1) gives the definition of two-flux FAPAR, ignoring contributions of horizontal fluxes, PAR albedo at background level and PAR albedo at the top-of-canopy level:

$$FAPAR_{\text{two-flux}} = 1 - \frac{PAR_{\text{trans}}}{PAR_{\text{in}}} \quad (\text{A.1})$$

where FAPAR_{two-flux} is the two-flux Fraction of Absorbed Active Radiation, PAR_{trans} is the PAR transmission down to background-level and PAR_{in} is the incoming PAR in $\mu\text{mol m}^{-2} \text{s}^{-1}$.

Appendix B

Fig. B1 shows environmental conditions at Graswang in 2015 and 2016.

Appendix C

Fig. C1 illustrates how the region of interest was defined for daily photos of automated camera in autumn 2016 and spring 2017.

- 1) For **solar zenith angle (SZA)**, we found an overestimation by 0.06 for SZA above 60° and clear sky conditions, thereby crossing the target accuracy set by GCOS (2011).
- 2) Regarding the influence of **wind speed (WS)**, we found indications for an underestimation. Further, the variability of FAPAR estimates was found to be increased under higher WS (above 5 m s⁻¹). We conclude that WS as a potential source of uncertainty for FAPAR observations should be addressed in further investigations at sites with higher WS occurring more frequently.
- 3) For **leaf color (LC)**, we found an overestimation by up to 0.05 around peak color period despite the relatively low percentage of beech trees at our site. We conclude that at a different site where deciduous trees are the dominating species, the influence of LC on two-flux FAPAR could be higher.
- 4) For **snow coverage (SC)**, we found a slight tendency for an overestimation by 0.01 which contrasts with previous findings. Given these discrepancies, we recommend that the validation of satellite-derived FAPAR should be avoided when snow is present.

Overall, the permanent monitoring with a Wireless Sensor Network in combination with the monitoring of other environmental variables demonstrated the potential to quantify sources variability and uncertainty of two-flux FAPAR observations without a priori information on forest structure or spectral properties of canopies. We see future potential to improve algorithms for satellite FAPAR products over forested areas, presenting similar forest structure and composition as the described permanent monitoring site. As uncertainties of FAPAR ground observations are assessable in field conditions, we recommend that they should be considered in upcoming validation activities of FAPAR satellite products.

Acknowledgements

This work was supported by a MICMoR Fellowship through KIT/IMK-IFU (Garmisch-Partenkirchen, Germany) and by funding from Helmholtz Association and the Federal Ministry of Education and Research (BMBF) in the framework of TERENO (Terrestrial Environmental Observatories) (grant no. 01LL0801B). The WSN technology and technical training was provided by the University of Alberta, Edmonton, CA, receiving funding from the Natural Science and Engineering Research Council of Canada (NSERC) Discovery Grant Program. The DEM was provided by the Free State of Bavaria. We thank Matthias Mauder and Matthias Zeeman (KIT/IMK-IFU) for their advice on the data acquired by the TERENO station Graswang. The authors sincerely thank two anonymous reviewers for their helpful comments.

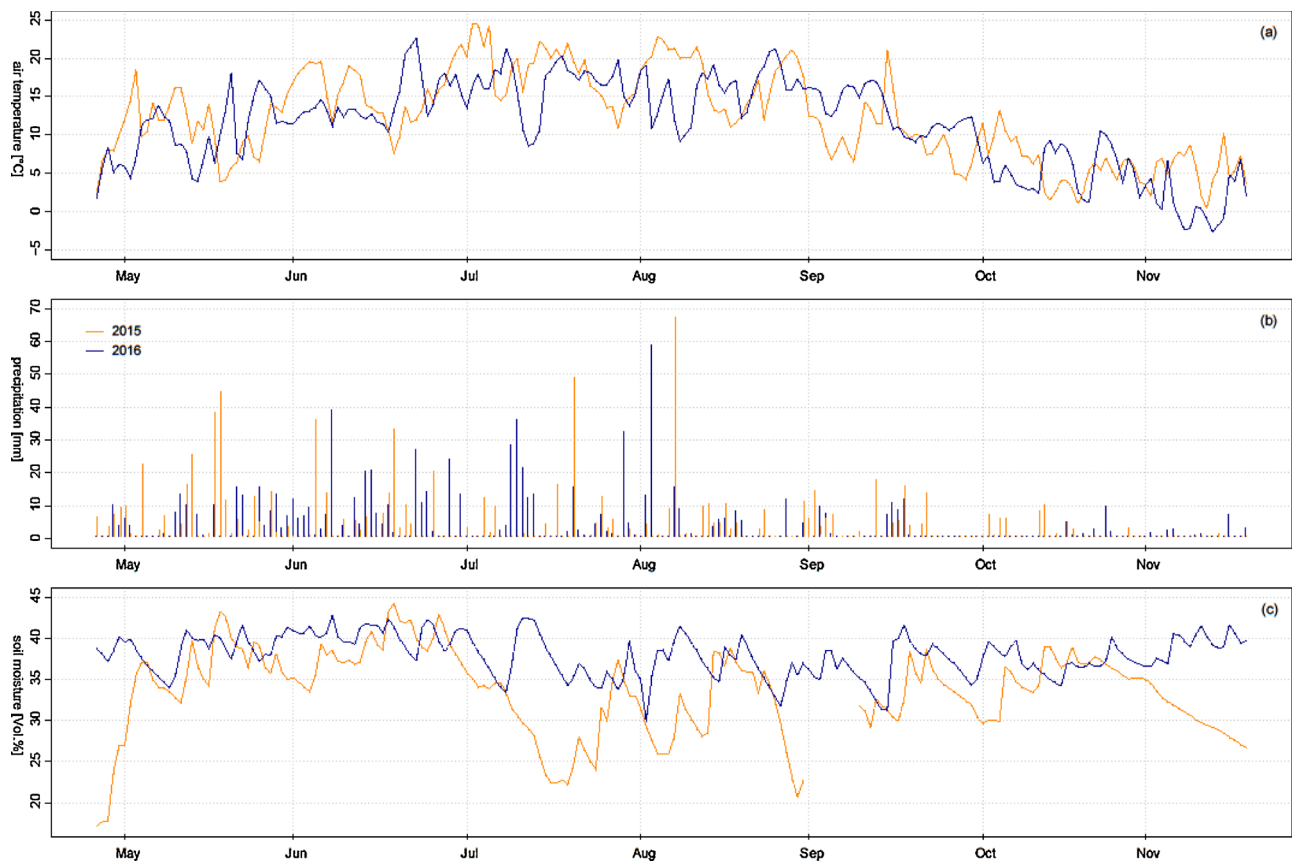


Fig. B1. (a) Daily mean air temperature outside the forest (measured by TERENO station on grassland), (b) daily precipitation sum outside the forest (measured by TERENO station on grassland) and (c) daily mean soil water content in 5 cm depth (measured the WSN in the forest).

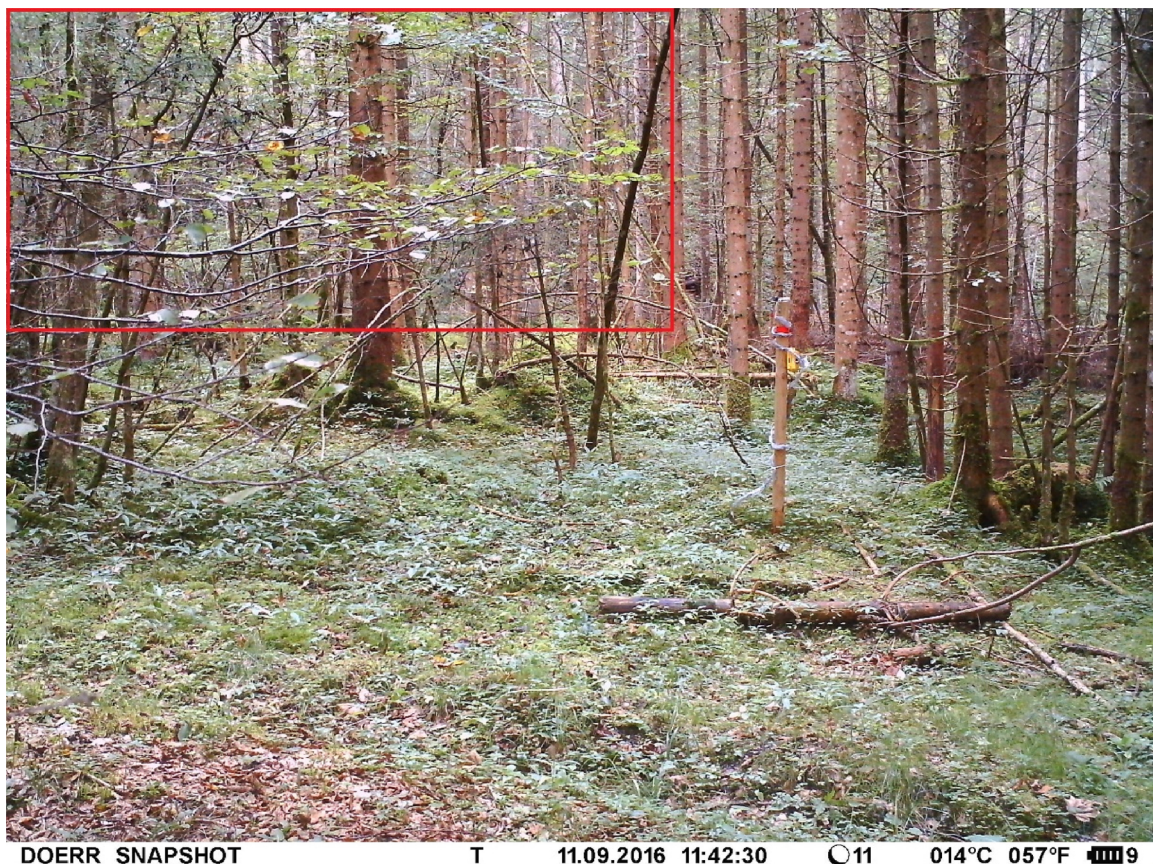


Fig. C1. Subset with region of interest (red area) for calculating greenness and redness in the daily photos of the automated camera. (For interpretation of the references to colour in this figure legend, the reader is referred to the web version of this article).

References

- GCOS, G. C. O. S., 2011. Systematic Observation Requirements for Satellite-Based Data Products for Climate.
- Morgan, D.C., Warrington, I.J., Rook, D.A., 1985. Some observations on the spectral distribution characteristics of short-wave radiation within *Pinus radiata* D. Don canopies. *Plant Cell Environ.* 8, 201–206. <https://doi.org/10.1111/1365-3040.ep11604610>.
- Akitsu, T., Nasahara, K.N., Hirose, Y., Ijima, O., Kume, A., 2017. Quantum sensors for accurate and stable long-term photosynthetically active radiation observations. *Agric. For. Meteorol.* 237, 171–183. <https://doi.org/10.1016/j.agrformet.2017.01.011>.
- Asner, G.P., 1998. Biophysical and biochemical sources of variability in canopy reflectance. *Remote Sens. Environ.* 64, 234–253. [https://doi.org/10.1016/S0034-4257\(98\)00014-5](https://doi.org/10.1016/S0034-4257(98)00014-5).
- Awal, M.A., Koshi, H., Ikeda, T., 2006. Radiation interception and use by maize/peanut intercrop canopy. *Agric. For. Meteorol.* 139, 74–83. <https://doi.org/10.1016/j.agrformet.2006.06.001>.
- Baldocchi, D., Hutchison, B., Matt, D., McMillen, R., 1986. Seasonal variation in the statistics of photosynthetically active radiation penetration in an oak-hickory forest. *Agric. For. Meteorol.* 36, 343–361. [https://doi.org/10.1016/0168-1923\(86\)90013-4](https://doi.org/10.1016/0168-1923(86)90013-4).
- Baret, F., Hagolle, O., Geiger, B., Bicheron, P., Miras, B., Huc, M., Berthelot, B., Nino, F., Weiss, M., Samain, O., Roujean, J.-L., Leroy, M., 2007. LAI, fAPAR and fCover CYCLOPES global products derived from VEGETATION part 1: principles of the algorithm. *Remote Sens. Environ.* 110, 275–286. <https://doi.org/10.1016/j.rse.2007.02.018>.
- Carrer, D., Roujean, J.-L., Lafont, S., Calvet, J.-C., Boone, A., Decharme, B., Delire, C., Gastellu-Etcheberry, J.-P., 2013. A canopy radiative transfer scheme with explicit FAPAR for the interactive vegetation model ISBA-A-gs: impact on carbon fluxes. *J. Geophys. Res. Biogeosci.* 118, 888–903. <https://doi.org/10.1002/jgrg.20070>.
- Chen, J.M., 1996. Canopy architecture and remote sensing of the fraction of photosynthetically active radiation absorbed by boreal conifer forests. *IEEE Trans. Geosci. Remote Sens.* 34, 1353–1368. <https://doi.org/10.1109/36.544559>.
- D'Odorico, P., Gonsamo, A., Pinty, B., Gobron, N., Coops, N., Mendez, E., Schaepman, M.E., 2014. Intercomparison of fraction of absorbed photosynthetically active radiation products derived from satellite data over Europe. *Remote Sens. Environ.* 142, 141–154. <https://doi.org/10.1016/j.rse.2013.12.005>.
- Disney, M., Muller, J.-P., Kharbouche, S., Kaminski, T., Voßbeck, M., Lewis, P., Pinty, B., 2016. A New global fAPAR and LAI dataset derived from optimal Albedo estimates: comparison with MODIS products. *Remote Sens.* 8, 275.
- Fensholt, R., Sandholt, I., Rasmussen, M.S., 2004. Evaluation of MODIS LAI, fAPAR and the relation between fAPAR and NDVI in a semi-arid environment using in situ measurements. *Remote Sens. Environ.* 91, 490–507. <https://doi.org/10.1016/j.rse.2004.04.009>.
- Ganguly, S., Nemani, R.R., Baret, F., Bi, J., Weiss, M., Zhang, G., Milesi, C., Hashimoto, H., Samanta, A., Verger, A., Singh, K., Myneni, R.B., 2014. Green leaf area and fraction of photosynthetically active radiation absorbed by vegetation. In: Hanes, J.M. (Ed.), *Biophysical Applications of Satellite Remote Sensing*. Springer Berlin Heidelberg, Berlin, Heidelberg, pp. 43–61.
- Gobron, N., Pinty, B., Mélin, F., Taberner, M., Verstraete, M.M., Belward, A., Lavergne, T., Widlowski, J.L., 2005. The state of vegetation in Europe following the 2003 drought. *Int. J. Remote Sens.* 26, 2013–2020. <https://doi.org/10.1080/01431160412331330293>.
- Gower, S.T., Kucharik, C.J., Norman, J.M., 1999. Direct and indirect estimation of leaf area index, fAPAR, and net primary production of terrestrial ecosystems. *Remote Sens. Environ.* 70, 29–51. [https://doi.org/10.1016/S0034-4257\(99\)00056-5](https://doi.org/10.1016/S0034-4257(99)00056-5).
- Hovi, A., Lukeš, P., Rautiainen, M., 2017. Seasonality of albedo and FAPAR in a boreal forest. *Agric. For. Meteorol.* 247, 331–342. <https://doi.org/10.1016/j.agrformet.2017.08.021>.
- Huemrich, K.F., Privette, J.L., Mukelabai, M., Myneni, R.B., Knyazikhin, Y., 2005. Time-series validation of MODIS land biophysical products in a Kalahari Woodland, Africa. *Int. J. Remote Sens.* 26, 4381–4398. <https://doi.org/10.1080/01431160500113393>.
- Hutchison, B.A., Matt, D.R., McMillen, R.T.: Effects of sky brightness distribution upon penetration of diffuse radiation through canopy gaps in a deciduous forest, 22, 1980.
- Kobayashi, H., Suzuki, R., Nagai, S., Nakai, T., Kim, Y., 2014. Spatial scale and landscape heterogeneity effects on FAPAR in an open-canopy black spruce forest in interior Alaska. *IEEE Geosci. Remote Sens. Lett.* 11, 564–568. <https://doi.org/10.1109/LGRS.2013.2278426>.
- Leblanc, S., Chen, J., Kwong, M., 2002. Tracing Radiation and Architecture of Canopies. TRAC MANUAL Version 2.1.3.
- Leuchner, M., Hertel, C., Menzel, A., 2011. Spatial variability of photosynthetically active radiation in European beech and Norway spruce. *Agric. For. Meteorol.* 151, 1226–1232. <https://doi.org/10.1016/j.agrformet.2011.04.014>.
- Li, W., Weiss, M., Waldner, F., Defourny, P., Demarez, V., Morin, D., Hagolle, O., Baret, F., 2015. A generic algorithm to estimate LAI, FAPAR and FCOVER variables from SPOT4 HRVIR and landsat sensors: evaluation of the consistency and comparison with ground measurements. *Remote Sens.* 7, 15494.
- Majasalmi, T., Stenberg, P., Rautiainen, M., 2017. Comparison of ground and satellite-based methods for estimating stand-level fPAR in a boreal forest. *Agric. For. Meteorol.* 232, 422–432. <https://doi.org/10.1016/j.agrformet.2016.09.007>.
- Manninen, T., Stenberg, P., 2009. Simulation of the effect of snow covered forest floor on the total forest albedo. *Agric. For. Meteorol.* 149, 303–319. <https://doi.org/10.1016/j.agrformet.2008.08.016>.
- McCallum, I., Wagner, W., Schullius, C., Shvidenko, A., Obersteiner, M., Fritz, S., Nilsson, S., 2010. Comparison of four global FAPAR datasets over Northern Eurasia for the year 2000. *Remote Sens. Environ.* 114, 941–949. <https://doi.org/10.1016/j.rse.2009.12.009>.
- Meroni, M., Fasbender, D., Kayitakire, F., Pini, G., Rembold, F., Urbano, F., Verstraete, M., 2014. Early detection of biomass production deficit hot-spots in semi-arid environment using FAPAR time series and a probabilistic approach. *Remote Sens. Environ.* 142, 57–68. <https://doi.org/10.1016/j.rse.2013.11.012>.
- Mortazavi, S.H., Salehe, M., MacGregor, M.H., 2014. Maximum WSN coverage in environments of heterogeneous path loss. *Int. J. Sensor Networks* 16, 185–198. <https://doi.org/10.1504/ijnsnet.2014.066788>.
- Möttus, M., 2004. Measurement and modelling of the vertical distribution of sunflecks. *Penumbra Umbra Willow Coppice* 79–91.
- Möttus, M., Sulev, M., Frederic, B., Lopez-Lozano, R., Reinart, A., 2011. Photosynthetically active radiation. *Meas. Model.* 7970–8000.
- Myneni, R.B., Ramakrishna, R., Nemani, R., Running, S.W., 1997. Estimation of global leaf area index and absorbed par using radiative transfer models. *IEEE Trans. Geosci. Remote Sens.* 35, 1380–1393. <https://doi.org/10.1109/36.649788>.
- Nagelkerke, N.J.D., 1991. A note on a general definition of the coefficient of determination. *Biometrika* 78, 691–692. <https://doi.org/10.2307/2337038>.
- Nestola, E., Sánchez-Zapero, J., Latorre, C., Mazzenga, F., Matteucci, G., Calfapietra, C., Camacho, F., 2017. Validation of PROBA-V GEOV1 and MODIS C5 & C6 fAPAR products in a deciduous beech forest site in Italy. *Remote Sens.* 9, 126.
- Ollinger, S.V., 2011. Sources of variability in canopy reflectance and the convergent properties of plants. *New Phytol.* 189, 375–394. <https://doi.org/10.1111/j.1469-8137.2010.03536.x>.
- Pastorello, G., Sanchez-Azofeifa, G.A., Nascimento, M., 2011. *Enviro-net: from networks of ground-based sensor systems to a web platform for sensor data management*. *Sensors* 11, 6454.
- Pickett-Heaps, C.A., Canadell, J.G., Briggs, P.R., Gobron, N., Haverd, V., Paget, M.J., Pinty, B., Raupach, M.R., 2014. Evaluation of six satellite-derived fraction of absorbed photosynthetically active radiation (FAPAR) products across the Australian continent. *Remote Sens. Environ.* 140, 241–256. <https://doi.org/10.1016/j.rse.2013.08.037>.
- Pinty, B., Jung, M., Kaminski, T., Lavergne, T., Mund, M., Plummer, S., Thomas, E., Widlowski, J., 2011. L.: Evaluation of the JRC-TIP 0.01° products over a mid-latitude deciduous forest site. *Remote Sens. Environ.* 115, 3567–3581. <https://doi.org/10.1016/j.rse.2011.08.018>.
- Prince, S.D., Goward, S.N., 1995. Global primary production: a remote sensing approach. *J. Biogeogr.* 22, 815–835. <https://doi.org/10.2307/2845983>.
- Rahman, M.M., Lamb, D.W., Stanley, J.N., 2015. The impact of solar illumination angle when using active optical sensing of NDVI to infer fAPAR in a pasture canopy. *Agric. For. Meteorol.* 202, 39–43. <https://doi.org/10.1016/j.agrformet.2014.12.001>.
- Reifsnyder, W.E., Furnival, G.M., Horowitz, J.L., 1971. Spatial and temporal distribution of solar radiation beneath forest canopies. *Agric. Meteorol.* 9, 21–37. [https://doi.org/10.1016/0002-1571\(71\)90004-5](https://doi.org/10.1016/0002-1571(71)90004-5).
- Ross, J., Sulev, M., Saarelaid, P., 1998. Statistical treatment of the PAR variability and its application to willow coppice. *Agric. For. Meteorol.* 91, 1–21. [https://doi.org/10.1016/S0168-1923\(98\)00066-5](https://doi.org/10.1016/S0168-1923(98)00066-5).
- Senna, M.C.A., Costa, M.H., Shimabukuro, Y.E., 2005. Fraction of photosynthetically active radiation absorbed by Amazon tropical forest: a comparison of field measurements, modeling, and remote sensing. *J. Geophys. Res. Biogeosci.* 110. <https://doi.org/10.1029/2004JG000005>.
- Serrano, L., Gamon, J.A., Penuelas, J., 2000. Estimation of canopy photosynthetic and nonphotosynthetic components from spectral transmittance. *Ecology* 81, 3149–3162. <https://doi.org/10.2307/177407>.
- Sinclair, T.R., Knoerr, K.R., 1982. Distribution of photosynthetically active radiation in the canopy of a loblolly pine plantation. *J. Appl. Ecol.* 19, 183–191. <https://doi.org/10.2307/2403003>.
- Sonnentag, O., Hufkens, K., Teshera-Sterne, C., Young, A.M., Friedl, M., Braswell, B.H., Milliman, T., O'Keefe, J., Richardson, A.D., 2012. Digital repeat photography for phenological research in forest ecosystems. *Agric. For. Meteorol.* 152, 159–177. <https://doi.org/10.1016/j.agrformet.2011.09.009>.
- Steinberg, D.R., Goetz, S.J., Hyer, E.J., 2006. Validation of MODIS F/sub PAR/ products in boreal forests of Alaska. *IEEE Trans. Geosci. Remote Sens.* 44, 1818–1828. <https://doi.org/10.1109/TGRS.2005.862266>.
- Stenberg, P., Möttus, M., Rautiainen, M., 2016. Photon recollision probability in modeling the radiation regime of canopies — a review. *Remote Sens. Environ.* 183, 98–108. <https://doi.org/10.1016/j.rse.2016.05.013>.
- Tao, X., Liang, S., Wang, D., 2015. Assessment of five global satellite products of fraction of absorbed photosynthetically active radiation: intercomparison and direct validation against ground-based data. *Remote Sens. Environ.* 163, 270–285. <https://doi.org/10.1016/j.rse.2015.03.025>.
- Tao, X., Liang, S., He, T., Jin, H., 2016. Estimation of fraction of absorbed photosynthetically active radiation from multiple satellite data: model development and validation. *Remote Sens. Environ.* 184, 539–557. <https://doi.org/10.1016/j.rse.2016.07.036>.
- Ter-Mikaelian, M.T., Wagner, R.G., Bell, F.W., Shropshire, C., 1999. Comparison of photosynthetically active radiation and cover estimation for measuring the effects of interspecific competition on jack pine seedlings. *Can. J. For. Res.* 29, 883–889. <https://doi.org/10.1139/x99-088>.
- Venables, W.N., Ripley, B.D., 2002. *Modern Applied Statistics with S*. Springer-Verlag, New York.
- Verhoef, W., 1984. Light scattering by leaf layers with application to canopy reflectance modeling: the SAIL model. *Remote Sens. Environ.* 16, 125–141. [https://doi.org/10.1016/0034-4257\(84\)90057-9](https://doi.org/10.1016/0034-4257(84)90057-9).
- Wang, H., 2006. Extending the linear model with R: generalized linear, mixed effects and

- nonparametric regression models. In: In: Faraway, J.J. (Ed.), *Biometrics*, vol. 62 https://doi.org/10.1111/j.1541-0420.2006.00596_12.x. 1278–1278.
- Wang, Y., Xie, D., Liu, S., Hu, R., Li, Y., Yan, G., 2016. Scaling of FAPAR from the field to the satellite. *Remote Sens.* 8. <https://doi.org/10.3390/rs8040310>.
- Widlowski, J.-L., 2010. On the bias of instantaneous FAPAR estimates in open-canopy forests. *Agric. For. Meteorol.* 150, 1501–1522. <https://doi.org/10.1016/j.agrformet.2010.07.011>.
- Younis, M., Akkaya, K., 2008. Strategies and techniques for node placement in wireless sensor networks: a survey. *Ad Hoc Networks* 6, 621–655. <https://doi.org/10.1016/j.adhoc.2007.05.003>.
- Zacharias, S., Bogena, H., Samaniego, L., Mauder, M., Fuß, R., Pütz, T., Frenzel, M., Schwank, M., Baessler, C., Butterbach-Bahl, K., Bens, O., Borg, E., Brauer, A., Dietrich, P., Hajsek, I., Helle, G., Kiese, R., Kunstmann, H., Klotz, S., Munch, J.C., Papen, H., Priesack, E., Schmid, H.P., Steinbrecher, R., Rosenbaum, U., Teutsch, G., Vereecken, H., 2011. A network of terrestrial environmental observatories in Germany. *Vadose Zone J.* 10, 955.

3.2 Paper II: Accuracy assessment on the number of flux terms needed to estimate in situ fAPAR. In: International Journal of Applied Earth Observation and Geoinformation

Citation: BIRGITTA PUTZENLECHNER, PHILIP MARZAHN AND ARTURO SÁNCHEZ-AZOFEIFA (2019): *Accuracy assessment on the number of flux terms needed to estimate in situ fAPAR*. International Journal of Applied Earth Observation and Geoinformation, *under review*.

Journal: International Journal of Applied Earth Observation and Geoinformation (Elsevier), 88, 102061
5-year Impact Factor: 5.194

Status: published

Research Outline: This article builds on the findings of paper I by investigating uncertainties not only for two-flux FAPAR estimates, but also for three- and four-flux FAPAR estimates. Therefore, measurements of the TOC PAR albedo as well the albedo of the forest floor were carried out. In addition to that, the investigations were carried out in three different ecosystems: the mixed-coniferous forest of the site Graswang, Germany, the boreal-deciduous forest of the Peace River site, Canada, and the tropical dry forest (TDF) site at Santa Rosa, Costa Rica. As the four-flux FAPAR estimate considers the highest amount of flux terms to describe the canopy absorption in the PAR domain (i.e., only horizontal PAR fluxes are ignored), this quantity was assumed to be closest to “true FAPAR”. Uncertainty of two- and three-flux estimates was investigated by calculating the difference with the four-flux estimate. The resulting quantity is then referred to as bias. As the bias of certain FAPAR estimate is known to vary with environmental conditions both from previous RTM simulations (Widlowski, 2010) and the findings of Paper I, the influence of several environmental conditions was assessed. As a reference, the bias found was compared with the GCOS accuracy threshold set for FAPAR products of 10% (or 0.05) (GCOS, 2011). The paper addresses the following research questions:

Q1: How can the bias of instantaneous FAPAR observations be assessed in field-conditions?

Q2: Which environmental conditions are key sources of uncertainty in FAPAR ground observations?

Q4: What is the bias of FAPAR ground observations associated to the estimating scheme?

Scientific value: The paper presents the first examination of the bias of two- and three-flux estimates in field-conditions. In addition to that, previous RTM simulations have focused on one forest ecosystem only. In this regard, the findings close a knowledge gap and clarify under which condition a certain estimating approach should be used. Several practical recommendations for planning future experimental set-ups with direct PAR measurements are given.

Authors' contributions: Study conception and methodology were developed by BP. Acquisition and curation of data was carried out by BP and AS-A. Formal analysis and interpretation of data was carried out by BP. Supervision was given by AS-A. Funding was acquired by AS-A. Project administration was

carried out by all authors. The original draft was written by BP, while PM and AS-A commented and revised critically and thus contributed to the final draft.



Accuracy assessment on the number of flux terms needed to estimate in situ fAPAR



Birgitta Putzenlechner^a, Philip Marzahn^a, Arturo Sanchez-Azofeifa^{b,*}

^a Department of Geography, Ludwig-Maximilians University, Luisenstr. 37, 80333 Munich, Germany

^b Earth and Atmospheric Sciences Department, University of Alberta, 1-26 Earth Sciences Building, University of Alberta, Edmonton, T6G2E3, Alberta, Canada

ARTICLE INFO

Keywords:

fAPAR
 Fraction of absorbed photosynthetically active radiation
 Forest
 Wireless sensor network
 In situ
 Bias

ABSTRACT

The fraction of Absorbed Photosynthetically Active Radiation (fAPAR) is a crucial variable for assessing global carbon balances and currently, there is an urgent need for reference data to validate satellite-derived fAPAR products. However, it is well-known that fAPAR ground measurements are associated with considerable uncertainties. Generally, fAPAR measurements can be carried out with two-, three- and four-flux approaches, depending on the number of flux terms measured. Currently, not much is known about the number of flux terms needed to satisfactorily reduce systematic errors. This study investigates the accuracy of different fAPAR estimates based on permanent, 10-min PAR measurements using Wireless Sensor Networks (WSNs) at three forest sites, located in Central Europe (mixed-coniferous forest), North America (boreal-deciduous forest) and Central America (tropical dry forest). All fAPAR estimates reflect the seasonal course of fAPAR. The highest average biases of different fAPAR estimates account to 0.02 at the temperate, 0.08 at the boreal and -0.05 at the tropical site, respectively, thereby generally fulfilling the uncertainty threshold of a maximum of 10 % or 0.05 fAPAR units set by the Global Climate Observing System (GCOS, 2016). During high wind speed conditions at the boreal site, the bias of the two-flux fAPAR estimate exceeded the 0.05-uncertainty threshold. Three-flux fAPAR estimates were not found to be advantageous, especially at the tropical site. Our findings are beneficial for the development of sampling protocols that are needed to validate global satellite-derived fAPAR products.

1. Introduction

Accurate estimates of biophysical variables such as the fraction of Absorbed Photosynthetically Active Radiation (fAPAR) are crucial input variables for many climate and biophysical models (Faticchi et al., 2016; Ryu et al., 2019). By linking available Photosynthetic Active Radiation (PAR) in the wavelength region between 400 and 700 nm to the absorption of plants (Gobron and Verstraete, 2009), fAPAR quantifies the status and dynamics of vegetation and is involved in many ecosystem processes (Möttus et al., 2011). Thus, fAPAR has been considered as one of the terrestrial Essential Climate Variables (ECVs) by the Global Climate Observing System (GCOS) (GCOS, 2011, GCOS, 2016). Long-term observations of fAPAR are required for assessing and understanding global carbon balances which are an important constraint in understanding global change (Prince and Goward, 1995; Xiao et al., 2018). On the one hand, continuous and spatially distributed reflectance measurements of vegetation by satellite remote sensing have led to an increasing availability of global fAPAR datasets (MODIS products by Myneni et al. (2002) and Pinty et al. (2011); SPOT VEGETATION

product by Baret et al. (2011); SPOT VEGETATION & PROBAV products by Camacho et al. (2013); Sentinel-2 product by Weiss and Baret (2016)) and the development of product enhancements and new retrieval algorithms is ongoing (e.g., Cammalleri et al., 2019; Disney et al., 2016; Gitelson, 2019; Li et al., 2017a; Liu et al., 2019, 2018). On the other hand, studies on the validation of global fAPAR products have reported discrepancies against in situ estimates based on various (measurement) approaches (D'odorico et al., 2014; Martínez et al., 2013; McCallum et al., 2010; Pickett-Heaps et al., 2014; Pinty et al., 2011; Tao et al., 2015) that exceed the current uncertainty requirements set by the Global Climate Observing System (GCOS) for fAPAR products, which is the maximum value between 10 % and 0.05 fAPAR units for spatially distributed fAPAR products (i.e. maps) (GCOS, 2011, GCOS, 2016). Discrepancies between different fAPAR products have been mainly attributed to a priori assumptions on the biome type and assumed scattering properties as well as different underlying fAPAR definitions (Pickett-Heaps et al., 2014). In this regard, it should be noted that satellite-derived fAPAR products based on RTM simulations often relate to absorption by green vegetation elements only, referred to

* Corresponding author.

E-mail address: arturo.sanchez@ualberta.ca (A. Sanchez-Azofeifa).

as “green fAPAR” (GCOS, 2011). However, in field conditions, PAR radiation is also attenuated by trunks and branches so that measurements obtained by PAR sensors consider the absorption of all vegetation components and thus relate to the concept of “total fAPAR” (GCOS, 2011). Another difference related to the definition of fAPAR that is often found in satellite-derived fAPAR products relates to the direction of the illumination source. Whereas “black-sky” fAPAR considers only direct light, “white-sky fAPAR” results from diffuse radiation only (GCOS, 2011). Typically, satellite-derived fAPAR products only consider “black-sky fAPAR”, whereas direct PAR measurements also contain “white-sky fAPAR” (Liu et al., 2019).

Several studies have emphasized that discrepancies between fAPAR products are highest in forest ecosystems (D’odorico et al., 2014; McCallum et al., 2010; Pickett-Heaps et al., 2014; Tao et al., 2015) and particularly high in tropical forest regions (Xiao et al., 2018; Xu et al., 2018). To improve current retrieval algorithms and radiative transfer models (RTMs), several recent studies have emphasized the need for fAPAR ground observations in forest ecosystems (Gobron, 2015; Xu et al., 2018). However, ground observations of fAPAR that are needed for validation studies are generally scarce and compromised in two respects: First, indirect measurement techniques are used, such as fAPAR retrieved from digital hemispherical photography (DHP) (Li et al., 2015; Liu et al., 2019), LAI (Fensholt et al., 2004; Pinty et al., 2011) or fractional (vegetation) cover (Liu and Treitz, 2018; Pickett-Heaps et al., 2014). Recently, more modeling approaches have been preferred (Majasalmi et al., 2017; Wu et al., 2018). Second, existing experimental set-ups for direct fAPAR measurements with the aim of validating satellite-derived products often lack representative sample sizes as only few PAR sensors are used (e.g., D’odorico et al., 2014; Tao et al., 2015). It is well-known that fAPAR varies considerably across different ecosystems and within single forest stands (Leuchner et al., 2011; Ollinger, 2011; Putzenlechner et al., 2019a) so that multiple samples are required (Reifsnnyder et al., 1971; Widlowski, 2010).

In theory, direct measurements of fAPAR would require measuring all five flux components of radiative transfer in canopies: incoming PAR, top-of-canopy reflected PAR, transmitted PAR through the canopy, PAR reflected from the soil and PAR fluxes entering the target canopy horizontally (Widlowski et al., 2006). As capturing all five quantities is unfeasible with currently available measurement techniques, fAPAR is estimated by ignoring certain flux terms or making assumptions upon. Depending on the number of flux terms being measured, direct fAPAR measurements are distinguished into two-, three- and four-flux estimates (Widlowski, 2010): The four-flux fAPAR (fAPAR₄) estimate ignores horizontal PAR fluxes; the three-flux fAPAR (fAPAR₃) estimate makes assumptions on PAR reflected from the background by either assuming PAR reflected from the background to equal to top-of-canopy reflected PAR (fAPAR₃₍₁₎) or by ignoring PAR reflected from the background (fAPAR₃₍₂₎); the two-flux fAPAR estimate (fAPAR₂) only considers incoming PAR and transmitted PAR through the canopy.

In general, it is known that depending on the selected fAPAR estimate and environmental conditions, in situ fAPAR will be affected by a considerable bias (Widlowski, 2010). In simulations with RTMs, it has been shown that the accuracy of fAPAR measurements depends on illumination conditions, seasonal changes in leaf color as well as changes in albedo of the forest surface (Widlowski, 2010). As for illumination conditions, it has been confirmed in field experiments (Leuchner et al., 2011; Putzenlechner et al., 2019b) that fAPAR estimates are affected by a considerable bias under high solar zenith angles (SZA) (i.e., above 60°) when the ratio of diffuse radiation to incident radiation is low, especially at conifer-dominated forest stands (Majasalmi et al., 2017; Putzenlechner et al., 2019a; Widlowski, 2010). As horizontal fluxes are ignored in all fAPAR estimates, the bias due to SZA can be limited by preferring fAPAR acquired during diffuse light conditions or, more practicable for validation activities, fAPAR acquired closely around the solar noon when SZA is lowest. Concerning the accuracy of fAPAR₂, it

has been simulated and observed in field conditions that the accuracy of fAPAR₂ is affected by seasonal changes in leaf color (i.e. during senescence period), with a possible influence also of wind speed (Putzenlechner et al., 2019b). Among various fAPAR estimators investigated in RTM simulations, fAPAR₂ was found to perform best in open forest canopies under typical summer conditions (Widlowski, 2010). These findings, however, seem to be in contrast with the current scientific practice based on available tower-base top-of-canopy reflected PAR. In this regard, the majority of studies using direct fAPAR measurements has preferred to perform three-flux measurements (D’odorico et al., 2014; Nestola et al., 2017; Rankine et al., 2014; Senna et al., 2005; Tao et al., 2015). Given the diversity of experimental set-ups used for direct fAPAR measurements in existing studies (Liu and Treitz, 2018; Nestola et al., 2017; Putzenlechner et al., 2019a; Senna et al., 2005; Steinberg et al., 2006; Tao et al., 2015; Ter-Mikaelian et al., 1999), there seems to be no overall consensus on which measurement approach, i.e. considering two-, three or four flux terms for the estimation of fAPAR, to choose. Thus, it becomes clear that the current situation is characterized by a lack of both well-defined field protocols and understanding of uncertainties involved in fAPAR measurements (Gobron, 2015).

During the last decade, WSNs have opened up new possibilities in environmental monitoring by ensuring cost and labor efficient options for multi-sensor and multi-temporal sampling also in forest ecosystems (Pastorello et al., 2011). Although WSNs have already demonstrated their potential for fAPAR observations and the validation of satellite-derived fAPAR products (Nestola et al., 2017; Putzenlechner et al., 2019a), WSN with multiple PAR sensors have not been used to evaluate the accuracy of two-, three and four-flux estimating schemes. Thus, former studies could not refer to any practical guidelines for sampling protocols on how to select a certain estimating scheme. To bridge this gap, the aim of this study is to assess the bias involved in different fAPAR estimates with direct PAR measurements using WSNs at three different forest sites: a temperate mixed-coniferous forest in Central Europe, Germany, a boreal-deciduous forest in Alberta, Canada and a tropical dry forest (TDF) in Costa Rica. Given existing findings from RTMs (Widlowski, 2010) and first experiences with uncertainties of two-flux fAPAR observations available at the temperate site (Putzenlechner et al., 2019b), one could assume that the two-flux fAPAR estimate does not exceed the uncertainty requirements set by the GCOS (2016). Thus, we will assess the hypothesis that the absolute differences between two- and three-flux estimates compared to the four-flux estimate remain within 0.05 in fAPAR units during the vegetation period irrespective of the type of ecosystem. Our approach follows the underlying assumption that the four-flux approach is very close to “true” fAPAR. Our main objectives were then to a) perform permanent, multi-sensor two-, three- and four-flux fAPAR measurements, b) assess the estimation bias associated with different fAPAR estimates and c) assess and evaluate uncertainties associated with certain seasonal or environmental conditions that have been found to lead to bias, such as the presence of colored autumn leaves, snow covered forest floor, or higher wind speeds. Our evaluation on the bias involved in different fAPAR estimating schemes in three different forest ecosystems will improve the knowledge on uncertainties involved in fAPAR ground estimates. We will also derive practical recommendations on how to improve experimental set-ups and sampling protocols needed to validate satellite-derived fAPAR products.

2. Materials and methods

2.1. Study sites

Permanent fAPAR observations were carried out in three different forest ecosystems: a mixed-coniferous forest in Central Europe, a boreal-deciduous forest in North America and a tropical dry forest (TDF) in Central America (Fig. 1). The European site “Graswang” is

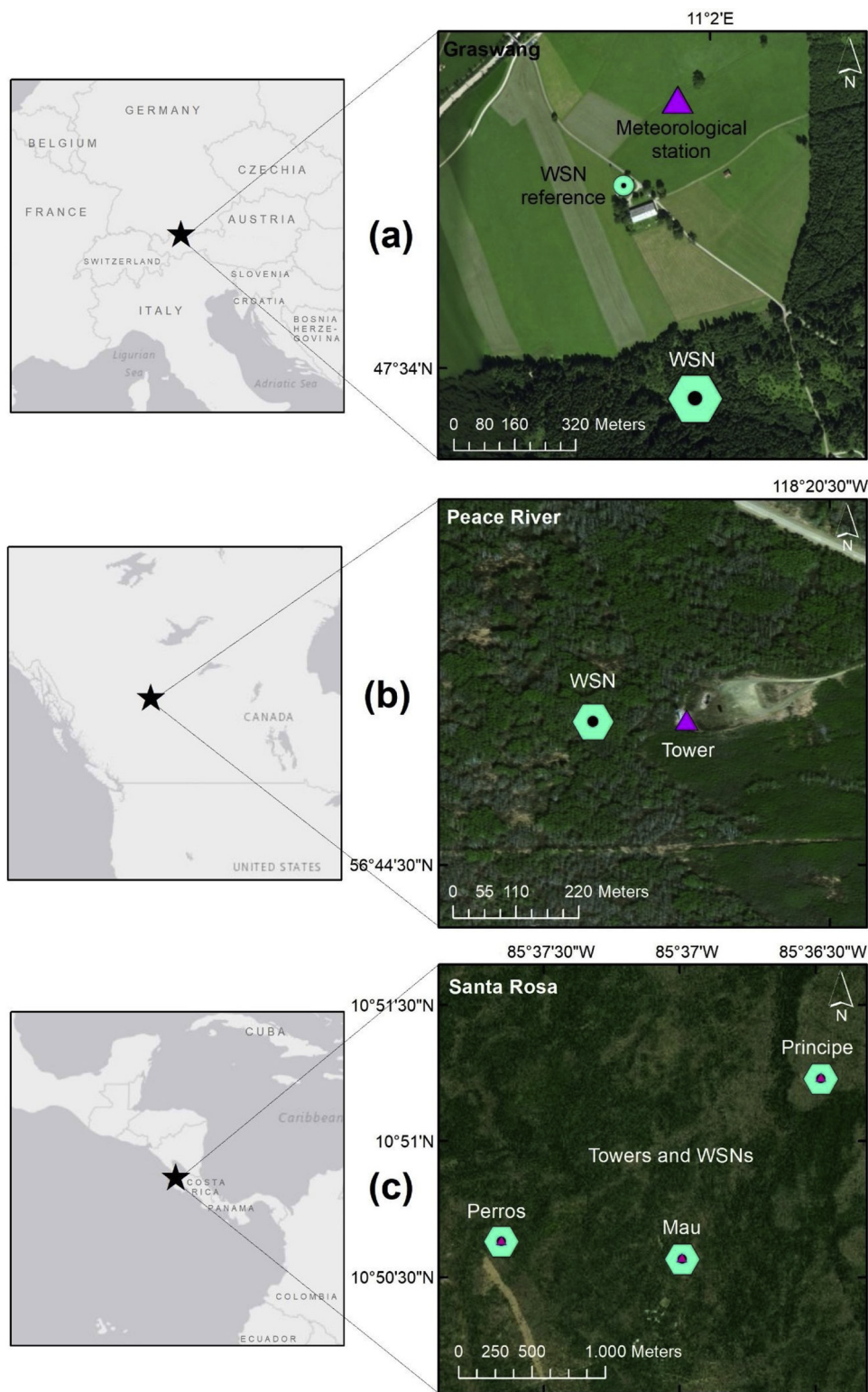


Fig. 1. Locations and set-up of the three WSN study sites for permanent fAPAR observations: (a) Graswang, (b) Peace River and (c) Santa Rosa. Hexagonal symbols refer to WSNs, triangles refer to towers with meteorological and carbon/water flux eddy covariance stations.

located in Southern Germany in a sub-alpine valley and comprises a mid-aged forest stand composed of both conifers (82 % Norway spruce/*Picea abies* (L.) H.Karst) and broadleaf tree species (14 % European beech/*Fagus sylvatica* L., 4 % sycamore maple/*Acer pseudoplatanus* L.). The understorey vegetation comprises low growing herbs not taller than 30 cm (i.e., wood sorrel/*Oxalis acetosella* L., dog's mercury/*Mercurialis perennis* L.). Climate is warm-temperate and fully humid,

with a vegetation period typically starting in late April and ending in late September. Snowfall occurs frequently throughout the dormant period. The site is part of the pre-Alpine TERENO research observatories (Zacharias et al., 2011). In addition to existing environmental monitoring equipment (e.g. meteorological station outside the forest) (Zeeman et al., 2017), the site was equipped with a WSN of PAR sensors to carry out permanent fAPAR observations (Putzenlechner

et al., 2019b). A forest inventory revealed that average tree height accounted 15 m, stem density and basal area accounted 231 stems $(0.1 \text{ ha})^{-1}$ and $4.8 \text{ m}^2 (0.1 \text{ ha})^{-1}$, respectively.

The North American “Peace River Environmental Monitoring Super Site” (“Peace River”) is located in Northern Alberta, Canada (Fig. 1) and comprises an old-growth boreal-deciduous forest stand with tree heights reaching up between 15 and 20 m (Rankine et al., 2014; Taheriazad et al., 2016). The forest stand is dominated by trembling aspen (*Populus tremuloides Michx.*) which is typical for the Northern Albertan biome of aspen parkland (Parks, 2006). The understory vegetation comprises a second vertical layer of canopy (predominantly mountain alder/*Alnus crispa*, prickly rose/*Rosa acicularis Lindl.*), reaching up to 4 m (Rankine et al., 2014). Average tree height accounts to 27 m, basal area and stem density is $4.1 \text{ stems } (0.1 \text{ ha})^{-1}$ and $2.4 \text{ m}^2 (0.1 \text{ ha})^{-1}$, respectively. The climate can be classified as humid-continental, with cool summers and snowy winters and thus a relatively short vegetation period, typically spanning from mid of May to mid of September. The site is part of the joint industry-research forestry region for Ecosystem Management Emulating Natural Disturbance (EMEND) for large-scale boreal forest preservation and harvest experimentation (Spence and Volney, 1999). Besides the WSN, the site comprises a 30 m tall flux tower for detailed meteorological and carbon/water flux observations.

The Central American “Santa Rosa National Park Environmental Monitoring Super Site” (“Santa Rosa”) is located in the Province of Guanacaste, Costa Rica (Fig. 1) and comprises a TDF under different levels of successional stages. In the tropical-monsoonal climate, vegetation period spans typically from May to December, followed by a 5-months dry season. Annual precipitation is approx. 1750 mm but can be highly variable Kalacska et al., 2004). Before the area became a conservation area in 1971, Santa Rosa was a cattle ranch. Today, the park is a mosaic of forests under different successional stages of secondary dry forests (Li et al., 2017b). For this study, we used data from three sub-sites, named “Kakubari”, “Perros” and “Principe” which are all located in TDF of an intermediate successional stage. This stage is characterized by two layers of canopy with a large variety of deciduous and few evergreen species (e.g., bastard cedar/*Guazama ulmifolia Lam.*, *Luehea speciosa Willd.*, *Lonchocarpus minimiflorus Donn. Smith*, *Byrsonima crassifolia (L.) Kunth*) and an understory composed of lianas and shade tolerant species (e.g., *Amphilophium paniculatum (L.) Kunth*, *Davilla kunthii A. St.-Hil.*, *Annona reticulata L.*, *Ocotea veraguensis (Meisn.) Mez*, *Hirtella racemosa Lam.*) (Arroyo-Mora et al., 2005; Kalacska et al., 2004). In a forest inventory, average tree height and basal area for all three sub-sites accounted 10–15 m, 120 stems $(0.1 \text{ ha})^{-1}$ and $1.9 \text{ m}^2 (0.1 \text{ ha})^{-1}$, respectively. All sub-sites are equipped with 35–40 m high carbon flux towers, each of them surrounded by a WSN (“Kakubari”, “Perros” and “Principe”, Fig. 1).

2.2. Wireless sensor networks for permanent fAPAR observations

At all three sites, WSNs were deployed for permanent fAPAR observations. The set-up for fAPAR observations included commercially available quantum PAR sensors (model SQ-110, Apogee, Logan, UT, USA; field of view 180° ; uncertainty estimates: cosine response $\pm 5\%$ at 75°SZA , temperature response $0.06 \pm 0.06\%$ per $^\circ\text{C}$, calibration uncertainty $\pm 5\%$ and non-stability $< 2\% \text{ y}^{-1}$) that were connected to self-powered nodes (model ENV-Link-Mini-LXRS, LORD MicroStrain, Cary, NC, USA). The configuration of the WSNs and scheduled data downloads during maintenance activities were carried out with a portable receiver (frequencies ranging from 2.405 GHz to 2.480 GHz). This “base station” was equipped with USB interface (model WSDA-Base-104 USB Base Station, MicroStrain, Cary, NC, USA) so that it can be connected to a portable computer equipped with the software “Node Commander” for network configuration and downloads (version 2.17.0, LORD MicroStrain, Cary, NC, USA). Due to the reduced accessibility of the sites Peace River and Santa Rosa, data aggregation was also carried

out operationally with a base station equipped with an outdoor receiver (model WSDA-1000 Wireless Sensor Data Aggregator, MicroStrain, Cary, NC, USA) positioned on the towers. A cellular GSM modem pointed at the nearest cellular tower enabled internet access most of the times and a battery bank (200 Ah) combined with solar panels (75 W) ensured power supply (Pastorello et al., 2011; Rankine et al., 2014). At all sites, WSN nodes were configured to measure instantaneous PAR every 10 min synchronously ($\sim 1 \text{ ns}$). Data was uploaded to “Enviro-Net” (<http://www.enviro-net.org/>), a web platform for sensor data management, near real-time visualization and analysis (Pastorello et al., 2011). For this study, PAR data acquired at the three study sites during the respective vegetation periods of the year 2016 was used.

2.2.1. Measurements of incoming and transmitted PAR

Sensors for monitoring incoming (PAR_{in}) and transmitted PAR ($\text{PAR}_{\text{trans}}$) were installed directed upward and mounted on wooden poles at 1.3 m height to avoid influences from ground-level vegetation. Angle connectors were used to ensure correct leveling of sensors. At Graswang, the reference sensor for PAR_{in} was located on open grassland (Fig. 1c), while it was measured right above the WSNs on towers at Peace River and Santa Rosa Environmental Monitoring Super Sites (Fig. 1a-b). All sensors for $\text{PAR}_{\text{trans}}$ were deployed in hexagonal geometry (Fig. 2) since this sampling scheme has been found to ensure signal quality and connectivity (Mortazavi et al., 2014; Younis and Akkaya, 2008) while at the same time maximizing the sensing area covered by a given number of nodes which, in turn, is important to reduce sampling bias (Widlowski, 2010). From previous investigations on the spatial variability of the radiation field in forests, it is known that fAPAR will depend mainly on the chance of sensor location when less than ten nodes are used for calculating the domain fAPAR (Putzenlechner et al., 2019b; Widlowski, 2010). To ensure the representativity of domain fAPAR, we deployed a minimum of 16 sensors per site. $\text{PAR}_{\text{trans}}$ was acquired with 16 sensors at Graswang, 22 sensors at Peace River and 35 sensors at Santa Rosa (19 at “Kakubari”, 10 at

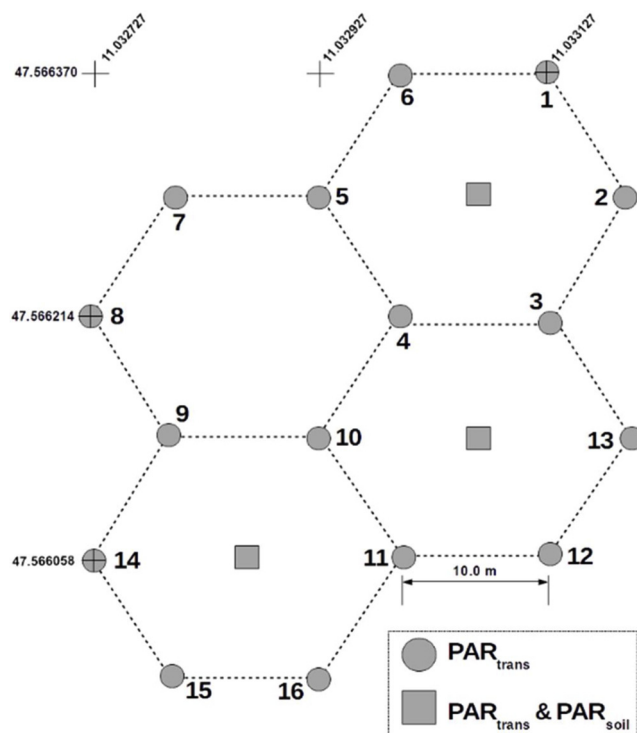


Fig. 2. Example of the experimental setups of the WSN nodes, consisting of a hexagonal sampling scheme; at the temperate site Graswang, the WSN consisted of 16 nodes with sensors for transmitted PAR and three nodes for transmitted and soil-reflected PAR to calculate the forest background albedo (R_{soil}).

“Principe” and 6 at “Perros”), respectively. As average canopy heights are different among the study sites, we considered different spatial footprints of PAR_{trans} measurements by deploying WSN nodes with 20 m spacing at Peace River and Santa Rosa and 10 m spacing at Graswang.

2.2.2. Observations of top-of-canopy PAR albedo

Observations of top-of-canopy PAR albedo (R_{TOC}) are required to calculate three- and four-flux $fAPAR$ estimates. Ideally, R_{TOC} is determined continuously for each timestep from the following equation:

$$R_{TOC_n} = \frac{1}{n} \sum_{i=1}^n \frac{PAR_{TOC_i}}{PAR_{in_i}} \quad (1)$$

With sensor location i , number of sensors n , PAR_{TOC} as PAR reflected upward from top-of-canopy and PAR_{in} as incoming PAR. At the sites Peace River and Santa Rosa (including sub-sites “Kakubari”, “Perros” and “Principe”), R_{TOC} was determined continuously every 10 min at the 30 m high flux towers with two opposite quantum PAR sensors connected to an environmental monitoring node which was synchronized with all WSN observations. At Graswang, the installation of a tower was not possible due to site-specific legal restrictions. Instead, R_{TOC} was approximated by PAR observations carried out with an Unmanned Aircraft Vehicle (UAV) (Brody et al., 2017) twice per year to cover the partly and fully foliated vegetation periods (Appendix A, Table A1). Therefore, an environmental monitoring node with a downward looking PAR sensor was mounted onto a commercially available hexacopter (model DJI F550 Flame Wheel, DJI Innovations, Shenzhen, China) to measure the reflected PAR above the canopy at 1 Hz temporal resolution. The hexacopter was equipped with an autopilot (Pixhawk, 3DR, Berkeley, USA) and an external GPS (LEA-6 u-blox 6, u-blox, Thalwil, Switzerland). Flight specific data was logged on board (altitude angles as well as engine output at 10 Hz, the accelerometer and gyroscope data at 50 Hz and GPS at 5 Hz), temporally aggregated to 1 Hz and joined with the PAR measurements. The takeoff weight including devices for PAR measurements accounted to approx. 2 kg which limited battery life and thus flight durations to 10 min. The UAV was programmed to aim for a relative altitude around 35 m after departure to ensure a vertical distance of 20 m to the tree crowns. As the UAV was started from the grassland approx. 100 m away from the area occupied by the WSN, the geo-coordinates tracked by the onboard GPS systems were used to select the timesteps for which the device was flying right above the WSN. For R_{TOC} , the ratio between PAR_{TOC} (as acquired during flights) and PAR_{in} (on the grassland) was calculated. To avoid influences of different illumination conditions resulting from moving clouds, flights were only carried out during clear sky conditions. Further, flights could not be carried out during high wind speeds or diffuse illumination conditions due to poor visibility of the UAV. Finally, the mean of the resulting four values for R_{TOC} (Appendix A, Table A1), which accounted to 0.03, was used as constant to calculate the four-flux $fAPAR$ estimate at Graswang.

2.2.3. Observations of forest background PAR albedo

Permanent observations of forest background albedo (R_{soil}) are needed to calculate the four-flux $fAPAR$ estimate. Therefore, measurements of PAR reflected from the forest soil (PAR_{soil}) were carried out with downward directed PAR sensors with 10 min sampling interval (synchronized with all other WSN observations). The forest background PAR albedo R_{soil} for the whole site for each timestep was calculated as follows:

$$R_{soil} = \frac{1}{n} \sum_{i=1}^n \frac{PAR_{soil_i}}{PAR_{trans_i}} \quad (2)$$

With sensor location i , number of sensors n , PAR_{soil} as PAR reflected upward from the forest floor and PAR_{trans} as transmitted PAR from the canopy.

At Graswang, three WSN nodes were installed at 3 m height across the area covered by the WSN (Fig. 1d, Fig. 2). Measurements of PAR_{soil} were amended by another sensor for PAR_{trans} pointed upward into the leafy canopy. The nodes with the two opposite quantum PAR sensors were covered and protected from weathering in plastic boxes that were attached to four neighboring trees with solid plastic ropes, respectively. Correct leveling of the constructions was checked every 10–20 days. At the Peace River and Santa Rosa Environmental Monitoring Super Sites, installations in trees were not possible due to various site/ecosystem constraints. Specifically, constructions hanging in trees were devastated by wildlife (i.e., bears) shortly after their installation at Peace River and too difficult to install and maintain at Santa Rosa due to the poor accessibility of the forest due to the natural occurrence of lianas. In addition to these practical reasons, the presence of two distinct vertical layers of canopy and especially its high volumetric variability in the TDF would have complicated the selection of representative areas for measuring forest background albedo from several meters above the forest floor. Instead, downward directed PAR_{soil} sensors were mounted at three nodes for PAR_{trans} of the WSNs at Peace River and 6 at Santa Rosa (i.e. at sub-site “Kakubari”), respectively.

2.2.4. Processing of PAR data and calculation of $fAPAR$ estimates

Before calculating $fAPAR$ estimates, site-specific pre-processing of PAR data was carried out for data acquired at the site Graswang. Due to the surrounding slopes, we had to consider that the WSN was periodically affected by topographic shadowing. Therefore, potentially affected time steps were determined and deleted for each sensor location based on the solar position and a Digital Elevation Model (DEM 5 m, Free State of Bavaria, <https://www.ldbv.bayern.de>) using the R-package “insol” (Corripio, 2003). As the WSNs at Santa Rosa and Peace River are located on relatively flat terrain, topographic shadowing did not occur. At Graswang site, we also had to consider that moving clouds may cause bias in $fAPAR$ estimates, as sensors for PAR_{in} and PAR_{trans} are separated by 300 m. For the case that the reference sensor outside the forest was shadowed by clouds, we checked whether PAR_{trans} exceeded PAR_{in} and eliminated respective timesteps from the dataset. Regarding Peace River and Santa Rosa Environmental Monitoring Super Sites, we assumed errors caused by cloud shadowing to be negligible as PAR_{in} and PAR_{TOC} were acquired on flux towers adjacent to sensors for PAR_{trans} and PAR_{soil} .

Subsequently, PAR measurements carried out at 10 min temporal resolution were processed to two-, three- and four-flux $fAPAR$ estimates. The domain-level (i.e. representative for one study site) two-flux $fAPAR$ estimate $fAPAR_{2n}$ was calculated as follows:

$$fAPAR_{2n} = \frac{1}{n} \sum_i^n 1 - \frac{PAR_{trans_i}}{PAR_{in_i}} \quad (3)$$

with sensor location i , number of sensors n , PAR_{trans} as PAR transmitted through the canopy and PAR_{in} as incoming PAR. For the domain-level three-flux $fAPAR$ estimates ($fAPAR_{3n}$), we distinguished into $fAPAR_{3(1)n}$ (hypothesis: $R_{soil} = R_{TOC}$) and $fAPAR_{3(2)n}$ (hypothesis: $R_{soil} = 0$) which were calculated as follows:

$$fAPAR_{3(1)n} = \frac{1}{n} \sum_i^n (1 - R_{TOC_n}) \left(1 - \frac{PAR_{trans_i}}{PAR_{in_i}}\right) \quad (4)$$

$$fAPAR_{3(2)n} = \frac{1}{n} \sum_i^n 1 - R_{TOC_n} - \frac{PAR_{trans_i}}{PAR_{in_i}} \quad (5)$$

with top-of-canopy PAR albedo R_{TOC} . The domain-level four-flux $fAPAR$ estimate $fAPAR_{4n}$ was calculated as follows:

$$fAPAR_{4n} = \frac{1}{n} \sum_i^n 1 - R_{TOC_n} - \frac{PAR_{trans_i}}{PAR_{in_i}} (1 - R_{soil_n}) \quad (6)$$

with PAR albedo of the forest floor R_{soil} .

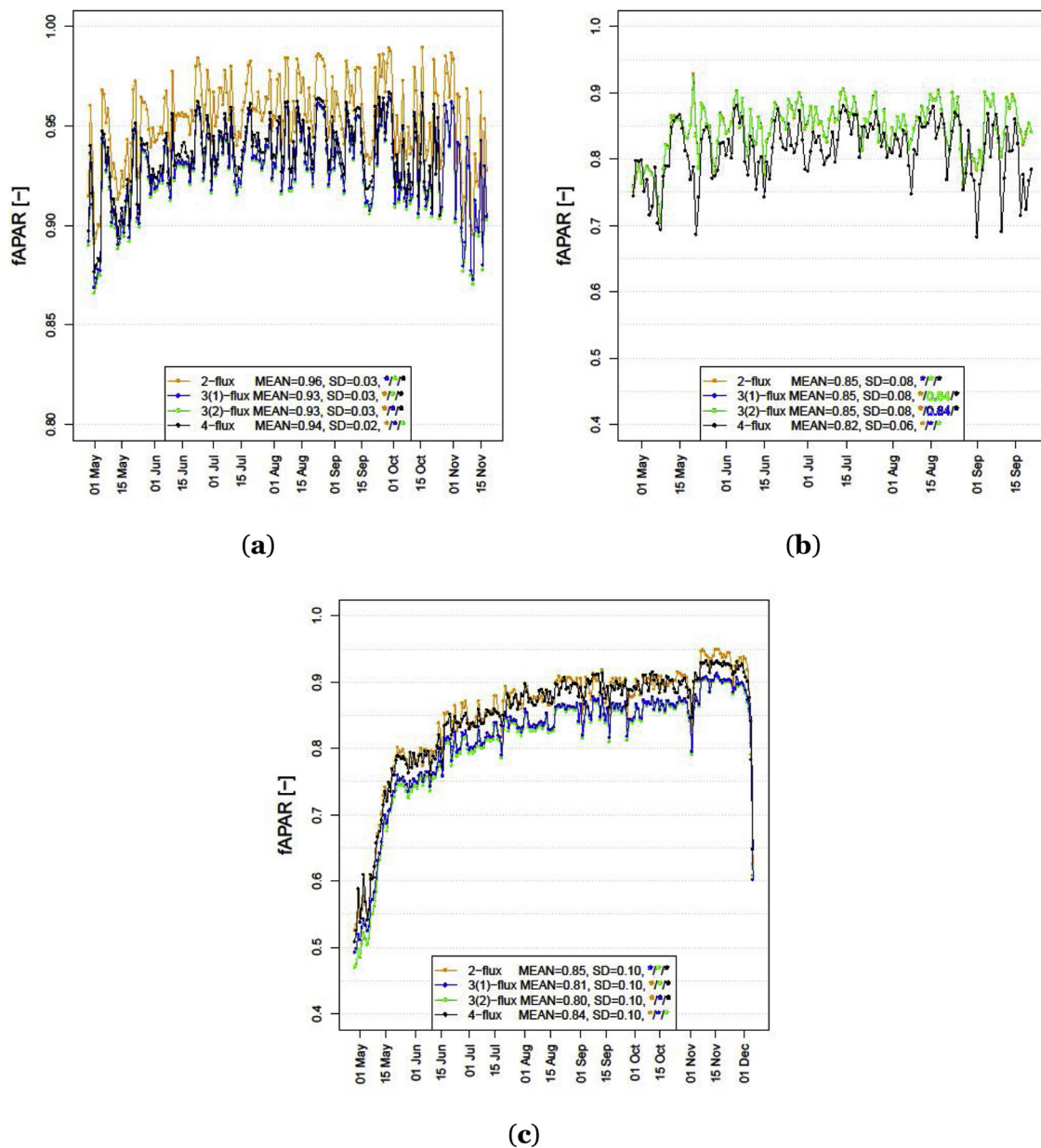


Fig. 3. Seasonal course of daily aggregated two-, three- and four-flux 10-min fAPAR estimates at the three study sites for the year 2016 at (a) Graswang, (b) Peace River and (c) Santa Rosa. Note that value ranges on y-axis are different for (a) compared to (b, c). The legend shows MEAN, SD of the whole time series and gives p-values obtained from a KS test for pairs of fAPAR distributions, with * indicating $p < 0.05$; the colors indicate pairs of comparison.

2.3. Meteorological and phenological observations

At Graswang, records of wind speed were used from the TERENO meteorological station (model WXT520, Vaisala, Vantaa, Finland) on open grassland (Appendix B, Figure B1a). Information on forest phenology and the occurrence of snow were retrieved from an automated camera (model SnapShot Mini 5.0, Dörr, Neu-Ulm, GER) installed at 1.3 m height and directed horizontally towards the center of the WSN in the forest. Based on visual inspection of daily photos, we classified the phenological status of the canopy as “no leaves”, “green leaves”, “yellow leaves” and “red leaves”. Regarding the factor snow, we distinguished into no occurrences of snow (“no”) and partly or closed snow cover (“yes”). Dates and representative photos for these conditions are shown in Appendix C (Table C1, Table C2, Figure C3). At Peace River, wind speed was acquired with the meteorological station (HOBO Energy Pro, OneTemp Pty Ltd, Adelaide, AU) at the flux tower above the forest. At Santa Rosa, records were taken at the towers of each of the

sub-sites (same product specification as at Peace River). As the environmental conditions and circumstances at Peace River and Santa Rosa did not allow for permanent observations with automated cameras, the phenological status was approximated by subletting the fAPAR observations by season, i.e. acquired during fully foliated season (i.e., Peace River: 01 Jun-31 Aug; Santa Rosa: 01 Jun-30 Sep) and partly or defoliated season (i.e., rest of available fAPAR time series).

2.4. Statistical analysis

This study assessed and explored absolute and relative differences between fAPAR estimates ($fAPAR_2$, $fAPAR_3$, $fAPAR_4$) and the influence of phenological and meteorological conditions upon these differences. This was done by the means of statistical testing, calculation of performance metrics and a multifactorial ANOVA. To test fAPAR distributions up on equality of distributions as null hypothesis (0.05-significance level), the nonparametric Kolmogorov-Smirnov test (KS test)

was applied. Further, a correlation analysis between different fAPAR estimates was performed using BIAS and R2 as performance metrics. For assessing systematic relative offsets, we calculated the mean difference between value pairs (BIAS), i.e. the average tendency of fAPAR₂ and fAPAR₃ estimates to be larger or smaller than the fAPAR₄ estimate. Note that we considered fAPAR₄ as reference (“closest to truth”) as it incorporates the highest number of measured flux terms of the radiative equation for fAPAR. We compared BIAS following the uncertainty requirements set by the GCOS (2016), demanding an uncertainty of the maximum between 10 % and 0.05 (“MAX(10 %; 0.05)”) for spatially distributed fAPAR products (i.e., maps). In our study, the 0.05-threshold was chosen as a fixed baseline as our dataset is based on point measurements (not maps, as defined by the GCOS) and thus contained single timesteps for fAPAR values acquired at individual sensor locations below 0.05, especially during early and late vegetation period. Further, we calculated the squared Pearson correlation coefficient (R²) to indicate the goodness of fit regarding a linear regression model between fAPAR₂ or fAPAR₃ estimates and fAPAR₄.

A multifactorial analysis of variation (ANOVA) was applied to evaluate the effect of environmental conditions on the difference of fAPAR estimates. As high wind speeds occurred less frequently at all three sites and high wind speeds have been suspected to decrease observed fAPAR values in previous investigations (Putzenlechner et al., 2019b), we classified wind speed data into two levels: wind speed < 2 ms⁻¹ and wind speed ≥ 5 ms⁻¹. As detailed phenological and meteorological observations were available at Graswang, we investigated the influence of leaf status, occurrence of snow and (classified) wind speed as factors on the difference between fAPAR₂ or fAPAR₃ and fAPAR₄ at each 10-min timestep (bias_{2to4}, bias_{3(1)to4}, bias_{3(2)to4}), respectively. At the sites Peace River and Santa Rosa, we investigated the influence of season (only distinguished into levels “fully foliated” and “partly foliated/defoliated”) and (classified) wind speed on bias_{2to4}, bias_{3(1)to4}, bias_{3(2)to4}, respectively. Significant differences in respective values of bias_{2to4}, bias_{3(1)to4}, or bias_{3(2)to4} according to environmental conditions were identified from *F*- and respective *p*-values.

3. Results

3.1. Seasonal dynamics of different fAPAR estimates and bias

The permanent monitoring resulted in almost continuous time series of different fAPAR estimates at all three sites (Fig. 3). At Graswang, fAPAR₄ was not available from end October onwards due to failures of sensors for PAR_{soil} (Fig. 3a). The seasonal courses of all fAPAR estimates reflect the phenological development, showing an increase of fAPAR in spring, a decrease of fAPAR values at the end of the growing season and in-between a plateau phase that is most pronounced at the temperate site. Compared to the other sites, the temperate site Graswang exhibits a relatively low range of fAPAR values (approx. 0.15 fAPAR units), with all estimates showing values rarely below 0.90. In contrast, a relatively high seasonal range (approx. 0.20 fAPAR units at Peace River and approx. 0.40 fAPAR units at Santa Rosa) is observed at the deciduous forests of Peace River and Santa Rosa (Fig. 3b-c). Apart from the differences in seasonal dynamics, mean values of all fAPAR estimates (0.93-0.96) at Graswang are considerably higher than at Peace River (0.82-0.85) and Santa Rosa (0.80-0.85).

Seasonal dynamics of different fAPAR estimates appear similar in Fig. 3 which is confirmed by the strong linear relationships depicted in Fig. 4, showing R² between 0.93 and 0.98. Across all sites, minimum BIAS between different fAPAR estimates account to -0.50 at Graswang, 3.30 at Peace River and 0.40 at Santa Rosa (Fig. 4b, f, g). Still, there are significant differences between most fAPAR estimates (KS test: *p* < 0.05, see legends in Fig. 3). It can be seen that at the temperate and boreal sites, BIAS between fAPAR₂, fAPAR₃₍₁₎ or fAPAR₃₍₂₎ and fAPAR₄ decrease with increasing number of flux terms considered (Fig. 4a-f): At Graswang, the lowest and highest BIAS (-0.01; 0.02) with fAPAR₄ was

obtained for fAPAR₂ and fAPAR₃₍₁₎, respectively; at Peace River, fAPAR₂ shows considerably higher BIAS (0.08) when related to fAPAR₄ than fAPAR₃₍₁₎ (BIAS: 0.03). However, at the tropical site, fAPAR₂ shows marginal deviations with fAPAR₄ compared to fAPAR₃₍₁₎ and fAPAR₃₍₂₎ (Fig. 4g-i).

Apart from absolute values of BIAS, another feature to be considered in the evaluation of different fAPAR estimates is the sign of BIAS. In this regard, value distributions of the bias depicted in Fig. 5 show that most values obtained for bias_{2to4} are positive. Thus, fAPAR₂ overestimated fAPAR₄ at all three sites. Further, even though value distributions of bias_{3(1)to4} and bias_{3(2)to4} show similar shape and the same median values at each of the sites, values are both positively and negatively signed. As a striking feature, the median of 0.05 obtained at the boreal site (Fig. 5b) indicates that for half of the timesteps, bias_{2to4} has crossed the uncertainty target following the GCOS (2016).

3.2. Environmental conditions and their effect on bias between fAPAR estimates

We investigated, whether environmental conditions, i.e. the factors wind speed and season at Peace River and Santa Rosa or rather the factors wind speed, leaf status and snow at Graswang, influenced the bias between two- or three-flux estimates and fAPAR₄ (i.e., bias_{2to4}, bias_{3(1)to4}, bias_{3(2)to4}). Table 1 presents the results of the respective two- or three-factorial ANOVAs with bias_{2to4}, bias_{3(1)to4}, bias_{3(2)to4} as target variables (for MEAN and SD, see Appendix D).

3.2.1. Seasonal and phenological effects

For all sites, the ANOVA results show significant (i.e., *p* < 0.05) seasonal (i.e. factor season) or phenological (i.e. factor leaf status) effects on the bias of fAPAR estimates (Table 1, Fig. 6). At Graswang, bias_{2to4} was increased for the leaf status “yellow” and “no leaves”, while for the three-flux estimates, a slightly higher bias was obtained for red leaves, even though the effect was less pronounced for bias_{3(1)to4} (Fig. 6b). In contrast to leaf status, no significant effect of snow was found (Table 1, Fig. 6a). At the boreal and tropical site, the more generalized factor “season” showed significant effects on the bias of several fAPAR estimates (bias_{2to4} at Peace River and bias_{3(1)to4} at Santa Rosa and Peace River, see Table 1). The higher *F*-values obtained from the ANOVA indicates that the effect of season on the bias of fAPAR was more pronounced at the boreal site. In addition to that, the median of bias_{2to4} crosses the 0.05-uncertainty threshold following the GCOS (2016) requirements for both foliated and defoliated season (Fig. 6c), while at the tropical site, values of bias_{2to4}, bias_{3(1)to4} and bias_{3(2)to4} stay within the -0.05 and 0.05-range irrespective of the fAPAR estimate (Fig. 6d).

3.2.2. Influence of wind speed

Wind speed influenced the bias of fAPAR estimates to various extents, depending on the site and fAPAR estimate. At Graswang, all estimates show deviations to fAPAR₄ below 0.05 (Fig. 7a), which is also reflected in the similar *F*-values in the ANOVA (Table 1). Here, only for bias_{3(1)to4} a significant effect (*p* < 0.05) was found. At the boreal and tropical sites, the effect of wind speed on the bias was found to be highly significant (*p* < 0.001) for almost all estimates (Table 1). At Peace River, it is clearly visible that the 0.05-uncertainty threshold is crossed permanently for bias_{2to4} during wind speeds between 2 and 3 ms⁻¹ as well as above 4 ms⁻¹ (Fig. 7b). At Santa Rosa, the effect of wind speed is significant, but fulfill the uncertainty requirements (Fig. 7c). Wind speed was found to affect top-of-canopy PAR albedo (R_{TOC}). In this regard, Fig. 8 shows that with increasing wind speed, R_{TOC} increases by 36–38 % at Santa Rosa and Peace River, respectively.

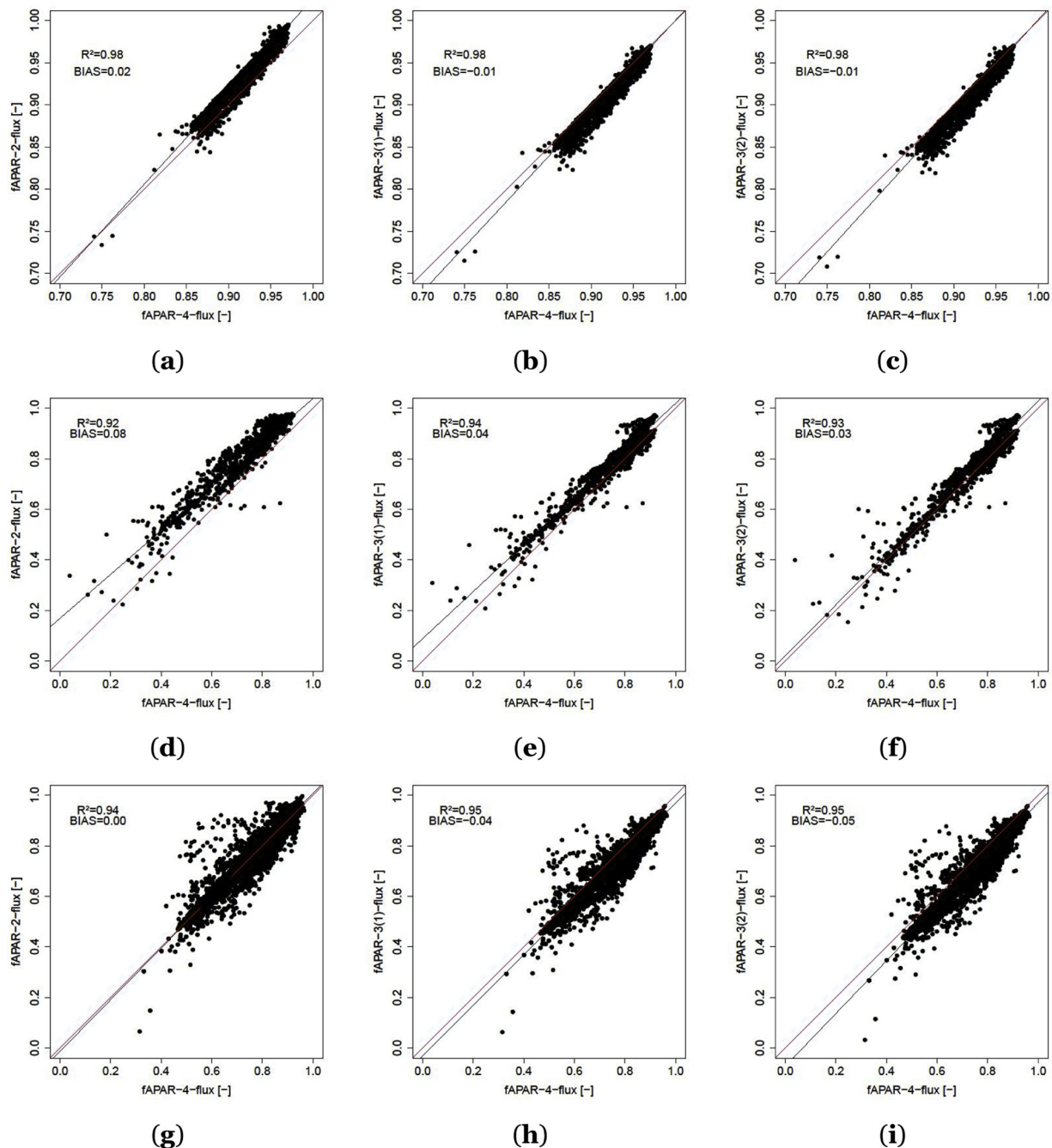


Fig. 4. Scatterplots of $fAPAR_2$, $fAPAR_{3(1)}$ and $fAPAR_{3(2)}$ vs. $fAPAR_4$ at (a-c) Graswang, (d-f) Peace River and (g-i) Santa Rosa. Mean average deviation between pairs of values (BIAS) and coefficient of determination (R^2) are shown. The continuous black line corresponds to slopes and intercepts of the linear regression, while the red line marks the 1:1 line. (For interpretation of the references to colour in the Figure, the reader is referred to the web version of this article).

4. Discussion

4.1. Consistency of $fAPAR$ estimates and overall accuracy

We presented time series of two-, three- and four-flux $fAPAR$ measurements (referred to as “ $fAPAR$ estimates”) for the vegetation period of 2016 using WSNs in three different forest ecosystems: the temperate mixed-coniferous forest site Graswang, Germany, the boreal-deciduous forest site Peace River in Northern Alberta, Canada and the tropical dry forest (TDF) site Santa Rosa, Costa Rica. All $fAPAR$ estimates reflect the seasonal increase and decrease of $fAPAR$ values and show relatively high $fAPAR$ with absolute values above 0.7 during the growing season (Fig. 3), which is typical for forests (e.g., Leuchner et al., 2011;

Majasalmi et al., 2017; Nestola et al., 2017). The relatively low seasonal dynamic with a seasonal range of only 0.15 $fAPAR$ units at Graswang reflects the dominance of evergreen conifers at this site (Fig. 3a). Additionally, the relatively high values could be attributed to the higher basal area and stem density when compared to Peace River and Santa Rosa.

Based on the $fAPAR$ time series, we assessed overall differences between $fAPAR$ estimates with several performance metrics (Fig. 4). The high overall correlations with R^2 above 0.9 between $fAPAR$ estimates indicate that adding information on top-of-canopy PAR albedo (R_{TOC}) and forest background albedo (R_{soil}) did not alter the time series in terms of seasonal dynamics considerably. This can be explained by the fact that PAR_{trans} represents the flux component with by far the

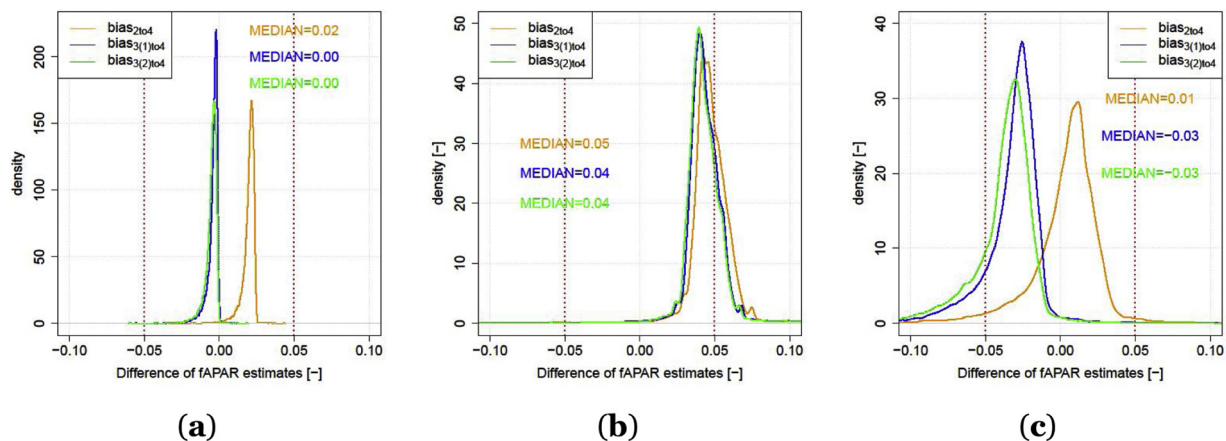


Fig. 5. Density of the difference between two- or three-flux estimates and the four-flux fAPAR estimate ($bias_{2to4}$, $bias_{3(1)to4}$, $bias_{3(2)to4}$) calculated for each 10-min timestep for the year 2016 at (a) Graswang, (b) Peace River and (c) Santa Rosa.

highest proportion in the absorption in the PAR range (Widłowski, 2010). As average bias between $fAPAR_2$, $fAPAR_{3(1)}$ and $fAPAR_{3(2)}$ with $fAPAR_4$ was found to be lower than the uncertainty requirements following the GCOS (2016), our initial hypothesis that the bias of two- and three-flux fAPAR estimates are within acceptable ranges, could be confirmed. Under the assumption that $fAPAR_4$ was closest to “true” fAPAR, we found an overestimation bias of $fAPAR_2$ at all three sites (i.e., majority of values of $bias_{2to4}$ with positive sign in Fig. 5), which is in accordance with previous findings from RTM simulations (Widłowski, 2010). For $fAPAR_3$, results were not as distinct (Fig. 5) and when taking a closer look at overall bias between the time series, it is striking that differences between fAPAR estimates did not necessarily decrease with increasing number of flux terms considered (Fig. 4).

In theory, one would expect that considering additional flux terms for fAPAR decreased the estimation bias. However, we could only see a reduction of the bias at the temperate site Graswang (Fig. 4a-c). At the boreal site, bias was barely reduced for the three-flux estimates and it is particularly striking that $fAPAR_2$ presented lower deviations to $fAPAR_4$ than the three-flux fAPAR estimates at the tropical site Santa Rosa. As for Peace River, the fact that there was almost no difference between the value distributions of three-flux fAPAR estimates (Fig. 5b) suggests that R_{soil} was very different to R_{TOC} and could thus not be approximated with R_{TOC} ($fAPAR_{3(1)}$) or zero ($fAPAR_{3(2)}$) at this site. Indeed, the forest floor at Peace River presents almost no green vegetation and could thus have very different spectral properties than the top-of-canopy layer of the primary and secondary canopy layers that are dominated by aspen and green alder, respectively. As for Santa Rosa, the fact that $fAPAR_2$ presented less bias than $fAPAR_3$ (Fig. 4g-i) could indicate that measurements of R_{TOC} were not representative for the whole area covered by the WSN. This is supported by the fact that only one measurement of PAR_{TOC} (per tower and sub-site) was carried out - in contrast to multiple sensors for PAR_{soil} . Compared to both other sites, the TDF site presents the highest number of different species. As fAPAR is influenced by both leaf properties and structure (Ollinger, 2011), the higher

number of species will increase the variety of geometries, particularly with the occurrence of both lianas and trees (Li et al., 2017b). In addition to that, previous research has shown that lianas present a higher percentage of woody biomass than tree species (Sánchez-Azofeifa et al., 2009), which could lead to a higher spatial variability of R_{TOC} . Thus, one single measurement of R_{TOC} per site, as carried out also in other studies (e.g., Nestola et al., 2017; Senna et al., 2005; Tao et al., 2015), may not be appropriate, particularly in tropical forests. In sum, our findings indicate that adding additional flux terms besides PAR_{in} and PAR_{trans} need to be well-considered. Without proper investigations on spatial variability of R_{TOC} and R_{soil} , there is a risk of introducing a sampling bias (i.e. statistical error) which could hamper the goal of decreasing estimation bias (i.e. systematic error due to assumptions in the radiative transfer equations).

4.2. The role of environmental conditions for the accuracy of fAPAR estimates

The significant effects of season and phenology on the difference between two- and three-flux estimates with the four-flux fAPAR estimate found in the ANOVA (Table 1) are in accordance with previous findings from both simulations with RTMs and field experiments (Putzenlechner et al., 2019a, b; Widłowski, 2010). Particularly, the strong effect of colored leaves found in the mixed-coniferous forest at Graswang (Fig. 6b) is attributed to changes in reflectance properties of beech and maple leaves, as yellow leaves present higher brightness than green leaves, thereby leading to an overestimation bias known from previous investigations (Putzenlechner et al., 2019b; Widłowski, 2010). As $fAPAR_2$ does not consider R_{TOC} , the effect on $bias_{2to4}$ is strongest. Interestingly, the effect is almost as strong for $bias_{3(2)to4}$, for which the corresponding $fAPAR_{3(2)}$ contains the assumption that forest background albedo equals zero. As the effect on $bias_{3(1)to4}$ is much lower, it can be implied that at this site, the approximation of R_{soil} equalizing R_{TOC} for the three-flux estimate is more robust because spectral

Table 1

ANOVA of the bias of fAPAR estimates and environmental conditions at the three study sites; Respective *F*- and *p*-values are shown.

| Bias of fAPAR | Graswang | | | | Peace River | | Santa Rosa | |
|------------------|-------------|------|------------|----------|-------------|--------|------------|--|
| | Leaf status | Snow | Wind speed | Season | Wind speed | Season | Wind speed | |
| $bias_{2to4}$ | 17.98*** | 3.39 | 3.34 | 52.27*** | 102.76*** | 0.29 | 112.67*** | |
| $bias_{3(1)to4}$ | 4.81* | 1.35 | 3.86* | 28.91*** | 26.95*** | 9.29** | 38.91*** | |
| $bias_{3(2)to4}$ | 17.88*** | 3.39 | 3.34 | 0.02 | 8.97** | 0.29 | 31.46*** | |

* $p < 0.05$.
 ** $p < 0.01$.
 *** $p < 0.001$.

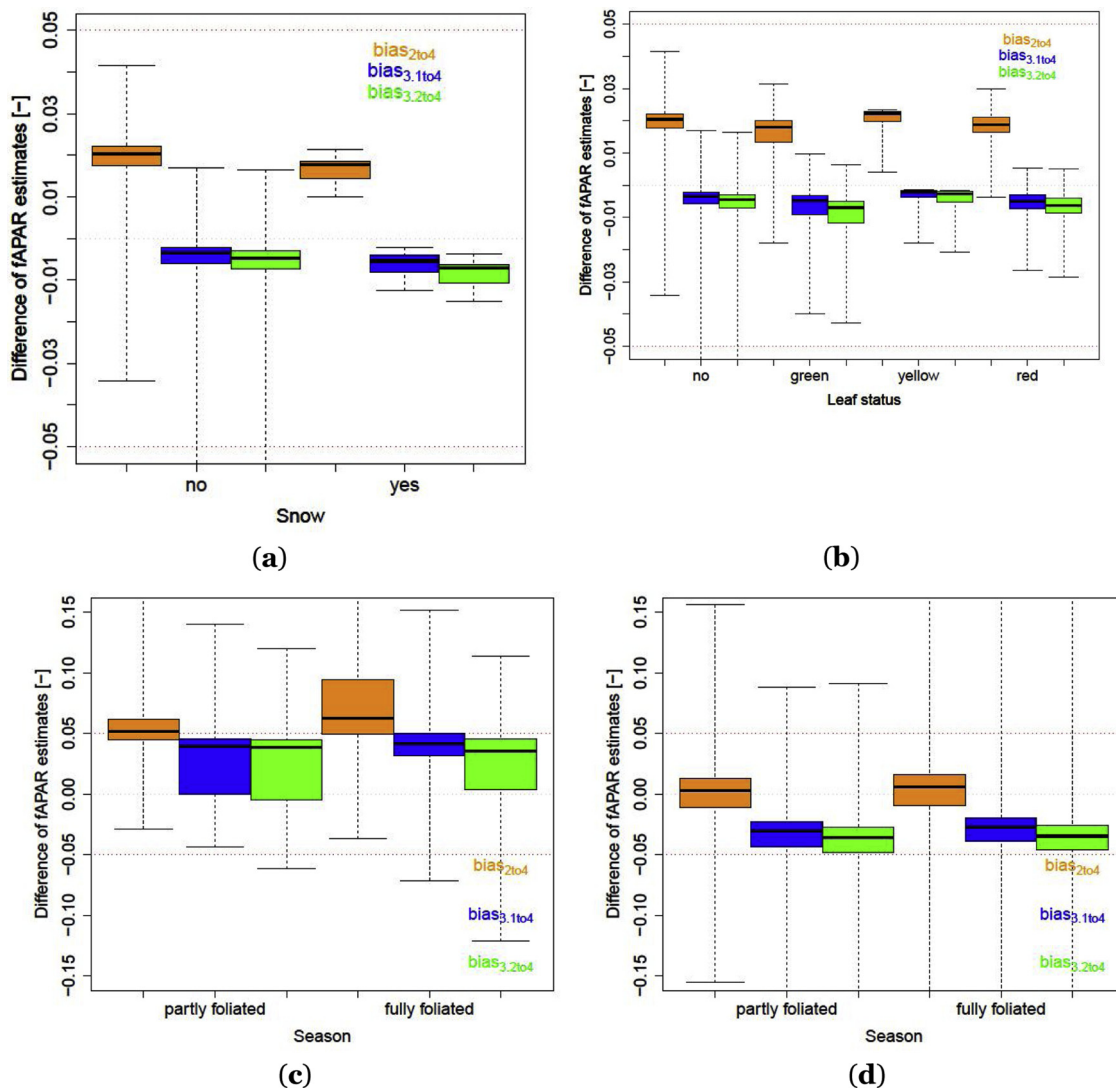


Fig. 6. Bias of fAPAR estimates for various seasonal factors: (a) snow and (b) leaf status at Graswang; season at (c) Peace River and (d) Santa Rosa. The dashed red lines indicate the 0.05-uncertainty threshold following the product requirements set by the GCOS (2016). Note that the scale of the y-axis is different for (a-b). Only data acquired under low wind speed conditions (i.e., 2 ms^{-1}) is shown. (For interpretation of the references to colour in the Figure, the reader is referred to the web version of this article).

properties of the top-of-canopy region and the forest floor were relatively similar at Graswang. This can be explained by the fact that the herbal understory experiences a brown-down as well and (colored) leaves will soon cover the forest floor during senescence period. We found that the factor season had generally stronger effects on the bias of fAPAR estimates at the boreal site than at the TDF site (Table 1). While the boreal deciduous forests of the Albertan aspen parkland are characterized by a short senescence period due to a sharp decline of air temperature in September (Beaubien and Freeland, 2000), TDFs are known for their gradually brown-down which is attributed to progressing drought during dry season (Kalacska et al., 2004). The bright yellow aspen leaves at Peace River will lead to an increase in R_{TOC} which could explain the accuracy decrease of fAPAR₂. It should be considered, however, that the strong effect attributed to the factor leaf color and season could be attenuated by effects of low LAI, which has been simulated to lead to a weak underestimation bias of fAPAR estimates (> -0.05) (Widlowski, 2010). Thus, the effect of the factors season and leaf color on the bias of different fAPAR estimates could vary within years, depending on the amount of foliage present during the period of peak color change.

In addition to that, the factor season may also incorporate early

snowfalls, which could also have influenced the bias at the boreal site. However, no significant effects on the bias of fAPAR was found during snowy conditions at Graswang, even though simulations with RTMs of previous studies have simulated an underestimation bias for the two- and three-flux estimates (Widlowski, 2010). In previous investigations on the bias of fAPAR₂ at this site, it has been suspected that PAR sensors could be affected by snow accumulation (Putzenlechner et al., 2019b). It must be admitted that such uncertainties related to the experimental set-up limit the usage of ground data for validation purposes during the occurrence of snow in forest ecosystems. Nevertheless, it must be considered as well, that the accuracy of satellite-derived fAPAR products may be compromised by effects of spectral mixing between vegetation and snow reflectance values. Even though Widlowski (2010) simulated a strong effect of high forest background albedo on the bias of fAPAR, the meaningfulness of validation studies carried during the occurrence of snow could be questionable in general.

For the factor wind speed, we found significant effects on the bias of fAPAR estimates at the boreal and TDF site (Table 1). Indications for wind speed influencing the uncertainty of two-flux fAPAR estimates have first been discovered at Graswang in previous investigations (Putzenlechner et al., 2019b), even though the influence was also not

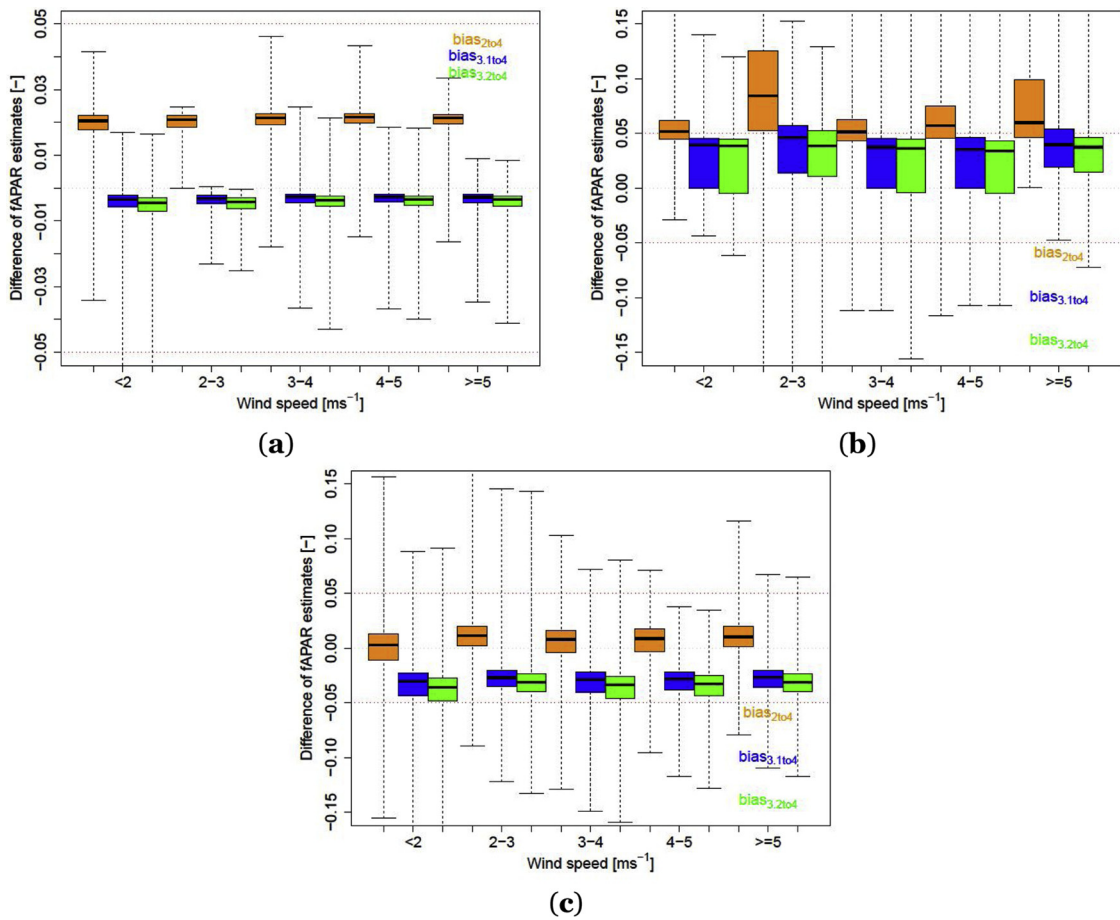


Fig. 7. Bias of fAPAR estimates for different wind speed conditions at (a) Graswang (factor leaf status = “green”), (b) Peace River (factor season = “fully foliated”) and (c) Santa Rosa (factor season = “fully foliated”). The dashed red lines shows the 0.05-uncertainty threshold following the uncertainty requirements set by the GCOS (2016). Note that scale of y-axis is different for (a). (For interpretation of the references to colour in the Figure, the reader is referred to the web version of this article).

found to be significant. The site’s special topographic setting with surrounding mountains giving shelter from high wind speeds compared to the other sites (Appendix B, Figure B1) could explain why the effect of wind speed is weak. At Peace River and Santa Rosa, we could see that

the effect of wind speed could be attributed mainly to increased R_{TOC} experienced under higher wind speed conditions (Fig. 8). It is well-documented that spectral properties of leaves depend on the vertical position in the canopy (Gara et al., 2018), which are altered with wind

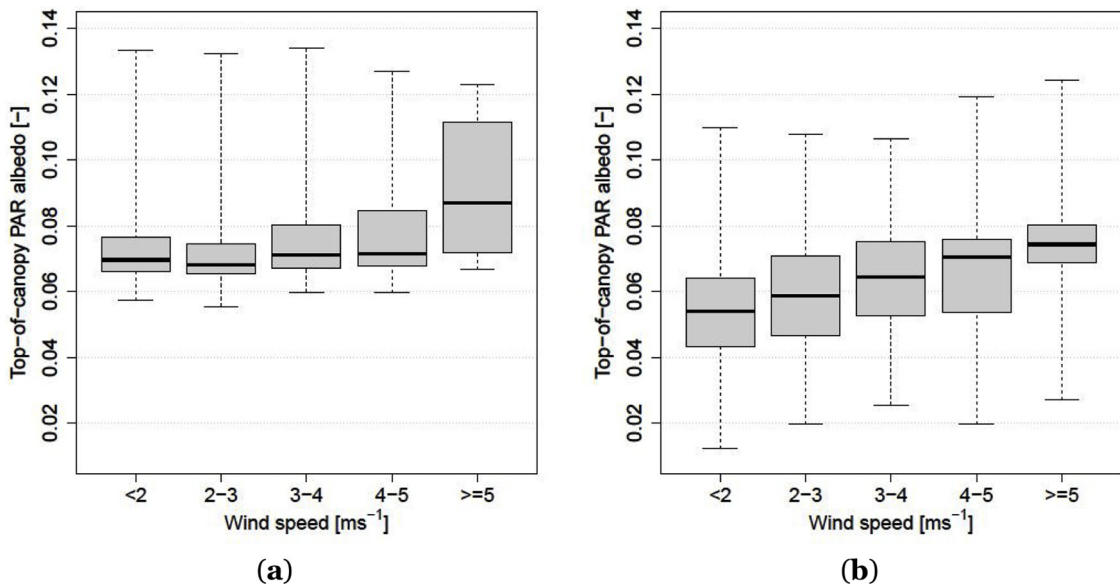


Fig. 8. Top-of-canopy PAR albedo (R_{TOC}) acquired under different wind speed conditions during fully foliated season at (a) Peace River and (b) Santa Rosa.

speed conditions. Exceeding the 0.05-uncertainty threshold also during lower wind speeds at the boreal site (bias_{2to4} for 2–3 ms⁻¹, Fig. 7b) coincides with the highest frequency of wind speed conditions (Appendix B, FigureB1) and thus shows the general disadvantage of the two-flux fAPAR estimate at this site. In fact, trembling aspen, the dominating species at Peace River, are named after their characteristic leaf flutter already during low wind speed conditions (Gara et al., 2018). The fluttering of the top-of-canopy leaves (often referred to as “sun leaves”) creates uniform photon flux densities so that incoming PAR is distributed in the canopy regardless of variation in leaf orientation and solar position (Roden, 2003). Consequently, the effect of wind speed on the bias of fAPAR was highest at Peace River and in addition to that crossed the GCOS uncertainty requirements (Fig. 7b). Based on our findings, we therefore recommend opting for three-flux fAPAR estimates at sites that frequently experience higher wind speeds.

4.3. Evaluation of the methodological approach for the bias assessment

Despite these distinct findings on the performance of different fAPAR estimates from our study we must discuss limitations of our approach in terms of 1) the experimental approach itself and 2) its context of using in situ fAPAR estimates to validate satellite-derived fAPAR products. Regarding 1), it should be considered that the four-flux fAPAR estimate was assumed to be closest to the truth. While ignoring the contribution of horizontal PAR fluxes was found to be problematic only for small experimental sites (Widlowski et al., 2006), this estimate could still be affected by horizontal fluxes. In this regard, SZA is a potential source of bias, that was not investigated as pyranometers required to classify fAPAR timesteps according to the ratio of diffuse-to-direct incoming radiation were not available at all the sites. Previous research at the temperate site has shown that during high SZAs, the bias of the two-flux fAPAR estimate exceeded 0.05 fAPAR units (Putzenlechner et al., 2019b). However, there is currently no experimental technique developed for quantifying horizontal fluxes with commercially available hemispherical PAR sensors as used in this study and it could thus be interesting to investigate the bias of the four-flux fAPAR estimate with spherical PAR sensors, as applied by Leuchner et al. (2011) in an ecological context (i.e., PAR radiation as a driver for competition). Finally, another limitation of the four-flux fAPAR estimate represented the restriction to meteorological conditions (i.e., clear sky, calm air) at the site Graswang with the UAV approach, resulting in only several estimates of R_{TOC} which showed considerable variability.

In the context of using fAPAR estimates for validating satellite-derived fAPAR products, underlying fAPAR definitions should be considered. In contrast to satellite-derived fAPAR products, which mostly relate to “green” fAPAR (Gobron, 2015), PAR sensors measure “total” fAPAR, referring to the PAR absorption of both green and non-green vegetative elements (Gobron, 2015). Authors of existing studies have stated that the exact contribution of such bias is difficult to quantify, but could be below 10 % (Nestola et al., 2017; Zhang et al., 2013). The bias between “total” and “green” fAPAR could be particularly high at the tropical site, as liana species are known for their higher ratio of woody biomass (Sánchez-Azofeifa et al., 2009). Given the facts that recent studies have raised attention on discrepancies of satellite-derived fAPAR products in tropical forest regions (Xiao et al., 2018; Xu et al., 2018), we see the need for future investigations on the bias between “green” and “total” fAPAR especially in tropical forests. Investigating the bias between “green” and “total” fAPAR could be done by evaluating direct fAPAR measurements with DHPs at the sensor locations or by the means of in situ RTM simulations. Another issue related to different fAPAR definitions is that our measurements were acquired during all illumination conditions. In future bias investigations, a clear differentiation into “black-sky” and “white-sky” fAPAR would be favorable for improving the comparability to satellite-derived fAPAR products, which mostly relate to “black-sky” fAPAR (Gobron, 2015). In return, we welcome satellite-derived fAPAR products based on retrieval

algorithms for both “white-sky” and “black-sky” conditions as recently proposed by Liu et al. (2019) as an important step towards an improved comparability of fAPAR maps and ground measurements.

Nevertheless, our investigations have provided the first insights into the accuracy of different fAPAR estimates varying with ecosystem type and environmental conditions based on direct PAR measurements which we consider beneficial for the implementation of sampling protocols in the context of validation activities of satellite-derived fAPAR products.

5. Conclusions

This study presented an assessment on the differences and uncertainties of different fAPAR estimates at three forest sites: a conifer-dominated forest in Southern Germany, a boreal-deciduous forest in Northern Alberta at the Peace River Environmental Monitoring Super Sites, Canada and a tropical dry forest (TDF) at the Santa Rosa National Park Environmental Monitoring Super Site, Costa Rica. Based on permanent measurements with Wireless Sensor Networks (WSNs) of incoming, transmitted PAR as well as PAR albedos of the top-of-canopy region and the forest floor, we performed two-, three and four-flux fAPAR measurements, depending on the number of flux terms considered. As four-flux fAPAR considers the highest amount of flux terms to describe the canopy absorption in the PAR domain (i.e., only horizontal PAR fluxes are ignored), we assumed this quantity closest to “true fAPAR”. Thus, to evaluate the uncertainty of two- and three-flux estimates, we calculated their differences with the four-flux estimate and referred to this quantity as bias. As the bias of a certain fAPAR estimate is known to vary with environmental conditions, we assessed the influence of several environmental conditions with multifactorial ANOVAs.

In our analysis, we were particularly interested whether bias of certain fAPAR estimates fulfill the 0.05-uncertainty threshold following the product requirements set by the GCOS (2016). In this regard, we found that the highest average biases of different fAPAR estimates accounted to 0.02 at the temperate site, 0.08 at the boreal site and -0.05 at the tropical site. Thus, the uncertainty requirements set by the GCOS (2016) were fulfilled at the temperate and tropical site. At all three sites, the two-flux fAPAR estimate was found to consistently overestimate the four-flux fAPAR estimate. It is important to stress, however, that the three-flux fAPAR estimates, which have been favored frequently in previous studies, were not found to necessarily reduce overall bias, especially at the tropical site. We argued that higher bias of the three-flux estimates could arise from non-representative measurements of R_{TOC} due to higher number of tree species and thus higher spatial variability of fAPAR in the TDF forest. Concerning the influence of environmental factors referring to seasonal and phenological changes, such as bright colored autumn leaves, we found significant influences on the bias of fAPAR. The effect was considerably pronounced for the two-flux fAPAR estimate at the temperate and boreal sites, even though uncertainty requirements remained fulfilled. A significant effect of higher wind speed conditions on the bias of two- and three-flux estimates was found at the boreal and TDF sites. This effect was found to be mainly attributed to increases in the top-of-canopy albedo during higher wind speeds. At the boreal site, the absolute bias of the two-flux fAPAR estimate exceeded the 0.05-uncertainty threshold already during lower wind speed conditions. Based on our findings, the following conclusions could serve as practical recommendations for planning future experimental set-ups with direct PAR measurements, aiming at validating satellite-derived fAPAR products:

- 1 The bias of two-flux fAPAR observations, which are relatively cost and labor efficient, is bearable under typical summer conditions (i.e. green leaves, no snow, low wind speed).
- 2 At sites with frequently higher wind speed conditions, at least three-flux observations (better four-flux) should be carried out.

- 3 At sites where top-of-canopy albedo can be expected to differ considerably from forest background albedo (e.g., due to different species composition or fractional cover), an approximation of forest background albedo with top-of-canopy albedo in the three-flux estimate should be avoided as this approximation will increase the bias compared to two-flux estimate; in this case, top-of-canopy albedo should either be approximated with zero or measurements of forest-background albedo should be carried out so that the four-flux fAPAR estimate can be calculated.
- 4 To reduce statistical errors (i.e. sampling bias), multi-sensor approaches as possible with WSNs should be favored not only for measurements for transmitted PAR, but also for PAR fluxes reflected from the top-of-canopy region as well as the forest floor. In this regard, forests with high diversity of plant species will require special attention.

In sum it has been demonstrated that WSNs serve for assessing the bias of different fAPAR estimates which is needed for developing transparent sampling protocols for in situ fAPAR observations. Overall, investigating the bias of fAPAR in very different forest ecosystems allows the conclusion to be drawn that two-flux fAPAR observations present a good compromise between accepting uncertainties involved under specific environmental conditions and providing permanent fAPAR datasets suitable and urgently needed for the validation of satellite-derived fAPAR products.

Declaration of Competing Interest

The authors declare no conflict of interest.

Funding:

This work was supported by the Natural Science and Engineering Research Council of Canada (NSERC) Discovery Grant Program, the Inter-American Institute for Global Change Research (IAI) Collaborative Research Network Program (CRN3-023), the Canada Foundation for Innovation (CFI), and a MICMoR Fellowship to B.P. through KIT/IMK-IFU (Garmisch-Partenkirchen, Germany). The Helmholtz Association and the German Federal Ministry of Education and Research (BMBF) in the framework of TERENO (Terrestrial Environmental Observatories) (grant no. 01LL0801B) provided support also to the German site.

CRedit authorship contribution statement

Birgitta Putzenlechner: Conceptualization, Data curation, Formal analysis, Investigation, Methodology, Software, Validation, Writing - original draft. **Philip Marzahn:** Project administration, Resources, Methodology, Writing - review & editing. **Arturo Sanchez-Azofeifa:** Data curation, Project administration, Resources, Supervision, Writing - review & editing.

Acknowledgments

The authors thank Caroline Brody (KIT/IMK-IFU) for performing the UAV flights at German site as well as Ralf Ludwig (LMU Munich) and Ralf Kiese (KIT/IMK-IFU) for their constant advice. Collection of data in Alberta and Costa Rica was done by the support of Saulo Castro and Iain Sharp. We also thank Ronny Hernandez, Roger Blanco and Maria Marta Chavarria from the Guanacaste Conservation Area, Costa Rica as well as Jim Witt from Daishowa-Marubeni International Ltd. (DMI), Alberta, Canada. The authors thank two anonymous reviewers for their thoughtful comments and advice.

Appendix A. Supplementary data

Supplementary material related to this article can be found, in the

online version, at doi:<https://doi.org/10.1016/j.jag.2020.102061>.

References

- Arroyo-Mora, J.P., Sánchez-Azofeifa, G.A., Kalacska, M.E.R., Rivard, B., Calvo-Alvarado, J.C., Janzen, D.H., 2005. Secondary forest detection in a neotropical dry forest landscape using landsat 7 ETM+ and IKONOS Imagery1. *Biotropica* 37, 497–507.
- Baret, F., Makhmara, H., Lacaze, R., Smets, B., 2011. BioPar Product User Manual LAI,FAPAR, FCOVER, NDVI Version 1 From SPOT/VEGETATION Data.
- Beaubien, E.G., Freeland, H.J., 2000. Spring phenology trends in Alberta, Canada: links to Ocean temperature. *Int. J. Biometeorol.* 44, 53–59.
- Brosy, C., Krampf, K., Zeeman, M., Wolf, B., Junkermann, W., Schaefer, K., Emeis, S., Kunstmann, H., 2017. Simultaneous multicopter-based air sampling and sensing of meteorological variables. *Atmos. Meas. Tech.* 10, 2773–2784.
- Camacho, F., Cernicharo, J., Lacaze, R., Baret, F., Weiss, M., 2013. Geov1: lai, Fapar essential climate variables and FCOVER global time series capitalizing over existing products. Part 2: validation and intercomparison with reference products. *Remote Sens. Environ.* 137, 310–329.
- Cammalleri, C., Verger, A., Lacaze, R., Vogt, J.V., 2019. Harmonization of GEOV2 fAPAR time series through MODIS data for global drought monitoring. *Int. J. Appl. Earth Obs. Geoinf.* 80, 1–12.
- Corripio, J.G., 2003. Vectorial algebra algorithms for calculating terrain parameters from DEMs and solar radiation modelling in mountainous terrain. *Int. J. Geogr. Inf. Sci.* 17, 1–23.
- D'odorico, P., Gonsamo, A., Pinty, B., Gobron, N., Coops, N., Mendez, E., Schaepman, M.E., 2014. Intercomparison of fraction of absorbed photosynthetically active radiation products derived from satellite data over Europe. *Remote Sens. Environ.* 142, 141–154.
- Disney, M., Muller, J.-P., Kharbouche, S., Kaminski, T., Voßbeck, M., Lewis, P., Pinty, B., 2016. A new global fAPAR and LAI dataset derived from optimal albedo estimates: comparison with MODIS products. *Remote Sensing* 8, 275.
- Faticchi, S., Pappas, C., Ivanov, V.Y., 2016. Modeling plant–water interactions: an eco-hydrological overview from the cell to the global scale. *Wiley Interdiscip. Rev. Water* 3, 327–368.
- Fensholt, R., Sandholt, I., Rasmussen, M.S., 2004. Evaluation of MODIS LAI, fAPAR and the relation between fAPAR and NDVI in a semi-arid environment using in situ measurements. *Remote Sens. Environ.* 91, 490–507.
- Gara, W.T., Darvishzadeh, R., Skidmore, K.A., Wang, T., 2018. Impact of vertical canopy position on leaf spectral properties and traits across multiple species. *Remote Sens.* 10.
- Geos, 2011. Systematic Observation Requirements for Satellite-based Data Products for Climate. Global Climate Observing System (GCOS), Geneva, Switzerland. https://library.wmo.int/index.php?lvl=notice_display&id=12907#.XjgbTSMxmUk.
- Geos, 2016. The Global Climate Observing System for Climate: Implementation Needs. Global Climate Observing System (GCOS), Geneva, Switzerland. https://library.wmo.int/doc_num.php?explnum_id=3417.
- Gitelson, A.A., 2019. Remote estimation of fraction of radiation absorbed by photosynthetically active vegetation: generic algorithm for maize and soybean. *Remote Sens. Lett.* 10, 283–291.
- Gobron, N., 2015. Report on Satellite Derived ECV Definition and Field Protocols. European Commission, Joint Research Centre (JRC), Institute for Environment & Sustainability.
- Gobron, N., Verstraete, M.M., 2009. Ecv T10: fraction of absorbed photosynthetically active radiation (FAPAR). Essential Climate Variables. Food and Agriculture Organization (FAO), Rome Version 8.
- Kalacska, M., Sanchez-Azofeifa, G.A., Calvo-Alvarado, J.C., Quesada, M., Rivard, B., JANZEN, D.H., 2004. Species composition, similarity and diversity in three successional stages of a seasonally dry tropical forest. *For. Ecol. Manage.* 200, 227–247.
- Leuchner, M., Hertel, C., Menzel, A., 2011. Spatial variability of photosynthetically active radiation in European beech and Norway spruce. *Agric. For. Meteorol.* 151, 1226–1232.
- Li, W., Weiss, M., Waldner, F., Defourny, P., Demarez, V., Morin, D., Hagolle, O., Baret, F., 2015. A generic algorithm to estimate LAI, fapar and fcover variables from Spot4_Hrvir and landsat sensors: evaluation of the consistency and comparison with ground measurements. *Remote Sens.* 7, 15494.
- Li, W., Baret, F., Weiss, M., Buis, S., Lacaze, R., Demarez, V., Dejoux, J.-F., Battude, M., Camacho, F., 2017a. Combining hectometric and decametric satellite observations to provide near real time decametric FAPAR product. *Remote Sens. Environ.* 200, 250–262.
- Li, W., Cao, S., Campos-Vargas, C., Sanchez-Azofeifa, G.A., 2017b. Identifying Tropical Dry Forests Extent and Succession Via the Use of Machine Learning Techniques. pp. 63.
- Liu, N., Treitz, P., 2018. Remote sensing of arctic percent vegetation cover and fapar on Baffin Island, Nunavut, Canada. *Int. J. Appl. Earth Obs. Geoinf.* 71, 159–169.
- Liu, R., Huazhong, R., Liu, S., Liu, Q., Yan, B., Gan, F., 2018. Generalized FPAR estimation methods from various satellite sensors and validation. *Agric. For. Meteorol.* 260, 55–72.
- Liu, L., Zhang, X., Xie, S., Liu, X., Song, B., Chen, S., Peng, D., 2019. Global white-sky and black-sky fapar retrieval using the energy balance residual method: algorithm and validation. *Remote Sens.* 11.
- Majasalmi, T., Stenberg, P., RAUTIAINEN, M., 2017. Comparison of ground and satellite-based methods for estimating stand-level fPAR in a boreal forest. *Agric. For. Meteorol.* 232, 422–432.
- Martínez, B., Camacho, F., Verger, A., García-Haro, F.J., Gilabert, M.A., 2013. Intercomparison and quality assessment of MERIS, MODIS and SEVIRI FAPAR

- products over the Iberian Peninsula. *Int. J. Appl. Earth Obs. Geoinf.* 21, 463–476.
- Mccallum, L., Wagner, W., Schullius, C., Shvidenko, A., Obersteiner, M., Fritz, S., Nilsson, S., 2010. Comparison of four global fapar datasets over northern Eurasia for the year 2000. *Remote Sens. Environ.* 114, 941–949.
- Mortazavi, S.H., Salehe, M., Macgregor, M.H., 2014. Maximum wsn coverage in environments of heterogeneous path loss. *Int. J. Sens. Netw.* 16, 185–198.
- Möttus, M., Sulev, M., Frederic, B., Lopez-Lozano, R., Reinart, A., 2011. Photosynthetically Active Radiation: Measurement and Modeling.
- Myneni, R.B., Hoffman, S., Knyazikhin, Y., Privette, J.L., Glassy, J., Tian, Y., Wang, Y., Song, X., Zhang, Y., Smith, G.R., Lotsch, A., Friedl, M., Morisette, J.T., Votava, P., Nemani, R.R., Running, S.W., 2002. Global products of vegetation leaf area and fraction absorbed PAR from year one of MODIS data. *Remote Sens. Environ.* 83, 214–231.
- Nestola, E., Sánchez-Zapero, J., Latorre, C., Mazzenga, F., Matteucci, G., Calfapietra, C., Camacho, F., 2017. Validation of Proba-V Geov1 and modis C5 & C6 fapar products in a deciduous beech forest site in Italy. *Remote Sens.* 9, 126.
- Ollinger, S.V., 2011. Sources of variability in canopy reflectance and the convergent properties of plants. *New Phytol.* 189, 375–394.
- Parks, A., 2006. Natural regions and subregions of Alberta. A Framework For Alberta's Parks. Alberta Parks., Edmonton.
- Pastorello, G., Sanchez-Azofeifa, G.A., Nascimento, M., 2011. Enviro-net: from networks of ground-based sensor systems to a web platform for sensor data management. *Sensors* 11, 6454.
- Pickett-Heaps, C.A., Canadell, J.G., Briggs, P.R., Gobron, N., Haverd, V., Paget, M.J., Pinty, B., Raupach, M.R., 2014. Evaluation of six satellite-derived fraction of absorbed photosynthetically active radiation (Fapar) products across the Australian continent. *Remote Sens. Environ.* 140, 241–256.
- Pinty, B., Jung, M., Kaminski, T., Lavergne, T., Mund, M., Plummer, S., Thomas, E., Widlowski, J.L., 2011. Evaluation of the jrc-tip 0.01° products over a mid-latitude deciduous forest site. *Remote Sens. Environ.* 115, 3567–3581.
- Prince, S.D., Goward, S.N., 1995. Global primary production: a remote sensing approach. *J. Biogeogr.* 22, 815–835.
- Putzenlechner, B., Castro, S., Kiese, R., Ludwig, R., Marzahn, P., Sharp, I., Sanchez-Azofeifa, A., 2019a. Validation of Sentinel-2 fapar products using ground observations across three forest ecosystems. *Remote Sens. Environ.* 232, 111310.
- Putzenlechner, B., Marzahn, P., Kiese, R., Ludwig, R., Sanchez-Azofeifa, A., 2019b. Assessing the variability and uncertainty of two-flux fapar measurements in a conifer-dominated forest. *Agric. For. Meteorol.* 264, 149–163.
- Rankine, C.J., Sanchez-Azofeifa, G.A., Macgregor, M.H., 2014. Seasonal Wireless Sensor Network Link Performance In Boreal Forest Phenology Monitoring. In: Eleventh Annual Ieee International Conference On Sensing, Communication, And Networking (Secon). 30 June–3 July 2014 2014. pp. 302–310.
- Reifsnyder, W.E., Furnival, G.M., Horowitz, J.L., 1971. Spatial and temporal distribution of solar radiation beneath forest canopies. *Agric. Meteorol.* 9, 21–37.
- Roden, J.S., 2003. Modeling the light interception and carbon gain of individual fluttering aspen (*Populus tremuloides* Michx) leaves. *Trees* 17, 117–126.
- Ryu, Y., Berry, J.A., Baldocchi, D.D., 2019. What is global photosynthesis? history, uncertainties and opportunities. *Remote Sens. Environ.* 223, 95–114.
- Sánchez-Azofeifa, G.A., Kalácska, M., Espírito-Santo, M.M.D., Fernandes, G.W., Schnitzer, S., 2009. Tropical dry forest succession and the contribution of lianas to wood area index (Wai). *For. Ecol. Manage.* 258, 941–948.
- Senna, M.C.A., Costa, M.H., Shimabukuro, Y.E., 2005. Fraction of photosynthetically active radiation absorbed by Amazon tropical forest: a comparison of field measurements, modeling, and remote sensing. *J. Geophys. Res. Biogeosci.* 110 N/A-N/A.
- Spence, J., Volney, J., 1999. Emend: ecosystem management emulating natural disturbance. Sustainable Forest Manage. Network Project Report.
- Steinberg, D.C., Goetz, S.J., Hyer, E.J., 2006. Validation of modis F/Sub par/ products in boreal forests of Alaska. *Ieee Trans. Geosci. Remote. Sens.* 44, 1818–1828.
- Taheriazad, L., Moghadas, H., Sanchez-Azofeifa, A.A., 2016. New approach to calculate plant area density (Pad) using 3d ground-based Lidar. *Spie Remote Sens.* 10 Spie.
- Tao, X., Liang, S., Wang, D., 2015. Assessment of five global satellite products of fraction of photosynthetically active radiation: intercomparison and direct validation against ground-based data. *Remote Sens. Environ.* 163, 270–285.
- Ter-Mikaelian, M.T., Wagner, R.G., Bell, F.W., Shropshire, C., 1999. Comparison of photosynthetically active radiation and cover estimation for measuring the effects of interspecific competition on Jack pine seedlings. *Can. J. For. Res.* 29, 883–889.
- Weiss, M., Baret, F., 2016. S2toolbox Level 2 Products: Lai, Fapar, Fcover.
- Widlowski, J.-L., 2010. On the Bias Of instantaneous fapar estimates in open-canopy forests. *Agric. For. Meteorol.* 150, 1501–1522.
- Widlowski, J.-L., Pinty, B., Lavergne, T., Verstraete, M.M., Gobron, N., 2006. Horizontal radiation transport in 3-D forest canopies At multiple spatial resolutions: simulated impact on canopy absorption. *Remote Sens. Environ.* 103, 379–397.
- Wu, M., Scholze, M., Voßbeck, M., Kaminski, T., Hoffmann, G., 2018. Simultaneous assimilation of remotely sensed soil moisture and fapar for improving terrestrial carbon fluxes At multiple sites using ccdas. *Remote Sens.* 11.
- Xiao, Z., Liang, S., Sun, R., 2018. Evaluation of three long time series for global fraction of absorbed photosynthetically active radiation (Fapar) products. *Ieee Trans. Geosci. Remote. Sens.* 56, 5509–5524.
- Xu, B., Park, T., Yan, K., Chen, C., Zeng, Y., Song, W., Yin, G., Li, J., Liu, Q., Knyazikhin, Y., Myneni, R., 2018. Analysis of global Lai/Fpar products from viirs and modis sensors for spatio-temporal consistency and uncertainty from 2012–2016. *Forests* 9, 73.
- Younis, M., Akkaya, K., 2008. Strategies and techniques for node placement in wireless sensor networks: a survey. *Ad Hoc Netw.* 6, 621–655.
- Zacharias, S., Bogena, H., Samaniego, L., Mauder, M., Fuß, R., Pütz, T., Frenzel, M., Schwank, M., Baessler, C., Butterbach-Bahl, K., Bens, O., Borg, E., Brauer, A., Dietrich, P., Hajsek, I., Helle, G., Kiese, R., Kunstmann, H., Klotz, S., Munch, J.C., Papen, H., Priesack, E., Schmid, H.P., Steinbrecher, R., Rosenbaum, U., Teutsch, G., Vereecken, H., 2011. A network of terrestrial environmental observatories in Germany. *Vadose Zone J.* 10, 955.
- Zeeman, M.J., Mauder, M., Steinbrecher, R., Heidbach, K., Eckart, E., Schmid, H.P., 2017. Reduced snow cover affects productivity of upland temperate grasslands. *Agric. For. Meteorol.* 232, 514–526.
- Zhang, Q., Middleton, E.M., Cheng, Y.-B., Landis, D.R., 2013. Variations of foliage chlorophyll fapar and foliage non-chlorophyll fapar (Faparchl, Faparnonchl). *Harvard Forest.* 6, 2254–2264.

3.3 Paper III: Validation of Sentinel-2 FAPAR products using ground observations across three forest ecosystems. In: Remote Sensing of Environment

Citation: BIRGITTA PUTZENLECHNER, SAULO CASTRO, RALF KIESE, RALF LUDWIG, PHILIP MARZAHN, IAIN SHARP AND ARTURO SÁNCHEZ-AZOFEIFA (2019): *Validation of Sentinel-2 FAPAR products using ground observations across three forest ecosystems*. Remote Sensing of Environment, 232, 111310.

Journal: Remote Sensing of Environment (Elsevier)

5-year Impact Factor: 8.791

Status: published

Research outline: Paper III presents a validation study of the recent S2 FAPAR product and adds to the discussion on uncertainties of both ground data and satellite derived FAPAR products. In this regard, the paper applies the lessons learnt on uncertainties of in situ FAPAR identified in Paper I and II at the three study sites Graswang, Peace River and Santa Rosa. The paper explicitly focuses on the two-flux FAPAR estimate as the general hypothesis, that the uncertainties of this estimate are acceptable under typical summer conditions has been confirmed in both Paper II. Nevertheless, bias of ground data related to the presence of colored leaves and influences of SZA is discussed again under the aspect of temporal aggregation. For the investigation of SZA, the S2 FAPAR product is validated with different instantaneous ground FAPAR estimates (e.g. instantaneous FAPAR at 10:00 and 14:00 local solar time) and daily average FAPAR. Deviations were referred to the GCOS accuracy threshold of 10% (or 0.05).

Q5: What is the bias between ground data and recent satellite derived FAPAR products under uncertainty constraints?

Q6: How does ecosystem complexity influence deviations between ground and satellite derived FAPAR estimates?

Scientific value: The paper presents the first validation of the S2 FAPAR product as well as the first validation study considering uncertainties of FAPAR ground data. In addition to that, the very different settings of forest ecosystems investigated in this study allow to test the hypothesis that deviations between in situ FAPAR and satellite derived FAPAR are a function of ecosystem complexity. Finally, the high spatial and temporal resolution of FAPAR ground data as possible with the WSN monitoring approach enable a validation of the representativeness of spatial and temporal variability acquired by decametric multispectral remote sensing products.

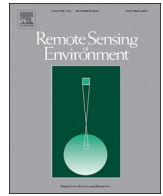
Authors' contributions: The study conception and methodology was developed by BP and AS-A. Data acquisition and curation was done by BP, SC, IS and AS-A. Formal analysis and interpretation of data was carried out by BP. Supervision was given by RL and AS-A. Funding was acquired by RL, RK and AS-

A. Project administration was carried out by RK, RL, PM and BP. The original draft was written by BP, while all other authors commented and revised critically and thus contributed to the final draft.



Contents lists available at ScienceDirect

Remote Sensing of Environment

journal homepage: www.elsevier.com/locate/rse

Validation of Sentinel-2 fAPAR products using ground observations across three forest ecosystems



Birgitta Putzenlechner^a, Saulo Castro^b, Ralf Kiese^c, Ralf Ludwig^a, Philip Marzahn^a, Iain Sharp^b, Arturo Sanchez-Azofeifa^{b,*}

^a Department of Geography, Ludwig-Maximilians Universität, Luisenstr. 37, 80333 Munich, Germany

^b Centre for Earth Observation Sciences (CEOS), University of Alberta, 1-26 Earth Sciences Building University of Alberta, Edmonton T6G2E3, Alberta, Canada

^c Institute of Meteorology and Climate Research - Atmospheric Environmental Research (IMK-IFU), Karlsruhe Institute of Technology, Kreuzeckbahnstr. 19, 82467 Garmisch-Partenkirchen, Germany

ARTICLE INFO

Keywords:

fAPAR
In-situ
Sentinel-2
Validation
Forest
Uncertainty
Essential Climate Variables

ABSTRACT

Accurate estimates of Essential Climate Variables (ECV) such as the fraction of Absorbed Photosynthetically Active Radiation (fAPAR) are essential for assessing global carbon balances. ESA's Sentinel-2 (S2) mission with its decametric resolution enables to derive fAPAR information at single forest stand. Validation studies on previously existing satellite-derived fAPAR products have found considerable discrepancies, especially in forest ecosystems that exceed relative discrepancies of 10% (i.e. 0.05 for absolute values) set as target accuracy by the Global Climate Observing System (GCOS).

This study presents the validation of S2 fAPAR products using direct radiation measurements of 2017 at three different forests, located in Central Europe (mixed-coniferous forest in temperate mid-latitude), North America (boreal-deciduous forest) and Central America (tropical dry forest, TDF). We measured incoming and transmitted PAR every 10 min synchronously using Wireless Sensor Networks (WSN) and calculated a two-flux fAPAR estimate. We validated the S2 fAPAR product with different instantaneous ground fAPAR estimates (e.g. instantaneous fAPAR at 10:00 and 14:00 local solar time) and daily average fAPAR. We considered uncertainties of ground data, i.e. bias related to the presence of colored autumn leaves and influences of solar zenith angle.

Overall, we found high discrepancies between the S2 fAPAR product and ground measurements, indicating that the S2 fAPAR product systematically underestimated (negative values for bias in percent) the ground observations. The highest agreement was observed at the boreal-deciduous forest stand with a bias of -13% ($R^2 = 0.67$). The Central American and European sites reported deviations of -20% ($R^2 = 0.68$) and -25% ($R^2 = 0.26$), respectively. At all sites, we found evidence that particularly the influence of colored leaves during the senescence periods lead to bias of the ground data. Further, the choice of temporal fAPAR estimate, i.e. daily average fAPAR or a certain instantaneous fAPAR estimate, lead to partly different results in the correlation analysis with the S2 fAPAR product. However, considering sources of uncertainties of ground data, we emphasize that only the boreal-deciduous site in Canada fulfilled the accuracy requirements set by the GCOS.

In contrast to absolute values, we found strong agreement on phenological changes at all three sites. Specifically, the influence of species composition on seasonal variability of fAPAR across the European mixed-coniferous site was well-represented in the S2 fAPAR product. As for the representation of spatial variability, we found highest agreement at the boreal-deciduous forest stand (BIAS = -22% , $R^2 = 0.93$), whereas spatial variability was least represented at the TDF site (BIAS = 125% , $R^2 = 0.97$). We conclude that the S2 fAPAR product has strong capabilities for assessing temporal variability of fAPAR, but due to low accuracy of absolute values currently limited options to feed global production efficiency models and assess global carbon balances.

* Corresponding author.

E-mail addresses: b.putzenlechner@iggf.geo.uni-muenchen.de (B. Putzenlechner), scastro@ualberta.ca (S. Castro), ralf.kiese@kit.edu (R. Kiese), r.ludwig@lmu.de (R. Ludwig), p.marzahn@iggf.geo.uni-muenchen.de (P. Marzahn), iain@ualberta.ca (I. Sharp), arturo.sanchez@ualberta.ca (A. Sanchez-Azofeifa).

<https://doi.org/10.1016/j.rse.2019.111310>

Received 12 December 2018; Received in revised form 17 June 2019; Accepted 6 July 2019

0034-4257/ © 2019 Elsevier Inc. All rights reserved.

1. Introduction

Satellite remote sensing of vegetation has evolved rapidly, offering global information on the status and dynamics of biophysical variables, such as the fraction of Absorbed Photosynthetically Active Radiation (fAPAR). fAPAR links available Photosynthetic Active Radiation (PAR) in the wavelength region between 400 and 700 nm to the absorption of plants (Gobron and Verstraete, 2009). As fAPAR represents a key role in many ecosystem processes (Möttus et al., 2011) and is needed for assessing global plant productivity and carbon balances (Gower et al., 1999; Prince and Goward, 1995), it has been considered an Essential Climate Variable (ECV) by the Global Climate Observing System (GCOS) (GCOS, 2011). Satellite-derived fAPAR products have been used for the monitoring of photosynthetic activity (Gobron et al., 2006), biomass production (Meroni et al., 2014), the evolution of drought events (Gobron et al., 2005), tree phenology (Gond et al., 1999) and variations of foliage chlorophyll (Zhang et al., 2013).

Over the last decade, several satellite missions have led to an increased availability of fAPAR products based on the development of new retrieval algorithms (Gobron, 2015). Besides the empirical retrieval of fAPAR from vegetation indices such as the Normalized Difference Vegetation Index (NDVI) (Fensholt et al., 2004; Myneni and Williams, 1994), operational fAPAR products are commonly generated using Radiative Transfer Models (RTM), Artificial Neural Networks (ANN), Lookup Tables (LUT) or combinations thereof (Baret et al., 2007; Carrer et al., 2013; Li et al., 2015; Myneni et al., 1997; Tao et al., 2016; Yuan et al., 2015). fAPAR products have commonly been available at kilometeric (e.g. GEOV1 fAPAR product from SPOT/VEGETATION) and hectometric (e.g. PROBA-V fAPAR product) spatial resolutions, thereby not perfectly matching the spatial resolution desired for agricultural and forestry applications (Clevers and Gitelson, 2013). Thus, efforts have been made to downscale products by using auxiliary optical remote sensing observations (e.g. Li et al., 2017a; Wang et al., 2016). Since 2015, ESA's satellite mission Sentinel-2 (S2) offers a fAPAR product with decametric spatial resolution, thereby facilitating the monitoring of vegetation productivity and dynamics on the scale of single agricultural fields and forest stands (Drusch et al., 2012; Frampton et al., 2013). The S2 mission consists of two identical satellites (S2A since June 2015 and S2B since March 2017), thereby ensuring image acquisition for a given site every five days.

While the evaluation of the scientific capabilities of the S2 mission is already ongoing for a wide range of applications (e.g., Clasen et al., 2015; Dotzler et al., 2015; Immitzer et al., 2016; Korhonen et al., 2017; Majasalmi and Rautiainen, 2016; Mura et al., 2018), the validation of derived fAPAR products has not been done yet. In this regard, validation means the process of analytically comparing a satellite product with a reference dataset assumed to represent the "true" value of the remotely sensed target which can be carried out directly or indirectly (Trevithick et al., 2015). Direct validation requires ground measurements as a reference data source that is usually quite scarce. Indirect validation, i.e. inter-comparison of different satellite-products, offers the advantage of higher temporal and spatial coverage (Justice et al., 2000), and has thus been carried out more frequently (e.g., Disney et al., 2016; D'Odorico et al., 2014; Martínez et al., 2013; McCallum et al., 2010; Morissette et al., 2006; Xu et al., 2018). Over the last decade, numerous studies conducted with the goal of intercomparing and validating existing satellite-derived fAPAR products have found considerable discrepancies, especially within forest ecosystems (D'Odorico et al., 2014; Martínez et al., 2013; McCallum et al., 2010; Pickett-Heaps et al., 2014; Pinty et al., 2011; Tao et al., 2015). As fAPAR is determined by both ecosystem function and structure (Ollinger, 2011) and therefore varies across different ecosystems (Gower et al., 1999) and within single forest stands (Leuchner et al., 2011; Möttus, 2004), existing studies on the evaluation of different fAPAR products have stressed the need for independent in-situ data in different ecosystems (Camacho et al., 2013; D'Odorico et al., 2014;

Gobron, 2015; Wang et al., 2016).

Unfortunately, outcomes of direct validation studies with the objective of using in-situ data have been compromised by a) either the use of indirect fAPAR retrieval methods or b) a limited number of PAR sensors at the ground level to generate the fAPAR estimate. As direct measurements are costly and labor-intensive, fAPAR is often retrieved indirectly from Digital Hemispherical Photography (DHP) (Li et al., 2015; Nestola et al., 2017), measurements of Leaf Area Index (LAI) (Fensholt et al., 2004; Pinty et al., 2011) or 3D simulations which require prior information on canopy structure and spectral properties of the canopies (Hovi et al., 2017; Majasalmi et al., 2017; Stenberg et al., 2013). For the rare case that direct PAR measurements are available to generate a fAPAR ground reference, only few sites are equipped to perform a multi-temporal validation of satellite-derived fAPAR products (Gobron, 2015). Instead, often only few sensors are used even though existing studies have stressed the need for taking multiple samples in forest ecosystems (Reifsnyder et al., 1971; Widlowski, 2010). For example, the assessments of different satellite-derived fAPAR products by D'Odorico et al. (2014) and Tao et al. (2015) relied on PAR flux measurements acquired at one single location per site, thereby limiting their outcome for a comprehensive validation.

Besides a sufficient number of samples needed for direct fAPAR observations, validation studies have to consider that also direct in-situ fAPAR observations may incorporate considerable uncertainties (Trevithick et al., 2015). In fact, discrepancies between ground data and satellite-derived fAPAR products mainly arise from (a) the estimating scheme and influences from environmental conditions (Widlowski, 2010), (b) different underlying fAPAR definitions (Gobron and Verstraete, 2009), and (c) spatial and temporal aggregation methods applied (Majasalmi et al., 2017; Wang et al., 2016). As for the estimation scheme (a), physically complete fAPAR estimates would require simultaneous measurements of all components of the radiation balance, including incoming solar radiation in the PAR domain, PAR reflectance at the top-of-canopy level, PAR transmission down to surface-level, PAR albedo of the surface as well as the contribution of horizontal fluxes entering and exiting the canopy target (Chen, 1996; Widlowski, 2010). As it is unfeasible to measure all these quantities in practice, certain terms must be ignored or approximated and the resulting fAPAR estimates are then differentiated by the number of considered flux contributions (Widlowski, 2010). The so-called two-flux fAPAR estimate, for example, only considers incoming and transmitted PAR and has the advantage that no tower for measuring the PAR reflectance at the top-of-canopy level is required. It has been shown that the accuracy of two-flux fAPAR measurements are mainly affected by illumination conditions, seasonal changes in leaf color (i.e. during senescence period) as well as changes in albedo of the forest surface during the presence of snow (Putzenlechner et al., 2019; Widlowski, 2010). As for the definition of fAPAR (b), satellite fAPAR products usually consider the contribution of the living green vegetation elements (denominated as "green fAPAR"), whereas direct radiation measurements refer to all contributions from vegetation elements, known as "total fAPAR" (Gobron, 2015). Regarding the temporal aggregation method applied (c), Majasalmi et al. (2017) found considerable discrepancy between daily averaged and instantaneous fAPAR at a boreal forest site in Finland, thereby questioning the common assumption of instantaneous fAPAR acquired at 10:00 or 14:00 local solar time being a good approximation of daily integrated fAPAR (Baret et al., 2011; Camacho et al., 2013; Martínez et al., 2013). Recently, Nestola et al. (2017) presented the results of a validation study of two satellite-derived fAPAR products at a mountainous deciduous forest site and found high agreement of different ground measurement methods, e.g. between direct fAPAR observations based on PAR sensors and DHP measurements. However, it remains unclear whether the fAPAR ground data was affected by commonly known sources of uncertainties, such as the presence of colored leaves during the senescence period or systematic errors introduced by topographic shadowing. In this regard, it

has been shown that PAR sensors arranged in so-called Wireless Sensor Network (WSN) are an efficient way to offer long-term observations of fAPAR with uncertainty information (Putzenlechner et al., 2019; Rankine et al., 2014), thereby opening new opportunities for validating decametric biophysical products.

In this article, we present the first validation study of the S2 fAPAR product based on direct fAPAR ground estimates carried out in three different ecosystems: a temperate mixed-coniferous forest in Germany, a boreal-deciduous forest in Alberta, Canada and a tropical dry forest (TDF) in Costa Rica. These forest ecosystems have substantial phenological variations in common, even though the underlying meteorological drivers for these changes are different (i.e. dormant periods due to the absence of rainfall at the TDF site vs. low temperatures and lack of sunlight at the temperate and boreal site). Further, the sites present different species composition and forest structure. This leads us to the hypothesis that not only the representation of absolute values could differ between fAPAR ground measurements and the S2 fAPAR product, but also the representation of temporal and spatial variability as well. Thus, our main objectives were to a) validate the S2 fAPAR with fAPAR ground estimates, b) assess the differences between forest ecosystems and c) discuss the role of uncertainties related to two-flux fAPAR ground estimates. Therefore, we used WSNs for continuous and synchronized measurements of incoming and transmitted PAR at all sites and compared the resulting two-flux fAPAR observations with the S2 fAPAR product. We collected additional information on species composition, meteorological and phenological conditions to discuss the role of uncertainties of ground data. To our knowledge, we hereby present the first validation of the S2 fAPAR product based on direct fAPAR measurements and a comparison of fAPAR acquired in different forest ecosystems.

This article is organized as follows: Section 2 introduces the study sites located in three different ecosystems (2.1), explains the acquisition of ground data (2.2) and the S2 fAPAR product (2.3) and describes the validation approach and statistical analysis applied (2.4). Section 3 presents the results of obtained fAPAR ground observations (3.1) and their level of agreement with the S2 fAPAR product (3.2), including the representation of temporal and spatial variability. Section 4 discusses the findings regarding absolute value representation (4.1) as well as temporal and spatial consistency (4.2) of the S2 fAPAR product and evaluates the validation approach (4.3). Section 5 provides conclusions and recommendations on the usage and future potentials of the investigated S2 fAPAR product.

2. Materials and methods

2.1. Study sites

Study sites for permanent fAPAR ground observations comprise three different forest biomes: A Central European mixed-coniferous forest, a North American boreal-deciduous forest and a Central American TDF (Table 1). The Central European site “Graswang” (Fig. 1a) is located in Southern Germany in a sub-alpine valley which is surrounded by the Ammer Mountains. It comprises a mid-aged spruce-dominated forest stand, with 82% Norway spruce (*Picea abies*), 14% European beech (*Fagus sylvatica*) and 4% Sycamore maple (*Acer pseudoplatanus*). The climate can be classified as warm-temperate fully-humid climate with warm summers (Köppen’s classification), with mean annual precipitation around 1300 mm and a mean annual air temperature of 6.8 °C (monthly mean temperatures range from −2.5 °C in January to 15.6 °C in July). Snowfall occurs frequently between November and March so that the vegetation period typically spans from late April to the end of September. The site is part of the pre-Alpine TERENO research project (Terrestrial Environmental Observatories) for long-term environmental research (Zacharias et al., 2011) and was equipped with a WSN for continuous fAPAR observations in 2015.

The Peace River Environmental Monitoring Super Site in Northern

Alberta, Canada (“Peace River”) (Fig. 1b) comprises an old-growth boreal-deciduous forest stand dominated by trembling aspen (*Populus tremuloides*) with a broadleaf deciduous canopy (Rankine et al., 2014; Taheriazad et al., 2016). The site is part of the joint industry-research forestry region for Ecosystem Management Emulating Natural Disturbance (EMEND) for large-scale boreal forest preservation and harvest experimentation (Spence and Volney, 1999). The climate is humid-continental with cool summers and snowy winters, with a mean annual temperature of 1.2 °C and annual precipitation sum of 400 mm. The vegetation period is relatively short, usually starting not before mid of May and ending until the mid of September. The forest stand is characterized by two distinct vertical layers of vegetation with an observed decreasing woody density with height; the understory canopy reaches up to 4 m and the upper canopy layer up to 15–20 m height (Rankine et al., 2014). A 30 m tall flux tower located at the Super Site was used for meteorological observations. The monitoring with the WSN began in 2012 and is ongoing.

The Santa Rosa National Park Environmental Monitoring Super Site (“Santa Rosa”) is located in the Province of Guanacaste, Costa Rica. The climate is tropical-monsoonal with a 6-month dry season (December to May) and a highly variable precipitation ranging from 900 to 2600 mm with an average around 1600 mm (Kalacska et al., 2004). Deforestation activities have happened across the entire region of the study site due to clearing lands for pasture, agriculture, timber extraction and tourism, resulting in various stages of 0–400-year-old secondary forest successions (Li et al., 2017b). We used data of two WSNs (“Principe” and “Perros” in Fig. 1c) located in forests of an intermediate successional stage that typically consists of two vertical canopy layers. The upper canopy layer is composed of fast growing deciduous species and few evergreen species (< 10%) whereas the understory consists of lianas and shade tolerant species (Arroyo-Mora et al., 2005; Kalacska et al., 2004). Both WSN sites operate since 2013 and include 35–40 m high carbon flux towers.

Forest structure variables and species composition as summarized in Table 1 were assessed during forest inventories carried out in 2018 at Santa Rosa and 2015 at Graswang and Peace River, respectively. Species composition (trees and understory), species density S (total number of species per 0.1 ha), diameters at breast height (DBH) of all trees with DBH > 5 cm, stem density D (number of stems per 0.1 ha), basal area B (stem area per 0.1 ha) and tree heights H were inventoried within the WSNs including a buffer of 10 m. Additionally, detailed information on the spatial distribution of individual trees was assessed at Graswang which was used to validate the representation of species composition in the satellite-derived fAPAR product. Therefore, basal area of all species and percentages of different species were assessed for the 10 m surrounding of each node, ranging from 37.9 to 68.3 m²/ha for all tree species (thereof 77.7–96.7% occupied by spruce, 3.3–20.8% beech and 0.0–26.8% maple). Based on the assessed site characteristics, we calculated the Holdridge Complexity Index (HCI) as a measure of ecosystem complexity (Holdridge and Tosi, 1967) following Eq. (1):

$$HCI = \frac{HDBS}{10^3} \quad (1)$$

where H is the mean tree height, D the number of stems per 0.1 ha, B the basal area in m² per ha and S the total number of tree species. We used the modified HCI of Lugo et al. (1978) who adopted the HCI for secondary forests, considering all trees with DBH > 5 cm.

2.2. Ground observations

2.2.1. Instrumentation and set-up of Wireless Sensor Networks

The experimental set-up for the fAPAR measurements consisted of WSNs of self-powered nodes (model ENV-Link-Mini-LXRS, LORD MicroStrain, Cary, NC, USA) equipped with quantum PAR sensors (model SQ-110, Apogee, Logan, UT, USA; field of view 180°; uncertainty estimates: cosine response ± 5% at 75° SZA, temperature

Table 1
Species composition and forest structure variables of the study sites.

| Site names | Graswang, Germany | Peace River, Canada | Santa Rosa, Costa Rica |
|---|--|--|--|
| Geographical locations and altitudes | 47.5708° N, 11.0326° E; 864 m | 56.7441° N, 118.3439° W; 870 m | "Principe": 10.8543° N, 85.6080° W; 305 m; "Perros": 10.8437° N, 85.6275° W; 292 m |
| Forest biomes | Temperate mixed-coniferous forest | Boreal-deciduous forest | Tropical dry forest (TDF) |
| Trees: names of dominant species | <i>Picea abies</i> (Norway spruce), <i>Fagus sylvatica</i> (European beech), <i>Acer pseudoplatanus</i> (sycamore maple) | <i>Populus tremuloides</i> (trembling aspen), <i>Populus balsamifera</i> (balsam poplar) | <i>Luehea speciosa</i> , <i>Lonchocarpus minimiflorus</i> , <i>Guazuma ulnifolia</i> (bastard cedar), <i>Byrsonima crassifolia</i> |
| Understory vegetation: names of dominant species | <i>Oxalis acetosella</i> (wood sorrel), <i>Mercurialis perennis</i> (dog's mercury) | <i>Alnus crispa</i> (green alder), <i>Rosa acicularis</i> (prickly rose) | <i>Amphilophium paniculatum</i> , <i>Davilla kunthii</i> , <i>Annona reticulata</i> , <i>Ocotea veraguensis</i> , <i>Hirtella racemosa</i> |
| Species density S [no. of tree species (0.1 ha) ⁻¹] | 3 | 2 | 29 |
| DBH: MEAN ± SD [cm] | 13.4 ± 9.5 | 30.6 ± 8.2 | 12.5 ± 7.8 |
| Stem density D [no. of stems (0.1 ha) ⁻¹] | 231 | 4.1 | 120 |
| Basal area B [m ² (0.1 ha) ⁻¹] | 4.8 | 2.4 | 1.9 |
| Tree height H: MEAN ± SD [m] | 14.4 ± 2.3 | 26.5 ± 4.5 | 9.6 ± 3.2 |
| HCI | 48 | 1 | 64 |

response $0.06 \pm 0.06\%$ per °C, calibration uncertainty $\pm 5\%$ and non-stability $< 2\%$ y^{-1}). The PAR sensors were mounted at 1.3 m height on wooden poles using angle connectors to ensure correct leveling. Sensors were aimed upward to either measure incoming PAR (PAR_{in})

outside the forests or transmitted PAR (PAR_{trans}) inside the forests. Sensors were deployed in a hexagonal topology (Fig. 2) since this sampling scheme was found to a) maximize the sensing area covered by a given number of nodes and b) ensure signal quality and connectivity

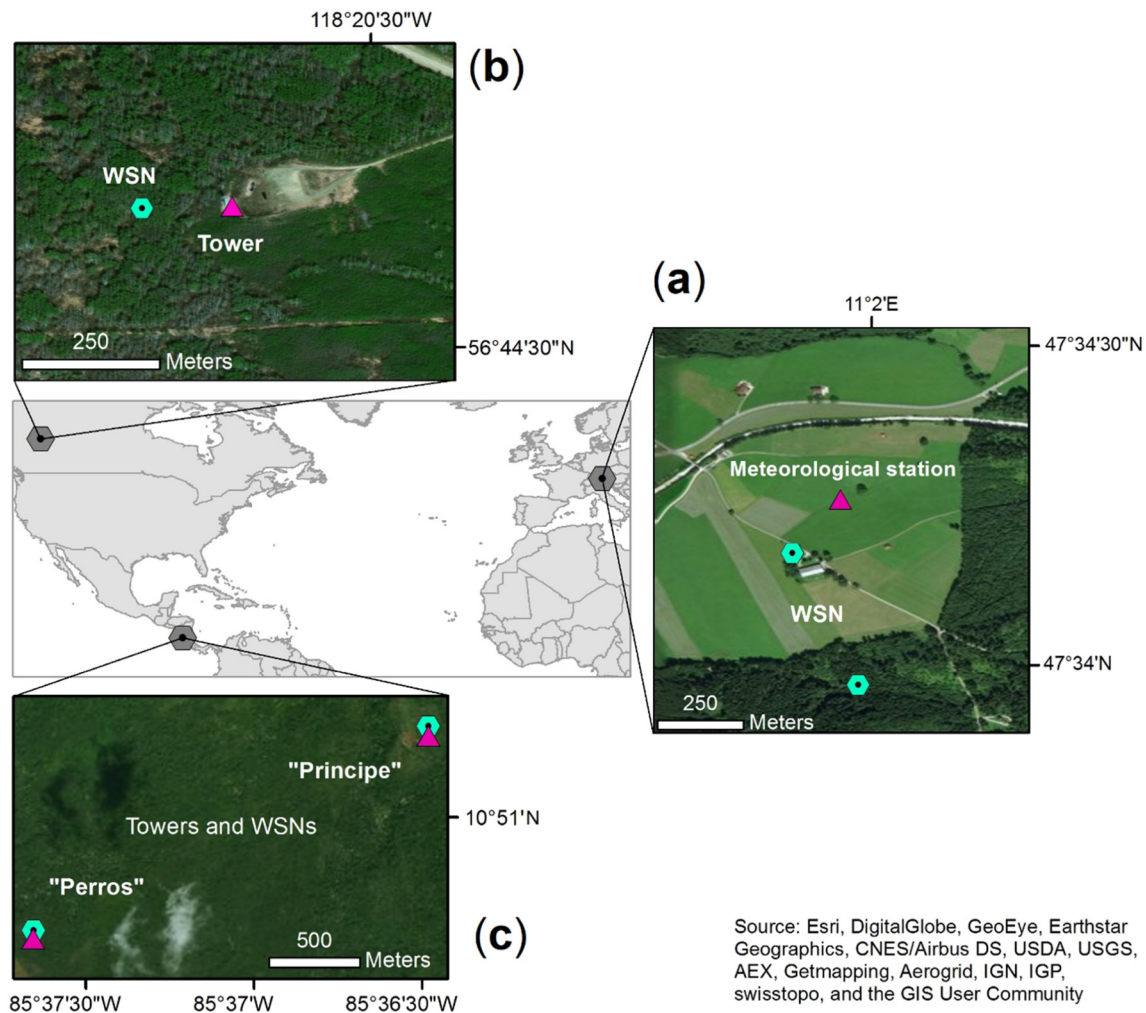


Fig. 1. Locations of the three sites equipped with WSNs: (a) At Graswang TERENO site, the reference sensor for incoming PAR is located on grassland outside the forest, transmitted PAR was measured inside the forest with 16 WSN nodes (each of them equipped with PAR sensors, Fig. 2); (b) The Peace River Environmental Super Site was equipped with 22 WSN nodes for transmitted PAR inside the forest, incoming PAR was measured on top of a flux tower; (c) At Santa Rosa National Park Environmental Monitoring Super Site, data of two WSN sites was used: "Principe" and "Perros", with 10 and 6 WSN nodes with sensors for transmitted PAR and incoming PAR measured on top of two flux towers, respectively.

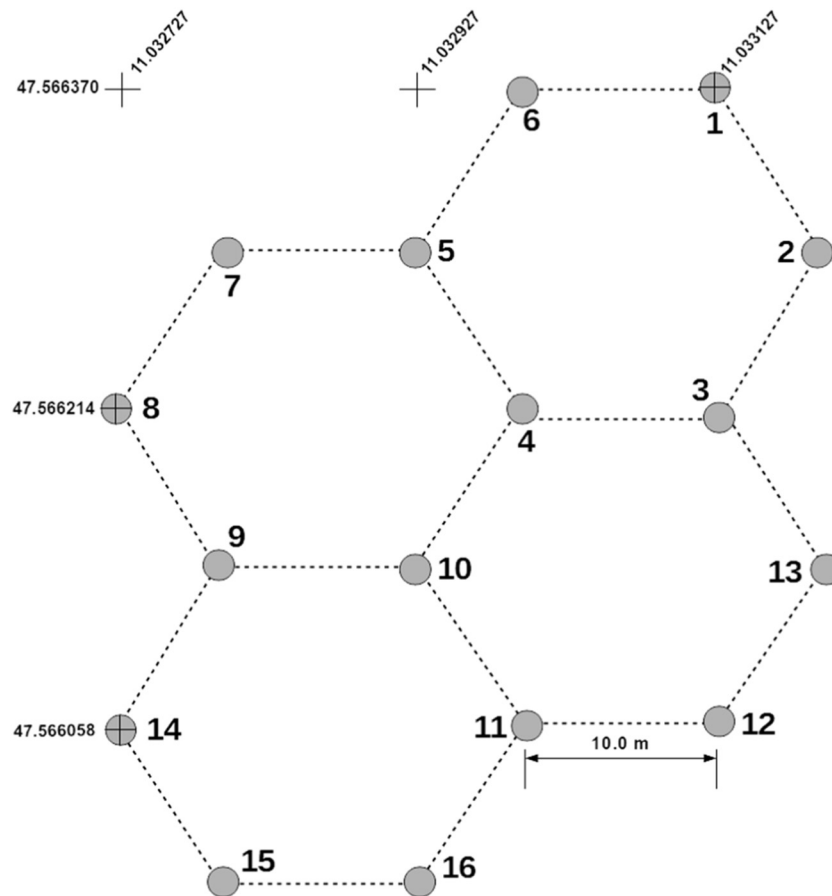


Fig. 2. Experimental setup of the WSN nodes with 16 sensors for transmitted PAR at the TERENO site Graswang, Germany.

(Mortazavi et al., 2014; Younis and Akkaya, 2008). To account for the different footprint which is dependent on the height of the canopy and based on previous investigations on the spatial autocorrelation of light in forests (Montgomery and Chazdon, 2001), nodes were deployed in 20 m spacing at the sites Santa Rosa and Peace River and 10 m spacing at Graswang.

At Graswang, PAR_{in} was measured with one PAR sensor approx. 300 m outside the forest in open grassland, while PAR_{trans} was measured simultaneously with 16 PAR sensors inside the forest (Figs. 1a, 2), covering an area of approx. 2000 m². At Peace River, PAR_{in} was measured on a flux tower outside the forest, while PAR_{trans} was measured with 22 nodes inside the forest, covering an area of approx. 5000 m² (Fig. 1b). At Santa Rosa, PAR was measured with two synchronized WSNs (“Santa Rosa/Principe”, “Santa Rosa/Perros”), with PAR_{in} measured on adjacent towers, and PAR_{trans} acquired with 10 (“Santa Rosa/Principe”) and 6 (“Santa Rosa/Perros”) sensors, respectively, covering an area of approx. 2000 m² in total (Fig. 1c).

The configuration of the WSN and data download were carried out with a portable receiver (frequencies ranging from 2.405 GHz to 2.480 GHz) equipped with USB interface (model WSDA-Base-104 USB Base Station, MicroStrain, Cary, NC, USA) to connect to a portable computer equipped with the software “Node Commander” (version 2.17.0, LORD MicroStrain, Cary, NC, USA). At Peace River and Santa Rosa, data aggregation was operationally carried out with a base station equipped with an outdoor transceiver (model WSDA-1000 Wireless Sensor Data Aggregator, MicroStrain, Cary, NC, USA) positioned on the towers. Internet access was obtained using a cellular GSM modem pointed at the nearest cellular tower. A battery bank (200 Ah) and solar panels (75 W) were used for power management (Pastorello et al., 2011; Rankine et al., 2014). At all sites, sensors were configured to measure instantaneous PAR every 10 min synchronously (~1 ns). Data

was uploaded to “Enviro-Net”, a web platform for sensor data management, near real-time visualization and analysis (Pastorello et al., 2011).

2.2.2. Meteorological and phenological observations

At Graswang, records of temperature, shortwave incoming radiation and precipitation (model WXT520, Vaisala, Vantaa, Finland) was used from the TERENO meteorological station. Further, observations of forest phenology were carried out using an automated camera (model SnapShot Mini 5.0, Dörr, Neu-Ulm, GER) installed at 1.3 m height and directed horizontally towards the center of the WSN. Measurements of the diffuse radiation, obtained from a sunshine pyranometer (model SPN1, Delta-T, Cambridge, UK) were used to select $fAPAR$ acquired under direct light conditions. We defined values of the ratio of diffuse-to-total incident radiation (d/Q) below 0.2 as direct light conditions for which an influence of the solar zenith angle (SZA) on $fAPAR$ is present (Leuchner et al., 2011; Widłowski, 2010). At Peace River, meteorological data (HOBO Energy Pro, OneTemp Pty Ltd., Adelaide, AU) was acquired at the flux tower outside the forest. At Santa Rosa, air temperature and precipitation were measured with two meteorological stations adjacent to the WSNs (same implementation as at Peace River).

2.2.3. Processing of PAR data and calculation of $fAPAR$ estimates

Measurements of PAR_{in} and PAR_{trans} carried out at 10 min temporal resolution were processed to two-flux $fAPAR$ estimates. $fAPAR$ was calculated a) individually at each sensor location in the forest (“individual $fAPAR$ ”) following Eq. (2) and b) as spatial average (“domain $fAPAR$ ”) following Eq. (3):

$$fAPAR_{i,t} = 1 - \frac{PAR_{trans,i,t}}{PAR_{in,t}} \quad (2)$$

$$fAPAR_{n,t} = \frac{1}{n} \sum_i^n fAPAR_{i,t} \quad (3)$$

where $fAPAR_{i,t}$ is the individual fAPAR at a time step t at an individual PAR_{trans} sensor location i ; $fAPAR_{n,t}$ is the domain mean fAPAR at a given time step t based on all n PAR_{trans} sensor locations. We chose the two-flux approach as it has the advantage of being relatively cost and labor efficient as measurements of top-of-canopy reflectance and thus the installation of a tower is not required. The main disadvantage of the two-flux fAPAR approach is its susceptibility to changes in background albedo which is mainly altered by the occurrence of snow (Widłowski, 2010). Thus, we focus our analysis on non-winter conditions.

At the sub-alpine site Graswang, the WSN was periodically affected by topographic shadowing. We determined all potentially affected time steps for each sensor location based on the solar position and a Digital Elevation Model (DEM 5 m, Free State of Bavaria, <https://www.ldbv.bayern.de>) using the R-package “insol” (version 1.2, <https://cran.r-project.org/web/packages/insol/insol.pdf>). Data affected by topographic shadowing was excluded from the dataset. Further, we considered shadowing of moving clouds, as sensors for PAR_{in} and PAR_{trans} are separated by 300 m. Therefore, we excluded all time steps for which PAR_{trans} exceeded PAR_{in} which would occur for the case that the reference sensor outside the forest was shadowed by a cloud. Errors introduced by the opposite case, i.e. sensors in the forests affected by a cloud shadow, were limited by excluding all PAR data acquired under mixed illumination conditions ($0.2 \leq d/Q < 0.9$). As the WSNs at Santa Rosa and Peace River are located on relatively flat terrain, topographic shadowing did not occur. Further, as PAR_{in} was acquired on flux towers adjacent to sensors for PAR_{trans} at these sites, we assumed errors caused by cloud shadowing to be negligible.

As the S2 fAPAR product refers to daily integrated fAPAR, we considered daily average fAPAR ($fAPAR_{DAY}$) calculated from all daylight time steps as our main reference of comparison. However, recent research (Majasalmi et al., 2017) has questioned the underlying assumption that the daily integrated fAPAR corresponds to instantaneous fAPAR at 10:00 (or 14:00) solar time used in several satellite-derived fAPAR products (Baret et al., 2011; Camacho et al., 2013; Martínez et al., 2013). Therefore, we further distinguished between several temporal (i.e. instantaneous and aggregated) fAPAR estimates: fAPAR acquired at 10:00 ($fAPAR_{INST10}$), 12:00 ($fAPAR_{INST12}$) and 14:00 ($fAPAR_{INST14}$) local solar time, average fAPAR of $fAPAR_{INST10}$ and $fAPAR_{INST14}$ ($fAPAR_{INST10\&14}$) as well as average fAPAR between 10:00 and 14:00 local solar time ($fAPAR_{INST10TO14}$). At Graswang, we distinguished individual $fAPAR_{DAY}$ according to the proportions of basal area of spruces ($fAPAR_{spruces} > 90\%$ spruces) and beeches ($fAPAR_{beeches} < 80\%$ spruces) in the 10 m-surrounding of each sensor for PAR_{trans} .

fAPAR ground estimates may be affected by systematic diurnal changes in illumination conditions, particularly at the tropical site where thunderstorms are typically occurring in the afternoon (Yang and Slingo, 2001). Thus, we selected PAR acquired during clear sky conditions ($PAR_{in} > 900 \mu\text{mol m}^{-2} \text{s}^{-1}$) to calculate “black-sky fAPAR”. For assessing the differences between temporal fAPAR estimates, we calculated the mean (MEAN) and standard deviation (SD) of domain fAPAR ground estimates and applied the non-parametric Kolmogorov-Smirnov test (KS test) with 0.05-significance level to test on the equality of value distributions between domain $fAPAR_{INST10}$, $fAPAR_{INST14}$, $fAPAR_{INST10\&14}$, $fAPAR_{INST10TO14}$ and domain $fAPAR_{DAY}$, respectively.

2.3. Processing of the Sentinel-2 fAPAR product

S2 data is available since 2015 from the Copernicus Open Access Hub (<https://scihub.copernicus.eu/>). The two S2 satellites, S2A and S2B, are identical and ensure a combined constellation revisit of five days with a spatial resolution of 10–60 m depending on the band number (Drusch et al., 2012; Malenovsky et al., 2012). For all three

study sites, cloud-free scenes were downloaded for the year 2017 as Top-Of-Atmosphere (TOA) Level-1C products (WGS84 UTM projection) which include radiometric and geometric corrections. To retrieve the Bottom-Of-Atmosphere (BOA) corrected reflectance Level-2A product, atmospheric correction was performed using the module “Sen2Cor” (version 2.3) (Mueller-Wilm, 2018) from the “Sentinel-2 Toolbox” embedded in ESA’s free software “SNAP”, version 6.0 (<http://step.esa.int/main/toolboxes/snap/>). Besides the atmospheric correction, the processing step includes a scene classification algorithm, considering clouds, shadows, vegetation, soils/deserts, water and snow (ESA, 2015). Level-2A scenes as well as scene classification outputs were inspected visually at the study sites to exclude pixels affected by cloud cover or shadows from clouds or topography.

From Level-2A scenes, the S2 Level-2B product with fAPAR and several other biophysical variables was calculated using the “L2B biophysical processor” (version 1.1) (Weiss and Baret, 2016). The implemented algorithm is an evolution of algorithms that have been applied to retrieve biophysical products from sensors of VEGETATION, MERIS, SPOT, and LANDSAT satellites (Li et al., 2015; Weiss and Baret, 2016). The algorithm was developed with a neuronal network trained over the PROSPECT+SAIL radiative transfer model on S2 TOC reflectances to derive LAI, fAPAR and FCOVER and does not require prior information on land cover.

The product definition of fAPAR corresponds to daily integrated fAPAR values, following the assumption that daily integrated values of fAPAR under clear sky conditions (“black-sky fAPAR”) are close to the instantaneous fAPAR values obtained at 10:00 (or 14:00) local solar time (Baret et al., 2011). Further, the S2 fAPAR product refers to green parts of the canopy (“green fAPAR”). The algorithm uses vegetation bands of different spatial resolution (10 m spatial resolution: B3, B4, B8; 20 m: B5, B6, B7, B11, B12). To avoid oversampled data without increasing the spectral information, we carried out the validation at 20 m spatial resolution, corresponding to the spatial resolution of S2 bands 5–7 and 11–12. Finally, processed S2 fAPAR products ($fAPAR_{S2}$) were only used for validation when quality indicators were inconspicuous (“QA = 0 0 0: data is OK”).

2.4. Validation approach

A summary of the preprocessing steps of ground and satellite-derived fAPAR and the validation approach outlined in the following is illustrated in Fig. 3.

2.4.1. Linking the S2 fAPAR product to ground measurements

The S2 fAPAR product with its relatively high spatial resolution of 20 m matches the decametric resolution of the ground observations. To link fAPAR-S2 to ground observations, we considered buffer areas (radius of 10 m at Graswang and Santa Rosa and 20 m at Peace River to account for different footprints due to different average tree height) around each sensor location i for PAR_{trans} . For each date when an S2 image was available, all m_i intersecting S2 pixels j_i for the footprint area of a sensor location i were identified (and then also for all n sensor locations of the WSN) (Fig. 4). Based on the proportion share w_{j_i} , the fAPAR-S2 product at sensor location i corresponding to individual fAPAR (Eq. (2)) $fAPAR_{S2_i}$ was calculated as weighted average following Eq. (4). The fAPAR-S2 product corresponding to domain fAPAR (Eq. (3)) $fAPAR_{S2_n}$ was calculated following Eq. (5).

$$fAPAR - S2_i = \sum_{j_i}^{m_i} w_{j_i} fAPAR - S2_{j_i} \quad (4)$$

$$fAPAR - S2_n = \frac{1}{n} \sum_i^n fAPAR - S2_i \quad (5)$$

When referring to the common terminology used in validating studies (e.g., Morisette et al., 2006), individual fAPAR measured

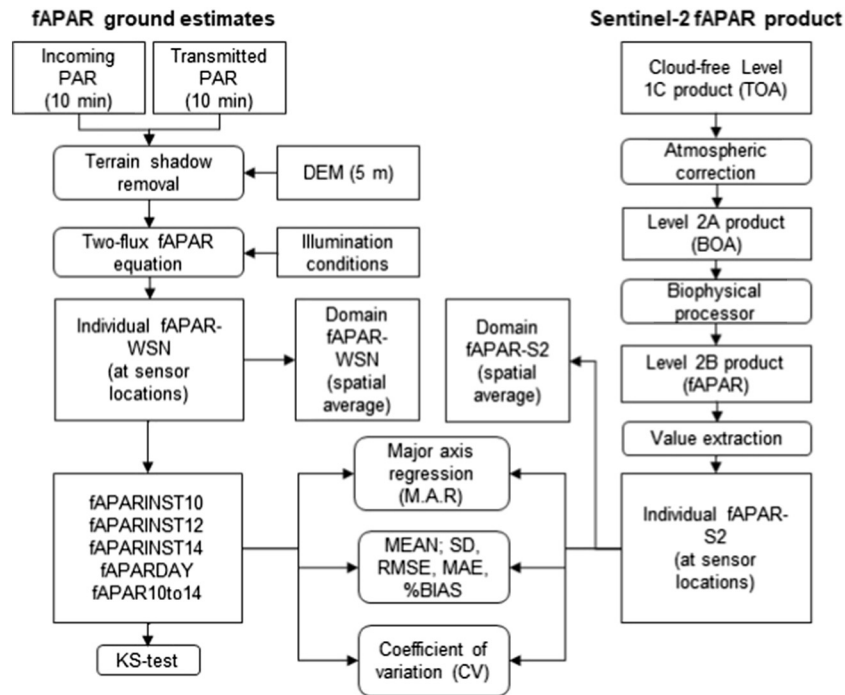


Fig. 3. Workflow of the validation strategy of the S2 fAPAR product in three different ecosystems.

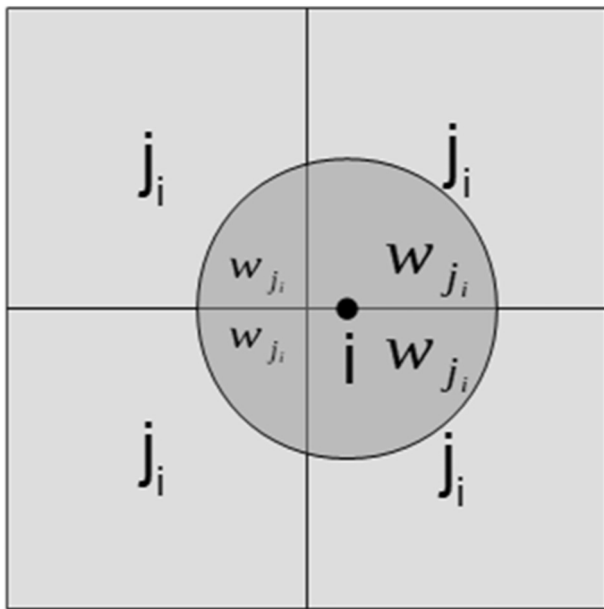


Fig. 4. Schematic example for variables of interest for extracting the S2 fAPAR value and link it to measured fAPAR; j_i as an individual S2 pixel which intersects with the footprint area around sensor location i and w_{j_i} as the intersecting area of j_i with the footprint area of i as area proportion.

(extracted) at (around) a single sensor location refers to secondary sampling units (SSU) while domain fAPAR as spatial average refers to the elementary sampling unit (ESU), thereby representing the spatial variability across the study site.

2.4.2. Statistical analysis

We performed a correlation analysis between individual fAPAR-S2 and individual fAPAR estimates (i.e. fAPAR_{DAY}, fAPAR_{INST10}, fAPAR_{INST12}, fAPAR_{INST14}, fAPAR_{INST10&14} and fAPAR_{INST10to14}) using several performance metrics. We calculated the Root Mean Square Error (RMSE) as usually recommended for the validation of satellite products

(Fernandes et al., 2014) and the Mean Absolute Error (MAE) to assess the accuracy (total error) of both datasets in units of fAPAR. Compared to RMSE, MAE is less sensitive to outliers and sometimes considered as easier to interpret (Pontius et al., 2008). We calculated the mean difference between value pairs in percent (%BIAS) to assess systematic offsets, i.e. the average tendency of the ground observations to be larger or smaller than fAPAR-S2. We assumed both ground estimates and fAPAR-S2 to be affected by uncertainties based on previous investigations (D’Odorico et al., 2014; Tao et al., 2015; Widlowski, 2010). Therefore, we chose Major Axis Regression (M.A.R.) as Ordinary Least Square Regression (OLS) is known to underestimate the slope of the linear relationship when both variables contain considerable errors (Legendre and Legendre, 2012). We computed the 95%-confidence intervals for the slope and intercept parameters of the linear regression model as well as the squared Pearson correlation coefficient (R^2) to assess the goodness of fit. We compared our results with the requirements set by GCOS (2011), demanding a maximum bias of 10% (0.05) for fAPAR products.

To compare the site-specific spatial variability in both datasets, we calculated the Coefficient of Variation (i.e. ratio of the standard deviation to the mean in percent; CV) as a function of the number of samples for individual fAPAR_{DAY} and fAPAR-S2. Therefore, we determined all possible combinations of sensor locations (i.e. SSUs) for the total number of sensors for PAR_{trans} per site with the binomial coefficient and then calculated the maximum CV of fAPAR for each of these combinations. Based on the obtained CV values per number of samples, we calculated the above-mentioned performance metrics and M.A.R. to assess the agreement between ground measurements and the S2 fAPAR product.

3. Results

3.1. fAPAR ground observations

Seasonal courses of domain and individual fAPAR_{DAY} are depicted in Fig. 5. As can be seen the permanent monitoring of fAPAR at the three sites resulted in almost continuous time series for the year 2017, with data gaps in June for two weeks at Peace River and for ten days at

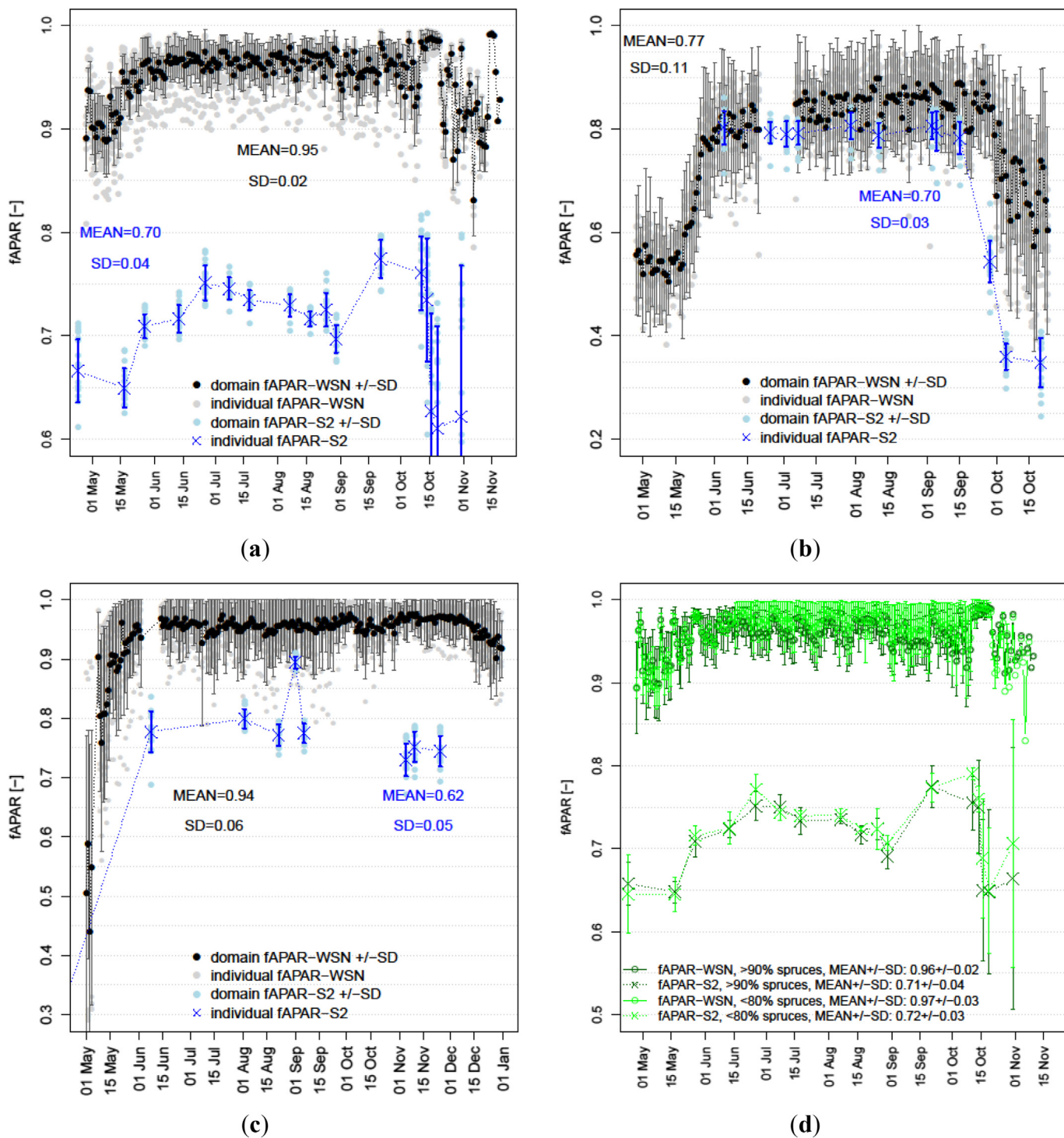


Fig. 5. Domain and individual $fAPAR_{DAY}$ measured with WSNs and $fAPAR-S2$ for the year 2017 at (a) Graswang, (b) Peace River and (c) Santa Rosa. Panel (d) shows domain and individual $fAPAR_{DAY}$ and $fAPAR-S2$ distinguished for $fAPAR_{spruces}$ and $fAPAR_{beeches}$.

Santa Rosa due to outage of reference sensors (PAR_{in}). Domain $fAPAR$ at Graswang (MEAN = 0.95) and Santa Rosa (MEAN = 0.94) was almost constantly above 0.90 (Fig. 5a, c), whereas $fAPAR$ remained always below this value at Peace River (MEAN = 0.77) (Fig. 5b). Seasonal variability, expressed in SD of domain $fAPAR_{DAY}$, was comparatively weak at Graswang (SD = 0.02) and more distinct at Peace River (SD = 0.11) and Santa Rosa (SD = 0.06). Fig. 5d shows that the weak seasonality was mainly attributed to the dominance of conifers at this site, altered by the phenology of beech trees, with $fAPAR_{beeches}$ showing higher $fAPAR$ than $fAPAR_{spruces}$ during the summer

months. Fig. 5 illustrates differences in value distributions of individual $fAPAR_{DAY}$. At all sites, $fAPAR$ followed a unimodal left-skewed distribution. The distributions at Graswang and Santa Rosa show a rather narrow specification with pronounced peaks above 0.95, whereas at Peace River, the distribution is more expanded, showing no pronounced peak and a local maximum around 0.58.

3.1.1. Evaluation of phenological changes

At Peace River and Graswang, $fAPAR_{DAY}$ showed relatively abrupt

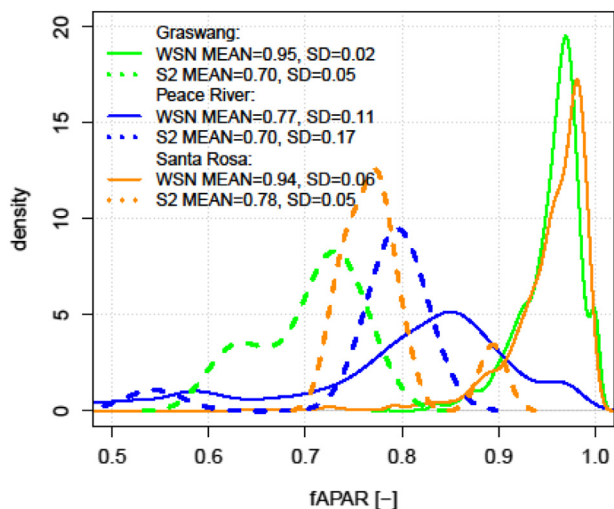


Fig. 6. Kernel density distributions of individual $fAPAR_{DAY}$ of WSN and $fAPAR-S2$ at Graswang, Peace River and Santa Rosa.

changes across one single month in both spring and autumn (Fig. 5a–b). At Santa Rosa, $fAPAR_{DAY}$ increased abruptly only in spring, shortly after the first rainfalls in May (Fig. A1) and showed slowly decreasing $fAPAR$ towards the end of the vegetation period. After the green-up, plateau phases with only marginal fluctuations of $fAPAR$ occurred, with $fAPAR$ staying around 0.97 at Graswang and around 0.92 at Santa Rosa between June and September. At Peace River, $fAPAR$ continued to increase throughout the whole vegetation period. At all three sites and for periods between two to four weeks, highest $fAPAR$ values were recorded just before the decrease of $fAPAR$ in the senescence period set in: highest $fAPAR$ was reached at Graswang (max = 0.99) between October 1st and 19th (Fig. 5a), at Peace River (max = 0.91) between September 15th and 17th (Fig. 5b) and at Santa Rosa (max = 0.96) between October 17th and December 1st (Fig. 5c). For Peace River and Graswang, the periods with highest values are represented with the local maxima at the right end of the value distributions in Fig. 6. At the end of the season, $fAPAR$ showed high day-by-day fluctuations in combination with high SDs at both Peace River (± 0.10) and Graswang (± 0.05).

3.1.2. Differences of temporal $fAPAR$ estimates

We calculated several temporal $fAPAR$ estimates, i.e. $fAPAR_{INST12}$, $fAPAR_{INST10}$, $fAPAR_{INST14}$, $fAPAR_{INST10to14}$ and $fAPAR_{INST10&14}$ and compared their distributions to domain $fAPAR_{DAY}$. Although Table 2 shows similar MEAN and SD of different temporal estimate (i.e., maximum difference for the MEAN ± 0.02 and for SD ± 0.06 of distributions), we found significant to $fAPAR_{DAY}$. At Graswang, $fAPAR_{INST10}$ and $fAPAR_{INST12}$ were significantly different from $fAPAR_{DAY}$ (KS test: p -value < 0.05); at Peace River, $fAPAR_{INST12}$ differed significantly from $fAPAR_{DAY}$ and at Santa Rosa, $fAPAR_{INST12}$, $fAPAR_{INST14}$ and $fAPAR_{INST10to14}$ were found to differ significantly from $fAPAR_{DAY}$. Thus, the common hypothesis of $fAPAR_{DAY}$ corresponding to $fAPAR_{INST10&14}$ is not supported by our measurements in the TDF.

3.2. Validation of the Sentinel-2 $fAPAR$ product with ground measurements

The processing of S2 data resulted in 19 $fAPAR$ product maps available for Graswang, 12 for Peace River and 15 for Santa Rosa (see examples in Fig. 7). For Peace River and Santa Rosa, no $fAPAR$ products could be derived for the early vegetation period due to frequent cloud cover. Accordingly, no satellite-derived $fAPAR$ could be obtained for the end of the vegetation period at Santa Rosa. When evaluating time series depicted in Fig. 5 it becomes clear that $fAPAR-S2$ was generally lower than measured $fAPAR$ at all three sites, though to various extents.

Further, Fig. 6 shows that measured $fAPAR$ and $fAPAR-S2$ disagreed on the order of value ranges for the different sites: highest average $fAPAR$ was measured at Graswang and lowest values at Peace River; however, $fAPAR-S2$ showed highest $fAPAR$ at Santa Rosa and similar value ranges for Graswang and Peace River. From Figs. 5 and 6 can be seen that the discrepancy between measured and satellite-derived $fAPAR$ was clearly highest at Graswang and lowest at Peace River.

Fig. 8 shows scatter-plots and performance metrics for the relationship between measured individual $fAPAR$ ($fAPAR_{DAY}$) and $fAPAR-S2$. The scatterplots show nearly vertical point accumulations for highest and lowest $fAPAR$ values at Graswang ($fAPAR \sim 0.62$ and $fAPAR \sim 0.77$) and Peace River ($fAPAR \sim 0.37$ and $fAPAR \sim 0.80$), suggesting for a saturation effect. At Graswang, weak correlations (highest $R^2 = 0.27$ for $fAPAR_{INST10to14}$) and comparatively poor accuracies (RMSE = 0.24) were obtained between $fAPAR$ estimates and $fAPAR-S2$ (Table 2). All $fAPAR$ estimates showed absolute discrepancies around 25% (lowest %BIAS = -24.6 for $fAPAR_{INST12}$), thereby exceeding the threshold accuracy demanded by the GCOS (2011) by more than two times. At Santa Rosa, slightly higher agreement was observed, with BIAS around -20% (highest $R^2 = 0.68$) obtained from several $fAPAR$ estimates (Table 2). Best agreement was obtained at Peace River, with BIAS between -16 and -13% (highest $R^2 = 0.67$, lowest RMSE = 0.16) depending on the choice of $fAPAR$ estimate. In Fig. 6 can be seen that $fAPAR-S2$ also followed a bimodal and rather expanded value distribution as obtained from the ground measurements.

3.2.1. Representation of temporal variability

We compared the representation of seasonal dynamics between $fAPAR$ -WSN and $fAPAR-S2$. At Graswang, both datasets agreed upon the beginning of the spring green-up, showing an increase of $fAPAR$ between 17th and 27th of May (Fig. 5a) that coincided with the beginning of leaf development observed in the photos of the automated camera (Fig. B1). Fig. 5d shows that for most of the acquisition dates from June to September, the slightly higher values for $fAPAR_{beeches}$ were also represented by $fAPAR-S2$. Accordingly, lower values of $fAPAR_{spruces}$ for the early and late vegetation period were well-reflected in $fAPAR-S2$. Thus, S2 captured the local differences in species composition despite the dominance of spruce trees at this site. We also found agreement between the beginnings of leaf senescence at all sites. At Graswang, observations of the automated camera confirm that leaves had completely fallen on October 31st when $fAPAR-S2$ was lowest (Fig. B1n). During the winter dormant periods at Graswang and Peace River, the S2 $fAPAR$ product also showed highest SD.

3.2.2. Representation of spatial variability

We investigated how the spatial variability was represented in the S2 $fAPAR$ product compared to ground measurements. In this regard, Fig. 9 shows varying levels of agreement between individual $fAPAR$ across the sites. At Graswang, variation of %BIAS was comparatively low, ranging from -30 to -20 across the site (Fig. 9a, d). Contrarily, %BIAS varied more at Peace River and Santa Rosa, ranging from -26 to 11 and from -32 to 25, respectively (Fig. 9b–d).

In Fig. 10a–c is displayed how the spatial variability of $fAPAR$, expressed with the Coefficient of Variation (CV), decreased as a function of sample size in ground and satellite-derived $fAPAR$ products. For a minimum combination of two sensors in the WSN, the highest incident CV (43%) was obtained at Peace River, followed by Graswang (34%) and Santa Rosa (24%). With increasing sample size, Peace River showed the highest reduction of CV achievable with the same sample size ($n = 16$). Contrarily, the S2 $fAPAR$ product presented the highest incident CV for Santa Rosa (49%), followed by Graswang (40%) and Peace River (29%) while the reduction of CV with increasing sample size was most pronounced at Graswang. With a positive %BIAS obtained at Graswang (68) and Santa Rosa (125), the S2 $fAPAR$ product presented higher spatial variability than ground observations (Fig. 10d).

Table 2

Overview of the MEAN and SD of distributions of different temporal fAPAR estimates of domain fAPAR; correlation analysis and performance metrics of temporal fAPAR estimates vs. fAPAR-S2 are shown. Significant differences ($n = 206$, KS test: $p < 0.05$) between value distributions of fAPAR estimates and fAPAR_{DAY} are indicated with *.

| Estimate | MEAN | SD | RMSE | MAE | %BIAS | R ² | M.A.R. | |
|------------------------|------|------|------|------|-------|----------------|-----------|-------|
| | | | | | | | Intercept | Slope |
| Graswang, Germany | | | | | | | | |
| 10:00–14:00 | 0.95 | 0.03 | 0.24 | 0.24 | –24.9 | 0.27 | 2.6 | –1.8 |
| 10:00* | 0.96 | 0.03 | 0.24 | 0.24 | –25.3 | 0.23 | 2.22 | –1.40 |
| 14:00 | 0.95 | 0.03 | 0.24 | 0.24 | –24.9 | 0.24 | 2.11 | –1.30 |
| 10:00 & 14:00 | 0.95 | 0.03 | 0.24 | 0.24 | –25.0 | 0.26 | 2.24 | –1.42 |
| 12:00* | 0.94 | 0.04 | 0.24 | 0.23 | –24.6 | 0.22 | 2.60 | –1.75 |
| Daily average | 0.95 | 0.02 | 0.24 | 0.24 | –25.2 | 0.22 | 3.18 | –2.32 |
| Peace River, Canada | | | | | | | | |
| 10:00–14:00 | 0.78 | 0.07 | 0.17 | 0.12 | –14.6 | 0.67 | –1.57 | 2.75 |
| 10:00 | 0.78 | 0.07 | 0.16 | 0.12 | –14.6 | 0.67 | –1.57 | 2.75 |
| 14:00 | 0.78 | 0.07 | 0.17 | 0.12 | –14.6 | 0.67 | –1.57 | 2.75 |
| 10:00 & 14:00 | 0.78 | 0.07 | 0.17 | 0.12 | –14.6 | 0.67 | –1.57 | 2.75 |
| 12:00* | 0.78 | 0.13 | 0.18 | 0.14 | –15.5 | 0.43 | –1.29 | 2.38 |
| Daily average | 0.77 | 0.11 | 0.16 | 0.11 | –13.4 | 0.64 | –1.59 | 2.81 |
| Santa Rosa, Costa Rica | | | | | | | | |
| 10:00–14:00 | 0.94 | 0.05 | 0.19 | 0.19 | –20.0 | 0.64 | –0.10 | 0.91 |
| 10:00 | 0.95 | 0.06 | 0.20 | 0.19 | –19.9 | 0.56 | 0.03 | 0.76 |
| 14:00* | 0.94 | 0.05 | 0.20 | 0.19 | –20.5 | 0.57 | –0.36 | 1.18 |
| 10:00 & 14:00* | 0.94 | 0.05 | 0.20 | 0.19 | –20.3 | 0.61 | –0.08 | 0.88 |
| 12:00* | 0.93 | 0.07 | 0.19 | 0.18 | –19.8 | 0.68 | –0.12 | 0.93 |
| Daily average | 0.94 | 0.06 | 0.20 | 0.20 | –20.7 | 0.59 | –0.40 | 1.22 |

Despite these disagreements, CV obtained for highest sample sizes are in a relatively similar range at Graswang (Fig. 10a) and convergence is observed with increasing sample size at Peace River (Fig. 8b). This suggests that S2 reasonably captured the spatial variability encountered across the forest stand at Graswang and Peace River. At Santa Rosa, however, spatial variability assessed with the WSN was overestimated by the S2 fAPAR product even for the highest number of samples by > 100% (Fig. 10d).

4. Discussion

4.1. Consistency of absolute fAPAR values

We presented the results of the validation of the S2 fAPAR product for the vegetation period of 2017 based on WSN ground measurements carried out in a temperate mixed-coniferous forest at the TERENO site Graswang, Germany, in a boreal-deciduous forest site at the Peace River Environmental Super Site, Northern Alberta, Canada, and in a tropical dry forest (TDF) at the Santa Rosa National Park Super Site, Costa Rica. In general, we found high discrepancies (i.e. $-25 \leq \%BIAS \leq -13$) between ground measurements and the S2 fAPAR product (Fig. 8), irrespective of the fAPAR estimate chosen, i.e. daily aggregated or instantaneous fAPAR estimates (Table 2). Here, our results agree with previous studies on the validation of satellite-derived fAPAR products other than S2 who reported unacceptably high discrepancies in forested areas (D'Odorico et al., 2014; Tao et al., 2016; Tao et al., 2015). Discrepancies may result from characteristics of the S2 algorithm (Weiss and Baret, 2016) as well as from uncertainties of ground measurements.

4.1.1. Role of the Sentinel-2 fAPAR product specifications

The generic nature of the retrieval algorithm, as clearly stated by Weiss and Baret (2016) in the S2 algorithm description document, could be a major reason for the high discrepancies. Specifically, the algorithm does not require priori information on land cover classes and a global land cover classification product serving the decametric resolution of S2 is not available. Disagreements were particularly high at the conifer-dominated site Graswang and the TDF site Santa Rosa. As for Graswang, the high discrepancies could be the result of a

misclassification which is favored by the mixture of different crown architectures of deciduous and coniferous trees. In this regard, Fang et al. (2013) noted that coniferous forests presented the highest risks of biome misclassification due to their relatively open canopy structure and thus larger contributions from understory to forest reflectance. For tropical sites such as Santa Rosa, previous research has identified difficulties of correct classification particularly for TDFs due to a lack of consideration of phenological changes as well as different successional stages and their implications for canopy reflectance (Sanchez-Azofeifa et al., 2009). A misclassification as a reason for the high deviations is also supported by the fact that spatial variability was higher in the S2 fAPAR product (Fig. 10). Further, the forest stands Graswang and Santa Rosa are characterized by higher ecosystem complexity (i.e. Graswang: HCI = 48; Santa Rosa: HCI = 64, Table 1) than Peace River (HCI = 1), also containing only deciduous species. The combination of lower HCI with only deciduous species at Peace River could explain the highest overall agreement between ground measurements and the S2 fAPAR product regarding both the representation of absolute fAPAR values (Fig. 8b) and spatial variability (Fig. 10d).

Further, the algorithm is based on the coupled PROSPECT+SAIL model, which has originally been developed for agricultural crops and mostly been validated for broadleaf canopies (Jacquemoud and Baret, 1990; Jacquemoud et al., 2009). Regarding the representation of needle leaf canopies, it was argued that the model still gave reasonable representation despite the “plate assumption” by Allen et al. (1969), assuming that the leaf consists of one or several absorbing plates with rough surfaces to account for isotropic scattering. Here, we see the need for validating the S2 fAPAR product at a purely coniferous forest to comprehensively assess the performance of the algorithm. However, based on our results, we clearly support the suggestion of Li et al. (2015) of making the S2 fAPAR algorithm “more specific”.

Observed discrepancies could also be attributed to different underlying fAPAR definitions of ground measurements and the S2 fAPAR product. In contrast to the ground measurements that are influenced by all absorbing elements and thus refer to “total fAPAR”, the S2 fAPAR product considers absorption by green vegetation components only. It is difficult to quantify the exact contribution of such bias in validation studies, as also acknowledged by Nestola et al. (2017). Zhang et al.

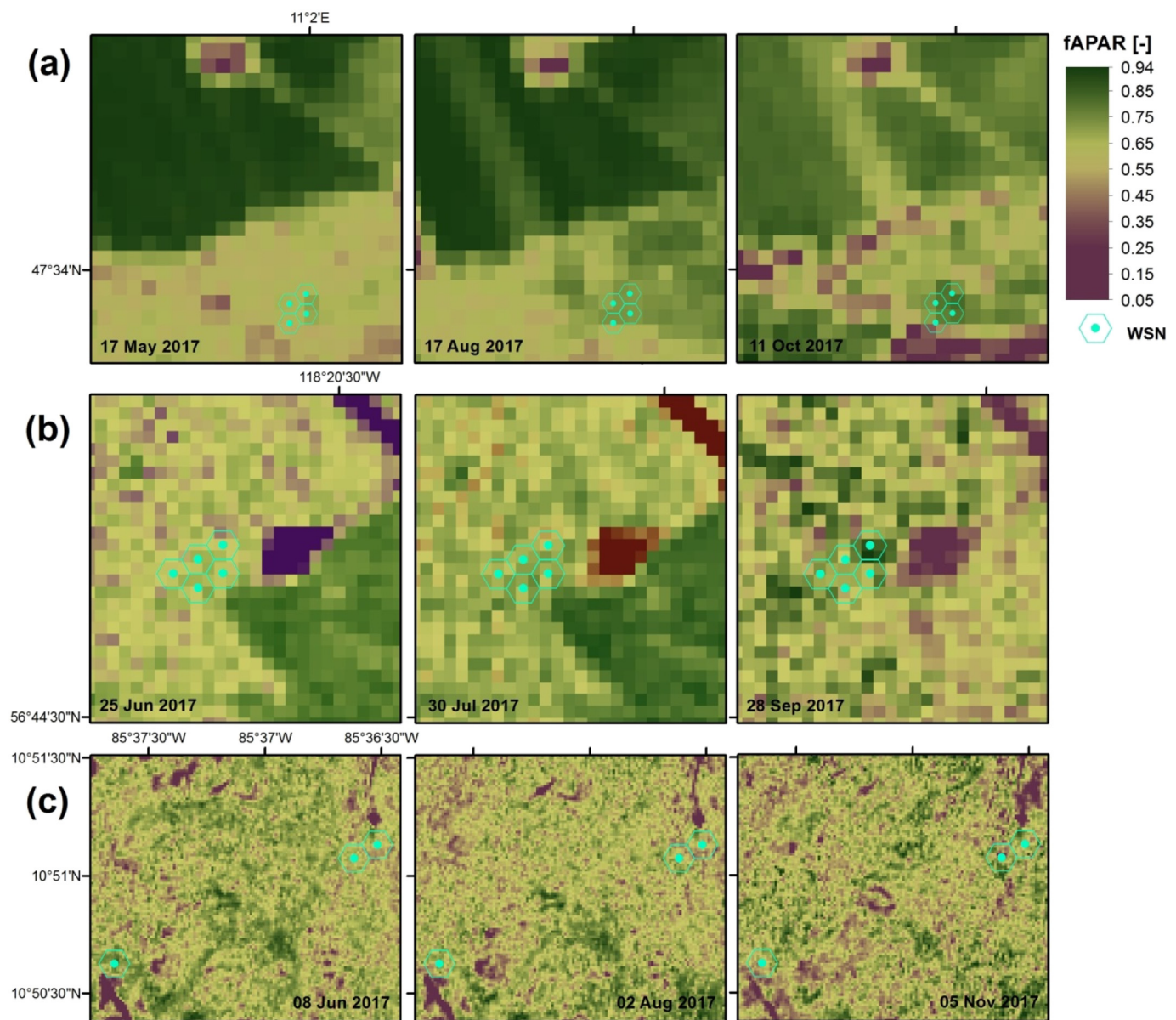


Fig. 7. The S2 fAPAR products at (a) Graswang, (b) Peace River and (c) Santa Rosa for several dates, representing early, peak and end of vegetation periods.

(2013) expected the relative contribution of non-photosynthetic components to total fAPAR to be < 0.1 during the peak season, which corresponds to a bias of 10%. Considering this contribution, accuracy requirements would still only be met at the boreal-deciduous site Peace River, with a minimum discrepancy thus accounting to 3%. For the tropical site Santa Rosa, the occurrence of lianas could increase the bias between green and total fAPAR. In this regard, previous research has shown that lianas present a higher percentage of woody biomass than tree species and it has been demonstrated that the contribution of Wood Area Index (WAI) is relevant for the correct estimation of LAI (Sánchez-Azofeifa et al., 2009). Thus, we consider the bias at our tropical site to be somewhat higher and clearly see the need for future investigations on the bias of fAPAR due to liana occurrence.

Further, validation results are dependent on the choice of temporal fAPAR estimate. Our results showed significant differences between $fAPAR_{DAY}$ and other instantaneous or aggregated fAPAR ground estimates (Table 2). Nevertheless, the common assumption that the daily integrated fAPAR corresponds to instantaneous fAPAR at 10:00 (or 14:00) local solar time (Baret et al., 2011) was supported by the results obtained at the temperate and boreal site (i.e. Graswang and Peace

River). At the tropical site Santa Rosa, distributions of $fAPAR_{DAY}$ and $fAPAR_{INST10&14}$ were significantly different even though only black-sky fAPAR was used. As such, we see the need for further investigations at other tropical sites.

4.1.2. Role of uncertainties of ground measurements

Discrepancies may also be attributed to uncertainties of ground measurements. Ground measurements of fAPAR were in the value range of 0.55–0.95 as previously obtained for forested areas (Leuchner et al., 2011; Nestola et al., 2017; Senna et al., 2005; Steinberg et al., 2006). For example, at the European site, a similar value range (0.93–0.96) was reported for a mountainous beech forest in Italy by Nestola et al. (2017). The high fAPAR values recorded at Graswang are in accordance with the dense canopy cover, expressed with the highest value for basal area and relatively high stem density compared to the other sites (Table 1). Accordingly, lowest fAPAR was recorded at Peace River as the forest is characterized by lower stem density. In contrast to the sites Graswang and Peace River that were characterized by a sudden change of fAPAR during green-up and senescence periods (Fig. 5a–b), the TDF at Santa Rosa showed a slow decrease during the senescence period

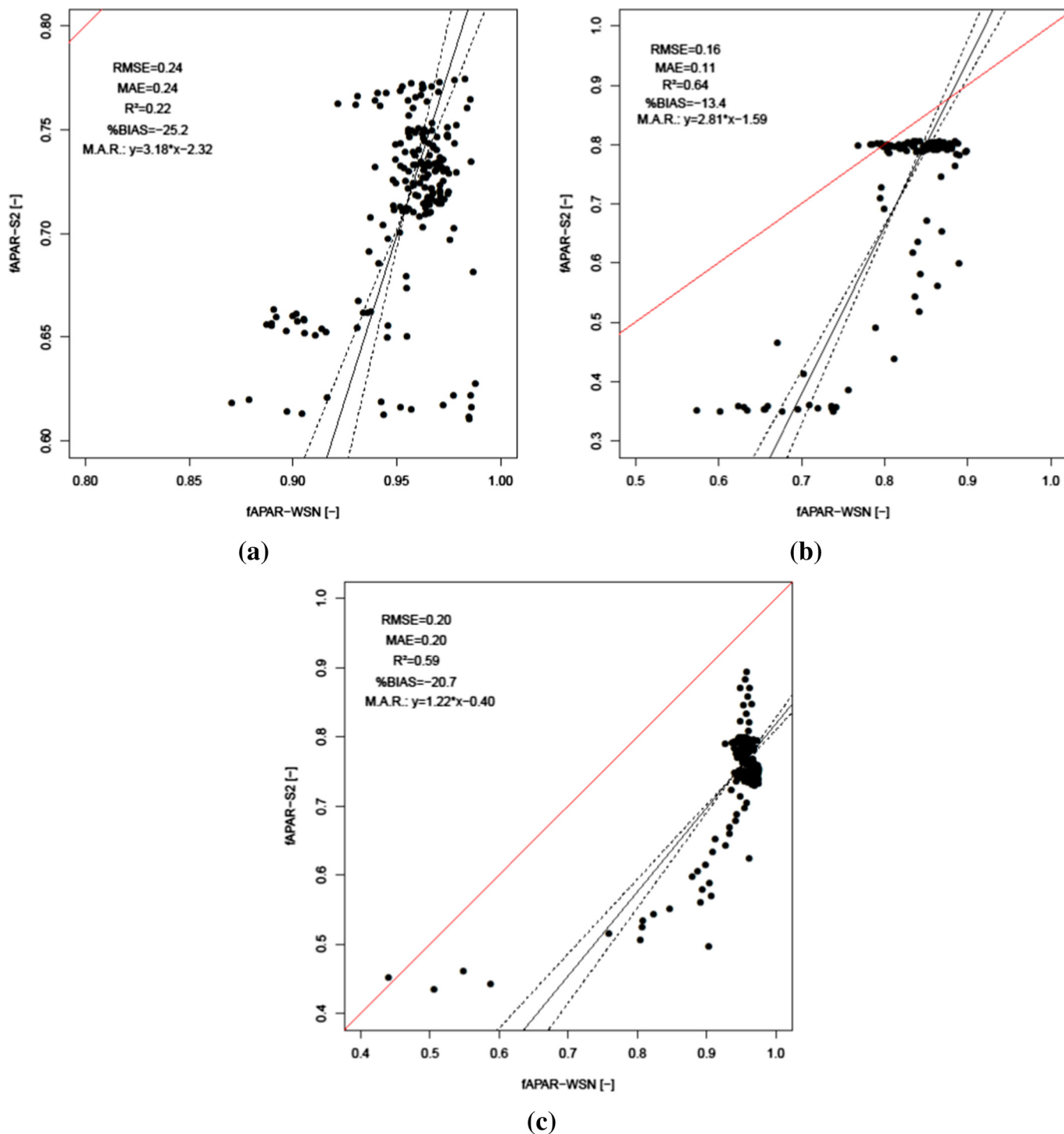


Fig. 8. Individual $fAPAR_{DAY}$ of WSN vs. S2 at (a) Graswang, (b) Peace River and (c) Santa Rosa. Root Mean Square Error (RMSE), Mean Absolute Error (MAE), coefficient of determination (R^2), Major Axis Regression (M.A.R.) and percent bias (%BIAS) are shown. The continuous black lines correspond to slopes and intercepts of the M.A.R.s, the dashed lines display the 95%-significance level. The red line marks the 1:1 line. (For interpretation of the references to color in this figure legend, the reader is referred to the web version of this article.)

(Fig. 5c). While the vegetation period at the temperate and boreal site can be expected to be mainly controlled by air temperature and light supply, the slowly decreasing $fAPAR$ at the tropical site could be attributed to the gradually drying out of soils with the absence of efficient rainfalls from November onwards (Fig. A1). The slow decrease of $fAPAR$ at Santa Rosa is also supported by findings of Kalacska et al. (2004) who reported substantial diversity for the timing of leaf fall among different tree species. In comparison to the temperate and boreal

sites, the tropical site is rich in different species (Table 1), incorporating 29 different species compared to 2–3 species at the other sites. Thus, the gradually decrease of $fAPAR$ could result from different phenological patterns of resident trees and understory vegetation, particularly due to the presence of few evergreen species as well as lianas. According to Kalacska et al. (2005), lianas present a longer phenological cycle as tree species, losing the greatest proportion of leaves during the driest time of the year.

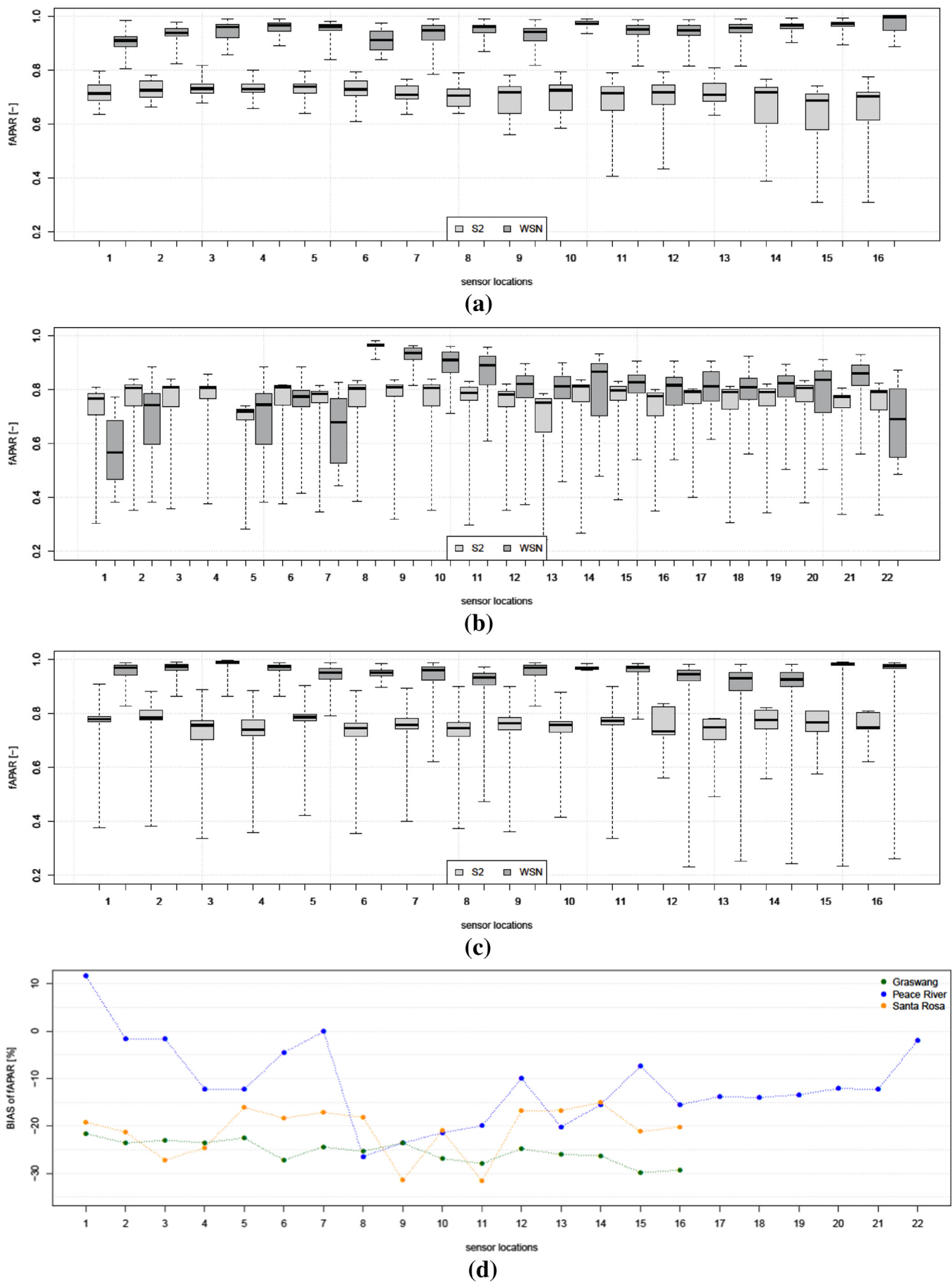


Fig. 9. Boxplots of individual $fAPAR_{DAY}$ of WSN and S2 at (a) Graswang, (b) Peace River, (c) Santa Rosa and (d) %BIAS thereof.

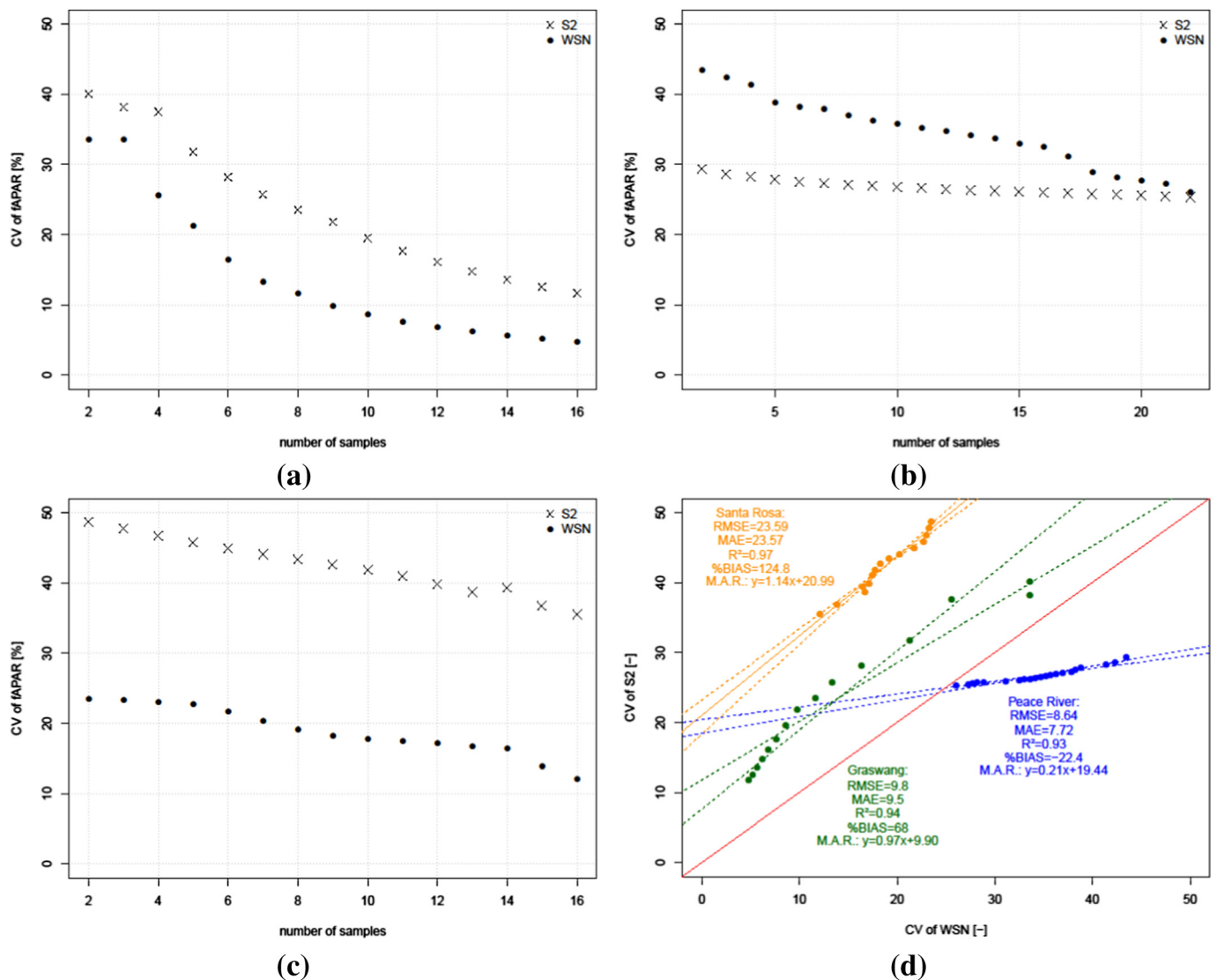


Fig. 10. The Coefficient of Variation (CV) of individual $fAPAR_{DAY}$ and $fAPAR-S2$ as a function of sample size at (a) Graswang, (b) Peace River and (c) Santa Rosa and (d) M.A.R. as well as performance metrics thereof.

At all sites, we observed highest $fAPAR$ values shortly before the decrease of $fAPAR$ during senescence (Fig. 5a–c). At least for Graswang, it can be noted that the period of highest $fAPAR$ values clearly coincided with the peak coloring of beech leaves observed around October 11th (Fig. B1m). The increase of $fAPAR$ occurred without rainfall (Fig. A1), so that the period can be assigned to the senescence period and is therefore suspected as bias due to the presence of colored autumn leaves. Widłowski (2010) simulated an overestimation bias of $fAPAR$ during the presence of colored leaves in experiments with RTMs for open canopy forests of various deciduous species. For the given site Graswang, Putzenlechner et al. (2019) have specified this overestimation bias to up to 0.05, which was similar to the value simulated by Widłowski (2010) for open beech forest. Accordingly, the overestimation bias due to colored autumn leaves could account to 0.03–0.07 at the aspen forest at Peace River, referring to simulations of Widłowski (2010) for open birch forest. For the tropical forest at Santa Rosa, it is difficult to assess the role of an overestimation bias due to the lack of existing studies. However, due to the observed gradual onset of leaf senescence, we consider the attributed bias to be somewhat smaller compared to the other sites.

After the period of highest $fAPAR$ at the beginning of senescence period, we observed frequent fluctuations of $fAPAR$ during the

senescence periods at the temperate and boreal site. Our observations are in agreement with Nestola et al. (2017) who explained this phenomenon with short-term changes of canopy gaps due to the progress of leaf fall. In addition to that, we consider a combination of changes of leaf color (with the associated overestimation bias of $fAPAR$) as an explanation for this phenomenon. It is further known that two-flux $fAPAR$ observations during high SZAs (above 60°) such as in late autumn or early morning tend to overestimate $fAPAR$ by up to 0.06 (Leuchner et al., 2011; Putzenlechner et al., 2019; Widłowski, 2010), particularly in coniferous forests. Thus, daily integrated $fAPAR$ ($fAPAR_{DAY}$) is generally more prone to be affected by biases caused by high SZAs. At the temperate conifer-dominated site Graswang, $fAPAR_{DAY}$ indeed showed higher values than other $fAPAR$ estimates, however, not significantly (Table 2). For the boreal-deciduous forest site Peace River, the influence of SZA was not indicated, as $fAPAR_{INST12}$ was higher than $fAPAR_{DAY}$. Thus, the contribution of an overestimation bias due to high SZAs seemed to have no crucial effect for the accuracy of the validation of S2. Still, the significant difference found between the daily aggregated $fAPAR$ ($fAPAR_{DAY}$) and instantaneous $fAPAR$ at the solar noon ($fAPAR_{INST12}$) when SZA is lowest, could indicate that using daily aggregated $fAPAR$ to validate satellite-derived $fAPAR$ products could indeed be hampered by biased ground data, as reported by Majasalmi

et al. (2017) for a boreal-coniferous forest site.

In sum, when considering common sources of uncertainties, discrepancies could be explained by up to 11%, given that black-sky fAPAR was acquired during high SZAs at a coniferous site (overestimation bias ≤ 0.06) and colored leaves were present (overestimation bias ≤ 0.05). If any, accuracy targets would only be reached temporarily at the site Peace River, with actual observed percent bias of 15% reduced to $< 10\%$ when considering sources of uncertainty for two-flux estimates.

4.2. Agreement on temporal and spatial variability

Similar to validation studies on other satellite-derived fAPAR products, we found good agreement between S2 and ground data on the seasonal dynamics, although existing validation studies have focused on mid/high-latitudes (McCallum et al., 2010; Nestola et al., 2017; Pinty et al., 2011; Steinberg et al., 2006) or semi-arid environments (Fensholt et al., 2004; Huemmrich et al., 2005; Martínez et al., 2013; Pickett-Heaps et al., 2014). The representation of relative differences of fAPAR values according to species composition at the mixed-coniferous forest site Graswang (Fig. 5d) emphasizes the capabilities of S2 to be suitable for forest applications.

As for the representation of spatial variability, we found that the level of agreement between ground measurements and S2 fAPAR product varied across forest stands and sites, with higher variations of % BIAS reported at Santa Rosa and Peace River (Fig. 9d). As the seasonal differences of fAPAR attributed to species composition were well-represented in the S2 fAPAR product at Graswang, this could imply that species composition was the major driver of spatial variability at this site and, in turn, explain the low spatial variation of discrepancies (Fig. 9d). With the crown architectures of spruce and beech trees being very different, different distribution of gaps are produced which are known to largely determine the spatial variability of fAPAR (Leuchner et al., 2011). Further, the high stem density at Graswang could explain the low variations of discrepancies between ground observations and S2 fAPAR product. Peace River and Santa Rosa have in common that they are characterized by at least two distinct vertical layers of canopy, leading to different contributions of tree species and understory vegetation. The low stem density at Peace River and thus larger contributions of the understory vegetation could thus explain the high variations of discrepancies. Compared to Peace River, the forest structure at Santa Rosa is considered more complex due to the higher number of species and thus the variety of geometries, in particularly with the occurrence of both lianas and trees (Li et al., 2017b). Previous investigations on the relationship between forest structure and light environment in tropical rain forests have suspected the vertical distribution of foliage as more influential than structural variables such as stem density and basal area, for which no significant relationship was found (Montgomery and Chazdon, 2001). Nevertheless, the level of complexity could explain the results obtained from the investigation of the representation of spatial variability with increasing sample sizes (Fig. 10d). In this regard, highest agreement (%BIAS = -22) was obtained at the boreal site for which ecosystem complexity (HCI = 1) is lowest, whereas highest discrepancies were obtained at the tropical site (%BIAS = -125) for which ecosystem complexity (HCI = 64) is highest.

4.3. Evaluation of the validation approach

A summary of presented and discussed results are given in Table 3. However, several limitations of our validation approach need to be considered when developing suggestions and recommendations for future validation activities as well as the usage of the S2 fAPAR product. As a practical issue, cloud contamination limited the validation of the seasonal course of fAPAR at the North and Central American sites in the green-up and senescence periods, especially at the tropical site. Thus,

we see the need to improve the temporal consistency of S2 fAPAR products which could be achieved by the means of product combinations and data fusion techniques as is has been done for other fAPAR products so far (Li et al., 2017a; Tao et al., 2018). From a theoretical perspective, it has to be considered that our validation approach validates satellite-derived fAPAR with two-flux fAPAR measurements, which are known to be affected by changes in background albedo, mostly under the occurrence of snow (Widlowski, 2010). As tropical dry forests present drastic phenological changes also of the understory vegetation, we see further need to quantify the benefits of three- or four-flux approaches in terms of uncertainty reduction of ground measurements in (tropical) field conditions, which has not been done yet. In this regard, another crucial point is that the bias between “green” and “total fAPAR” at the tropical site is currently unknown and thus will also need further research attention. As our direct validation approach relies on direct measurements, it should be noted that the observed discrepancies are site-specific and thus do not enable judging the performance of the S2 fAPAR product for the investigated ecosystems universally.

Despite these limitations, however, it has been shown that our observations across the three different sites give valuable insights on the actual performance of the S2 fAPAR product which has been found to be limited in terms of absolute value representation at sites with higher ecosystem complexity. In this regard, we assessed HCI as a measure of ecosystem complexity as a novelty in satellite validation studies and recommend this procedure for future validation activities. With the multi-sensor sampling approach with WSNs it was possible to investigate the representation of spatial variability in the S2 fAPAR product, demonstrating the potential of S2 to capture dynamics resulting from varying species composition. Finally, the high temporal resolution of the measurements enabled us to validate different temporal fAPAR estimates and specifically observe uncertainties of ground data arising at certain phenological phases (i.e. senescence period) which should be considered in future validation protocols.

5. Conclusions

This work presented the results of a validation study of the Sentinel-2 (S2) fAPAR product with two-flux fAPAR ground measurements obtained from Wireless Sensor Networks (WSNs) at three forest sites: a conifer-dominated forest in Southern Germany, a boreal-deciduous forest in Northern Alberta at the Peace River Environmental Monitoring Super Sites, Canada and a tropical dry forest (TDF) at the Santa Rosa National Park Environmental Monitoring Super Site, Costa Rica.

Our results show discrepancies of absolute fAPAR values throughout the whole vegetation period of 2017 between 13 and 25% (lower bound for Peace River and higher bound for Graswang), thereby exceeding the target accuracy of 10% set by the GCOS (2011) for fAPAR products. At all three sites, we found strong evidence that the change of leaf color during senescence periods resulted in an overestimation of fAPAR by up to 5%. We suggest that this bias needs to be considered when validating satellite products exclusively during the period of leaf senescence. The choice of temporal fAPAR estimate (i.e. daily average fAPAR and several instantaneous estimates) resulted in different performance metrics for the correlation analysis with the S2 fAPAR product. Even though the common assumption underlying the S2 fAPAR product as well many other satellite-derived fAPAR products that the daily integrated fAPAR is a good approximation of the instantaneous fAPAR at 10:00 (or 14:00) local solar time was supported by the ground observations at the boreal-deciduous and mixed-coniferous site, we recommend that the choice of temporal fAPAR estimate should be carefully argued in validation protocols. Overall, we found that uncertainties of ground data could not explain the high discrepancies of absolute fAPAR values.

Regarding the temporal consistency of the S2 fAPAR product, we found strong agreement on the onset of spring leaf unfolding and the beginning of leaf fall during the senescence periods at all sites where S2 data was available. Our analysis on the representation of spatial

Table 3
Outcome of the validation study: key results, implications and suggestions for future work.

| Agreement/disagreement | Validation method(s) | Possible reason(s) | Implications/instructive suggestion(s) |
|--|--|--|---|
| - Highest disagreement of absolute fAPAR values at the mixed-coniferous forest stand (Graswang), lowest at the boreal deciduous forest (Peace River) | - Graswang: performance metrics: $R^2 = 0.27$; RMSE = 0.24; %BIAS = -24.6; HCI = 48 - Peace River: performance metrics: $R^2 = 0.67$, RMSE = 0.16, %BIAS = -13; HCI = 1 | - Generic nature of retrieval algorithm - Possible misclassification of canopy as a result of different crown architectures | - Studies that rely on the accuracy of absolute fAPAR values should preferably be carried out at sites with low ecosystem complexity. - The performance of fAPAR-S2 in coniferous forests should be further validated. |
| High discrepancies exceeding GCOS target accuracy also at the tropical site (Santa Rosa) | Santa Rosa: performance metrics: $R^2 = 0.56$, RMSE = 0.19, %BIAS = -19.8; HCI = 64 | - Possible misclassification of canopy due to lacking consideration of phenological phases in tropical dry forests - Different underlying fAPAR definitions: bias between “total” and “green fAPAR” could be higher than at other sites due to liana occurrence | - Spectral characteristics of tropical forest ecosystems relevant for validation need further attention. - Specifically, the bias between “green” and “total fAPAR” should be quantified. |
| Increased fAPAR ground values during senescence periods at all sites | MEAN 5% higher in the period of leaf color change (observed with automated camera) compared to fully foliated period | Overestimation bias due to colored leaves as described in literature (e.g. Widlowski, 2010) | - Validation activities should be avoided in the senescence period. |
| Validation results dependent on the choice of temporal fAPAR estimate | Significant differences (KS-test) between daily integrated fAPAR and other instantaneous or aggregated fAPAR ground estimates | Daily integrated two-flux fAPAR known to be more prone to be affected by biases (up to 0.06) caused by high solar zenith angles, especially in coniferous forests | The choice of temporal fAPAR estimate should be carefully considered in validation protocols. |
| Agreement on the beginning of leaf development and leaf senescence at all three study sites; however, limitations due to cloud cover | Phenological observations from automated camera at Graswang; qualitative evaluation of one-year time series | Suitability of temporal resolution of S2 to monitor forest phenology | The temporal consistency of S2 fAPAR products needs further efforts, e.g. by the means of product combinations and data fusion techniques, to better validate fAPAR-S2 at tropical sites. |
| Effect of species composition on fAPAR-WSN values at the mixed-coniferous forest stand well-reflected by fAPAR-S2 | Classification of sensor locations according to high and low percentages of spruces | The decametric resolution captures spatial variability caused by differences in species composition. | The fAPAR-S2 product could be used for monitoring changes in species composition of forest ecosystems. |
| Highest agreement on the representation of spatial variability at Peace River site | %BIAS of the Coefficient of Variation (CV) of individual fAPAR as a function of samples size | Best representation of spatial variability at sites with low ecosystem complexity | The representation of spatial variability by satellite-derived fAPAR products should be included in validation protocols. |

variability in the S2 fAPAR product demonstrated the need for a sufficiently high number of samples for any validation studies. We highlight that at the conifer-dominated site, the variability of fAPAR attributed to species composition was well-represented in the S2 fAPAR product. Finally, we found the representation of both absolute and spatial variability across single forest stands to be related to ecosystem complexity (i.e. number of species present, basal area, stem density). Given these results, the following conclusions could serve as recommendations for planning future validation activities as well as for the usage of the current S2 fAPAR product:

- 1) Studies that rely on the accuracy of absolute values of the S2 fAPAR product in forested area should currently focus their investigations on areas with low ecosystem complexity.
- 2) Multi-sensor sampling approaches and permanent monitoring activities are key to a) understand uncertainties of ground data and b) validate the representation of temporal and spatial variability of recent decametric fAPAR products.
- 3) The choice of temporal fAPAR estimate and uncertainties of ground data should be carefully documented and argued in future validation protocols.
- 4) Given the promising results on the representation of species composition in the mixed-coniferous forest, the potential of S2 to monitor long-term forest dynamics and forestry programs should be further explored.

Overall, the very different settings of our three study sites allow the conclusion to be drawn that the current S2 fAPAR product demonstrates already strong performance for monitoring dynamics and spatial variability of fAPAR but will need further improvement to be useful for feeding global production efficiency or biogeochemical models.

Author contributions

B.P. was the primary author, performed the experiments at the German site and processed and analyzed all data, I.S. was largely involved in carrying out the experiments at the Canadian and Costa Rican site. A.S.-A. conceived and designed all experiments, R.L. arranged for and R.K. and P.M. assisted in carrying out the experiments at the German site. All authors contributed to the scientific discussions presented in the manuscript and assisted in finalizing the article.

Funding

This work was supported by the Natural Sciences and Engineering Research Council of Canada (NSERC) Discovery Grant Program, the Inter-American Institute for Global Change Research (IAI) Collaborative Research Network Program (CRN3-023), the Canada Foundation for Innovation (CFI), and a MICMoR Fellowship to B.P. through KIT/IMK-IFU (Garmisch-Partenkirchen, Germany). The Helmholtz Association and the German Federal Ministry of Education and Research (BMBF) in the framework of TERENO (Terrestrial Environmental Observatories) (grant no. 01LL0801B) provided support also to the German site

Acknowledgments

The authors thank Matthias Mauder and Matthias Zeeman (KIT/IMK-IFU) for their advice on the data acquired by the TERENO station at the German site. Collection of data in Costa Rica was done by the support of Ronny Hernandez. We also thank Roger Blanco and Maria Marta Chavarria from the Guanacaste Conservation Area, Costa Rica as well as Jim Witt from Daishowa-Marubeni International Ltd. (DMI), Alberta, Canada. Finally, we sincerely thank the two anonymous reviewers for their thoughtful comments.

Appendix A

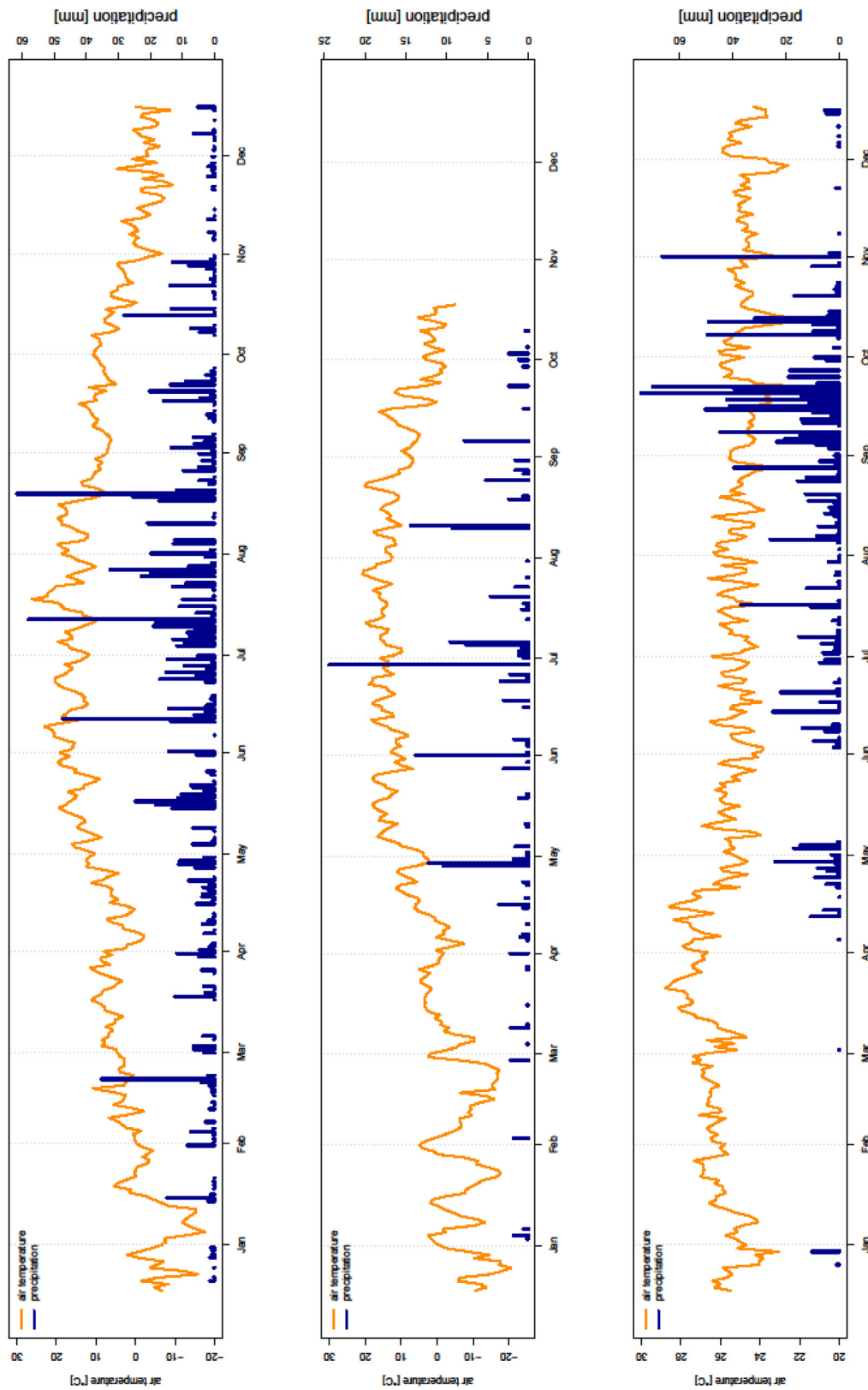


Fig. A1. Daily mean air temperature and daily precipitation sums at the three study sites for the year 2017: (top panel) Graswang, Germany; (middle panel) Peace River, Alberta, Canada; (bottom panel) Santa Rosa, Costa Rica.

Appendix B

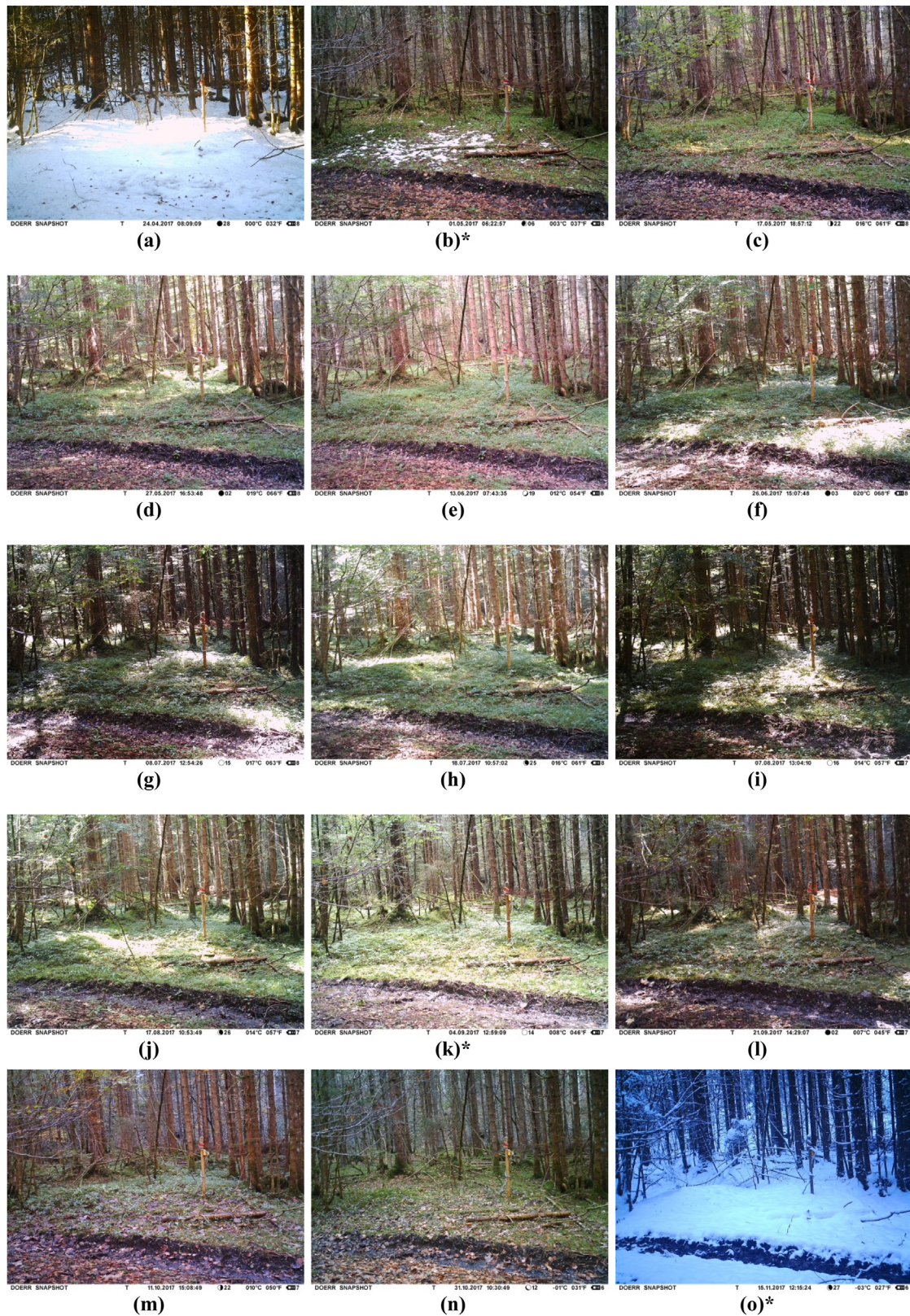


Fig. B1. Photos taken by an automated camera at Graswang at different dates in 2017 (format: MM-DD): (a) 04-24; (b) 05-01*; (c) 05-17; (d) 05-27; (e) 06-13; (f) 06-26; (g) 07-08; (h) 07-18; (i) 08-07; (j) 08-17; (k) 09-04*; (l) 09-21; (m) 10-11; (n) 10-31; (o) 11-15*. Note that dates without available FAPAR-S2 are marked with *.

References

- Allen, W.A., Gausman, H.W., Richardson, A.J., Thomas, J.R., 1969. Interaction of isotropic light with a compact plant leaf*. *J. Opt. Soc. Am.* 59, 1376–1379. <https://doi.org/10.1364/JOSA.59.001376>.
- Arroyo-Mora, J.P., Sánchez-Azofeifa, G.A., Kalacska, M.E.R., Rivard, B., Calvo-Alvarado, J.C., Janzen, D.H., 2005. Secondary forest detection in a neotropical dry forest landscape using Landsat 7 ETM+ and IKONOS Imagery1. *Biotropica* 37, 497–507. <https://doi.org/10.1111/j.1744-7429.2005.00068.x>.
- Baret, F., Hagolle, O., Geiger, B., Bicheron, P., Miras, B., Huc, M., Berthelot, B., Nino, F., Weiss, M., Samain, O., Roujean, J.-L., Leroy, M., 2007. LAI, fAPAR and fCover CYCLOPES global products derived from VEGETATION part 1: principles of the algorithm. *Remote Sens. Environ.* 110, 275–286. <https://doi.org/10.1016/j.rse.2007.02.018>.
- Baret, F., Makhmara, H., Lacaze, R., Smets, B., 2011. *BioPar Product User Manual LAI, FAPAR, FCOVER, NDVI Version 1 From SPOT/VEGETATION Data*.
- Camacho, F., Cernicharo, J., Lacaze, R., Baret, F., Weiss, M., 2013. GEOV1: LAI, FAPAR essential climate variables and FCOVER global time series capitalizing over existing products. Part 2: validation and intercomparison with reference products. *Remote Sens. Environ.* 137, 310–329. <https://doi.org/10.1016/j.rse.2013.02.030>.
- Carrer, D., Roujean, J.-L., Lafont, S., Calvet, J.-C., Boone, A., Decharme, B., Delire, C., Gastellu-Etchegorry, J.-P., 2013. A canopy radiative transfer scheme with explicit FAPAR for the interactive vegetation model ISBA-A-gs: impact on carbon fluxes. *Journal of Geophysical Research: Biogeosciences* 118, 888–903. <https://doi.org/10.1002/jgrg.20070>.
- Chen, J.M., 1996. Canopy architecture and remote sensing of the fraction of photosynthetically active radiation absorbed by boreal conifer forests. *IEEE Trans. Geosci. Remote Sens.* 34, 1353–1368. <https://doi.org/10.1109/36.544559>.
- Clasen, A., Somers, B., Pipkins, K., Tits, L., Segl, K., Brell, M., Kleinschmit, B., Spengler, D., Lausch, A., Förster, M., 2015. Spectral unmixing of forest crown components at close range, airborne and simulated Sentinel-2 and EnMAP spectral imaging scale. *Remote Sens.* 7. <https://doi.org/10.3390/rs71115361>.
- Clevers, J.G.P.W., Gitelson, A.A., 2013. Remote estimation of crop and grass chlorophyll and nitrogen content using red-edge bands on Sentinel-2 and -3. *Int. J. Appl. Earth Obs. Geoinf.* 23, 344–351. <https://doi.org/10.1016/j.jag.2012.10.008>.
- Disney, M., Muller, J.-P., Kharbouche, S., Kaminski, T., Voßbeck, M., Lewis, P., Pinty, B., 2016. A new global fAPAR and LAI dataset derived from optimal albedo estimates: comparison with MODIS products. *Remote Sens.* 8, 275.
- D'Odorico, P., Gonsamo, A., Pinty, B., Gobron, N., Coops, N., Mendez, E., Schaeppman, M.E., 2014. Intercomparison of fraction of absorbed photosynthetically active radiation products derived from satellite data over Europe. *Remote Sens. Environ.* 142, 141–154. <https://doi.org/10.1016/j.rse.2013.12.005>.
- Dotzler, S., Hill, J., Buddenbaum, H., Stoffels, J., 2015. The potential of EnMAP and Sentinel-2 data for detecting drought stress phenomena in deciduous forest communities. *Remote Sens.* 7, 14227.
- Drusch, M., Del Bello, U., Carrier, S., Colin, O., Fernandez, V., Gascon, F., Hoersch, B., Isola, C., Laberinti, P., Martimort, P., Meygret, A., Spoto, F., Sy, O., Marchese, F., Bargellini, P., 2012. Sentinel-2: ESA's optical high-resolution mission for GMES operational services. *Remote Sens. Environ.* 120, 25–36. <https://doi.org/10.1016/j.rse.2011.11.026>.
- ESA, 2015. *E. S. A.: Sentinel-2 User Handbook*. 64 European Space Agency (ESA) User Guide.
- Fang, H., Li, W., and B. Myneni, R.: The Impact of Potential Land Cover Misclassification on MODIS Leaf Area Index (LAI) Estimation: A Statistical Perspective, 830–844 pp., 2013.
- Fensholt, R., Sandholt, I., Rasmussen, M.S., 2004. Evaluation of MODIS LAI, fAPAR and the relation between fAPAR and NDVI in a semi-arid environment using in situ measurements. *Remote Sens. Environ.* 91, 490–507. <https://doi.org/10.1016/j.rse.2004.04.009>.
- Fernandes, R., Plummer, S., Nightingale, J., Baret, F., Camacho, F., Fang, H., Garrigues, S., Gobron, N., Lang, M., Lacaze, R., LeBlanc, S., Meroni, M., Martinez, B., Nilsson, T., Pinty, B., Pisek, J., Sonntag, O., Verger, A., Welles, J., Weiss, M., Widlowski, J.L., 2014. *Global Leaf Area Index Product Validation Good Practices*. Land Product Validation Subgroup (WGCV/CEOS) pp. 76.
- Frampton, W.J., Dash, J., Watmough, G., Milton, E.J., 2013. Evaluating the capabilities of Sentinel-2 for quantitative estimation of biophysical variables in vegetation. *ISPRS J. Photogramm. Remote Sens.* 82, 83–92. <https://doi.org/10.1016/j.isprsjprs.2013.04.007>.
- GCOS, G. C. O. S., 2011. *Systematic Observation Requirements for Satellite-based Data Products for Climate*.
- Gobron, N., 2015. *Report on Satellite Derived ECV Definition and Field Protocols*. 29 European Commission, Joint Research Centre (JRC), Institute for Environment & Sustainability.
- Gobron, N., Verstraete, M.M., 2009. *ECV T10: Fraction of Absorbed Photosynthetically Active Radiation (FAPAR)*. Essential Climate Variables. Version 8. Food and Agriculture Organization (FAO), Rome, pp. 23.
- Gobron, N., Pinty, B., Mélin, F., Taberner, M., Verstraete, M.M., Belward, A., Lavergne, T., Widlowski, J.L., 2005. The state of vegetation in Europe following the 2003 drought. *Int. J. Remote Sens.* 26, 2013–2020. <https://doi.org/10.1080/01431160412331330293>.
- Gobron, N., Pinty, B., Taberner, M., Mélin, F., Verstraete, M.M., Widlowski, J.L., 2006. Monitoring the photosynthetic activity of vegetation from remote sensing data. *Adv. Space Res.* 38, 2196–2202. <https://doi.org/10.1016/j.asr.2003.07.079>.
- Gond, V., de Pury, D.G.G., Veroustraete, F., Ceulemans, R., 1999. Seasonal variations in leaf area index, leaf chlorophyll, and water content; scaling-up to estimate fAPAR and carbon balance in a multilayer, multispecies temperate forest. *Tree Physiol.* 19, 673–679. <https://doi.org/10.1093/treephys/19.10.673>.
- Gower, S.T., Kucharik, C.J., Norman, J.M., 1999. Direct and indirect estimation of leaf area index, fAPAR, and net primary production of terrestrial ecosystems. *Remote Sens. Environ.* 70, 29–51. [https://doi.org/10.1016/S0034-4257\(99\)00056-5](https://doi.org/10.1016/S0034-4257(99)00056-5).
- Holdridge, L.R., Tosi, J.A., 1967. *Life Zone Ecology*. Tropical Science Center, San Jose, Costa Rica 149 pp.
- Hovi, A., Lukeš, P., Rautiainen, M., 2017. Seasonality of albedo and FAPAR in a boreal forest. *Agric. For. Meteorol.* 247, 331–342. <https://doi.org/10.1016/j.agrformet.2017.08.021>.
- Huemmlrich, K.F., Privette, J.L., Mukelabai, M., Myneni, R.B., Knyazikhin, Y., 2005. Time-series validation of MODIS land biophysical products in a Kalahari woodland, Africa. *Int. J. Remote Sens.* 26, 4381–4398. <https://doi.org/10.1080/01431160500113393>.
- Immiter, M., Vuolo, F., Atzberger, C., 2016. First experience with Sentinel-2 data for crop and tree species classifications in Central Europe. *Remote Sens.* 8. <https://doi.org/10.3390/rs8030166>.
- Jacquemoud, S., Baret, F., 1990. PROSPECT: a model of leaf optical properties spectra. *Remote Sens. Environ.* 34, 75–91. [https://doi.org/10.1016/0034-4257\(90\)90100-Z](https://doi.org/10.1016/0034-4257(90)90100-Z).
- Jacquemoud, S., Verhoef, W., Baret, F., Bacour, C., Zarco-Tejada, P.J., Asner, G.P., François, C., Ustin, S.L., 2009. PROSPECT+SAIL models: a review of use for vegetation characterization. *Remote Sens. Environ.* 113, S56–S66. <https://doi.org/10.1016/j.rse.2008.01.026>.
- Justice, C., Belward, A., Morisette, J., Lewis, P., Privette, J., Baret, F., 2000. Developments in the 'validation' of satellite sensor products for the study of the land surface. *Int. J. Remote Sens.* 21, 3383–3390. <https://doi.org/10.1080/014311600750020000>.
- Kalacska, M., Sanchez-Azofeifa, G.A., Calvo-Alvarado, J.C., Quesada, M., Rivard, B., Janzen, D.H., 2004. Species composition, similarity and diversity in three successional stages of a seasonally dry tropical forest. *Ecol. Manag.* 200, 227–247. <https://doi.org/10.1016/j.foreco.2004.07.001>.
- Kalacska, M., Calvo-Alvarado, J., Sanchez-Azofeifa, G.A., 2005. Calibration and assessment of seasonal changes in leaf area index of a tropical dry forest in different stages of succession. *Journal of Tree Physiology* 25, 733–744.
- Korhonen, L., Hadi, Packalen, P., Rautiainen, M., 2017. Comparison of Sentinel-2 and Landsat 8 in the estimation of boreal forest canopy cover and leaf area index. *Remote Sens. Environ.* 195, 259–274. <https://doi.org/10.1016/j.rse.2017.03.021>.
- Legendre, P., Legendre, L., 2012. *Numerical ecology*. In: *Developments in Environmental Modelling*. Elsevier 1006 pp.
- Leuchner, M., Hertel, C., Menzel, A., 2011. Spatial variability of photosynthetically active radiation in European beech and Norway spruce. *Agric. For. Meteorol.* 151, 1226–1232. <https://doi.org/10.1016/j.agrformet.2011.04.014>.
- Li, W., Weiss, M., Waldner, F., Defourny, P., Demarez, V., Morin, D., Hagolle, O., Baret, F., 2015. A generic algorithm to estimate LAI, FAPAR and FCOVER variables from SPOT4/HRVIR and Landsat sensors: evaluation of the consistency and comparison with ground measurements. *Remote Sens.* 7, 15494.
- Li, W., Baret, F., Weiss, M., Buis, S., Lacaze, R., Demarez, V., Dejoux, J., Battude, M., Camacho, F., 2017a. Combining hectometric and decametric satellite observations to provide near real time decametric FAPAR product. *Remote Sens. Environ.* 200, 250–262. <https://doi.org/10.1016/j.rse.2017.08.018>.
- Li, W., Cao, S., Campos-Vargas, C., Sanchez-Azofeifa, G.A., 2017b. Identifying tropical dry forests extent and succession via the use of machine learning techniques. 63. <https://doi.org/10.1016/j.jag.2017.08.003>.
- Lugo, A.E., Gonzalez-Liboy, J.A., Cintron, B., Dugger, K., 1978. Structure, productivity, and transpiration of a subtropical dry forest in Puerto Rico. *Biotropica* 10, 278–291. <https://doi.org/10.2307/2387680>.
- Majasalmi, T., Rautiainen, M., 2016. The potential of Sentinel-2 data for estimating biophysical variables in a boreal forest: a simulation study. *Remote Sensing Letters* 7, 427–436. <https://doi.org/10.1080/2150704X.2016.1149251>.
- Majasalmi, T., Stenberg, P., Rautiainen, M., 2017. Comparison of ground and satellite-based methods for estimating stand-level fPAR in a boreal forest. *Agric. For. Meteorol.* 232, 422–432. <https://doi.org/10.1016/j.agrformet.2016.09.007>.
- Malenovsky, Z., Rott, H., Cihlar, J., Schaeppman, M.E., Garcia-Santos, G., Fernandes, R., Berger, M., 2012. Sentinels for science: potential of Sentinel-1, -2, and -3 missions for scientific observations of ocean, cryosphere, and land. *Remote Sens. Environ.* 120, 91–101. <https://doi.org/10.1016/j.rse.2011.09.026>.
- Martínez, B., Camacho, F., Verger, A., García-Haro, F.J., Gilabert, M.A., 2013. Intercomparison and quality assessment of MERIS, MODIS and SEVIRI FAPAR products over the Iberian Peninsula. *Int. J. Appl. Earth Obs. Geoinf.* 21, 463–476. <https://doi.org/10.1016/j.jag.2012.06.010>.
- McCallum, I., Wagner, W., Schullius, C., Shvidenko, A., Obersteiner, M., Fritz, S., Nilsson, S., 2010. Comparison of four global FAPAR datasets over Northern Eurasia for the year 2000. *Remote Sens. Environ.* 114, 941–949. <https://doi.org/10.1016/j.rse.2009.12.009>.
- Meroni, M., Fasbender, D., Kayitakire, F., Pini, G., Rembold, F., Urbano, F., Verstraete, M.M., 2014. Early detection of biomass production deficit hot-spots in semi-arid environment using FAPAR time series and a probabilistic approach. *Remote Sens. Environ.* 142, 57–68. <https://doi.org/10.1016/j.rse.2013.11.012>.
- Montgomery, R.A., Chazdon, R.L., 2001. Forest structure, canopy architecture, and light forest structure, canopy architecture, and light transmittance in tropical wet forests. *Ecology* 82, 2707–2718. [https://doi.org/10.1890/0012-9658\(2001\)082\[2707:FSCAAL\]2.0.CO;2](https://doi.org/10.1890/0012-9658(2001)082[2707:FSCAAL]2.0.CO;2).
- Morisette, J.T., Baret, F., Privette, J.L., Myneni, R.B., Nickeson, J.E., Garrigues, S., Shabanov, N.V., Weiss, M., Fernandes, R.A., Leblanc, S.G., Kalacska, M., Sanchez-Azofeifa, G.A., Chubey, M., Rivard, B., Stenberg, P., Rautiainen, M., Voipio, P., Manninen, T., Pilant, A.N., Lewis, T.E., Iames, J.S., Colombo, R., Meroni, M., Busetto, L., Cohen, W.B., Turner, D.P., Warner, E.D., Petersen, G.W., Seufert, G.,

- Cook, R., 2006. Validation of global moderate-resolution LAI products: a framework proposed within the CEOS land product validation subgroup. *IEEE Trans. Geosci. Remote Sens.* 44, 1804–1817. <https://doi.org/10.1109/TGRS.2006.872529>.
- Mortazavi, S.H., Salehe, M., MacGregor, M.H., 2014. Maximum WSN coverage in environments of heterogeneous path loss. *International Journal of Sensor Networks* 16, 185–198. <https://doi.org/10.1504/ijnsnet.2014.066788>.
- Möttus, M., 2004. Measurement and modelling of the vertical distribution of sunflecks. penumbra and umbra in willow coppice 79–91.
- Möttus, M., Sulev, M., Frederic, B., Lopez-Lozano, R., Reinart, A., 2011. Photosynthetically Active Radiation: Measurement and Modeling. pp. 7970–8000.
- Mueller-Wilm, U., 2018. S2 MPC-Sen2Cor configuration and user manual. European Space Agency (ESA) 54.
- Mura, M., Botallico, F., Giannetti, F., Bertani, R., Giannini, R., Mancini, M., Orlandini, S., Travaglini, D., Chirici, G., 2018. Exploiting the capabilities of the Sentinel-2 multi spectral instrument for predicting growing stock volume in forest ecosystems. *Int. J. Appl. Earth Obs. Geoinf.* 66, 126–134. <https://doi.org/10.1016/j.jag.2017.11.013>.
- Myneni, R.B., Williams, D.L., 1994. On the relationship between FAPAR and NDVI. *Remote Sens. Environ.* 49, 200–211. [https://doi.org/10.1016/0034-4257\(94\)90016-7](https://doi.org/10.1016/0034-4257(94)90016-7).
- Myneni, R.B., Ramakrishna, R., Nemani, R., Running, S.W., 1997. Estimation of global leaf area index and absorbed par using radiative transfer models. *IEEE Trans. Geosci. Remote Sens.* 35, 1380–1393. <https://doi.org/10.1109/36.649788>.
- Nestola, E., Sánchez-Zapero, J., Latorre, C., Mazzenga, F., Matteucci, G., Calfapietra, C., Camacho, F., 2017. Validation of PROBA-V GEOV1 and MODIS C5 & C6 fAPAR products in a deciduous beech forest site in Italy. *Remote Sens.* 9, 126.
- Ollinger, S.V., 2011. Sources of variability in canopy reflectance and the convergent properties of plants. *New Phytol.* 189, 375–394. <https://doi.org/10.1111/j.1469-8137.2010.03536.x>.
- Pastorello, G., Sanchez-Azofeifa, G.A., Nascimento, M., 2011. Enviro-net: from networks of ground-based sensor systems to a web platform for sensor data management. *Sensors* 11, 6454.
- Pickett-Heaps, C.A., Canadell, J.G., Briggs, P.R., Gobron, N., Haverd, V., Paget, M.J., Pinty, B., Raupach, M.R., 2014. Evaluation of six satellite-derived Fraction of Absorbed Photosynthetically Active Radiation (FAPAR) products across the Australian continent. *Remote Sens. Environ.* 140, 241–256. <https://doi.org/10.1016/j.rse.2013.08.037>.
- Pinty, B., Jung, M., Kaminski, T., Laverge, T., Mund, M., Plummer, S., Thomas, E., Widlowski, J.L., 2011. Evaluation of the JRC-TIP 0.01° products over a mid-latitude deciduous forest site. *Remote Sens. Environ.* 115, 3567–3581. <https://doi.org/10.1016/j.rse.2011.08.018>.
- Pontius, R.G., Thontteh, O., Chen, H., 2008. Components of information for multiple resolution comparison between maps that share a real variable. *Environ. Ecol. Stat.* 15, 111–142. <https://doi.org/10.1007/s10651-007-0043-y>.
- Prince, S.D., Goward, S.N., 1995. Global primary production: a remote sensing approach. *J. Biogeogr.* 22, 815–835. <https://doi.org/10.2307/2845983>.
- Putzenlechner, B., Marzahn, P., Kiese, R., Ludwig, R., Sanchez-Azofeifa, A., 2019. Assessing the variability and uncertainty of two-flux FAPAR measurements in a conifer-dominated forest. *Agric. For. Meteorol.* 264, 149–163. <https://doi.org/10.1016/j.agrformet.2018.10.007>.
- Rankine, C.J., Sanchez-Azofeifa, G.A., MacGregor, M.H., 2014. Seasonal wireless sensor network link performance in boreal forest phenology monitoring. *Eleventh Annual IEEE International Conference on Sensing, Communication, and Networking (SECON)* 2014, 302–310.
- Reifsnyder, W.E., Furnival, G.M., Horowitz, J.L., 1971. Spatial and temporal distribution of solar radiation beneath forest canopies. *Agric. Meteorol.* 9, 21–37. [https://doi.org/10.1016/0002-1571\(71\)90004-5](https://doi.org/10.1016/0002-1571(71)90004-5).
- Sanchez-Azofeifa, G.A., Castro, K., Kurz, W., Joyce, A., 2009. Monitoring carbon stocks in the tropics and the remote sensing operational limitations: from local to regional projects. *Ecological applications - Ecological Society of America* 19, 480–494. <https://doi.org/10.1890/08-1149.1>.
- Sánchez-Azofeifa, G.A., Kalácska, M., Espírito-Santo, M.M., Fernandes, G.W., Schnitzer, S., 2009. Tropical dry forest succession and the contribution of lianas to wood area index (WAI). *For. Ecol. Manag.* 258, 941–948. <https://doi.org/10.1016/j.foreco.2008.10.007>.
- Senna, M.C.A., Costa, M.H., Shimabukuro, Y.E., 2005. Fraction of photosynthetically active radiation absorbed by Amazon tropical forest: a comparison of field measurements, modeling, and remote sensing. *Journal of Geophysical Research: Biogeosciences* 110. <https://doi.org/10.1029/2004JG000005>. n/a-n/a.
- Spence, J., Volney, J., 1999. EMEND: Ecosystem Management Emulating Natural Disturbance. Sustainable Forest Management Network Project Report.
- Steinberg, D.C., Goetz, S.J., Hyer, E.J., 2006. Validation of MODIS F/sub PAR/products in boreal forests of Alaska. *IEEE Trans. Geosci. Remote Sens.* 44, 1818–1828. <https://doi.org/10.1109/TGRS.2005.862266>.
- Stenberg, P., Lukeš, P., Rautiainen, M., Manninen, T., 2013. A new approach for simulating forest albedo based on spectral invariants. *Remote Sens. Environ.* 137, 12–16. <https://doi.org/10.1016/j.rse.2013.05.030>.
- Taheriazad, L., Moghadas, H., Sanchez-Azofeifa, A., 2016. A new approach to calculate Plant Area Density (PAD) using 3D ground-based lidar. *SPIE Remote Sensing* 10.
- Tao, X., Liang, S., Wang, D., 2015. Assessment of five global satellite products of fraction of absorbed photosynthetically active radiation: Intercomparison and direct validation against ground-based data. *Remote Sens. Environ.* 163, 270–285. <https://doi.org/10.1016/j.rse.2015.03.025>.
- Tao, X., Liang, S., He, T., Jin, H., 2016. Estimation of fraction of absorbed photosynthetically active radiation from multiple satellite data: model development and validation. *Remote Sens. Environ.* 184, 539–557. <https://doi.org/10.1016/j.rse.2016.07.036>.
- Tao, X., Liang, S., Wang, D., He, T., Huang, C., 2018. Improving satellite estimates of the fraction of absorbed photosynthetically active radiation through data integration: methodology and validation. *IEEE Trans. Geosci. Remote Sens.* 56, 2107–2118. <https://doi.org/10.1109/TGRS.2017.2775103>.
- Trevithick, R., Soto-Berelov, M., Jones, S., Held, A., Phinn, S., Armston, J., Bradford, M., Broomhall, M., Cabello, A., Chisholm, L., Clarke, K., Davies, K., Farmer, E., Flood, N., Gill, T., Guerschman, J., Hacker, J., Howorth, E., 2015. AusCover Good Practice Guidelines: A Technical Handbook Supporting Calibration and Validation Activities of Remotely Sensed Data Products.
- Wang, Y., Xie, D., Liu, S., Hu, R., Li, Y., Yan, G., 2016. Scaling of FAPAR from the field to the satellite. *Remote Sens.* 8. <https://doi.org/10.3390/rs8040310>.
- Weiss, M., Baret, F., 2016. S2ToolBox Level 2 Products: LAI, FAPAR, FCOVER. 53.
- Widlowski, J.-L., 2010. On the bias of instantaneous FAPAR estimates in open-canopy forests. *Agric. For. Meteorol.* 150, 1501–1522. <https://doi.org/10.1016/j.agrformet.2010.07.011>.
- Xu, B., Park, T., Yan, K., Chen, C., Zeng, Y., Song, W., Yin, G., Li, J., Liu, Q., Knyazikhin, Y., Myneni, R., 2018. Analysis of global LAI/FAPAR products from VIIRS and MODIS sensors for spatio-temporal consistency and uncertainty from 2012–2016. *Forests* 9, 73.
- Yang, G.-Y., Slingo, J., 2001. The diurnal cycle in the tropics. *Mon. Weather Rev.* 129, 784–801. [https://doi.org/10.1175/1520-0493\(2001\)129<0784:TDCITT>2.0.CO;2](https://doi.org/10.1175/1520-0493(2001)129<0784:TDCITT>2.0.CO;2).
- Younis, M., Akkaya, K., 2008. Strategies and techniques for node placement in wireless sensor networks: a survey. *Ad Hoc Netw.* 6, 621–655. <https://doi.org/10.1016/j.adhoc.2007.05.003>.
- Yuan, H., Ma, R., Atzberger, C., Li, F., Loisele, S., Luo, J., 2015. Estimating forest fAPAR from multispectral Landsat-8 data using the invertible forest reflectance model INFORM. *Remote Sens.* 7, 7425.
- Zacharias, S., Bogena, H., Samaniego, L., Mauder, M., Fuß, R., Pütz, T., Frenzel, M., Schwank, M., Baessler, C., Butterbach-Bahl, K., Bens, O., Borg, E., Brauer, A., Dietrich, P., Hajsek, I., Helle, G., Kiese, R., Kunstmann, H., Klotz, S., Munch, J.C., Papen, H., Priesack, E., Schmid, H.P., Steinbrecher, R., Rosenbaum, U., Teutsch, G., Vereecken, H., 2011. A network of terrestrial environmental observatories in Germany. *Vadose Zone J.* 10, 955.
- Zhang, Q., Middleton, E.M., Cheng, Y.-B., Landis, D.R., 2013. Variations of Foliage Chlorophyll fAPAR and Foliage Non-chlorophyll fAPAR (fAPARchl, fAPARnonchl) at the Harvard Forest. 6. pp. 2254–2264. <https://doi.org/10.1109/jstars.2013.2275176>.

4 Synthesis

This thesis focused on the assessment of uncertainties of direct FAPAR measurements and the findings were published in three papers. The following sections summarize the main findings and conclusions and give an outlook on possible future research directions.

4.1 Conclusions

Differences and uncertainties of different FAPAR estimates were assessed based on direct PAR measurements at three forest sites: a conifer-dominated forest in Southern Germany, a boreal-deciduous forest in Northern Alberta at the Peace River Environmental Monitoring Super Sites, Canada, and a tropical dry forest at the Santa Rosa National Park Environmental Monitoring Super Site, Costa Rica. Uncertainties were considered in a validation experiment of the operational S2 FAPAR product. On the one hand, the presented results confirm several findings of previous RTM simulations on the bias of instantaneous FAPAR estimates (in particular the findings by Widłowski, 2010) that in situ FAPAR estimates are affected by considerable uncertainties which have to be considered in sampling protocols for the validation of satellite derived FAPAR products. On the other hand, the presented publications based on the experimental approach with WSNs in three different ecosystems reveal new insights in the temporal and spatial dynamics of FAPAR as well as relevant sources of uncertainty and bias connected to the sampling and estimating scheme. The main findings of this thesis are presented in the following conclusions according to the research questions outlined in section 2.1.

Q1: How can the bias of instantaneous FAPAR observations be assessed in field conditions?

The bias of instantaneous FAPAR observations can be assessed with multisensory and permanent PAR observations carried out with WSNs as well as additional phenological and meteorological observations. In this thesis, two methods have been developed and applied for a bias assessment. The first method is suitable for valuating the bias of the two-flux estimate given that measurements of diffuse radiation are available. Therefore, the difference between FAPAR acquired under diffuse light conditions versus clear-sky conditions can be investigated. The second method can be used without additional measurements of diffuse radiation but requires measurements of top-of-canopy (TOC) PAR albedo and PAR albedo of the forest background to calculate the four-flux FAPAR estimate. To quantify the bias of two- and three-flux FAPAR estimates, the difference with the four-flux estimate can be calculated. As uncertainties of FAPAR are now quantifiable in field-conditions, they should be considered in future validation studies.

Q2: Which environmental conditions are key sources of uncertainty in FAPAR ground observations?

FAPAR observations exhibited different seasonal variability according to differences in species composition (Graswang: 0.89 to 0.99 \pm 0.02; Peace River: 0.55 to 0.87 \pm 0.03; Santa Rosa: 0.45 to 0.97 \pm 0.06). However, during certain environmental conditions, this variability was a result of bias. An overestimation of FAPAR by 0.06 was found for SZA above 60°, thereby crossing the target accuracy set by the GCOS (2011). Further, an overestimation of FAPAR by up to 0.05 was found during the senescence periods with the occurrence of colored leaves at all sites. Regarding the influence of WS, it was found that the overestimation of FAPAR during high wind speeds (\geq 5 m s⁻¹) is crucial at the boreal site for the two-flux FAPAR estimate.

Q3: What is the bias of FAPAR ground observations associated to sampling size?

The spatial variability of FAPAR was investigated with the coefficient of variation as a function of sample size. The high initial variability achieved with two sensors across all forest sites (43% at Peace River, 34 % at Graswang, 24% at Santa Rosa) emphasizes the need for a multi-sensor approach for in situ FAPAR observations. Given the fact that optical remote sensing FAPAR products are dependent on clear sky conditions where spatial variability of FAPAR is highest, the recommendation by Widlowski (2010) was confirmed. Thus, ten PAR sensors should be the utmost minimum number of samples for reasonably accurate FAPAR observations.

Q4: What is the bias of FAPAR ground observations associated to the estimating scheme?

The highest average relative biases of the two-flux FAPAR estimate accounted to 2.1% at the temperate site, 8.4% at the boreal site and -4.5% at the tropical site. Thus, the accuracy threshold of 10% set by the GCOS was generally fulfilled. As an important finding, the three-flux FAPAR estimates, which have been favored frequently in previous studies, were not found to be beneficial for overall accuracy at the tropical site. Furthermore, the bias of FAPAR associated to the estimating scheme varied with environmental conditions so that the GCOS accuracy threshold was crossed during certain environmental conditions. Particularly, a significant effect of higher wind speed conditions on the bias of two- and three-flux estimates was found at the boreal and TDF sites which was attributed to increases in TOC PAR albedo. At the boreal site, the absolute bias of the two-flux FAPAR estimate under higher wind speed conditions (i.e., above 5 ms⁻¹) exceeded 0.05, thereby crossing the GCOS target accuracy.

Q5: What is the bias between ground data and recent satellite derived FAPAR products under uncertainty constraints?

The high discrepancies between the S2 FAPAR product and ground observations confirmed findings of existing validation studies for other satellite derived FAPAR products (e.g., D'Odorico et al., 2014, Pickett-Heaps et al., 2014, Tao et al., 2015, Xu et al., 2018). At all three sites, the S2 FAPAR product systematically underestimated the ground observations. The highest agreement was observed at the boreal-deciduous forest stand with a bias of -13% ($R^2=0.67$). The Central American and European

sites reported deviations of -20% ($R^2=0.68$) and -25% ($R^2=0.26$), respectively. In contrast to absolute values, strong agreement was found on phenological changes at all three sites. Specifically, the influence of species composition on seasonal variability of FAPAR across the European mixed-coniferous site was found to be well-represented in the S2 FAPAR product. As for the representation of spatial variability, highest agreement was found at the boreal-deciduous forest stand (%BIAS=-22%, $R^2=0.93$), whereas spatial variability is least represented at the TDF site (%BIAS=125%, $R^2=0.97$). Overall, when considering uncertainties of ground data, only the boreal site fulfilled the accuracy requirements set by the GCOS. Thus, due to low accuracy of absolute values, the current retrieval algorithm for the S2 FAPAR product will need further improvement to feed global production efficiency models and assess global carbon balances.

Q6: How does ecosystem complexity influence deviations between ground and satellite derived FAPAR estimates?

As a measure of ecosystem complexity, the HCI was considered as a novelty in satellite validation studies. The highest agreement (%BIAS=-22) between S2 and FAPAR ground measurements was obtained at the boreal site for which ecosystem complexity (HCI=1) is lowest, whereas highest discrepancies were obtained at the tropical site (%BIAS=-125) for which ecosystem complexity (HCI=64) is highest. Thus, the quality of the representation of both absolute and spatial variability of the S2 FAPAR product was found to be related to ecosystem complexity (i.e. number of species present, basal area, stem density). As such, these findings emphasize the need for intensified research in tropical forests, where ecosystem complexity is high.

Overall, the permanent monitoring with WSNs in combination with the monitoring of other environmental variables demonstrated the potential to quantify sources variability and uncertainty of two-flux FAPAR observations without a priori information on forest structure or spectral properties of canopies. Based on these conclusions, **Table 3** provides recommendations that could be used for the development of FAPAR sampling protocols.

Table 3: Practical recommendations for the development of sampling protocols for in situ FAPAR measurements with WSNs.

| Recommendations | Research question(s) |
|---|----------------------|
| The bias of instantaneous FAPAR observations should be investigated using multisensory and permanent PAR observations. It is recommended to employ WSNs as well as additional phenological and meteorological observations. | Q1 |

| | |
|--|--------|
| <p>The bias of in situ FAPAR attributed to colored leaves is significant and must be quantified and considered when validating satellite products during the senescence period. If the bias cannot be quantified, validation activities should be handled with caution during the senescence period.</p> | Q2 |
| <p>Wind speed is a potentially crucial source of uncertainty and bias for FAPAR observations; this has been overlooked in existing studies. Validation activities should be avoided at wind speeds higher than 5 ms⁻¹ when using two-flux FAPAR measurements. Instead, three- or four flux FAPAR measurements should be carried out to account for changes in TOC PAR albedo.</p> | Q2, Q4 |
| <p>The choice of the temporal aggregation scheme of FAPAR measurements for the validation of satellite FAPAR products must be carefully considered, as overestimation bias due to high SZA (above 60°) may cause bias in daily aggregated FAPAR.</p> | Q2, Q5 |
| <p>To reduce statistical errors (i.e., sampling bias), multi-sensor approaches as possible with WSNs are essential. This recommendation concerns not only measurements for transmitted PAR, but also for PAR fluxes reflected from the TOC region as well as the forest floor as needed for three- and four flux FAPAR estimates.</p> | Q3, Q4 |
| <p>The accuracy of the three-flux FAPAR estimate is not necessarily higher compared to two-flux FAPAR. At sites where TOC albedo can be expected to differ considerably from forest background albedo (e.g., due to different species composition or fractional cover), an approximation of forest background albedo with TOC albedo should be avoided; in this case, TOC PAR albedo should either be approximated with zero or measurements of forest-background albedo should be carried so that the four-flux FAPAR estimate can be calculated.</p> | Q4 |
| <p>The two-flux FAPAR estimate can be recommended as standard in situ quantity for FAPAR observations under typical summer conditions (i.e. green leaves, no snow, low wind speed) as its bias is negligible and the required experimental set-ups are relatively cost and labor efficient.</p> | Q2, Q4 |
| <p>Studies that rely on the accuracy of absolute values of the current S2 FAPAR product in forested area should currently focus their investigations on areas with low ecosystem complexity.</p> | Q6 |

4.2 Future Outlook

Several future research directions can be derived from the findings of this thesis.

First, the influence of sample bias on the accuracy of three- or four-flux FAPAR approaches could be studied. In this regard, the spatial variability of TOC reflectance, especially in tropical (dry) forests, could be a promising quantity to improve three-flux FAPAR estimates, which are currently based on single, tower-based measurements only. This could be done by means of UAV campaigns during different phenological development stages at the three study sites, preferably over tropical (dry) forests where ecosystem complexity is high.

Another interesting future research direction would be to quantify uncertainties related to different FAPAR definitions. As satellite derived FAPAR products focus on “green FAPAR” and WSNs monitor “total FAPAR”, it would be important to assess “green FAPAR” in field conditions. This could be done by evaluating direct FAPAR measurements with DHPs at the sensor locations or by the means of RTM simulations.

Third, the influence of different scales on the discrepancies between ground data and satellite derived FAPAR products should be investigated. Therefore, multispectral reflectance measurements of both UAV and satellite remote sensing imagery could be used to derive FAPAR with an RTM. The parameterization of an RTM could be based on 3D forest reconstructions from terrestrial LiDAR measurements.

Overall, as uncertainties of FAPAR ground observations are now assessable in field conditions, they should be considered also in upcoming validation activities of FAPAR satellite products. In this regard, the different settings of the three investigated forest sites hold the opportunity to improve algorithms for satellite FAPAR products over forested areas, presenting similar forest structure and composition as the described permanent monitoring site. Given the actual discrepancies between satellite derived FAPAR products and ground observations over forested areas, it seems worthwhile to improve FAPAR retrieval schemes by the means of RTMs that have been optimized for tall canopies. As an important step towards more accurate global FAPAR estimates, special attention should also be directed to tropical (dry) forests as they are currently underrepresented in validation studies.

References

- AKITSU, T., NASAHARA, K. N., HIROSE, Y., IJIMA, O. & KUME, A. 2017. Quantum sensors for accurate and stable long-term photosynthetically active radiation observations. *Agricultural and Forest Meteorology*, 237, 171-183.
- ANDERSON, M. C., NORMAN, J. M., MEYERS, T. P. & DIAK, G. R. 2000. An analytical model for estimating canopy transpiration and carbon assimilation fluxes based on canopy light-use efficiency. *Agricultural and Forest Meteorology*, 101, 265-289.
- ARROYO-MORA, J. P., SÁNCHEZ-AZOFEIFA, G. A., KALACSKA, M. E. R., RIVARD, B., CALVO-ALVARADO, J. C. & JANZEN, D. H. 2005. Secondary Forest Detection in a Neotropical Dry Forest Landscape Using Landsat 7 ETM+ and IKONOS Imagery1. *Biotropica*, 37, 497-507.
- BALDOCCHI, D., HUTCHISON, B., MATT, D. & MCMILLEN, R. 1986. Seasonal variation in the statistics of photosynthetically active radiation penetration in an oak-hickory forest. *Agricultural and Forest Meteorology*, 36, 343-361.
- BARET, F., HAGOLLE, O., GEIGER, B., BICHERON, P., MIRAS, B., HUC, M., BERTHELOT, B., NINO, F., WEISS, M., SAMAIN, O., ROUJEAN, J.-L. & LEROY, M. 2007. LAI, fAPAR and fCover CYCLOPES global products derived from VEGETATION Part 1: Principles of the algorithm. *Remote Sensing of Environment*, 110, 275-286.
- BARET, F., MAKHMARA, H., LACAZE, R. & SMETS, B. 2011. BioPar Product User Manual LAI, fAPAR, fCover, NDVI Version 1 from SPOT/VEGETATION data.
- BEER, C., REICHSTEIN, M., TOMELLERI, E., CIAIS, P., JUNG, M., CARVALHAIS, N., RÖDENBECK, C., ARAIN, M. A., BALDOCCHI, D., BONAN, G. B., BONDEAU, A., CESCATTI, A., LASSLOP, G., LINDROTH, A., LOMAS, M., LUYSSAERT, S., MARGOLIS, H., OLESON, K. W., ROUPSARD, O., VEENENDAAL, E., VIOVY, N., WILLIAMS, C., WOODWARD, F. I. & PAPALE, D. 2010. Terrestrial Gross Carbon Dioxide Uptake: Global Distribution and Covariation with Climate. *Science*, 329, 834.
- BURAS, A. & MENZEL, A. 2019. Projecting Tree Species Composition Changes of European Forests for 2061–2090 Under RCP 4.5 and RCP 8.5 Scenarios. *Frontiers in Plant Science*, 9.
- CAMACHO, F., CERNICCHARO, J., LACAZE, R., BARET, F. & WEISS, M. 2013. GEOV1: LAI, FAPAR essential climate variables and FCOVER global time series capitalizing over existing products. Part 2: Validation and intercomparison with reference products. *Remote Sensing of Environment*, 137, 310-329.
- CAMMALLERI, C., VERGER, A., LACAZE, R. & VOGT, J. V. 2019. Harmonization of GEOV2 fAPAR time series through MODIS data for global drought monitoring. *International Journal of Applied Earth Observation and Geoinformation*, 80, 1-12.
- CAMMALLERI, C. & VOGT, J. V. 2018. Non-stationarity in MODIS fAPAR time-series and its impact on operational drought detection. *International Journal of Remote Sensing*, 1-17.
- CAPERS, R. S. & CHAZDON, R. L. 2004. Rapid assessment of understory light availability in a wet tropical forest. *Agricultural and Forest Meteorology*, 123, 177-185.
- CARRER, D., ROUJEAN, J.-L., LAFONT, S., CALVET, J.-C., BOONE, A., DECHARME, B., DELIRE, C. & GASTELLU-ETCHEGORRY, J.-P. 2013. A canopy radiative transfer scheme with explicit FAPAR for the interactive vegetation model ISBA-A-gs: Impact on carbon fluxes. *Journal of Geophysical Research: Biogeosciences*, 118, 888-903.

- CASTRO, S. & SANCHEZ-AZOFEIFA, G. A. 2018. *Testing of Automated Photochemical Reflectance Index Sensors as Proxy Measurements of Light Use Efficiency in an Aspen Forest*.
- CHEN, J. M. 1996. Canopy architecture and remote sensing of the fraction of photosynthetically active radiation absorbed by boreal conifer forests. *IEEE Transactions on Geoscience and Remote Sensing*, 34, 1353-1368.
- CLAVERIE, M., VERMOTE, E. F., WEISS, M., BARET, F., HAGOLLE, O. & DEMAREZ, V. 2013. Validation of coarse spatial resolution LAI and FAPAR time series over cropland in southwest France. *Remote Sensing of Environment*, 139, 216-230.
- CLEVERS, J. G. P. W. & GITELSON, A. A. 2013. Remote estimation of crop and grass chlorophyll and nitrogen content using red-edge bands on Sentinel-2 and -3. *International Journal of Applied Earth Observation and Geoinformation*, 23, 344-351.
- D'ODORICO, P., GONSAMO, A., PINTY, B., GOBRON, N., COOPS, N., MENDEZ, E. & SCHAEPMAN, M. E. 2014. Intercomparison of fraction of absorbed photosynthetically active radiation products derived from satellite data over Europe. *Remote Sensing of Environment*, 142, 141-154.
- DISNEY, M., MULLER, J.-P., KHARBOUCHE, S., KAMINSKI, T., VOßBECK, M., LEWIS, P. & PINTY, B. 2016. A New Global fAPAR and LAI Dataset Derived from Optimal Albedo Estimates: Comparison with MODIS Products. *Remote Sensing*, 8, 275.
- DJAMAI, N., FERNANDES, R., WEISS, M., MCNAIRN, H. & GOÏTA, K. 2019. Validation of the Sentinel Simplified Level 2 Product Prototype Processor (SL2P) for mapping cropland biophysical variables using Sentinel-2/MSI and Landsat-8/OLI data. *Remote Sensing of Environment*, 225, 416-430.
- DRUSCH, M., DEL BELLO, U., CARLIER, S., COLIN, O., FERNANDEZ, V., GASCON, F., HOERSCH, B., ISOLA, C., LABERINTI, P., MARTIMORT, P., MEYGRET, A., SPOTO, F., SY, O., MARCHESE, F. & BARGELLINI, P. 2012. Sentinel-2: ESA's Optical High-Resolution Mission for GMES Operational Services. *Remote Sensing of Environment*, 120, 25-36.
- FAN, W., LIU, Y., XU, X., CHEN, G. & ZHANG, B. 2014. A New FAPAR Analytical Model Based on the Law of Energy Conservation: A Case Study in China. *IEEE Journal of Selected Topics in Applied Earth Observations and Remote Sensing*, 7, 3945-3955.
- FARQUHAR, G. D., VON CAEMMERER, S. & BERRY, J. A. 1980. A biochemical model of photosynthetic CO₂ assimilation in leaves of C₃ species. *Planta*, 149, 78-90.
- FENSHOLT, R., SANDHOLT, I. & RASMUSSEN, M. S. 2004. Evaluation of MODIS LAI, fAPAR and the relation between fAPAR and NDVI in a semi-arid environment using in situ measurements. *Remote Sensing of Environment*, 91, 490-507.
- FRAMPTON, W. J., DASH, J., WATMOUGH, G. & MILTON, E. J. 2013. Evaluating the capabilities of Sentinel-2 for quantitative estimation of biophysical variables in vegetation. *ISPRS Journal of Photogrammetry and Remote Sensing*, 82, 83-92.
- GANGULY, S., NEMANI, R. R., BARET, F., BI, J., WEISS, M., ZHANG, G., MILESI, C., HASHIMOTO, H., SAMANTA, A., VERGER, A., SINGH, K. & MYNENI, R. B. 2014. Green Leaf Area and Fraction of Photosynthetically Active Radiation Absorbed by Vegetation. In: HANES, J. M. (ed.) *Biophysical Applications of Satellite Remote Sensing*. Berlin, Heidelberg: Springer Berlin Heidelberg.
- GCOS, G. C. O. S. 2011. Systematic observation requirements for satellite-based data products for climate.

- GITELSON, A. A. 2019. Remote estimation of fraction of radiation absorbed by photosynthetically active vegetation: generic algorithm for maize and soybean. *Remote Sensing Letters*, 10, 283-291.
- GOBRON, N. 2015. Report on satellite derived ECV definition and field protocols. European Commission, Joint Research Centre (JRC), Institute for Environment & Sustainability.
- GOBRON, N., PINTY, B., MÉLIN, F., TABERNER, M., VERSTRAETE, M. M., BELWARD, A., LAVERGNE, T. & WIDLOWSKI, J. L. 2005. The state of vegetation in Europe following the 2003 drought. *International Journal of Remote Sensing*, 26, 2013-2020.
- GOBRON, N., PINTY, B., TABERNER, M., MÉLIN, F., VERSTRAETE, M. M. & WIDLOWSKI, J. L. 2006. Monitoring the photosynthetic activity of vegetation from remote sensing data. *Advances in Space Research*, 38, 2196-2202.
- GOND, V., DE PURY, D. G. G., VEROUSTRAETE, F. & CEULEMANS, R. 1999. Seasonal variations in leaf area index, leaf chlorophyll, and water content; scaling-up to estimate fAPAR and carbon balance in a multilayer, multispecies temperate forest. *Tree Physiology*, 19, 673-679.
- HEIMANN, M. & REICHSTEIN, M. 2008. Terrestrial ecosystem carbon dynamics and climate feedbacks. *Nature*, 451, 289-292.
- HOLDRIDGE, L. R. & TOSI, J. A. 1967. *Life Zone Ecology*, San Jose, Costa Rica, Tropical Science Center.
- HOUBORG, R., SOEGAARD, H. & BOEGH, E. 2007. Combining vegetation index and model inversion methods for the extraction of key vegetation biophysical parameters using Terra and Aqua MODIS reflectance data. *Remote Sensing of Environment*, 106, 39-58.
- HOVI, A., LUKEŠ, P. & RAUTIAINEN, M. 2017. Seasonality of albedo and fAPAR in a boreal forest. *Agricultural and Forest Meteorology*, 247, 331-342.
- HUEMMERICH, K. F., PRIVETTE, J. L., MUKELABAI, M., MYNENI, R. B. & KNYAZIKHIN, Y. 2005. Time-series validation of MODIS land biophysical products in a Kalahari woodland, Africa. *International Journal of Remote Sensing*, 26, 4381-4398.
- KALACSKA, M., SANCHEZ-AZOFEIFA, G. A., CALVO-ALVARADO, J. C., QUESADA, M., RIVARD, B. & JANZEN, D. H. 2004. Species composition, similarity and diversity in three successional stages of a seasonally dry tropical forest. *Forest Ecology and Management*, 200, 227-247.
- KNYAZIKHIN, Y., MARTONCHIK, J. V., MYNENI, R. B., DINER, D. J. & RUNNING, S. W. 1998. Synergistic algorithm for estimating vegetation canopy leaf area index and fraction of absorbed photosynthetically active radiation from MODIS and MISR data. *Journal of Geophysical Research: Atmospheres*, 103, 32257-32275.
- KOBAYASHI, H., SUZUKI, R., NAGAI, S., NAKAI, T. & KIM, Y. 2014. Spatial Scale and Landscape Heterogeneity Effects on fAPAR in an Open-Canopy Black Spruce Forest in Interior Alaska. *IEEE Geoscience and Remote Sensing Letters*, 11, 564-568.
- LARCHER, W. 2003. *Physiological Plant Ecology: Ecophysiology and Stress Physiology of Functional Groups*, Heidelberg, Springer.
- LEUCHNER, M., HERTEL, C. & MENZEL, A. 2011. Spatial variability of photosynthetically active radiation in European beech and Norway spruce. *Agricultural and Forest Meteorology*, 151, 1226-1232.
- LEUCHNER, M., HERTEL, C., RÖTZER, T., SEIFERT, T., WEIGT, R., WERNER, H. & MENZEL, A. 2012. Solar Radiation as a Driver for Growth and Competition in Forest Stands. In: MATYSSEK, R., SCHNYDER, H., OßWALD, W., ERNST, D., MUNCH, J. C. &

- PRETZSCH, H. (eds.) *Growth and Defence in Plants: Resource Allocation at Multiple Scales*. Berlin, Heidelberg: Springer Berlin Heidelberg.
- LI, W., BARET, F., WEISS, M., BUIS, S., LACAZE, R., DEMAREZ, V., DEJOUX, J.-F., BATTUDE, M. & CAMACHO, F. 2017a. Combining hectometric and decametric satellite observations to provide near real time decametric FAPAR product. *Remote Sensing of Environment*, 200, 250-262.
- LI, W., CAO, S., CAMPOS-VARGAS, C. & SANCHEZ-AZOFEIFA, G. A. 2017b. Identifying tropical dry forests extent and succession via the use of machine learning techniques. 63.
- LI, W., WEISS, M., WALDNER, F., DEFOURNY, P., DEMAREZ, V., MORIN, D., HAGOLLE, O. & BARET, F. 2015. A Generic Algorithm to Estimate LAI, FAPAR and FCOVER Variables from SPOT4_HRVIR and Landsat Sensors: Evaluation of the Consistency and Comparison with Ground Measurements. *Remote Sensing*, 7, 15494.
- LIU, L., ZHANG, X., XIE, S., LIU, X., SONG, B., CHEN, S. & PENG, D. 2019. Global White-Sky and Black-Sky FAPAR Retrieval Using the Energy Balance Residual Method: Algorithm and Validation. *Remote Sensing*, 11.
- LIU, N. & TREITZ, P. 2018. Remote sensing of Arctic percent vegetation cover and fAPAR on Baffin Island, Nunavut, Canada. *International Journal of Applied Earth Observation and Geoinformation*, 71, 159-169.
- LIU, R., HUAZHONG, R., LIU, S., LIU, Q., YAN, B. & GAN, F. 2018. Generalized FPAR estimation methods from various satellite sensors and validation. *Agricultural and Forest Meteorology*, 260, 55-72.
- LUGO, A. E., GONZALEZ-LIBOY, J. A., CINTRON, B. & DUGGER, K. 1978. Structure, Productivity, and Transpiration of a Subtropical Dry Forest in Puerto Rico. *Biotropica*, 10, 278-291.
- MAJASALMI, T. & RAUTIAINEN, M. 2016. The potential of Sentinel-2 data for estimating biophysical variables in a boreal forest: a simulation study. *Remote Sensing Letters*, 7, 427-436.
- MAJASALMI, T., STENBERG, P. & RAUTIAINEN, M. 2017. Comparison of ground and satellite-based methods for estimating stand-level fPAR in a boreal forest. *Agricultural and Forest Meteorology*, 232, 422-432.
- MARTÍNEZ, B., CAMACHO, F., VERGER, A., GARCÍA-HARO, F. J. & GILABERT, M. A. 2013. Intercomparison and quality assessment of MERIS, MODIS and SEVIRI FAPAR products over the Iberian Peninsula. *International Journal of Applied Earth Observation and Geoinformation*, 21, 463-476.
- MCCALLUM, I., WAGNER, W., SCHMULLIUS, C., SHVIDENKO, A., OBERSTEINER, M., FRITZ, S. & NILSSON, S. 2009. Satellite-based terrestrial production efficiency modeling. *Carbon Balance and Management*, 4, 8.
- MCCALLUM, I., WAGNER, W., SCHMULLIUS, C., SHVIDENKO, A., OBERSTEINER, M., FRITZ, S. & NILSSON, S. 2010. Comparison of four global FAPAR datasets over Northern Eurasia for the year 2000. *Remote Sensing of Environment*, 114, 941-949.
- MERONI, M., FASBENDER, D., KAYITAKIRE, F., PINI, G., REMBOLD, F., URBANO, F. & VERSTRAETE, M. M. 2014. Early detection of biomass production deficit hot-spots in semi-arid environment using FAPAR time series and a probabilistic approach. *Remote Sensing of Environment*, 142, 57-68.
- MONTEITH, J. L., MOSS, C. J., COOKE, G. W., PIRIE, N. W. & BELL, G. D. H. 1977. Climate and the efficiency of crop production in Britain. *Philosophical Transactions of the Royal Society of London. B, Biological Sciences*, 281, 277-294.

- MONTGOMERY, R. A. & CHAZDON, R. L. 2001. Forest structure, canopy architecture, and light forest structure, canopy architecture, and light transmittance in tropical wet forests. *Ecology*, 82, 2707-2718.
- MORTAZAVI, S. H., SALEHE, M. & MACGREGOR, M. H. 2014. Maximum WSN coverage in environments of heterogeneous path loss. *International Journal of Sensor Networks*, 16, 185-198.
- MÖTTUS, M., SULEV, M., FREDERIC, B., LOPEZ-LOZANO, R. & REINART, A. 2011. *Photosynthetically Active Radiation : Measurement and Modeling*.
- MOUGIN, E., DEMAREZ, V., DIAWARA, M., HIERNAUX, P., SOUMAGUEL, N. & BERG, A. 2014. Estimation of LAI, fAPAR and fCover of Sahel rangelands (Gourma, Mali). *Agricultural and Forest Meteorology*, 198-199, 155-167.
- MYNENI, R. B., HOFFMAN, S., KNYAZIKHIN, Y., PRIVETTE, J. L., GLASSY, J., TIAN, Y., WANG, Y., SONG, X., ZHANG, Y., SMITH, G. R., LOTSCH, A., FRIEDL, M., MORISSETTE, J. T., VOTAVA, P., NEMANI, R. R. & RUNNING, S. W. 2002. Global products of vegetation leaf area and fraction absorbed PAR from year one of MODIS data. *Remote Sensing of Environment*, 83, 214-231.
- MYNENI, R. B., RAMAKRISHNA, R., NEMANI, R. & RUNNING, S. W. 1997. Estimation of global leaf area index and absorbed par using radiative transfer models. *IEEE Transactions on Geoscience and Remote Sensing*, 35, 1380-1393.
- MYNENI, R. B. & WILLIAMS, D. L. 1994. On the relationship between FAPAR and NDVI. *Remote Sensing of Environment*, 49, 200-211.
- NESTOLA, E., SÁNCHEZ-ZAPERO, J., LATORRE, C., MAZZENGA, F., MATTEUCCI, G., CALFAPIETRA, C. & CAMACHO, F. 2017. Validation of PROBA-V GEOV1 and MODIS C5 & C6 fAPAR Products in a Deciduous Beech Forest Site in Italy. *Remote Sensing*, 9, 126.
- OLLINGER, S. V. 2011. Sources of variability in canopy reflectance and the convergent properties of plants. *New Phytologist*, 189, 375-394.
- PASTORELLO, G., SANCHEZ-AZOFEIFA, G. A. & NASCIMENTO, M. 2011. Enviro-Net: From Networks of Ground-Based Sensor Systems to a Web Platform for Sensor Data Management. *Sensors*, 11, 6454.
- PENG, J., MULLER, J. P., BLESSING, S., GIERING, R., DANNE, O., GOBRON, N., LUDWIG, R., MÜLLER, B., LENG, G., YOU, Q., DUAN, Z. & DADSON, S. 2019. Can We Use Satellite-Based FAPAR to Detect Drought? *Sensors*, 19, 3662.
- PICKETT-HEAPS, C. A., CANADELL, J. G., BRIGGS, P. R., GOBRON, N., HAVERD, V., PAGET, M. J., PINTY, B. & RAUPACH, M. R. 2014. Evaluation of six satellite-derived Fraction of Absorbed Photosynthetic Active Radiation (FAPAR) products across the Australian continent. *Remote Sensing of Environment*, 140, 241-256.
- PINTY, B., JUNG, M., KAMINSKI, T., LAVERGNE, T., MUND, M., PLUMMER, S., THOMAS, E. & WIDLOWSKI, J. L. 2011. Evaluation of the JRC-TIP 0.01° products over a mid-latitude deciduous forest site. *Remote Sensing of Environment*, 115, 3567-3581.
- PRINCE, S. D. & GOWARD, S. N. 1995. Global Primary Production: A Remote Sensing Approach. *Journal of Biogeography*, 22, 815-835.
- RAHMAN, M. M. & LAMB, D. W. 2016. Trigonometric correction factors renders the fAPAR-NDVI relationship from active optical reflectance sensors insensitive to solar elevation angle. *Computers and Electronics in Agriculture*, 121, 43-47.
- RANKINE, C. J., SANCHEZ-AZOFEIFA, G. A. & MACGREGOR, M. H. Seasonal wireless sensor network link performance in boreal forest phenology monitoring. 2014 Eleventh

- Annual IEEE International Conference on Sensing, Communication, and Networking (SECON), 30 June-3 July 2014 2014. 302-310.
- RODEN, J. S. 2003. Modeling the light interception and carbon gain of individual fluttering aspen (*Populus tremuloides* Michx) leaves. *Trees*, 17, 117-126.
- ROSS, J. & SULEV, M. 2000. Sources of errors in measurements of PAR. *Agricultural and Forest Meteorology*, 100, 103-125.
- RUNNING, S. W. 2012. A Measurable Planetary Boundary for the Biosphere. *Science*, 337, 1458.
- RYU, Y., BERRY, J. A. & BALDOCCHI, D. D. 2019. What is global photosynthesis? History, uncertainties and opportunities. *Remote Sensing of Environment*, 223, 95-114.
- SAKOWSKA, K., JUSZCZAK, R. & GIANELLE, D. 2016. Remote Sensing of Grassland Biophysical Parameters in the Context of the Sentinel-2 Satellite Mission. *Journal of Sensors*, 2016, 16.
- SANCHEZ-AZOFEIFA, G.-A. 1996. *Assessing Land Use/Cover Change in Costa Rica*. PhD Doctoral Dissertation, Universidad de Costa Rica.
- SELLERS, P. J., DICKINSON, R. E., RANDALL, D. A., BETTS, A. K., HALL, F. G., BERRY, J. A., COLLATZ, G. J., DENNING, A. S., MOONEY, H. A., NOBRE, C. A., SATO, N., FIELD, C. B. & HENDERSON-SELLERS, A. 1997. Modeling the Exchanges of Energy, Water, and Carbon Between Continents and the Atmosphere. *Science*, 275, 502.
- SELLERS, P. J., SCHIMMEL, D. S., MOORE, B., LIU, J. & ELDERING, A. 2018. Observing carbon cycle-climate feedbacks from space. *Proceedings of the National Academy of Sciences*, 115, 7860.
- SELLERS, P. J., TUCKER, C. J., COLLATZ, G. J., LOS, S. O., JUSTICE, C. O., DAZLICH, D. A. & RANDALL, D. A. 1994. A global 1° by 1° NDVI data set for climate studies. Part 2: The generation of global fields of terrestrial biophysical parameters from the NDVI. *International Journal of Remote Sensing*, 15, 3519-3545.
- SENNA, M. C. A., COSTA, M. H. & SHIMABUKURO, Y. E. 2005. Fraction of photosynthetically active radiation absorbed by Amazon tropical forest: A comparison of field measurements, modeling, and remote sensing. *Journal of Geophysical Research: Biogeosciences*, 110, n/a-n/a.
- SPENCE, J. & VOLNEY, J. 1999. EMEND: Ecosystem Management Emulating Natural Disturbance. Sustainable Forest Management Network Project Report.
- STEINBERG, D. C., GOETZ, S. J. & HYER, E. J. 2006. Validation of MODIS F/sub PAR/ products in boreal forests of Alaska. *IEEE Transactions on Geoscience and Remote Sensing*, 44, 1818-1828.
- STENBERG, P., LUKEŠ, P., RAUTIAINEN, M. & MANNINEN, T. 2013. A new approach for simulating forest albedo based on spectral invariants. *Remote Sensing of Environment*, 137, 12-16.
- TAHERIAZAD, L., MOGHADAS, H. & SANCHEZ-AZOFEIFA, A. A new approach to calculate Plant Area Density (PAD) using 3D ground-based lidar. *SPIE Remote Sensing*, 2016. SPIE, 10.
- TAO, X., LIANG, S., HE, T. & JIN, H. 2016. Estimation of fraction of absorbed photosynthetically active radiation from multiple satellite data: Model development and validation. *Remote Sensing of Environment*, 184, 539-557.
- TAO, X., LIANG, S. & WANG, D. 2015. Assessment of five global satellite products of fraction of absorbed photosynthetically active radiation: Intercomparison and direct validation against ground-based data. *Remote Sensing of Environment*, 163, 270-285.

- VERSTRAETE, M. M., GOBRON, N., AUSSÉDAT, O., ROBUSTELLI, M., PINTY, B., WIDLÓWSKI, J.-L. & TABERNER, M. 2008. An automatic procedure to identify key vegetation phenology events using the JRC-FAPAR products. *Advances in Space Research*, 41, 1773-1783.
- WANG, Q. & TENHUNEN, J. D. 2004. Vegetation mapping with multitemporal NDVI in North Eastern China Transect (NECT). *International Journal of Applied Earth Observation and Geoinformation*, 6, 17-31.
- WANG, Y., XIE, D., LIU, S., HU, R., LI, Y. & YAN, G. 2016. Scaling of FAPAR from the Field to the Satellite. *Remote Sensing*, 8.
- WEISS, M. & BARET, F. 2016. S2ToolBox Level 2 products: LAI, FAPAR, FCOVER.
- WIDLÓWSKI, J.-L. 2010. On the bias of instantaneous FAPAR estimates in open-canopy forests. *Agricultural and Forest Meteorology*, 150, 1501-1522.
- XIAO, Y., LI, X., ZHAO, S. & SONG, G. 2019. Characteristics and simulation of snow interception by the canopy of primary spruce-fir Korean pine forests in the Xiaoxing'an Mountains of China. *Ecology and Evolution*, 9.
- XIAO, Z., LIANG, S. & SUN, R. 2018. Evaluation of Three Long Time Series for Global Fraction of Absorbed Photosynthetically Active Radiation (FAPAR) Products. *IEEE Transactions on Geoscience and Remote Sensing*, 56, 5509-5524.
- XU, B., PARK, T., YAN, K., CHEN, C., ZENG, Y., SONG, W., YIN, G., LI, J., LIU, Q., KNYAZIKHIN, Y. & MYNENI, R. 2018. Analysis of Global LAI/FPAR Products from VIIRS and MODIS Sensors for Spatio-Temporal Consistency and Uncertainty from 2012–2016. *Forests*, 9, 73.
- YOUNIS, M. & AKKAYA, K. 2008. Strategies and techniques for node placement in wireless sensor networks: A survey. *Ad Hoc Networks*, 6, 621-655.
- YU, Z., YUHONG, T., KNYAZIKHIN, Y., MARTONCHIK, J. V., DINER, D. J., LEROY, M. & MYNENI, R. B. 2000. Prototyping of MISR LAI and FPAR algorithm with POLDER data over Africa. *IEEE Transactions on Geoscience and Remote Sensing*, 38, 2402-2418.
- YUAN, H., MA, R., ATZBERGER, C., LI, F., LOISELLE, S. & LUO, J. 2015. Estimating Forest fAPAR from Multispectral Landsat-8 Data Using the Invertible Forest Reflectance Model INFORM. *Remote Sensing*, 7, 7425.
- ZACHARIAS, S., BOGENA, H., SAMANIEGO, L., MAUDER, M., FUß, R., PÜTZ, T., FRENZEL, M., SCHWANK, M., BAESSLER, C., BUTTERBACH-BAHL, K., BENS, O., BORG, E., BRAUER, A., DIETRICH, P., HAJNSEK, I., HELLE, G., KIESE, R., KUNSTMANN, H., KLOTZ, S., MUNCH, J. C., PAPEN, H., PRIESACK, E., SCHMID, H. P., STEINBRECHER, R., ROSENBAUM, U., TEUTSCH, G. & VERECKEN, H. 2011. A Network of Terrestrial Environmental Observatories in Germany. *Vadose Zone Journal*, 10, 955.
- ZHANG, Q., MIDDLETON, E. M., CHENG, Y.-B. & LANDIS, D. R. 2013. Variations of Foliage Chlorophyll fAPAR and Foliage Non-Chlorophyll fAPAR (fAPARchl, fAPARnonchl) at the Harvard Forest. 6, 2254-2264.
- ZHU, Z., BI, J., PAN, Y., GANGULY, S., ANAV, A., XU, L., SAMANTA, A., PIAO, S., NEMANI, R. R. & MYNENI, B. R. 2013. Global Data Sets of Vegetation Leaf Area Index (LAI)_{3g} and Fraction of Photosynthetically Active Radiation (FPAR)_{3g} Derived from Global Inventory Modeling and Mapping Studies (GIMMS) Normalized Difference Vegetation Index (NDVI_{3g}) for the Period 1981 to 2011. *Remote Sensing*, 5.